UNIVERSITÀ DELLA CALABRIA

Dipartimento di Farmacia e Scienze della Salute e della Nutrizione

Universitat d'Alacant
Universidad de Alicante

Departamento de Química Orgánica
Istituto de Sintesis Organica (ISO)

PhD Thesis under International Joint Supervision

Deep Eutectic Solvents as Sustainable Media for Pharmaceutical Purposes

Doctoral Course in Translational Medicine, Cycle XXXVI

Supervisor (University of Calabria)
Prof. Maria Luisa Di Gioia

PhD Student
Dr. Debora Procopio

Supervisor (University of Alicante)
Prof. Diego J. Ramòn

PhD coordinator
Prof. Stefania Catalano

STEFANIA CATALANO
25.07.2024
14:28:12
UTC

ACADEMIC YEAR 2023/2024

Index

Index

Abbreviations list

[Ir(ppy)$_3$]: Tris(2-phenylpyridine) iridium

^{13}C NMR: Carbon-13 Nuclear Magnetic Resonance Spectroscopy

^{1}H NMR: Proton Nuclear Magnetic Resonance Spectroscopy

2-MeTHF: 2-methyltetrahydrofuran

5-ASA: 5-aminosalycilic acid

ACS GCIPR: American Chemistry Society Green Chemistry Industry Pharmaceutical Roundtable

ADES: Acidic Deep Eutectic Solvent

AE: Atom Economy

API: Active Pharmaceutical Ingredient

BA: Benzoic Acid

BADES: Brønsted Acidic Deep Eutectic Solvent

BCS: Biopharmaceutics Classification

Boc: Tert-butyl carbamate

Cds: Cadmium sulfide

ChCl: Choline Chloride

CO_2: Carbon Dioxide

DCC: Diciclohexylcarbodiimide

DCM: Dichloromethane

DES: Deep Eutectic Solvent

DIPEA: Diisopropylethylamine

DMSO: Dimethyl sulfoxide

DSC: Differential Scanning Calorimetry

EDC: 1-Ethyl-3-(3-dimethylaminopropyl) carbodiimide

EG: Ethylene glycol

Fmoc: Fluoromethyloxy carbonyl

GC-MS: Gas Chromatography coupled to Mass Spectrometry

Gly: Glycerol

HBA: Hydrogen Bond Acceptor

HBD: Hydrogen Bond Donor

HOBt: 1-hydroxybenzotriazole

HPA: Hydroxyphenylacetic acid

IBDUs: Inflammatory Bowel Diseases

ILs: Ionic Liquids

m.p: melting point

MeCN: Acetonitrile

Mes-Acr-ClO_4: 9-Mesityl-10-methylacridinium perchlorate

$MgSO_4$: Magnesium Sulphate

MI: Mass Intensity

NADESs: Natural Deep Eutectic Solvents

$NSAID_S$: Non-steroidal Ant inflammatory Drugs

OE: Optimum Efficiency

PA: Phenylacetic Acid

PG: Propylene Glycol

PMI: Process Mass Intensity

POM: Polarised Optical Microscope

pTSA: *p*-toluenesulfonic acid

RDES: Reactive Deep Eutectic Solvent

RME: Reaction Mass Economy

$Ru(bpy)_3Cl_2$: Tris(bipyridine) ruthenium (II) chloride

SCFs: Supercritical Fluids

SDGs: Sustainable Development Goals

TCT: 2,4,6-Trichloro-1,3,5-triazine

TEMPO: 2,2,6,6,-Tetramethylpiperidin 1-oxyl

TFA: Trifluoroacetic acid

THEDESs: Therapeutic Deep Eutectic Solvents

THF: Tetrahydrofuran

VOCs: Volatile Organic Compounds

Prologue

The research developed in this thesis has been carried out at Department of Pharmacy, Health and Nutritional Sciences of the University of Calabria, under the supervision of the Prof. Maria Luisa Di Gioia, and at the Institute of Organic Synthesis (ISO) of the University of Alicante, under the guidance of the Prof. Diego J. Ramón as supervisor and Prof. Gabriela Guillena as academic tutor. Part of the results reported in this thesis have already been published.

"Green solvents for the formation of amide linkages."
D. Procopio, C. Siciliano, S. Trombino, D. E. Dumitrescu, F. Suciu and M. L. Di Gioia.
Org. Biomol. Chem. **2022**, *20*, 1137-1149.

"An overview of the latest advances in the catalytic synthesis of glycerol carbonate."
D. Procopio and M. L. Di Gioia.
Catalysts **2022**, *12*, 50-72.

"Deep eutectic solvents for improving the solubilization and delivery of dapsone.
S. Trombino, C. Siciliano, D. **Procopio,** F. Curcio, A. S. Laganà, M. L. Di Gioia and R. Cassano.
Pharmaceutics, **2022**, *14*, 333-346.

"A Brønsted Acidic Deep Eutectic Solvent for N-Boc Deprotection".
D. Procopio, C. Siciliano, R. De Rose, S. Trombino, R. Cassano and M. L. Di Gioia.
Catalysts **2022**, *12*, 1480-1495.

"Visible-Light-Mediated Amide Synthesis in Deep Eutectic Solvents".
D. Procopio, X. Marset, G. Guillena, M. L. Di Gioia and D. J. Ramón.
Adv. Synth. Catal. **2024**, *366*, 870-876.

“Reactive deep eutectic solvents for EDC-mediated amide synthesis.”
D. Procopio, C. Siciliano and M. L. Di Gioia.
Org. Biomol. Chem., **2024**, *22*, 1400-1408.

“Reactive Deep Eutectic Solvent for an Eco-Friendly Synthesis of Cellulose Carbamate.”
V. Algieri, L. Maiuolo, **D. Procopio**, P. Costanzo, F. P. Nicoletta, S. Trombino, M. L. Di Gioia and A. De Nino.
Polymers **2024**, *16*, 757-773.

“Deep Eutectic Solvents for the Synthesis of Active Pharmaceutical Ingredients: a greener route to Atenolol”
D. Procopio, C. Siciliano, G. Guillena, D. J. Ramón and M. L. Di Gioia.
Manuscript submitted for publication, **2024.**

Scientific conferences participation

D. Procopio, C. Siciliano, S. Trombino, R. Cassano, F. Curcio and M. L. Di Gioia. (2021). Solubility of Mesalazine in Natural Deep Eutectic Solvents. 2nd International Meeting On Deep Eutectic Systems. Online, 15th-17th June. Book of Abstract, page 26. *ORAL PRESENTATION*

D. Procopio, M. Nardi, M. Oliverio, A. Procopio and M. L. Di Gioia. (2021) Deep Eutectic Solvents As Powerful Catalysts and Solvents for the Synthesis of Amides. 13th International Symposium on Pharmaceutical Sciences. Ankara, 22th-25th June, Book of Abstract P055, page 185. *POSTER PRESENTATION*

F. Curcio, R. Cassano, M. L. Di Gioia, **D. Procopio**, S. Trombino. (2021). Strategies for the solubilization and delivery of Dapsone in the Pharmaceutical field. In: 20th Advanced School in Pharmaceutical Technology. 27th-29th September. *POSTER PRESENTATION*

D. Procopio, C. Siciliano, A. Perri, G. Guillena, D. J. Ramón and M. L. Di Gioia. (2023) A Sustainable Synthesis of Atenolol in Deep Eutectic Solvents. 3rd International Meeting on Deep Eutectic Systems. Lisbon, 19th-22nd June. Book of Abstract P46, page 112. *POSTER PRESENTATION*

D. Procopio, M. Martos, Y. Perez-Almarcha, A. Nacher-Luis, D. J. Ramòn and I. M. Pastor. (2023) Catalytic protocols based on DES-type interactions using carboxy-funcionalized imidazolinium salts. XXXIX Reunión Bienal de la Sociedad Española de Química. Zaragoza, 25th-29th June. Book of Abstract S11-PP01, page 881. *POSTER PRESENTATION*

D. Procopio, X. Marset, T. Martí, M. L. Di Gioia and D. J. Ramón. (2023) Visible light-mediated synthesis of amides in deep eutectic solvents. XXXIX Reunión Bienal de la Sociedad Española de Química. Zaragoza 25th-29th June. Book of Abstract S11-PP10, page 890. *POSTER PRESENTATIO*

D. Procopio, X. Marset, G. Guillena, D. J. Ramón and M. L. Di Gioia. (2023) A Sustainable Approach towards Amide Bond Formation. 6th EuChemS Conference on Green Chemistry and Sustainable Chemistry, Salerno 3th-6th September. Book of Abstract P4 *POSTER PRESENTATION*

Riassunto

La presente tesi di dottorato si propone di esaminare l'uso di Deep Eutectic Solvents (DESs) come alternativa ecologica ai solventi convenzionali nelle comuni trasformazioni organiche e processi di formulazione nell'ambito dell'industria farmaceutica. A tale scopo, la tesi è stata suddivisa in cinque distinti capitoli:

Il Capitolo I si concentra sullo sviluppo di un approccio sostenibile per la sintesi di ammidi, utilizzando dei Reactive Deep Eutectic Solvents (RDESs) che servono sia come mezzo di reazione che come reagenti. Questo metodo innovativo mira ad eliminare solventi pericolosi, consentendo un recupero efficace dei prodotti, eludendo l'uso di ulteriori purificazioni cromatografiche. La sostenibilità del metodo sviluppato è stata stimata attraverso la valutazione e comparazione delle metriche di sostenibilità della procedura rispetto alle strategie industriali convenzionali.

Il Capitolo II delinea l'utilizzo pionieristico di un catalizzatore di rutenio semplice e commercialmente disponibile per la sintesi fotocatalizzata di ammidi in DES. L'impatto ambientale di questa nuova metodologia è stato valutato utilizzando specifiche metriche di sostenibilità.

Il Capitolo III presenta un metodo eco-sostenibile di rimozione del gruppo *ter*-butilossicarbonil (Boc), largamente utilizzato in chimica organica per la protezione delle funzioni amminiche. La procedura di *N*-Boc deprotezione è stata realizzata in assenza di solvente organico e utilizzando un DES a base di cloruro di colina e acido *p*-toluenesolfonico, che agisce sia da mezzo di reazione che da catalizzatore. Tale approccio è stato testato per la deprotezione di diversi *N*-Boc derivati. Anche in questo caso, l'impatto ambientale della metodologia sviluppata è stato valutato attraverso specifiche metriche di sostenibilità.

Il Capitolo IV mira a proporre una sintesi *green*, "one-pot", in due stadi, dell'Ingrediente Farmaceutico Attivo (API) Atenololo. Attualmente, l'Atenololo è tra i cinque farmaci più venduti al mondo, appartenente ad una classe di beta-bloccanti comunemente utilizzati per il trattamento dell'angina, dell'ipertensione e per ridurre il rischio di mortalità dopo infarto. La nuova metodologia di sintesi dell'atenololo

proposta utilizza un DES sia come mezzo di reazione che come catalizzatore, offrendo un'alternativa sostenibile e rispettosa dell'ambiente rispetto alle vie sintetiche industriali convenzionali. L'impatto ambientale di questa strategia sintetica è stato valutato utilizzando metriche di sostenibilità e confrontato con le procedure classiche.

Infine, il Capitolo V approfondisce il potenziale utilizzo sostenibile dei DESs come solventi alternativi nel settore farmaceutico, evidenziando la loro straordinaria capacità di migliorare notevolmente la solubilizzazione e il *delivery* di ingredienti farmaceutici attivi (API) scarsamente solubili in acqua (appartenenti alle Classi II e IV del Sistema di Classificazione Biofarmaceutica (BCS)), con potenziali implicazioni positive per l'industria farmaceutica, chimica e altri settori correlati.

Summary

This doctoral thesis explores the use of Deep Eutectic Solvents (DESs) as an environmentally friendly alternative to conventional solvents in common organic transformations and formulation processes within the pharmaceutical industry. For this purpose, the thesis has been divided into five distinct chapters:

Chapter I details the development of a sustainable approach for the synthesis of amides, using Reactive Deep Eutectic Solvents (RDESs) that serve both as a reaction medium and as reagents. This innovative method aims to eliminate hazardous solvents, allowing efficient product recovery and avoiding the need for additional chromatographic purifications. The sustainability of the developed method was estimated through the assessment and comparison of sustainability metrics on a large scale compared to conventional industrial strategies.

Chapter II delineates a pioneering use of a simple and commercially available ruthenium catalyst to carry out the photocatalytic amide synthesis in DES. Even in this case, the environmental impact of the new methodology has been assessed using green metrics.

Chapter III presents an eco-sustainable method for the removal of the tert-butyl carbamate (Boc) group, widely used in organic chemistry for the protection of amine functionalities. The *N*-Boc deprotection procedure was carried out in the absence of organic solvent, using a DES based on choline chloride and *p*-toluenesulfonic acid, which acts both as a reaction medium and catalyst. This approach was tested for the deprotection of various *N*-Boc derivatives. Furthermore, the impact of the developed methodology was evaluated using green metrics.

Chapter IV aims to propose a green, "one-pot" synthesis in two stages of the Active Pharmaceutical Ingredient (API) Atenolol. Currently, Atenolol ranks among the top five best-selling drugs worldwide, belonging to a class of beta-blockers commonly used for treating angina, hypertension, and reducing the risk of mortality after a heart attack. The novel synthetic methodology for Atenolol involves a DES which acts both as reaction medium and catalyst, providing a sustainable and environmentally

friendly alternative to conventional industrial synthetic routes. The environmental impact of this synthetic strategy has been assessed using sustainability metrics and compared with traditional procedures.

Finally, Chapter V aims to delve into how DESs can be sustainably utilized as alternative solvents in the pharmaceutical sector due to their extraordinary ability to significantly enhance the solubilization and delivery of poorly water-soluble Active Pharmaceutical Ingredients (APIs) belonging to Biopharmaceutics Classification System (BCS) Classes II and IV. This exploration holds potential positive implications for the pharmaceutical, chemical, and other related industries.

Resumen

La presente tesis doctoral explora el uso de mezclas no volátiles o mezclas eutécticas (DESs en inglés) como medios de reacción alternativos a los disolventes convencionales (VOCs en inglés), a fin de desarrollar nuevas metodologías de alto interés farmacéutico de forma sostenible y respetuosa con el medio ambiente. El estudio tiene como objetivo evaluar la viabilidad y eficiencia de los DESs para reemplazar procesos químicos tradicionales, considerando sus posibles beneficios en términos de sostenibilidad, rentabilidad y reducción del impacto ambiental. El trabajo se ha dividido en cinco capítulos diferentes:

El Capítulo I detalla el desarrollo de una metodología más sostenible para la síntesis de enlaces amida, fundamentales en productos farmacéuticos, agroquímicos y polímeros, utilizando DES reactivos, que sirven tanto como medio de reacción como reactivos. A este fin, se prepararon tres RDES con cloruro de colina como HBA y ácidos benzoico, fenilacético y 4-hidroxifenilacético como HBD. Con el fin de investigar los DES preparados por sus roles duales como solventes y reactivos en la síntesis de amidas, se realizó la *N*-amidación de anilina con ácido fenilacético, utilizado como componente del RDES. El método de síntesis mediado por RDES fue aplicable a todas las combinaciones de acoplamiento consideradas. La mayor eficiencia en términos de rendimiento de acoplamiento y pureza del producto se logró al utilizar 1-etil-3-(3-dimetilaminopropil)carbodiimida (EDC) como agente de acoplamiento. Con el objetivo de investigar el alcance y las limitaciones de la metodología optimizada, se evaluó la reacción de acoplamiento para una serie de aminas, empleando el mismo sistema RDES. En todos los casos, se obtuvieron las amidas correspondientes con rendimientos de buenos a excelentes. Además, hay que señalar que no se observó racemización al utilizar aminas enantiopuras. En consecuencia, la rapidez de la conversión lograda a través del protocolo desarrollado permitió evitar la necesidad de emplear HOBt como catalizador, mejorando la sostenibilidad general del proceso.

Con el fin de resaltar la generalidad del proceso, se utilizaron algunos de los mismos grupos de aminas para realizar reacciones de acoplamiento con los otros

dos RDES preparados. Los resultados mostraron que incluso al cambiar el componente ácido en el RDES, el rendimiento de los sistemas fue comparable con el primero, confirmando y ampliando el alcance del protocolo desarrollado. Con el objetivo de investigar la utilidad de la metodología desarrollada en la industria farmacéutica, se aplicaron las condiciones de reacción optimizadas para sintetizar 4-hidroxifenilacetamida, un intermediario sintético clave en la producción industrial de atenolol. El atenolol es uno de los cinco medicamentos más vendidos en el mundo, utilizado actualmente para tratar la angina de pecho, la hipertensión y reducir el riesgo de muerte después de un ataque cardíaco. En este contexto, la síntesis de 4-hidroxifenilacetamida representa el primer paso en la producción industrial de atenolol. A partir de la reacción entre cloruro de amonio y RDES basado en ácido 4-hidroxifenilacético, se recuperó la amida deseada con un rendimiento del 94%, utilizando EDC·HCl como agente de acoplamiento. Es importante enfatizar que una de las ventajas del método desarrollado es que, para todas estas amidaciones, el procedimiento de trabajo ideado aportó el producto de amida puro sin necesidad de purificacion por cromatografía.

Considerando la viabilidad de aplicar la ruta sintética desarrollada para la síntesis industrial de amidas, se procedió a realizar la síntesis a escala de gramos de N-fenetil-2-fenilacetamida. Al añadir agua a la mezcla de reacción al final del proceso de acoplamiento, el producto precipitado se recuperó exitosamente con rendimientos y pureza elevados mediante una simple filtración, sin necesidad de realizar procedimientos cromatográficos. Esta estrategia de recuperación del producto presenta ventajas significativas en términos de eficiencia y simplicidad del proceso. La adición de agua facilita la precipitación del compuesto deseado, permitiendo una separación fácil y efectiva de impurezas y subproductos. Este enfoque minimiza la necesidad de pasos adicionales y recursos asociados con técnicas cromatográficas, lo que resulta en una metodología más rentable y respetuosa con el tiempo. Los rendimientos y la pureza elevados obtenidos en esta etapa de síntesis a escala de gramos validan la aplicabilidad práctica y la eficacia de la ruta desarrollada.

Basándonos en los resultados de la literatura previa y nuestros experimentos, se propone un mecanismo plausible para la reacción de amidación en presencia de RDES. En un primer paso de reacción, la transferencia de protones desde el ácido carboxílico al átomo de nitrógeno débilmente básico en el EDC fue facilitada por interacciones de enlace de hidrógeno entre el RDES y el agente de acoplamiento, provocando el ataque nucleofílico del anión carboxilato resultante para llevar a la formación del intermediario de O-acilisourea. Luego, las mismas interacciones de enlace de hidrógeno permitieron el paso de aminólisis. Finalmente, la asistencia anquimérica guió la formación del producto de amida, junto con la producción de urea como subproducto.

Finalmente, con el fin de demostrar los beneficios ambientales de la metodología desarrollada, las métricas de química sostenible para la síntesis de la reacción piloto fueron calculadas. El método resultó altamente eficiente para producir la amida deseada con un rendimiento del 97% (a escala de gramos), con valores de PMI (Intensidad de Masa del Proceso) y *E*-factor mejores en comparación con el método industrial convencional. Estos resultados indican una mayor sostenibilidad ambiental de la ruta sintética propuesta. La eficiencia del proceso, junto con la reducción de residuos y la mejora en las métricas de sostenibilidad, respaldan la viabilidad y la idoneidad de la metodología desarrollada para aplicaciones prácticas a nivel industrial. Esta evaluación cuantitativa refuerza la contribución positiva de la nueva ruta sintética al objetivo general de reducir el impacto ambiental en la síntesis de productos químicos.

En resumen, la exitosa aplicación de RDES en la *N*-amidación ofrece una alternativa prometedora y respetuosa con el medio ambiente para la síntesis de amidas. La eficiencia, versatilidad, escalabilidad y alineación con los principios de química verde hacen de este método una valiosa contribución para avanzar en prácticas sostenibles en la industria farmacéutica.

El Capítulo II delinéa una metodología pionera para la síntesis de amidas mediante fotocatálisis en DES. El estudio tiene como objetivo la síntesis de amidas a partir de tioácidos con luz visible en DES, explorando sinergias para mitigar desafíos y evaluando beneficios ambientales al reemplazar disolventes peligrosos. Además, los objetivos son desbloquear por primera vez el potencial de los DES en combinación con la fotocatálisis en una síntesis de amidas más segura y sostenible.

A este fin, se realizaron pruebas con diversas mezclas eutécticas y fotocatalizadores para la formación de amidas a partir de ácido tioacético y anilina. El mejor resultado se obtuvo con la mezcla eutéctica ChCl:urea, sin necesidad de una base externa. Dado que el DES podría actuar como medio de reacción y base, la formación de amidas catalizada por fotocatálisis redox se logró sin la adición extra de la sal inorgánica o base, reduciendo así los residuos químicos. En cuanto a la eficiencia de los fotocatalizadores probados, los mejores resultados se obtuvieron con $Ru(bpy)_3Cl_2$, dando el producto deseado con un rendimiento cuantitativo en combinación con ChCl:urea durante 1 hora. Además, se observó una disminución abrupta del rendimiento cuando la reacción se realizó en la oscuridad con o sin catalizador, respaldando el mecanismo basado en la fotocatálisis redox. Curiosamente, otros fotocatalizadores dieron resultados similares, lo que es un aspecto importante para su implementación en procesos fotocatalíticos adicionales en medios DES.

La metodología optimizada muestra una alta versatilidad al producir amidas con altos rendimientos. Los efectos electrónicos de los sustituyentes en las aminas no parecen afectar significativamentea esta transformación. Las anilinas con sustituyentes tanto donadores como atrayentes de electrones dieron resultados similares. Además, anilinas con sustituyentes en posición *para*, *meta* y *orto* se transformaron en amidas con rendimientos razonables. El uso de *p*-aminofenol como substrato mostró una superioridad en la selectividad hacia la acilación del grupo amino en comparación con el grupo hidroxilo libre. Finalmente, se obtuvo *N*-(naftalen-1-il) acetamida a partir de 1-naftilamina con un rendimiento del 63%. Las aminas alifáticas también fueron toleradas bajo las mismas condiciones,

proporcionando los productos derivados de amida deseados con rendimientos de moderados a excelentes. Anilina y *p*-toluidina pueden reaccionar con ácido tiobenzoico para obtener las resultantes amidas con altos rendimientos. Para tioácidos alquílicos, se obtuvieron buenos rendimientos con sustratos como ciclohexilo, *ter*-butilo, *n*-pentilo y *n*-heptilo. Incluso las unidades terminales de alquenos, comúnmente usadas en la captura de intermediarios radicalarios, fueron toleradas; por ejemplo, el ácido undec-10-enoico pudo emplearse con éxito como socio de acoplamiento con anilina y *p*-toluidina, sin observar reacciones colaterales.

Con el fin de arrojar luz sobre la posible vía de reacción, se llevaron a cabo experimentos mecanísticos. A partir de los resultados obtenidos, se propuso un mecanismo plausible para la síntesis de amidas. En este contexto, al introducir 2,2,6,6-tetrametilpiperidina-1-oxilo (TEMPO) a la combinación de ácido tioacético y anilina, se obtuvo la amida correspondiente solo en cantidades mínimas. Por consiguiente, se planteó un mecanismo que involucraba al radical del tioácido. Para profundizar en la comprensión de la reacción vinculada al aislamiento de intermediarios activos, se expuso el ácido tiobenzoico a la luz visible durante 30 minutos, generando un esclarecedor intermediario de disulfuro con aproximadamente un 57% de rendimiento. Se llevó a cabo un experimento ortogonal utilizando ácido tioacético e intermediario de disulfuro bajo condiciones estándar, y los resultados obtenidos indicaron claramente la participación del intermediario de disulfuro en el mecanismo. En última instancia, se examinó la influencia del oxígeno atmosférico al realizar la reacción modelo bajo una atmósfera de argón. Se evidenció una significativa disminución en la velocidad de reacción, logrando solo un 46% de rendimiento de la amida deseada después de 2 horas, en contraste con el 99% observado en condiciones aeróbicas. Este descubrimiento subraya la relevancia del oxígeno atmosférico en la eficacia de la reacción. En resumen, los resultados respaldan la propuesta de un mecanismo que implica el radical del tioácido y subrayan la notable influencia del oxígeno en la cinética de la reacción. En base a los resultados de los estudios mencionados anteriormente, se propuso un mecanismo plausible para la síntesis de amidas.

Dado que el reciclaje de los DES y el catalizador es un punto crucial para la sostenibilidad del proceso desde el punto de vista industrial, se evaluó también la posibilidad de recuperar el sistema DES-catalizador y reutilizarlo. Los mejores resultados se obtuvieron cuando se empleó acetato de etilo. El reciclaje del DES y el catalizador fue posible hasta tres ciclos, destacando la sostenibilidad de la metodología. La capacidad de recuperar y reutilizar el sistema DES-catalizador contribuye significativamente a la sostenibilidad del proceso, reduciendo la generación de residuos y disminuyendo la dependencia de recursos. El hecho de que el reciclaje sea posible durante varios ciclos refuerza la viabilidad a largo plazo de la metodología propuesta. Estos descubrimientos respaldan la implementación práctica de la ruta sintética en un entorno industrial, donde la eficiencia y la sostenibilidad son factores críticos para el éxito a largo plazo.

Al fin de evaluar la eficiencia del método desarrollado, se analizaron métricas verdes y se compararon con la síntesis previamente reportada de amidas fotocatalíticas a partir de aminas y tioácidos. Se utilizó un análisis semicuantitativo llamado EcoScale, que considera rendimiento de reacción, costo, seguridad y facilidad de purificación. El valor de EcoScale para el presente protocolo en DES fue de 64, clasificándose como aceptable (50-75). Esto es relevante al compararse con informes que utilizan el mismo catalizador, con MeCN como disolvente o catalizadores como $MesAcrBF_4$ o CdS. Además, la economía de átomos para la síntesis de la reacción piloto fue del 79.9% con ácido tioacético y 65.2% con tioacetato de potasio.

En resumen, la metodología propuesta destaca por su innovación, sostenibilidad y eficiencia en la síntesis de amidas, abriendo nuevas perspectivas en la aplicación de DES y fotocatálisis.

En el capítulo III se presenta una metodología simple y conveniente para la desprotección de derivados *N*-Boc protegidos que conduce a los productos desprotegidos correspondientes con altas purezas y altos rendimientos, sin la necesidad de aplicar purificación post-reacción. El desarrollo de métodologias

generales para la eliminación del grupo protector Boc se ha identificado recentemente como una de las áreas prioritarias de investigación para el sector farmacéutico. A lo largo de los años, se han desarrollado varios procedimientos experimentales para la desprotección de Boc, típicamente implicando el uso de ácidos fuertes. La mayoría de estos métodos presentan varias desventajas, como alta acidez, uso de reactivos costosos, cantidades excesivas de catalizadores y disolventes orgánicos, baja quimioselectividad, altas temperaturas y desafíos en la recuperación del catalizador. En este sentido, el ácido trifluoroacético (TFA) sigue siendo el reactivo de elección para la eliminación del grupo Boc; sin embargo, este enfoque tiene sus inconvenientes, ya que el TFA es tóxico, volátil y perjudicial para el medio ambiente. Por lo tanto, el desarrollo de un método respetuoso con el medio ambiente, económico en átomos y sostenible en la desprotección de Boc sigue siendo un desafío contemporáneo en la química sintética y la industria química.

Dado que la desprotección selectiva del grupo Boc se lleva a cabo bajo condiciones ligeramente ácidas, se probó el comportamiento catalítico de diferentes DESs tipo ácido de Brønsted y ácido de Lewis. En particular, la sal de amonio cuaternario cloruro de colina (ChCl) se utilizó como HBA, ya que es una sal cuaternaria económica, biodegradable, no tóxica e incluso comestible, que se puede extraer de biomasa o sintetizar fácilmente a partir de reservas fósiles. Por otro lado, se eligieron *p*TSA, ácido oxálico, ácido cítrico, ácido malónico, ácido succínico y $FeCl_3$ como HBDs y catalizadores.

Todos los RDES preparados fueron sometidos a pruebas en la desprotección de *N*-Boc-bencilamina, la cual fue seleccionada como sustrato modelo. Para un análisis sistemático de la acción de los sistemas investigados, se llevaron a cabo todas las reacciones a temperatura ambiente, salvo en el caso del DES preparado con ácido cítrico, que requirió una temperatura de 50 °C debido a su alta viscosidad, limitando así su aplicación como medio de reacción. De manera satisfactoria, al tratar 1 mmol de N-Boc bencilamina en 1 mL de ChCl: *p*TSA (1:1) a temperatura ambiente, la desprotección se llevó a cabo en tan solo 10 minutos, logrando un

rendimiento del 98%. La presencia de la amina libre fue detectada mediante GC-MS. Sin embargo, al evaluar la reacción modelo en otros DESs de tipo ácido de Brønsted y ácido de Lewis, se observaron rendimientos más bajos en la formación de la amina libre. Esto podría estar relacionado con el carácter ácido más bajo de los ácidos utilizados en comparación con el primero mencionado.

Inspirados por los resultados iniciales, se exploró el alcance y las limitaciones del método perfeccionado en diversos *N*-terbutilcarbamatos alifáticos y aromáticos. La eficaz desprotección de varias aminas primarias y secundarias, anilinas, etc., se evidenció con rendimientos cuantitativos en tiempos de reacción de 10 a 30 minutos. El método se aplicó con éxito también a aminas alifáticas y heterocíclicas, con rendimientos notables incluso para aminas secundarias protegidas, aunque con tiempos de reacción más largos. La eficacia con la que se lleva a cabo la desprotección, junto con los rendimientos cuantitativos observados en varios casos, respaldan la robustez y la utilidad del método mejorado. Estos descubrimientos sugieren que la metodología podría tener aplicaciones amplias en la síntesis de diversas aminas y compuestos relacionados en la química orgánica.

Considerando el gran valor científico e industrial de la protección *N*-Boc en la síntesis de péptidos, se investigó la desprotección *N*-Boc de varios derivados de aminoácidos. Los ésteres metílicos de aminoácidos con cadenas laterales alifáticas, como L-alanina y D-alanina, se desprotegieron en solo 10 minutos, con rendimientos superiores al 98%. Estos ésteres fueron compatibles con las condiciones de reacción, sin observarse productos de degradación. En contraste, los ésteres metílicos de aminoácidos de cadena ramificada, como N-Boc L-leucina y *N*-Boc valina, requirieron tiempos de desprotección más largos (alrededor de 25 minutos) y mostraron rendimientos más bajos en comparación con los aminoácidos de cadenas laterales alifáticas. En este punto, se evaluó la ortogonalidad de las condiciones de reacción, sin afectar otros grupos protectores en las cadenas laterales de los aminoácidos. Los sustratos con grupos protectores ácido-lábiles, como el éter bencílico, se mantuvieron estables. Se utilizó también el O-Bencil-L-

tirosina metyl éster para demostrar la ortogonalidad, ya que la estrategia Boc/Bn es común en la síntesis de péptidos. La desprotección selectiva del grupo Boc sin afectar el éster bencílico se logró con éxito en el DES ChCl:*p*TSA. La estabilidad del grupo Fmoc en la cadena lateral del triptófano también se confirmó. La desprotección eficiente de un dipeptido *N*-Boc-L-fenilalanil-L-alanina metil éster resaltó la aplicabilidad del protocolo a sistemas más complejos. La recuperación sencilla de los productos finales, sin necesidad de purificación cromatográfica, subraya la ventaja del uso de DES en este procedimiento. Los productos se neutralizaron con $NaHCO_3$ y se obtuvieron rendimientos cuantitativos mediante evaporación al vacío tras extracción y lavado con acetato de etilo y salmuera.

Basándose en la literatura previamente reportada, se propuso una posible vía mecanística para la ruptura del Boc. En un primer paso, el sitio ácido de Brønsted del sistema de disolventes CHCl: *p*TSA activó el oxígeno del carbamato mediante protonación, debilitando y rompiendo así el enlace C=O y provocando la pérdida del carbocatión de terbutilo. La formación reversible de enlaces de hidrógeno entre el DES y el sustrato hizo que el ácido carbámico resultante experimentara una transferencia de protones seguida de una descarboxilación para proporcionar la amina desprotegida en forma de sal. La última etapa, con un medio básico, proporciona la amina libre. La evaluación del método en una escala mayor con *N*-Boc bencilamina mostró un rendimiento del 94%, destacando la eficiencia para la producción a gran escala.

Finalmente, se comparó la eficiencia ambiental del protocolo con otros métodos mediante la intensidad de masa del proceso (PMI) y el factor ambiental completo (E-factor). Con PMI y *E*-factor de 68 y 67, respectivamente, el protocolo demostró ser más sostenible y respetuoso con el medio ambiente que otras metodologías, destacando su viabilidad y contribución a la química verde, refuerzando la posición del protocolo como una opción más sostenible.

En resumen, el capítulo presenta una metodología novedosa y altamente eficiente para la desprotección de Boc utilizando RDES basados en *p*TSA. La versatilidad del método, su facilidad de operación y sus características respetuosas con el medio ambiente lo posicionan como una alternativa prometedora para la desprotección selectiva de derivados de N-Boc en una variedad de sustratos.

El Capítulo IV tiene como objetivo proponer una síntesis "one-pot" en dos etapas del Ingrediente Farmacéutico Activo (API) Atenolol. Actualmente, el Atenolol se encuentra entre los cinco medicamentos más vendidos a nivel mundial, perteneciente a la clase de beta-bloqueantes comúnmente utilizados para el tratamiento de la angina de pecho, la hipertensión y para reducir el riesgo de mortalidad después de un infarto. La ruta industrial típica para obtener el atenolol utiliza la reacción de la 4-hidroxifenilacetamida con la epiclorhidrina, seguida de la apertura del anillo del epóxido con la isopropilamina. Este enfoque clásico genera cantidades sustanciales de residuos y otros subproductos que deben ser eliminados adecuadamente. Por lo tanto, hay una creciente necesidad de una ruta sintética más conveniente que se alinee con los desafíos ambientales actuales.

La nueva metodología de síntesis de atenolol desarrollada utiliza un Disolvente Eutéctico (DES) como medio de reacción y catalizador, buscando así ofrecer una alternativa sostenible y respetuosa con el medio ambiente en comparación con las rutas sintéticas industriales convencionales.

En una primera fase, se optimizó el primer paso. En este contexto, el estudio comenzó investigando la reacción entre la 4-hidroxifenilacetamida y la epiclorhidrina, investigando diferentes DESs como medio de reacción y en ausencia de aditivos. Entre los DES evaluados, el DES ChCl: etilenglicol resultó ser el mejor medio de reacción para sintetizar los intermediarios, que dieron lugar al atenolol en un segundo paso, obteniéndolos en rendimientos cuantitativos.

Además, se exploró la recuperación y reutilización del DES para el primer paso, demostrando una pérdida mínima de actividad después de varios ciclos. Este enfoque contribuye a la sostenibilidad del proceso y destaca la viabilidad de utilizar el DES de manera repetida, reduciendo así el impacto ambiental y los costos asociados con la gestión de residuos.

Con estos datos y considerando que la etapa final de la producción industrial del Atenolol API implica una reacción de apertura de anillo o una reacción de sustitución nucleofílica bimolecular, se visualizó la viabilidad de realizar una síntesis "one-pot" en dos etapas de atenolol en ChCl:EG DES, obteniendo el atenolol correspondiente en un rendimiento global del 95%.

Además, se demostró con éxito la escalabilidad del proceso a la producción a escala de gramos, destacando su potencial para aplicaciones industriales. Conjuntamente, se exploró la recuperación y reutilización del DES para el primer paso, mostrando una pérdida mínima de actividad después de varios ciclos.

Para comprender la estructura del intermediario clave del proceso de síntesis del atenolol, se llevó a cabo una investigación a fondo con técnicas avanzadas de RMN mono- y bidimensionales. Basándose en los datos obtenidos, se propuso un mecanismo que sugiere la participación de enlaces de hidrógeno entre los componentes del DES y los materiales de partida, facilitando la apertura del anillo de epóxido y la formación consecutiva de atenolol. El papel crucial de ambos componentes (aceptor y donante de enlace de hidrógeno) del DES es crucial para el éxito de la reacción. Este enfoque novedoso resalta la importancia de la interacción de los componentes del disolvente eutéctico profundo en la reacción, subrayando cómo tanto el componente aceptor como el donante de enlace de hidrógeno desempeñan un papel fundamental en el proceso. La comprensión detallada del mecanismo proporciona información valiosa para optimizar y mejorar aún más la eficiencia de la síntesis de atenolol, teniendo en cuenta la importancia de la sostenibilidad y la reducción de residuos en el diseño de procesos químicos.

Finalmente, la evaluación de "sostenibilidad" mediante el First Pass CHEM21 Metrics Toolkit destacó la mayor economía de átomos, eficiencia de masa reactiva e intensidad total de masa del proceso de síntesis basado en DES en comparación con los métodos existentes. Además, se realizó una evaluación cualitativa utilizando la clasificación en categorías de banderas. Esta evaluación de la sostenibilidad ecológica de nuestro enfoque, en comparación con otros existentes, resalta la sostenibilidad del método desarrollado, enfatizando su sostenibilidad frente a las alternativas. Esta consideración incluye no solo la eficiencia y la seguridad intrínseca de los materiales utilizados, sino también la eficiencia energética del mismo proceso.

En resumen, el capítulo propone una novedosa síntesis "one-pot" en dos etapas del Atenolol, utilizando un Disolvente Eutéctico (DES). Tras optimizar el proceso, se identificó al DES ChCl: etilenglicol como el medio de reacción más eficaz. La viabilidad de esta síntesis en ChCl: etilenglicol DES para la producción de Atenolol se confirmó con un rendimiento destacado del 95%. Se resaltó la escalabilidad del proceso y la eficaz recuperación del DES. La evaluación de sostenibilidad subrayó la eficiencia del método en comparación con los enfoques convencionales, ofreciendo así una alternativa prometedora y respetuosa con el medio ambiente.

Finalmente, el capítulo V tiene como objetivo investigar de manera integral el uso de Disolventes Eutécticos (DES) para mejorar la solubilidad de fármacos, comprender las interacciones moleculares involucradas y evaluar el perfil de liberación de medicamentos disueltos en estos solventes.

Mejorar la permeabilidad y biodisponibilidad de los medicamentos es crucial para el éxito de la fabricación y desarrollo de fármacos. La solubilidad, una característica fundamental, es una consideración clave en las ciencias farmacéuticas y en la industria, ya que influye directamente en cómo se comporta un fármaco en el cuerpo. Cuando los medicamentos tienen una baja solubilidad en agua, su eficacia puede verse significativamente comprometida.

La capacidad de un Ingrediente Farmacéutico Activo para disolverse en un solvente específico es esencial para su reactividad, estabilidad y biodisponibilidad. Si el fármaco no puede disolverse adecuadamente en el entorno acuoso del cuerpo, sus efectos terapéuticos pueden estar limitados.

Dada la amplia utilización de solventes en la formulación de medicamentos, no solo es importante centrarse en su eficacia para disolver los compuestos deseados, sino también en su impacto ambiental. Los aspectos ambientales y de seguridad para la salud de los solventes se han convertido en consideraciones significativas en el desarrollo de medicamentos.

Para abordar estos desafíos, hay una creciente demanda de nuevos solventes o medios que puedan mejorar la solubilidad de los medicamentos manteniendo un compromiso con los estándares de seguridad ambiental y de salud.

En este contexto los disolventes eutécticos han surgido como una solución prometedora en este contexto. Estos solventes han atraído un interés sustancial como vehículos alternativos para la formulación de productos farmacéuticos. Su adopción se percibe como un enfoque estratégico para superar los problemas de solubilidad al tiempo que se cumplen los requisitos de seguridad ambiental y de salud en el desarrollo de medicamentos. Los DES ofrecen una solución potencial al delicado equilibrio entre la eficacia y seguridad de los fármacos, convirtiéndolos en un área de exploración destacada en la industria farmacéutica.

Los resultados obtenidos de nuestros estudios destacan el potencial de los DES para aumentar el perfil de solubilidad de fármacos insolubles en agua, centrándose específicamente en la mesalazina y la dapsona. A la luz del Sistema de Clasificación Biofarmacéutica (BCS, por sus siglas en inglés), la dapsona se clasifica como clase IV, lo que refleja su limitada solubilidad en agua, así como su permeabilidad reducida, lo que conduce a un índice terapéutico bajo. Debido a estas características, la vía de administración preferida para este medicamento es

la transdérmica en lugar de la oral. La mesalazina se clasifica en el esquema de clasificación biofarmacéutica como un medicamento de clase IV, ya que tiene baja permeabilidad y baja solubilidad en agua.

En ambos casos considerados, se evaluó la posibilidad de formar Disolventes Eutécticos Terapeuticos (THEDESs, por sus siglas en inglés), donde el fármaco constituía un componente directo del DES, y el uso de un DES como solvente para mejorar la solubilización de los fármacos en cuestión. En ambas situaciones, la formación de DES que contenían directamente al fármaco no fue posible, a pesar de la combinación con varios aceptores de hidrógeno (HBA). Sin embargo, es interesante destacar que se observó un notable aumento de la solubilidad de la dapsona en el DES ChCl:glicol propilénico, alcanzando los 500 mg/mL, en comparación con solo 380 mg/L en agua. Esto sugiere que el uso de este DES como solvente puede mejorar significativamente la solubilidad del fármaco. De manera similar, la solubilidad de la mesalazina aumentó significativamente (35 mg/mL) en el DES ChCl:ácido láctico, en comparación con su solubilidad en agua. Esto indica que el uso de este DES como solvente puede llevar a una mejora considerable en la solubilidad de la mesalazina. En resumen, aunque la formación directa de DES que contienen los fármacos puede no ser factible, el uso de ciertos DES como disolventes ha demostrado ser prometedor para mejorar la solubilidad de ambos fármacos considerados. la mejora en la solubilidad observada en estos sistemas ofrece la posibilidad de incrementar la biodisponibilidad y eficiencia tanto de la mesalazina como de la dapsona, abordando así un desafío clave en su aplicación farmacéutica.

El uso de técnicas como la Calorimetría Diferencial de Barrido (DSC), Resonancia Magnética Nuclear (RMN) y Espectroscopía Infrarroja por Transformada de Fourier (FT-IR) proporciona información valiosa acerca de las interacciones moleculares entre los fármacos considerados y los componentes de los DES. Comprender a fondo estas interacciones es crucial para optimizar las formulaciones de DES adaptadas a las propiedades únicas de estos fármacos, garantizando su estabilidad

y eficacia. En ambos los contextos de estudio, se ha observado la manifestación de fuertes interacciones de hidrógeno entre los grupos funcionales de los fármacos y los componentes de los DES. Estas interacciones emergen como el principal catalizador de un perfil de solubilidad notablemente mejorado en los DES, en comparación con el agua utilizada como parámetro de control. Estas interacciones no solo influyen positivamente en la solubilidad de los fármacos en los DES, sino que también tienen el potencial de dar forma al panorama de sus propiedades terapéuticas.

La posibilidad de aprovechar estas interacciones específicas en el diseño de formulaciones de DES específicas abre nuevas perspectivas para la creación de sistemas farmacéuticos más eficientes, estables y efectivos. La optimización de estas formulaciones según las características únicas de los fármacos considerados puede fomentar una mejor biodisponibilidad y resultados terapéuticos más favorables, contribuyendo así al progreso en la investigación farmacéutica.

Finalmente, la evaluación del perfil de liberación de mesalazina y dapsona disueltas en DES aporta información significativa sobre las propiedades de liberación sostenida. Esto es fundamental para diseñar sistemas de administración de fármacos que controlen y extiendan la liberación de estos medicamentos. Las posibles mejoras en los resultados terapéuticos y la minimización de efectos secundarios son especialmente relevantes en el contexto de los efectos antiinflamatorios de la mesalazina y el uso de la dapsona en diversas condiciones dermatológicas.

Para evaluar la idoneidad del DES en la liberación de dapsona, se llevaron a cabo estudios in vitro en diferentes intervalos de tiempo (15, 30, 60, 90 y 120 minutos) y a un pH de 7.4 y 34 °C, con el objetivo de replicar las condiciones fisiológicas. Se utilizó espectrometría UV-Vis para determinar el perfil de liberación del fármaco, expresado como el porcentaje acumulativo del fármaco liberado en función del tiempo (=0.908, =293 nm). El análisis de los datos reveló una liberación completa y

sustancial del fármaco en las primeras dos horas, sin observarse liberación en las horas siguientes. Este patrón de liberación puede considerarse altamente ventajoso y beneficioso para lograr el efecto terapéutico deseado. Específicamente, la liberación completa del fármaco cargado en 2 horas es bastante satisfactoria.

En el caso de la mesalazina, se llevaron a cabo experimentos de liberación del fármaco a dos niveles de pH diferentes (6.8 y 7.4), imitando condiciones intestinales. Los resultados indicaron que el sistema DES liberó gradualmente la mesalazina a pH 6.8 durante 24 horas, mientras que a pH 7.4, se observó una mayor liberación de la sustancia en las primeras 6 horas. Por lo tanto, estos hallazgos sugieren el potencial para la administración oral y respaldan el uso del sistema DES como portador de la mesalazina en el intestino.

En resumen, los objetivos de investigación proporcionan un marco para explorar a fondo los DES como un medio para mejorar la solubilidad, comprender las interacciones moleculares y evaluar los perfiles de liberación de mesalazina y dapsona. Los resultados de estas investigaciones aportan conocimientos valiosos al campo más amplio de la investigación farmacéutica, ofreciendo soluciones potenciales para mejorar la efectividad y aplicación de estos importantes agentes terapéuticos.

Preface

Over the last years, the scientific community has been involved in the development of pioneering methodologies that align with the fundamental principles of Green Chemistry.

In this regard, given the significant environmental concerns associated with the use of volatile organic compounds (VOCs) as solvents in pharmaceutical production, the group's research has been specifically motivated to explore alternative solvents, pursuing green and sustainable synthetic approaches. Particularly, Deep Eutectic Solvents (DESs) have been selected as the solvent of choice to avoid the use of traditional hazardous organic solvents.

The formation of the amide bond stands as one of the most widely employed transformations in the pharmaceutical industry, playing a pivotal role in the synthesis of various bioactive compounds and peptides. In this regard, traditional organic solvents, pose environmental concerns due to their hazardous nature. Consequently, there is a pronounced motivation within the scientific community to explore alternative solvents that are environmentally friendly and sustainable.

Despite the widespread application of DESs across various disciplines since their discovery at the beginning of this century, their use in Organic Synthesis has remained relatively unexplored.

The use of DESs as reaction media holds the promise of enhancing the sustainability of conventional organic transformations, potentially uncovering innovative methodologies and reactions for compounds with substantial added value.

On the other side, enhancing the solubility of poorly water-soluble drugs is a key challenge in drug manufacturing and development. The limited water solubility hinders formulation, bioavailability and may lead to side effects. On this matter,

traditional organic solvents, often toxic with unpleasant odors, pose challenges for pharmaceutical use.

In order to address these issues, exploring new media is essential, balancing drug solubility with environmental and health safety. In this regard, DESs have recently emerged as promising alternatives for pharmaceutical formulations, showing increased interest. Their potential lies in improving drug solubility, bioavailability, and safety, addressing critical challenges in the pharmaceutical industry.

The present research is inspired by this central idea. On this basis, alternative and eco-friendly routes were developed for amide production, employing Deep Eutectic Solvents (DESs) as a reaction medium. Concurrently, the study aims to demonstrate the suitability of DESs for effectively solubilizing poorly-soluble drugs.

The results and conclusions of this research work will be presented following this structure:

I. ABBREVIATIONS LIST

II. GENERAL INTRODUCTION

III. GENERAL OBJECTIVES

IV. MATERIALS, INSTRUMENTS AND GENERAL METHODS

V. RESULTS

CHAPTER I: Reactive Deep Eutectic Solvents for EDC-mediated Amide Synthesis

CHAPTER II: Visible-Light-Mediated Amide Synthesis in Deep Eutectic Solvents

CHAPTER III: A Brønsted Acidic Deep Eutectic Solvent for *N*-Boc Deprotection

CHAPTER IV: Synthesis of Atenolol in DESs: A Sustainable Approach

General Introduction

GI.I SUSTAINABLE CHEMISTRY

In recent years, sustainability has emerged as a pivotal and progressively influential concept within the scientific community[1]. This trend has been driven by the growing recognition of the detrimental environmental impact associated with economic and social activities. The imperative to address these negative consequences has driven topics such as waste management, the reduction of greenhouse gas emissions, as well as tackling resource exhaustion and pollution to the forefront of global discourse, underscoring the urgent need for a paradigm shift[2,3]. This awareness has culminated in the formulation and widespread acceptance of the Sustainable Development Goals (SDGs), a comprehensive framework aimed at addressing multifaceted global challenges[4]. The SDGs provide a guideline for sustainable development, emphasizing environmental stewardship, social equity, and economic resilience.

The advent of Green Chemistry marks a significant milestone in the scientific panorama, representing a proactive response to the environmental challenges posed by traditional chemical practices. Introduced by P. T. Anastas and J. Warner as a new approach aiming to develop more environmentally friendly chemical processes and products, it involves reducing or eliminating the use of hazardous substances and improving the overall sustainability of chemical manufacturing[5]. This new trend is outlined in 12 principles that delineate the criteria for designing chemical procedures and methodologies to guarantee process sustainability (Figure 1)[6]. In the last few years, several researchers have actively contributed to the progression of this sustainability pursuit[7–9]. Consequently, designing chemical processes following these principles would imply a noteworthy progress toward this goal. Nonetheless, achieving full compliance with all principles simultaneously remains a challenging feat with our existing technology and knowledge.

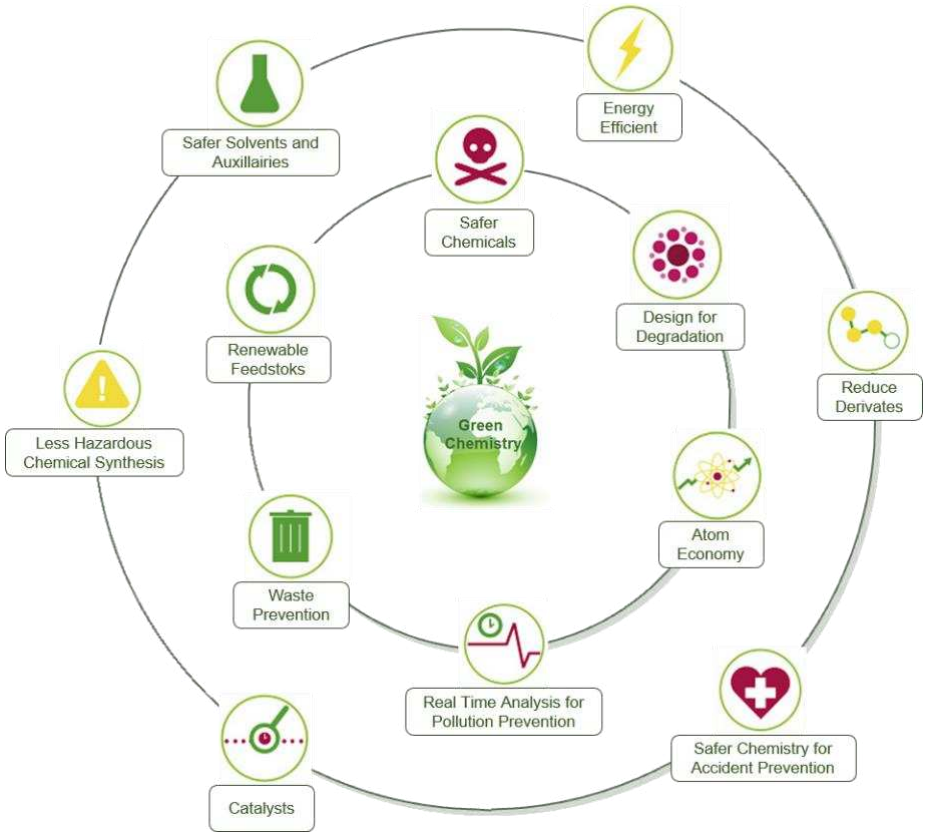

Figure 1. The 12 principles of Green Chemistry.

The implementation of green metrics in defining the greenness of chemical processes contributes to guide efforts towards more responsible chemical production. These metrics aim to carefully assess all key parameters involved in a chemical process, ensuring not only the optimization of individual steps but also a substantial enhancement in the overall methodology[10]. In this context, one of the pioneering metrics introduced in the early 90's was the *E*-factor[11], defined as the mass ratio of total waste substances (including all auxiliary substances, see equation below) to desired products.

$$Efactor = \frac{mass\ of\ total\ waste}{mass\ of\ the\ desired\ product}$$

More recently, the University of York has established the Metrics Toolkit as part of the CHEM21 consortium[12,13]. This toolkit serves the purpose of monitoring, measuring, comparing and evaluating the environmental impact of new reactions (Figure 2)[14]. It's crucial to emphasize that the toolkit does not intend to label something as *green,* rather provides information to assess whether a process is an improvement over the previous one and enables a direct comparison between several processes. Thus, the toolkit offers a method to clearly identify aspects that can be further improved, allowing for iterative enhancements in sustainability.

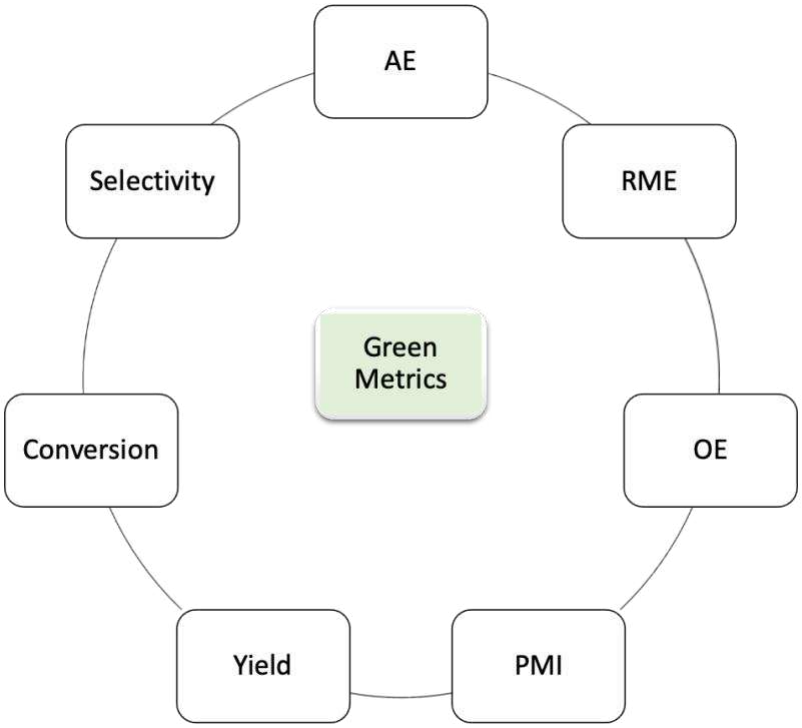

Figure 2. Green metrics for assessing the greenness of a process.

Atom Economy (AE) assesses the efficiency of a reaction by quantifying the atoms in the reagents introduced into the desired product[15,16]. It is obtained by dividing the molecular weight of the target product by the sum of the molecular weight of each reactant, assuming 100% yield and stoichiometric loading.

$$AE = \frac{MW\ product}{\Sigma MW\ reactants} \cdot 100$$

A comparable metric offering a more comprehensive insight into reagent utilization is Reaction Mass Efficiency (RME), as it is based on mass rather than molecular weight.

$$RME = \frac{mass\ of\ product}{\text{mass of}\ reactants} \cdot 100$$

Optimum efficiency (OE) involves a comparison of these two metrics, where AE represents the theoretical maximum efficiency, and RME provides the observed value.

$$OE = \frac{AE}{\text{RME}} \cdot 100$$

Process mass intensity (PMI) is defined as the total mass of reactants used to produce a specified mass of product, including solvents, work-up and purification steps, additives and catalysts[17]. It represents the most important metric for pharmaceutical companies in evaluating the greenness of a chemical process[18].

$$PMI = \frac{Total\ mass\ in\ the\ process}{\text{mass of the desired product}}$$

Yield, conversion, and selectivity were included, as they are widely used classical metrics[19].

In the last decades, it has become increasingly clear that fine chemistry, which encompasses sectors like pharmaceuticals, cosmetics, and agrochemicals, are faced with serious environmental concerns[20]. In particular, a pivotal aspect of sustainability involves the well-judged utilization of solvents[21]. In a classical chemical process, solvents are used extensively for dissolving reactants, work up

procedures and chromatographic purification, separating mixtures, cleaning reaction apparatus, and dispersing products for practical applications. In this regard, the conventional use of large amounts of solvents, particularly volatile organic compounds (VOCs), has long been associated with environmental and health concerns due to their typical characteristics as non-renewable petrochemicals, flammable substances, and potential hazards to both human health and the environment[22]. Their low boiling points and limited biodegradability contribute to their accumulation in the atmosphere, rivers, oceans, seas, and soil. Furthermore, solvents account for approximately 80-90% of the total mass of all chemicals involved in synthesizing an active pharmaceutical ingredient (API)[23,24]. In this perspective, numerous reports from leading pharmaceutical companies have detailed the guidelines and requirements for achieving greater sustainability and/or reducing the environmental and operational costs of conventional protocols. From these reports, it is evident that a key consideration to achieve this goal is the change in solvent selection[24–27]. With the onset of Green Chemistry, there is a concerted effort to explore and implement solvent alternatives that pose lesser harm to the environment, thereby aligning with the principles of sustainability and the circular economy[23].

GI.II ALTERNATIVE SOLVENTS

The exploration of eco-friendly options in solvent choices stands as a fundamental aspect of advancing sustainable practices. From the Green Chemistry perspective, the most appropriate solution would be to perform chemical processes under solvent-free conditions[28]. Solvent-free conditions align with green chemistry principles, significantly reducing hazardous waste generation and environmental pollution and offering advantages in reaction rates and purification simplicity[29]. However, achieving a completely solvent-free condition is challenging or may introduce additional difficulties in the process execution. Furthermore, the reaction medium plays a crucial role in the outcome of a reaction, such as enhanced homogeneity of reagents, better heat and mass transfer, stabilisation of key

transition intermediates and prevention of undesirable side-products. In consequence, an extensive array of solvents has been investigated as a viable alternative to the ideal condition of solvent-free reactions (Figure 3)[30,31]. An ideal and alternative solvent must be non-toxic, economic, recyclable, sustainable, easily available, having at the same time the properties that resemble those of the solvents to be replaced[32,33].

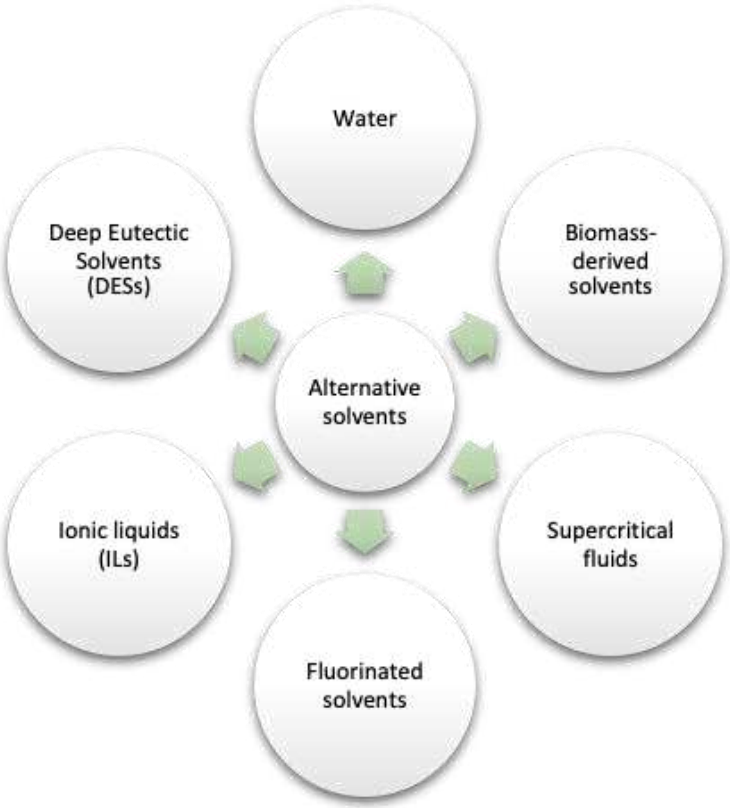

Figure 3. Alternatives solvents.

Water is the sustainable solvent of excellence for its cost-effectiveness, widespread availability, non-toxic and non-flammable nature, renewability and safety[34]. Its unique physicochemical properties influence organic reactions, serving as a moderator and thermal insulator, accelerating transformations, enhancing selectivity, and facilitating hydrogen bond exchange[35,36]. Despite these positive features, some drawbacks limit the use of water in classical synthetic

transformations. These drawbacks include low solvation ability for organics, incompatibility with water-sensitive compounds and highly basic and acidic reagents, as well as extremely high purification costs. As a solution, VOCs are used as a last possibility, balancing environmental benefits with practical considerations in specific synthetic applications.

In the pursuit of environmentally friendly solvents, biomass-derived options have proved to be promising, driven by rising oil prices and potential waste disposal cost reduction[37,38]. Produced from renewable resources, bio based solvents fulfil many of the criteria recommended by Gu and Jerome[38] for green solvents, including availability, renewability, low toxicity, biodegradability and reasonable prices. Thus, they are recognized as green solvents and their use is recommended by several selection guides[27]. Noteworthy for cost-effectiveness and safety, solvents like ethanol[39], γ-valerolactone[40], Cyrene™[41], limonene[42], or 2-methyltetrahydrofuran (2-MeTHF)[43] have been explored in several organic transformations. However, limitations such as flammability, limited polarity options, and small-scale production hinder their widespread use in organic synthesis.

Supercritical fluids (SCFs), particularly carbon dioxide (CO_2) at 31.1 °C and 73.8 bar, and water at 374 °C and 220 bar, have been considered as alternative solvents in both industry and academia[44]. SCFs are formed by simultaneous compression and heating above their critical point, exhibiting unique properties between the liquid and gas states[45]. One significant advantage is the complete removal of the solvent by degassing the system[46]. However, challenges such as high equipment costs, complex design, poor solubility of organic reagents, high energy consumption and incompatibility with certain reagents highlight the limitations of supercritical fluids.

Fluorinated solvents have gained recent attention for their noteworthy attributes, including low nucleophilicity, low toxicity, non-flammability, and non-polar characteristics[47,48]. However, their volatility poses a challenge as they can persist in the atmosphere. Additionally, their high production cost diminishes their appeal from

a sustainability perspective. Despite their advantageous properties, these drawbacks need to be addressed for fluorinated solvents to become more environmentally sustainable in practical applications.

Ionic liquids (ILs) have been proposed as highly suitable alternatives to VOCs owing to their advantageous properties in terms of sustainability[49,50]. ILs, constituted primarily of large organic cations like ammonium, phosphonium and imidazolium salts, paired with a non-nucleophilic inorganic anion, maintain a liquid state within a specific temperature range, typically below 100 °C[51]. Their appealing features encompass high thermal and chemical stability, negligible vapour pressure, low flammability, significant solvation ability, and customizable properties[49]. However, it is noteworthy that ILs have been identified as toxic and non-biodegradable, persisting in the environment, raising concerns regarding their alignment with Green Chemistry principles[52,53]. Additionally, their synthesis often involves multi-step procedures, leading to increased energy and time consumption, and frequently requires the utilization of VOCs.

Recently, a new class of solvents has emerged, sharing many advantages with ILs. Known as Deep Eutectic Solvents (DESs), these were introduced by Abbott[54] at the beginning of this century with the explicit purpose of overcoming the limitations associated with ILs.

GI.III DEEP EUTECTIC SOLVENTS

Deep eutectic solvents stand out as exemplary and versatile green solvents, with flexible designability. Introduced for the first time by Abbott[54], the term DES has been associated with a wide array of diverse definitions over the last years[55–57]. Due to the lack of a strict and clear definition of what a “deep eutectic solvent” is, this term is often abused.

A Deep Eutectic Solvent is a mixture of two or more pure compounds, typically comprising Lewis and Brønsted acids and bases, encompassing a diverse range of ionic and non-ionic species[58], in a determined ratio in which the mixture behaves as a pure compound in the phase transfer from mixture solid to mixture liquid. The adjective *deep* is intended to emphasize significant negative deviations that occur in a mixture compared to the expected ideal behaviour, with a eutectic point temperature significantly lower than that of its individual components (Figure 4).

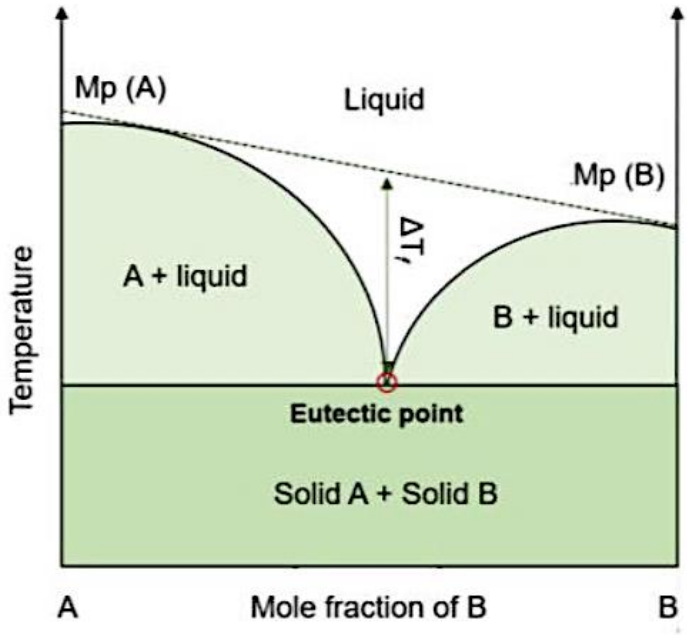

Figure 4. Phase diagram of a binary mixture.

This marked decrease in the melting point is attributed to the electrostatic interactions and strong hydrogen bond formations. These interactions hinder the precursors from establishing a well-defined crystalline structure, leading to mixtures with melting points generally in close proximity to room temperature[56].

3.1 Classification of DESs

In 2007, Abbott and his collaborators developed a classification system for DESs. They can be described by the general formula[59]:

$$Cat^{+}\ X^{-}\ zY$$

where X^- is a Lewis base, typically a halide anion, and Y is a Brønsted or Lewis acid. The adduct is formed between X^- and z units of Y. Currently, DESs are classified into five main categories, as reported in Figure 5.

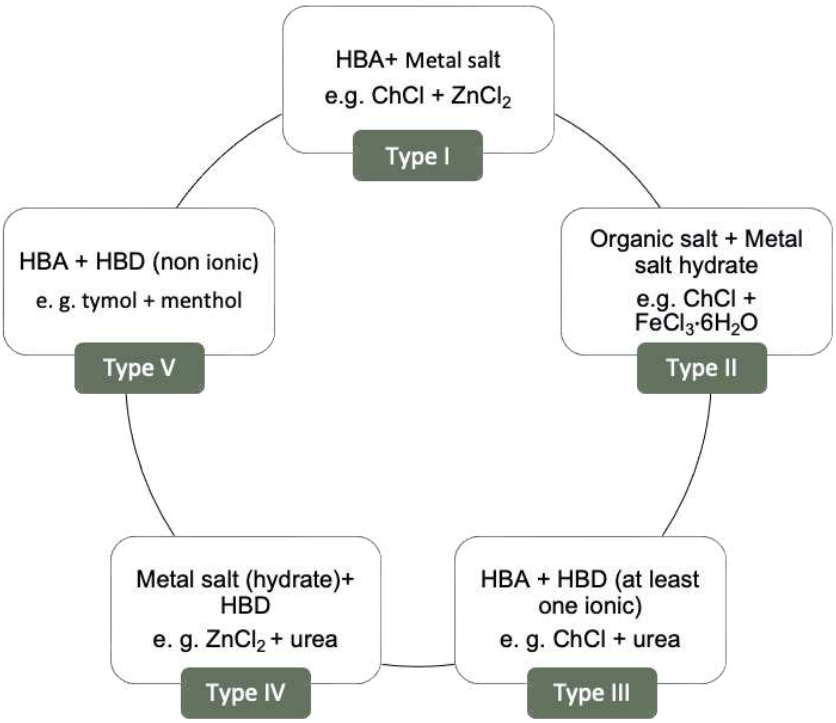

Figure 5. Classification of DESs depending on their composition.

Type I DESs are prepared from quaternary ammonium salt and metal halides such as $ZnCl_2$, $FeCl_2$, $CuCl_2$, $SnCl_2$. This type of DESs is generally more expensive and toxic compared to other DESs. This is because their preparation needs anhydrous metal halides. The analogous ones formed with hydrated metal halides (Type II) constitute a significant portion of DESs. These hydrated metal salts are more cost-effective and exhibit higher stability in the presence of air and moisture, resulting in a diverse range of mixtures with lower melting points. Moreover, metal salts can also provide eutectic mixtures when combined with different HBDs (Type IV).

DESs are readily prepared by simply mixing HBAs and HBDs components such as those illustrated in Figure 6[58]. The charge delocalization through hydrogen bonding contributes to reducing the lattice energy of the system and, consequently, the melting point of the mixture compared to the individual components ones.

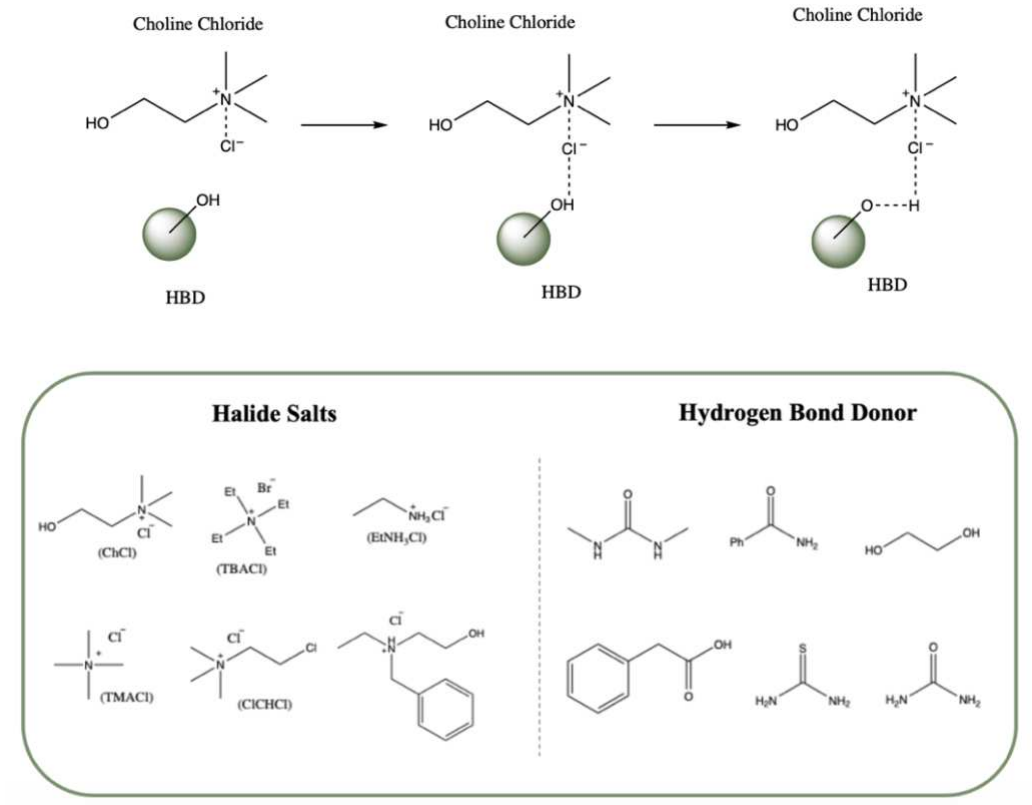

Figure 6. Structures of some halide salts and hydrogen bond donors used in the formation of DES.

Type III and V DESs are extensively studied and widely investigated due to their significant potential in terms of sustainability. Type III DESs must contain, at a minimum, one ionic compound. This category allows for the incorporation of ionic species in the mixture, expanding the range of possible interactions and properties. They are usually based on hydrogen bond acceptors generally represented by a quaternary ammonium salt, whereas the most common hydrogen bond donors are carboxylic acids, alcohols, amides. Choline chloride has been extensively adopted as HBA since it is relatively cheap, non-toxic, and biodegradable, as it is approved

as a natural additive food for several animal species[60]. The presence of an ionic compound contributes to the unique characteristics and properties of these DESs. Type V DESs are a relatively new class mixture of non-ionic molecular HBA and HBD. This category relies solely on non-ionic components, which can include a variety of organic and inorganic substances. The exclusion of ionic species simplifies the composition but still offers a wide range of possibilities for tailoring properties based on the non-ionic constituents used. Both Type III and V DESs provide alternatives that align with the principles of being non-toxic, biodegradable, safe, renewable, economical, and readily available. Their versatility and environmentally friendly characteristics make them promising candidates for various applications in industry and research. In this regard, a multitude of HBDs and HBAs have been extensively employed in the formulation of DESs. This includes natural products involved in biological processes, such as amino acids and carbohydrates, along with some active pharmaceutical ingredients (APIs). In such instances, DESs are referred to as Natural Deep Eutectic Solvents (NADESs)[62,63] and Therapeutic Deep Eutectic Solvents (THEDESs)[64,65], respectively.

Despite some studies indicating low toxicities and high biodegradability, it's important to note that the overall environmental impact and safety of DESs depend on the specific starting materials used, and caution should be exercised in labelling them as universally green, non-toxic, or economical[54,66].

3.2 Preparation methods of DESs

Conventionally, the chemical synthesis of any compound requires one or more chemical reactions between two or more reactants, leading to the formation of a product(s). In contrast, the preparation of DESs deviates from this conventional approach as it involves the simple mixing of a HBA and a HBD[67]. Therefore, DESs are prepared rather than synthesized, as there is no technical involvement of chemical reactions in their formation. DESs are prepared by 100% atom economy route and all other steps such as purification and waste disposal are not required.

A number of preparation methods have been employed to obtain DESs with low cost and high purity. In this regard, heating and stirring (HS) or grinding represent the most common employed methods. The heating and stirring method involves mixing components and heating under stirring until a homogeneous liquid is formed. Various studies have employed different temperatures, ranging from as low as room temperature to as high as 130 °C for a period of a few hours, depending on the melting point, boiling point and stability of the components. Care must be taken to avoid high temperatures that could lead to DES degradation, especially when choline chloride and carboxylic acids are involved[68]. On the other hand, the grinding method includes mixing the HBA and HBD components and grinding them in mortar and pestle at room temperature until a clear liquid is obtained[69]. Both approaches are environmentally benign, generating no waste and maximizing atom economy.

Other available preparation methods include freeze-drying aqueous solutions[69] and rotary evaporation[70], microwave irradiation method[71] and ultrasound-assisted preparation[71,72].

3.3 Physicochemical properties of DESs

In recent years many efforts have been devoted to the physicochemical characterization of DESs, including melting point, density, viscosity, conductivity, and pH, among others[73–75].

3.3.1 Melting point

As previously mentioned, DESs result from the self-association of their components *via* hydrogen bonds, leading to a liquid phase with a lower freezing point compared to individual components. For instance, when ChCl and urea are combined in a 1:2 molar ratio, the melting point of the eutectic is 12°C, significantly lower than the melting points of ChCl and urea, which are 302°C and 133°C, respectively. The interactions between the halide anion and the HBD component, such as urea, is crucial for this freezing point depression. For ChCl-based DESs, the choice of HBDs, like carboxylic acids or sugar-derived polyols, influences the

formation of room temperature liquid DESs (Table 1). The nature of organic salts and the anion in choline-derived salts also impact melting points, showing a correlation with the hydrogen bond strength. Additionally, the organic salt/HBD molar ratio significantly affects DES melting temperatures; for instance, a 1:1 and 1:2 ratio of ChCl and urea results in melting points > 50°C and 12°C, respectively[74].

HBD		ChCl: HBD (molar ratio)	T*m/°C	T*f/°C
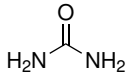	Urea	1:2	134	12
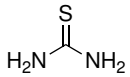	Thiourea	1:2	175	69
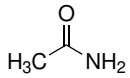	Acetamide	1:2	80	51
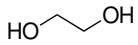	Ethylene glycol	1:2	-12.9	-66
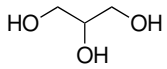	Glycerol	1:2	17.8	-40
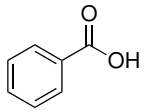	Benzoic acid	1:1	122	95
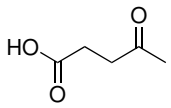	Levulinic acid	1:2	32	Liquid at RT
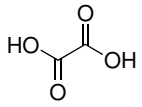	Oxalic acid	1:1	190	34

Table 1. Continuation

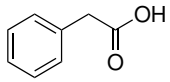	Phenylacetic acid	1:1	77	25

Table 1. Melting point (T*f) of the most common DESs. (T*m): melting point of pure HBD; RT= room temperature.

3.3.2 Density

Density is a crucial physical property for solvents and is typically measured using a specific gravity meter for DESs. Several factors contribute to the density values of DESs[76]. Specifically, the molecular organization and packing, along with the presence of holes and vacancies within the liquid DES, play a significant role. The Hole theory provides linkage between properties of DESs and available holes of approximate dimension and size of mobile species. DESs are assumed as a composition of holes. During the formation of DESs, when the HBD is added to HBA, the average size of holes changes, hence changing the density of the DES. For instance, when $ZnCl_2$ is mixed with urea, the average hole radius decreases, leading to a slight increase in DES density, compared to neat urea[77]. Other influential parameters affecting DES densities include the organic salt/HBD molar ratio, the alkyl chain length of the cation [78] and temperature[76].

3.3.3 Viscosity

Most DESs are characterized as viscous liquids (>100 cP) at room temperature, exhibiting significantly higher viscosity compared to water under similar conditions[79]. The elevated viscosity of DESs is often ascribed to the formation of an extensive hydrogen bond network among their components, leading to reduced mobility of free species within the DES. Viscosities of DESs are influenced by various factors, including the chemical nature of HBAs and HBDs, temperature, molar mass, water content, and the molar ratio. Given their potential applications as environmentally friendly solvents, there is a strong interest in developing DESs with lower viscosities.

Thus, in green technology, designing DESs with low viscosities can be achieved by considering factors such as the small size of HBD and cation, guided by the principles outlined in the Hole theory.

3.3.4 Conductivity

Owing to their relatively high viscosities, DESs exhibit poor conductivity at room temperature[80]. Therefore, the conductivity of DESs is influenced by the same factors that affect viscosity, including molar ratio of HBDs/HBAs, alkyl chain length of cation, and temperature. DES conductivities are primarily temperature-dependent; thus, an increase in temperature leads to an improvement in conductivity, attributed to a decrease in the viscosity of the DES.

3.3.5 Acidity or basicity

The assessment of the acidity and basicity of deep eutectic solvents stands as pivotal physical attributes, rendering them versatile in various industrial sectors. These characteristics, governed by the acidity of the hydrogen bond donor (HBD) and hydrogen bond acceptor (HBA) components, dictate the pH equilibrium within the DES system. In the case of acidic Deep Eutectic Solvents (ADESs), the acidity align with the intrinsic acidity of the HBD component. For BADESs (Brønsted Acidic Deep Eutectic Solvents), the Brønsted acidity strength can be accomplished through pH measurement or by assessing the Hammett acidity function[79]. Furthermore, the evaluation of Lewis acidity in Lewis acidic DESs (LADES) can be achieved through Fourier-transform infrared (FT-IR) investigation. On this matter, some DESs exhibit highly acidic characteristics with a negative pH, such as choline chloride: citric acid (1:1) and choline chloride: maleic acid (1:1). Conversely, there are basic DESs, including choline chloride: urea (1:2), choline chloride: triethanolamine (1:2), and potassium carbonate: glycerol (1:5). These differences in acidity and basicity highlight the distinct pH properties of DESs, enabling their application across a range of industrial contexts[80].

3.3.6 Hydrophilicity and hydrophobicity of DESs

Hydrophilic DESs, limited by their polarity, find constrained applicability in non-polar contexts. Van Osch *et al.* pioneered hydrophobic DES research[81], introducing compositions like decanoic acid and a quaternary ammonium salt paired with fatty acids. Hydrophobic DESs, crucial for solute extraction in biphasic systems, have gained particular interest in recent years. DES hydrophobicity is influenced by the chemical nature of HBAs and HBDs. Long alkyl chains in HBAs impart hydrophobicity, leading to low densities and moderate viscosity at room temperature. Anion size and temperature changes further influence the physical properties of hydrophobic DESs. When comparing DESs with conventional solvents, the role of polarity becomes crucial[81]. Hydrophilic DESs, due to their polar nature, exhibit a strong affinity for water molecules, making them less suitable for non-polar environments. Conversely, the hydrophobic DESs, with their reduced polarity facilitated by long alkyl chains, are better suited for solute extraction in non-polar contexts compared to their hydrophilic counterparts. This highlights the crucial interplay between polarity and hydrophobicity in defining the suitability of DESs for various applications, offering distinct advantages over conventional solvents in specific scenarios.

3.4 Application fields of DESs

Over the past two decades, DESs have received great interest in a wide variety of fields (Figure 7). Their unique properties, tunable through careful selection of the components, have opened up new possibilities in several processes, leading to a significant surge in research interest and widespread adoption across various sectors of chemistry.

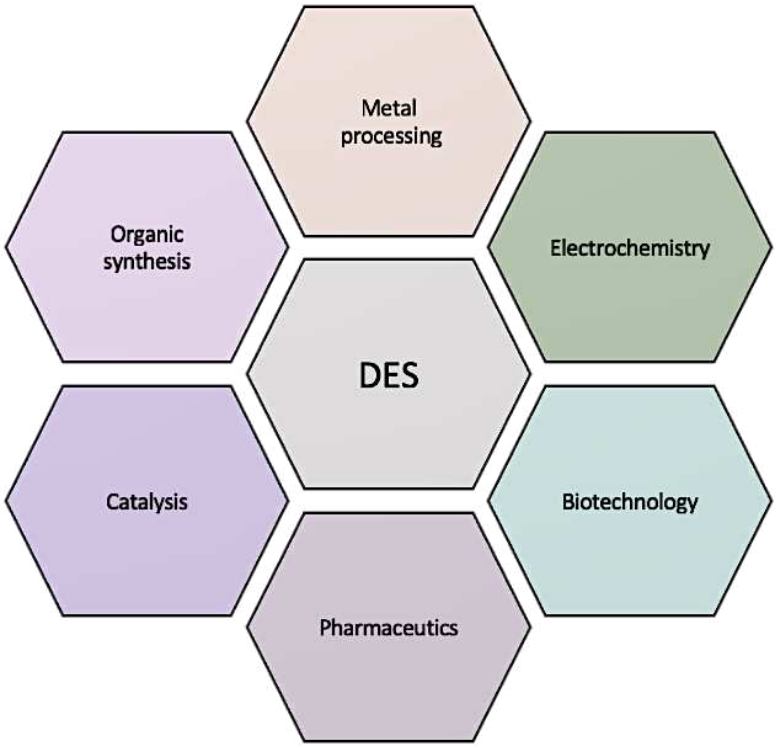

Figure 7. Application fields of DESs.

On this matter, DESs have attracted early interest for metallurgical applications due to their high solubility and conductivity for metals and metal salts[82]. DESs emerged as promising candidates for metal extraction, recycling, ore refining, electroplating[83] and electrodeposition[84,85], providing advantages such as enhanced metal salt solubility, absence of water, and superior conductivity compared to non-aqueous solvents.

Moreover, several features of DESs have drawn attention to their analytical applications[86], emerging as a sustainable alternative in extraction procedures[87]. In this sense, the tunability of DES components has given rise to hydrophobic DESs, offering potential solutions for extracting different compounds from water due to their immiscibility. Furthermore, lipophilic DESs have been used as novel green absorbents for capturing hydrophilic VOCs from the environment[88]. This capability offers opportunities to improve environmental and industrial processes, highlighting

DESs as promising tools for sustainability and efficiency in diverse applications. On this matter, the ionic nature of some DESs enables efficient capture of carbon dioxide (CO_2)[89,90] and sulfur dioxide (SO_2)[91], with the potential to transform these gases into value-added compounds.

On the other hand, DESs play a dual role as catalysts and co-solvents in biodiesel production. Owing to their high polarity, DESs have also been used to facilitate the purification and separation of impurities (mono-glyceride, di-glyceride, tri-glyceride, and residual catalyst) from the produced biodiesel[92].

Additionally, DESs have been extensively explored as potential drug delivery systems on account of their unique properties such as tunability and chemical and thermal stability[93–95]. On this matter, DESs contribute to solubilizing water-insoluble drugs[96,97], enabling transdermal drug delivery[98,99], synthesizing inorganic nanoparticles[100], and designing polymeric and self-assembled drug carriers[101]. The versatility of DESs in addressing various challenges makes them promising candidates for advancing drug delivery technologies, offering solutions for enhancing drug solubility, designing innovative carriers, and enabling novel routes of administration in the pharmaceutical field.

An emerging research frontier for DESs is their application in biotransformations. On this matter, DESs exhibit key traits, acting as versatile liquids that can support various substrates, enzymes, and bioactive solutes[102]. These characteristics pose DESs as potential candidates to facilitate novel biocatalytic pathways. They enhance the activity and stability of enzymes like lipase, protease, and cellulase, showcasing their potential to advance bioconversion processes and contribute to innovations in biotechnology and healthcare[103].

Focusing on the field of catalysis, other chemical transformations such as polymerisation[104] and more traditional organic transformations have been reproduced by using DES as reaction media.

3.5 Organic synthesis in DESs

In recent years, DESs have gained significant attention as green and sustainable media, aiming to enhance the efficiency of organic transformations[105–107]. These solvents offer a more ecologically friendly option, mitigating the environmental impact associated with VOCs. On this matter, DESs have been used not only as a reaction medium but also as a catalytic active species for some reactions and, in some cases, as part of the starting materials[105]. Nevertheless, there are also some challenges associated with using DESs as reaction medium. The high viscosity of some DESs can sometimes limit mass transfer and diffusion of reactants and products, affecting the reaction kinetics. Additionally, their high sensitivity to water and other impurities can alter their stability and catalytic activity.

3.5.1 DESs as catalysts

DESs have demonstrated outstanding catalytic activity in various chemical reactions[108]. These eutectic mixtures have been found to be effective as solvents or as catalysts, both in organic synthesis and catalytic reactions, including esterification, amidation, condensation, cross-coupling, cycloaddition and oxidation, highlighting their reuse in both homogeneous and heterogeneous catalytic reactions.

In Types I, II and IV DESs, the presence of metal salts such as $ZnCl_2$ gives DES a Lewis acidic character, expanding the use of this kind of DES not only as a reaction medium but also as a catalyst. On this matter, the DES containing ChCl and $ZnCl_2$ is widespreadly used as Lewis acid catalyst as well as a reaction medium for several reactions. The first report using this system as a solvent and as a catalyst was in some Diels–Alder reactions[109]. The Lewis acidity of the mixture accelerated the reaction. Interestingly, the products were separated from the DESs by simply decantation allowing the recyclability of the mixture up to five consecutive times.

ChCl-$ZnCl_2$ was also investigated for its performance as catalyst and solvent in the synthesis of primary amides from aldehydes and nitriles by Patil et al.[110] (Scheme 1). Nitriles bearing ortho-para electron-donating groups gave excellent results in DES-catalyzed reactions, while ortho-substituted ones needed long reaction times due to steric hindrance. Strong electron-withdrawing groups prolonged reactions. Important feature of the DES, was the possibility of recycling for three times, promoting green, atom-efficient synthesis by reducing waste and toxicity.

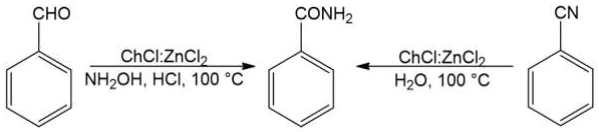

Scheme 1. Synthesis of primary amides from aldehydes and nitriles in DES.

In another study, ChCl:$ZnCl_2$ (1:3)[111] was used as both catalyst and reaction medium for the high regio- and chemoselectivity Friedel-Crafts acylation of anisole, using acid anhydrides under microwave irradiation. All acid anhydrides were found to provide ketone products having a majority of *p*-isomer (Scheme 2).

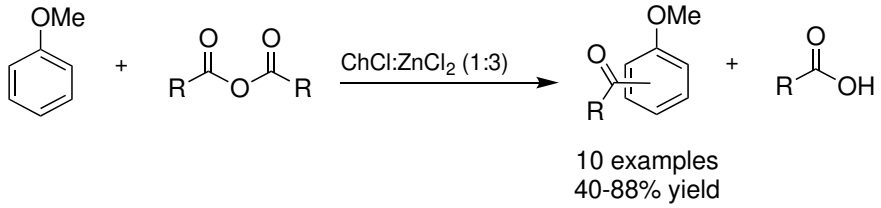

Scheme 2. Friedel-Crafts acylation of anisole with respect to acid anhydride catalyzed by ChCl-$ZnCl_2$ (1:3).

Also the synthesis of indoles via Fisher annulation was successfully performed in ChCl:$ZnCl_2$ (1:2) DES. This transformation gave rise to a wide range of indoles which were readily purified by sublimation as the vapour pressure of the DESs is negligible[112].

Some other standard transformations have been performed in ChCl:$ZnCl_2$ (1:2) DES, such as esterification[113], Friedel-Craft alkylation[114], Mannich reaction[115], O-acetylation[116], among others[108].

Also ChCl-$SnCl_2$ (1:2 molar ratio) has been explored as Lewis catalyst for chemoselective ring opening of epoxides with aromatic amines, thiols, alcohols, azide and cyanide, yielding the corresponding products, using just a 40 mol% of the mixture (Scheme 3). The system could be reused, maintaining the catalytic activity[117].

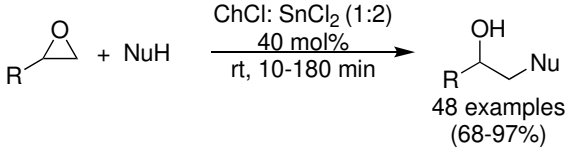

Scheme 3. Ring opening of epoxides in DES.

Non-metal containing metal DES (type III and V), can act as organocatalysts since it is possible to modulate their acidic/basic properties. On this matter, *p*-toluenesulfonic acid-based deep eutectic solvent, composed of *p*-toluenesulfonic acid and choline chloride (1:3), was found to be an efficient transesterification catalyst for biodiesel production.[118] The same DES in 1:1 molar ratio was used as Brønsted acid type DES in the one-pot synthesis of 2H-indazolo[2,1-b] phthalazine-trione derivatives.[119]

On the other hand, ChCl:urea (1:2) has been described as a basic catalyst for several organic transformations, such as Perkins reaction[120], Knoevenagel condensation,[121] or Paul-Knorr synthesis[122]. It showed to play a significant role in the activation of the starting materials for the synthesis of several pyran derivatives (Scheme 4)[123].

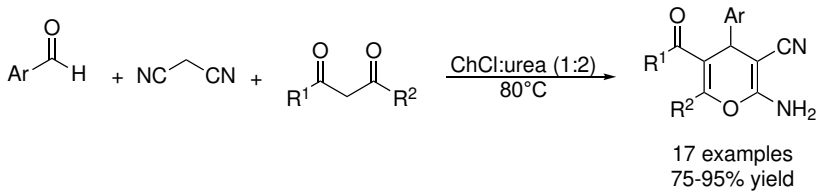

Scheme 4. Synthesis of pyran derivatives in basic catalyst DES.

3.5.2 DESs as reagents

Reactive Deep Eutectic Solvents (RDESs) represent an innovative class of solvents with unique properties that make them particularly versatile in various chemical processes. Unlike traditional solvents, these DESs are not only capable of serving as efficient reaction media but also actively participate in chemical reactions due to their inherent reactivity. On this matter, aldehydes heated in choline chloride: urea (1:2) DES reacted with the urea, producing the corresponding geminal diureas[124].

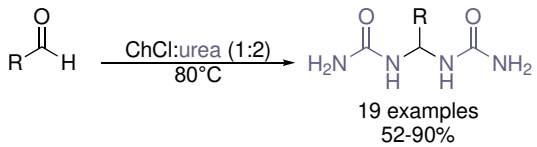

Scheme 5. Synthesis of gem-diureas in reactive DES.

Additionally, a range of dihydropyrimidinones has been synthesized through multicomponent reactions involving dimethylurea (DMU), aldehydes, and keto esters by using a DES comprised of the same DMU and tartaric acid (Scheme 6)[125].

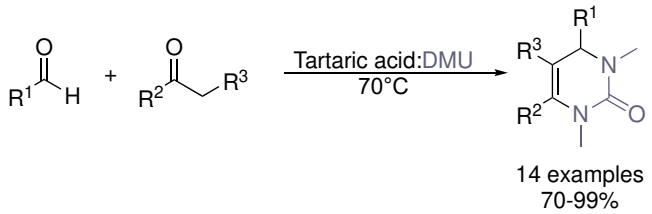

Scheme 6. Synthesis of dihydropyrimidinones in tartaric acid: DMU DES.

Furthermore, type III DES based on ChCl as HBA and *o*-phenylendiamine as HBD in 1:1 molar ratio was prepared and used as medium, and at the same time as a reagent, for the synthesis of benzimidazole derivatives (Scheme 7)[127].

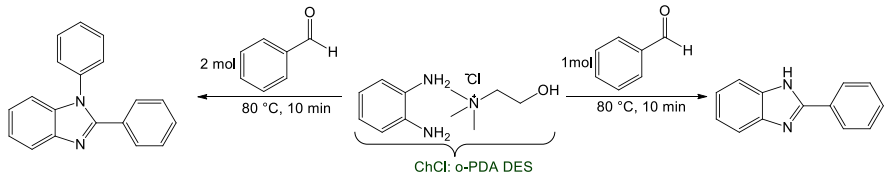

Scheme 7. Green synthesis of benzimidazole derivates in DES.

3.6 DESs for drug solubility enhancement

One of the main challenges in drug manufacturing and development is to increase the permeability and bioavailability by enhancement of the solubility of poorly water-soluble drugs[128]. The low water solubility of drugs largely limits their formulation and bioavailability and can also result in significant side effects[129,130]. However, most of the traditional organic solvents are not acceptable for pharmaceutical applications and present considerable constraints for manufacturing. Furthermore, besides being toxic, many of them have an unpleasant odour or taste. All these considerations require the exploration of new media, which would offer higher solubility of the drug, as well as ensure environmental and health safety. In this context, the use of DESs as alternative vehicles for the preparation of pharmaceutical formulations has recently gained deep interest[131,132]. Due to their high stabilization and solubilization power, DESs offer the ability to tune the solubility, permeation, and absorption of APIs by several folds when compared with water[133–136] (Table 2).

Table 2. Reported solubility enhancement of some APIs in DES solvents at room temperature.

API	Solubility in water ($mg.mL^{-1}$)	DES	Solubility in DES ($mg.mL^{-1}$)
Aspirin	7.03 ± 0.03	ChCl:1,2-propanediol (1:2)	202.00 ± 3.15
Acetaminophen	19.95 ± 0.12	ChCl:1,2-propanediol (1:2)	324.00 ± 4.23
Ibuprofen	0.07 ± 0.00	Camphor: menthol (1:1)	282.11 ± 6.67
		Tetrapropylammonium bromide:1,2- propanediol	383.40 ± 4.03
Lidocaine	3.63 ± 0.00	ChCl: glycolic acid: oxalic acid (1:1.7:0.3)	295.40 ± 6.80

Table 2. Continuation

Rutin	0.12 ± 0.05	ChCl: proline (3:1)	2.79 ± 0.10

Therefore, they represent an unconventional method to improve the dissolution and in vivo absorption of API with low aqueous solubility and/or low permeability. Furthermore, DESs could limit phenomena like polymorphism or degradation that represent serious problems encountered during drug formulation[137]. Promising results on the solubilization of poorly water-soluble drugs in DES have been reported, as summarized in Table 2. For instance, the NADES composed by menthol:camphor (1:1) proved to be a likely biocompatible solvent for ibuprofen, allowing to achieve a solubility of 40.4 ± 8.8 μg·mL^{-1} (vs. 9.81 ± 2.71 μg·mL^{-1} in water at the same temperature)[138]. Other non-steroidal anti-inflammatory drugs (NSAIDs), such as naproxen and ketoprofen, and analgesics like acetaminophen, are additional examples of drugs that have been investigated in this regard.[133]

3.6.1 Therapeutic deep eutectic solvents (THEDES)

Many APIs may act as either the HBDs or HBAs, and thus can be used as DES components. Since these DESs possess in their composition an API, and thereby exhibit therapeutic action, they are called therapeutic deep eutectic solvents (THEDES, or API-DES)[139]. Most of the THEDES reported up to date are prepared using the API as the HBD species, since most of them present amine, carboxylic acid and alcohol groups (Figure 8) in their structure.

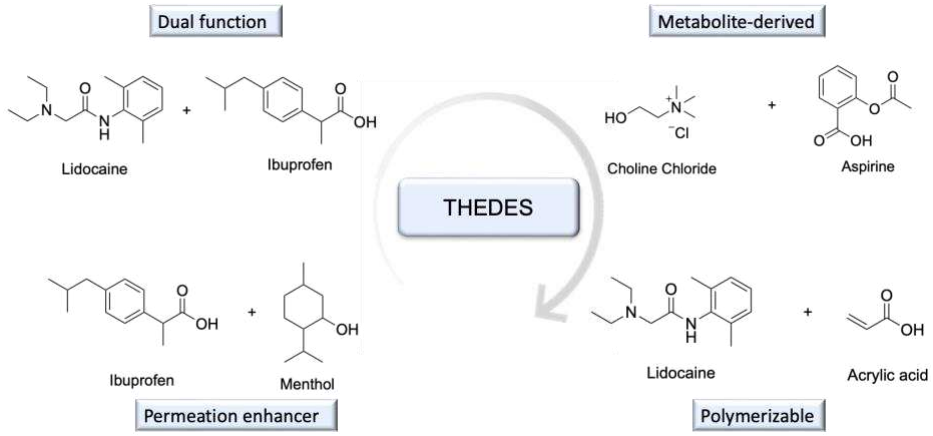

Figure 8. Strategies using different API as HBAs/HBDs with distinct biological properties and function.

Amongst THEDES, dual function is one of the most promising strategies since it allows the incorporation of two active ingredients in the same formulation, while avoiding the polymorphism of both APIs. For instance, a remarkable dual function API-DES based on ibuprofen and lidocaine was reported[140]. Additionally, THEDES can be prepared by combining the API with a wide variety of other compounds, including metabolites[140] or permeation enhancers[141,142]. API-DES can additionally present a polymerizable character when comprising APIs with polymerizable moieties, further allowing the adequate tuning of the delivery profile[143].

General Objectives

Based on the previously described backgrounds, the following general objectives were established for this doctoral thesis:

- To gain a deep insight into the dual role of DESs as solvents and reagents in common organic procedures: a comprehensive investigation into how DES acts not only as a solvent but also as a reagent/catalyst in organic processes has been conducted. Understanding both roles is crucial for exploiting the full potential of DES in assisting chemical reactions, and it may involve studying their interactions with reactants, products, and the overall reaction mechanisms;
- To design sustainable synthetic protocols using DESs: consideration has been given to the development of synthetic protocols utilizing DES, taking into account its dual role as both a solvent and a reagent. The emphasis is on designing procedures that are not only efficient but also sustainable. This may involve optimizing reaction conditions, exploring novel pathways enabled by DES reactivity, and minimizing the environmental impact associated with the synthesis. Amide synthesis has taken into account for this purpose, due to its importance in pharmaceutical industry;
- To assess the environmental impact of the protocols developed using the impact metrics and compare them with established methodologies: the evaluation of the environmental consequences of the synthetic protocols developed with DES has been a focal point. This involves using impact metrics to quantify the environmental footprint of the developed procedures. The comparison with established methodologies serves as a benchmark for understanding the potential environmental advantages or challenges posed by DES-based synthetic protocols.
- To comprehensively investigate the use of Deep Eutectic Solvents in enhancing drug solubility, understand the molecular interactions involved, and assess the release profile of drugs dissolved in these solvents. The findings from these investigations can contribute to the development of more effective and controlled drug delivery systems.

In summary, the doctoral thesis aims to explore the dual role of DES as solvents and reagents/catalyst in organic procedures, design sustainable synthetic protocols leveraging this dual functionality, and evaluate the environmental impact of these protocols using impact metrics and comparisons with established methodologies. Furthermore, the thesis aims to disclose the applicability of DESs for an efficient solubilization of poorly-soluble drugs. The primary goals is likely to contribute to the development of environmentally friendly and efficient methods in pharmaceutical realm.

Materials, Instruments and General Methods

E.1 Materials and Instruments

All starting materials were purchased from Acros (Fisher), Aldrich (Merck), Alfa Aesar (Fisher) and Fluorochem and used without further purification unless stated otherwise. Thin layer chromatography (TLC) was carried out on Schleicher&Schuell F1400/LS 254 plates coated with a 0.2 mm layer of silica gel; detection by UV254 light. P/UV254 silica gel with calcium sulfate supported on 20x20 cm glass plate was used for preparative thin layer chromatography.

Low-resolution mass spectra were performed using a spectrometer Agilent GC / MS-5973N, performing studies in the form of electron impact (EI) at 70 eV ionization source and helium as the mobile phase. Samples were introduced by injection through a gas chromatograph Hewlett-Packard HP-6890, equipped with a HP-5MS column 30 m length, 0.25 mm internal diameter and 0.25 μm film thickness (crosslinking 5% PH ME siloxane).

^{1}H NMR (300 or 400 MHz) spectra were recorded on Bruker AC-300 NMR spectrometers respectively in proton coupled mode. ^{13}C NMR (75.5 or 101 MHz) spectra were recorded on Bruker AC-300 NMR spectrometers respectively in proton decoupled mode at 20 °C; chemical shifts are given in δ (parts per million) and coupling constants (J) in Hertz. In both cases CDCl3, DMSO-d_6 and acetone were used as a solvent and, in some cases, durene as internal standard for ^{1}H.

Melting points of solid products were determined using a Reichert Thermovar apparatus, a widely used method known for its accuracy in measuring melting points in laboratory settings. The recorded temperatures, reported in degrees Celsius (°C), offer crucial insights into the thermal properties and stability of the substances under investigation. Additionally, the accuracy of these melting points serves as an indicator of the degree of purity of the compounds being examined.

FT-IR spectra were acquired using a JASCO 4100LE spectrophotometer equipped with a Pike Miracle ATR accessory. Solvents and reagents were utilized directly

from commercial sources without further purification. For solid samples, a specialized pellet was prepared by mixing the sample with potassium bromide (KBr) to form a homogeneous mixture. This pellet was then used for the FT-IR analysis to ensure consistent and reproducible results. In the case of liquid samples, a drop of the liquid was directly applied onto the ATR crystal surface of the spectrophotometer. This method allows for direct analysis of liquid samples without the need for additional preparation steps, ensuring efficient and accurate spectral acquisition.

HPLC analysis was performed to determine the ee % value (DIACEL Chiralcel OD-H, n-hexane [thin space (1/6-em)]:[thin space (1/6-em)]2-propanol = 90[thin space (1/6-em)]:[thin space (1/6-em)]10 (1 mL min−1), tr = 13.4 min (R) and tr = 18.1 min (S), 99% ee, S-enantiomer).

The DSC (Differential Scanning Calorimetry) experiments were conducted for different samples following a standardized procedure. Approximately 5–9 mg of the DESs solid drug compounds, or the drug dissolved in DESs were accurately weighed and placed into hermetically sealed sample pans. These sample pans were then subjected to thermal analysis using a DSC instrument (specifically, the DSC 200 PC Netzsch model). During the experiment, the temperature was ramped from 20 to 200 °C at a controlled rate of 5 °C per minute. This controlled heating rate ensured that all transitions, including melting points and glass transition temperatures (Tg), were accurately detected and recorded in the resulting thermograms.

Polarized Optical Microscopy (POM) analysis served as a valuable tool for qualitatively assessing the solubility of drugs in DESs. The method involves depositing a small droplet of DES containing incremental amounts of the drug onto a microscopic slide. The slide was then observed under a polarizing microscope at a magnification of 10x. Using the Nikon ECLIPSE LV100N polarizing microscope coupled with a Nikon DS-Fi2 camera, polarized light images were captured at room

temperature. In the absence of a solid crystalline structure, the polarized light image appeared uniformly black, indicating a lack of birefringence.

E.2 General methods

E.2.1 General procedure for the preparation of DESs

The different DESs were prepared by mixing a Hydrogen Bond Acceptor (HBA) and a Hydrogen Bond Donor (HBD) in a round-bottom flask under an inert atmosphere, typically nitrogen or argon, to prevent unwanted reactions. The specific molar ratio of HBA to HBD was carefully controlled according to the desired properties of the resulting DES. The resulting mixture was magnetically stirred at 60-80 °C, until a clear liquid was observed. The obtained DESs were directly utilized for subsequent experiments without undergoing any further purification steps. This approach minimizes potential contamination and preserves the integrity of the DES for use in various applications.

E.2.2 DES solubility measurement

To assess the solubility of drugs in the prepared DESs, a standardized procedure was followed. Excess amounts of the drug were added to approximately 1 mL of the eutectic mixtures. These mixtures were then continuously stirred for 24 hours at room temperature to ensure equilibrium conditions were reached. Following the saturation period, the samples underwent filtration using PTFE syringe filters with a 0.45 µm membrane. This step aimed to separate any macroscopic solid residues from the liquid phase containing the dissolved drug. Subsequently, the liquid phase was diluted in an appropriate solvent to ensure accurate UV spectrophotometric analysis. The choice of solvent depended on the compatibility with both the dissolved drug and the analytical technique. Common solvents such as methanol, ethanol, or water may be used based on the properties of the drug and the solvent system. The concentration of the drugs in the DESs was determined based on a calibration curve. This curve was established by dissolving pre-weighed amounts

of the drug in an appropriate solvent at various concentrations. By measuring the absorbance of these solutions and correlating it with the known concentrations, a calibration curve was generated. This curve allowed for the quantification of the drug concentration in the DESs, expressed as mass of the drug dissolved per milliliter of the solvent (mg/mL). Overall, this methodology provided a systematic approach to accurately determine the solubility of drugs in DESs, essential for optimizing drug delivery formulations and understanding their pharmaceutical behavior.

E.2.3 In vitro skin permeation of drugs

Permeation studies were conducted using Franz diffusion cells and excised rabbit skin obtained from a local slaughterhouse. The skin samples, sourced from New Zealand rabbits weighing between 2.9 and 3.1 kg, underwent a pre-treatment phase where they were equilibrated with a pH 7.4 buffer solution for 12 hours before mounting onto the Franz diffusion cells. Once mounted, the receptor compartment of the diffusion cells was filled with pH 7.4 buffer solution, serving as the diffusion medium. The cells were carefully maintained at a constant temperature of 37 ± 0.5 °C throughout the experiment to ensure consistent conditions. Before sample application, the skin was saturated with the dissolution medium for 1 hour to ensure uniformity. Drug-loaded Deep Eutectic Solvents (DESs) were then applied to the stratum corneum side of the skin, and the donor compartment was sealed with laboratory film (Parafilm®) to facilitate proper contact and prevent evaporation. Samples of the receiver solution were systematically withdrawn at predetermined time intervals (1, 2, 3, 4, 6, and 24 hours), and each withdrawal was replenished with an equivalent volume of fresh buffer to maintain sink conditions. The concentration of dapsone in the receiver solution samples was subsequently determined using UV–Vis spectrophotometry. All experimental procedures were meticulously conducted in triplicate (n = 3) to ensure the reliability and reproducibility of the results. This rigorously standardized protocol allowed for a comprehensive

evaluation of dapsone permeation through rabbit skin, providing invaluable insights into its potential as a transdermal delivery agent.

E.2.4 In vitro release studies of drugs

In vitro release studies of drugs from the Deep Eutectic Solvent (DES) were conducted over a 24-hour period at two pH values simulating intestinal conditions: pH 6.8 and pH 7.4. The drug-loaded DES formulation was placed in contact with cellulose acetate membranes immersed in the respective pH solutions at 37°C with agitation. At predefined time intervals (30 minutes, 45 minutes, 1 hour, 2 hours, 4 hours, 6 hours, and 24 hours), 2 mL samples were withdrawn from the solutions, and fresh medium was added to maintain a constant volume throughout the study. The concentration of the released drug was quantified using UV-Vis spectrophotometry at a specific wavelength relevant to the drug's maximum absorbance. This standardized procedure enabled the assessment of drug release kinetics from the DES formulation under simulated physiological conditions, providing crucial information for understanding its potential therapeutic efficacy and application in pharmaceutical formulations.

Results

CHAPTER I

Reactive Deep Eutectic Solvents for EDC-mediated Amide Synthesis

C1.1 Antecedents

In synthetic medicinal chemistry, the synthesis of amides stands as a crucial cornerstone, often dictating the efficacy and safety of drug candidates. Literature demonstrated that approximately 54% of the biologically tested compounds contain at least one amide bond. Additionally, more than 25% of known drugs consist of amide functionalities, as revealed by the analysis of the Comprehensive Medicinal Chemistry database (Figure 9)[144].

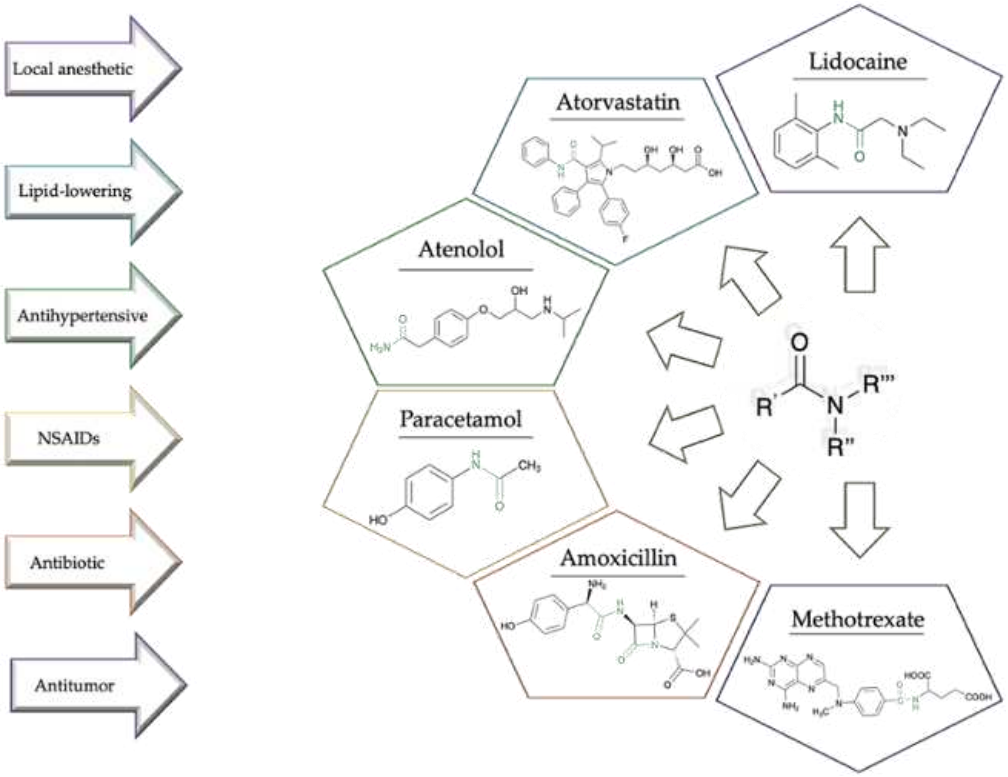

Figure 9. Examples of some amide-based drugs.

On this matter, amide synthesis was identified in the top 10 key research areas for the pharmaceutical industry by ACS Green Chemistry Institute Pharmaceutical Roundtable (ACS GCIPR)[145]. Notably, the existing processes for amide coupling reaction in manufacturing of API have a gap in reaction process efficiency and sustainability[146].

Traditional methods for amide formation frequently rely on stoichiometric reagents and harsh reaction conditions, leading to challenges in atom efficiency and undesirable by-products[147]. Moreover, the use of conventional solvents, characterized by toxicity and environmental concerns, increases further complexity to the synthetic process[148,149]. Thus, the green synthesis of amides assumes critical importance not only due to its intrinsic relevance but also as a transformative approach to address the limitations of conventional methods[145]. Among this framework, the search for eco-friendly alternatives to conventional solvents and reagents employed in amide synthesis becomes overriding.

In recent years, the panorama of amide synthesis has witnessed a profound transformation, driven by innovative green strategies that leverage novel reagents, catalytic systems, and reaction media[150]. On this matter, water, an abundant and benign solvent, has emerged as an attractive medium for amide bond formation under milder conditions, promoting atom efficiency and obviating the need for toxic additives[151,152]. A particularly promising opportunity involves the utilization of renewable and bio-derived solvents[153–155]. Finally, ionic liquids, with their unique solvent properties and potential for recycling, also offer a sustainable alternative to conventional solvents[156,157].

The emergence of DESs, characterized by their tunability and efficiency as both solvents/catalysts and reagents, presents an exciting frontier for a greener synthesis of amides. As mentioned in the general introduction, Reactive Deep Eutectic Solvents (RDESs) have emerged as a new promising class of media that combine the advantageous properties of DESs with the ability to actively participate in chemical reactions. The innovation of RDES builds upon these features, adding an extra dimension of functionality. RDES can be fine-tuned to exhibit different desired properties, such as acidity, basicity, or redox potential. This dual role as both solvent and reactant opens up opportunities for more sustainable, streamlined, and efficient synthetic routes, minimizing the use of external reagents and reducing waste generation.

On this matter, several research endeavours have emerged, delving into the multiple applications of DES in amide bond formation. Notably, Azizi and colleagues harnessed the synergistic capabilities of DES, particularly choline chloride: stannous chloride (ChCl:$SnCl_2$), which served both as a reaction medium and catalyst (Figure 10, A)[158]. Nevertheless, the approach was restricted to the formylation of aryl amines. Then, Salomone et al. approached a distinct route, by employing two different DES to perform the carbonylation of amines (Figure 10, B)[159]. Yet, they employed iodine surrogates to serve as source of carbonyl moieties. Parallel to these advances, Saberi's group highlighted the intrinsic potential of the uncomplicated DES ChCl: urea (Figure 10, C) in the direct condensation of amines and carboxylic acids using 2,4,6-trichloro-1,3,5-triazine (TCT) as a coupling reagent. However, the protocol involved the use of a base catalyst which enhanced the final amount of waste produced.

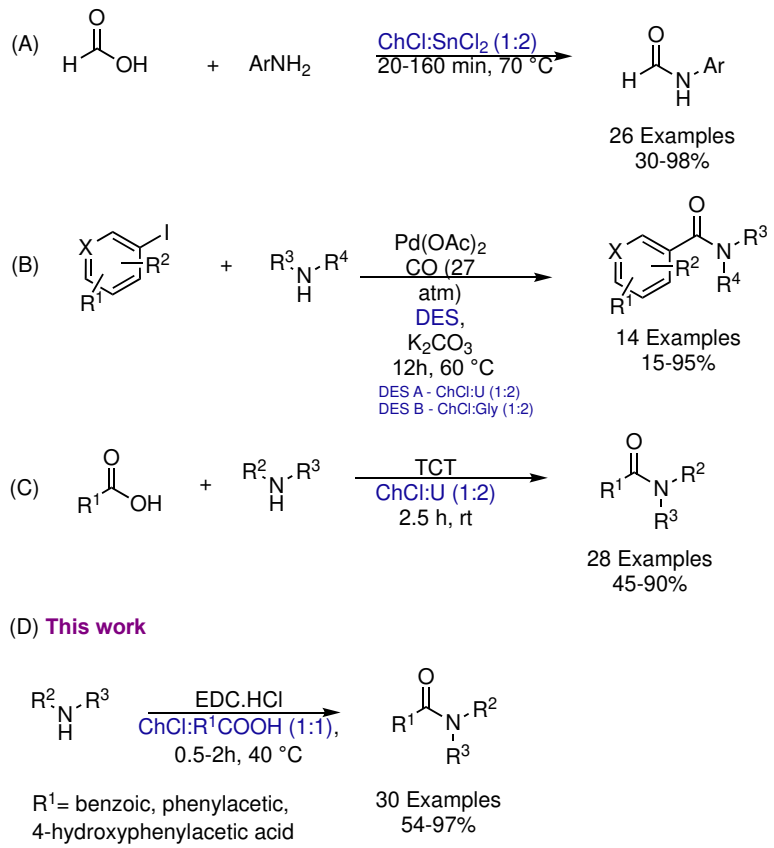

Figure 10. Synthesis of amides using DESs.

C1.2 Objectives

The industrial synthesis of amide bonds is crucial for pharmaceuticals, agrochemicals, and polymers. Current methods pose challenges with harsh conditions and environmental impact. Deep Eutectic Solvents, recognized for their unique properties, offer potential sustainability improvements in amide synthesis. Despite their green chemistry potential, DESs remain relatively unexplored in amide synthesis. Thus, as a part of our ongoing interest in the preparation of DES and investigation of their application in organic synthesis, the following objectives were established:

- To develop a green route for the *N*-amidation of amines with carboxylic acids, exploiting the unique properties of DESs as solvents. This aims to replace or improve upon existing methods that may have adverse environmental impacts;
- To design RDESs in order to contribute actively to amide synthesis: the focus is on creating DESs with tailored reactivity to actively participate in the amide synthesis process, potentially enhancing efficiency and selectivity;
- To evaluate the environmental footprint of the developed method in comparison to classical approaches.

These objectives collectively form a holistic approach towards improving the sustainability and efficiency of amide synthesis processes. By focusing on green routes, designing reactive solvents, and conducting a thorough environmental assessment, the research aims to contribute to the development of more environmentally friendly and efficient methods for industrial amide bond synthesis.

C1.3 Results and discussion

The investigation started with the preparation of three different RDESs. As the usual eutectic point is found about 1:1 molar ratio, we started preparing and analysing these mixtures. In particular, the quaternary ammonium salt choline chloride was used as the HBA, whereas benzoic acid (BA), phenylacetic acid (PA) and 4-hydroxyphenylacetic acid (HPA) were chosen as HBDs and reactants (Table

3). The selected HBA, ChCl, exhibits clear biocompatibility and benefits from its natural origin, which represents one of its significant advantages.

Hydrogen-bond Acceptor (HBA)		Hydrogen-bond Donors (HBD)		Molar ratio (HBA/HBD)
ChCl	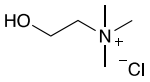	**BA**	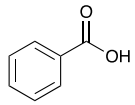	1:1
ChCl	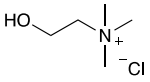	**PA**	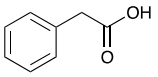	1:1
ChCl	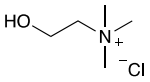	**HPA**	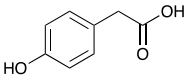	1:1

Table 3. Chemical structures of the HBA and HBDs used as RDESs components.

All RDESs were prepared by using a well-established protocol, by mixing the components in a defined molar ratio and heating them at 60-90 °C, under constant stirring in a round bottom flask, until a homogeneous colorless liquid phase was formed. A differential scanning calorimetry (DSC) analysis of the obtained mixtures as well as for the individual components was performed to prove the successful formation of the RDESs (Table 4).

HBA	HBDs	T^*_f (°C)	T^*_m HBD (°C)	Δ (°C)	Aspect
ChCl	**BA**	95	122.3	27.3	Viscous transparent liquid
ChCl	**PA**	25	76-77	51-52	Clear and transparent liquid
ChCl	**HPA**	19	147.6	129.6	Yellow viscous liquid

Table 4. Melting poiny (T*f) of the prepared RDESs with the corresponding melting point (Tm) of the pure HBDs.

All the RDESs prepared were used without the need of further purification.

In order to investigate the prepared DESs for their dual roles as solvents and reactants in the synthesis of amides, the *N*-amidation of aniline with phenylacetic acid, employed as a component of the RDES, was performed. To date, the preferred method in the pharmaceutical industry for large-scale amide synthesis is the activation of carboxylic acids using carbodiimides in combination with additives. At first, the model reaction was performed in the presence of *N,N*-diciclohexylcarbodiimide (DCC)/1-hydroxybenzotriazole (HOBt) as coupling reagent combination. After 60 minutes of magnetic stirring at room temperature, the desired amide was obtained in 61% yield (entry **1**, Table 5), indicating that the RDES could promote the amidation reaction. Encouraged by this promising outcome, the coupling reaction within the context of the RDES medium has been optimised. To this end, various combinations of coupling reagents across different temperature ranges have been systematically assessed, omitting the use of a basic catalyst. The progress of all reactions was monitored through thin layer chromatography (TLC) and gas chromatography/ mass spectrometry (GC/MS) analysis. As shown in Table 4, the RDES-mediated synthesis method was applicable to all coupling combinations considered. The greatest efficiency in terms of coupling performance and product purity was achieved by using 1-ethyl-3-(3-dimethylaminopropyl)carbodiimmide (EDC) as the coupling reagent (entry **6**, Table 5). This was justified by the fact that the EDC and the corresponding urea byproduct produced at the end of the reaction, are soluble in water, thus allowing an easier work up procedures. As a matter of fact, since the amide is insoluble in water, it precipitates and can be easily afforded by washing it with water, without any further purification or use of VOC solvents. In addition, from a green chemistry point of view, EDC is greener than other carbodiimides according to the GlaxoSmithKline reaction-selection guide, since the urea byproduct generated does not pose health and environmental hazard[160]. Finally, it is important to highlight that raising the temperature in EDC-mediated reactions did not affect the final product yield. On the other hand, when the reaction was performed in a conventional organic solvent like

dichloromethane, the desired amide was afforded in a good yield (entry **8**, Table 5). Nevertheless, the use of an organic base like diisopropilethylamine (DIPEA) was required and the product was recovered after chromatographic purification, thus revealing the strength of the RDES mediated procedure.

Table 5. *Optimization of Reaction Condition for N-acylation of Aniline with Benzoic Acid in RDES*

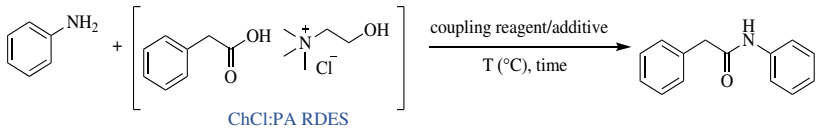

ChCl:PA RDES

Entry	Coupling Reagent	Additive	T (°C)	Time (min)	Yield (%)[d]
1[a]	DCC	HOBt	rt	60	61 %
2[a]	DCC	HOBt	40°C	60	76 %
3[a]	DIC	HOBt	40°C	60	68 %
4[b]	DIC	-	40°C	30	79 %
5[a]	EDC	HOBt	40°C	30	89 %
6[b]	**EDC**	**-**	**40 °C**	**60**	**93 %**
7[b]	EDC	-	70 °C	30	91 %
8[c]	EDC	-	rt	240	60 %[e]

[a] **Reaction conditions:** HOBt (1 equiv.) and the coupling reagent, (1 equiv.) were sequentially added in RDES (1 equiv.) and stirred for 10 min at the temperatures reported above. Successively, aniline, (1 equiv.) was added and stirred for the time reported above. [b] Reaction conditions: the coupling reagent, (1 equiv.) was added in RDES (1 equiv.) and stirred for 10 min at different temperatures. Successively, aniline, (1 equiv.) was added and stirred for the time reported above. [c] The reaction was performed in dichloromethane in the presence of DIPEA as the base. The amide product was purified by column chromatography. [d]% conversion calculated by GC/MS.

In order to investigate the scope and limitations of the optimized methodology the coupling reaction for a series of amines, by employing the same RDES system was assessed. First, phenylacetic-based RDES was subjected to the reaction with different aliphatic primary amines (entries **3c**, **3g-3i**, Table 6) affording the corresponding *N*-alkyl amides with good to excellent yields. The reaction of the same RDES with the secondary amine *N*-ethylbenzylamine lead to the corresponding compound in 78% yield, while the one with aniline afforded **3b** with

93% yield. When *p*-toluidine or *p*-anisidine were used as amine source, a slight reduction in yield was observed (entries **3d** and **3e**, Table 6), probably due to the reduced reactivity of the aromatic amine. Moreover, the presence of an additional functional group in amine framework did not interfere in the yield of the desired amide (entries **3g** and **3i**, Table 6). Besides the benzylamine, the reaction was also carried out with other substituted amines, confirming that the amine scope is wide. It was also find that halogen substituents such as chloride, are tolerated in the reaction (**3m**, Table 6). The reaction proceeded well with anilines bearing strong electron-withdrawing substituents like *p*-nitro or trifluoromethyl (**3n**, **3l**, Table 5). Tertiary amides could also be prepared, including examples derived from both cyclic and acyclic (**3f**, **3o** and **3p**, Table 6) secondary amines.

The additive HOBt is regularly employed in combination with EDC or other coupling reagents in order to reduce the risk of racemization in amide synthesis[161]. In particular, it acts as an activating agent for the carboxylic acid group, making it more reactive towards the amine. This activation reduces the time that the intermediates are exposed to potentially racemizing conditions, thus minimizing the chances of racemization occurring during the reaction. However, the inherent risks associated with HOBt have led to its regulation under the REACH (Registration, Evaluation, Authorization, and Restriction of Chemicals) framework[162]. This is due to its potential hazards to individuals for its capacity in causing skin and ocular irritation, as well as inhalation-related risks when not handled in accordance with established safety protocols. Furthermore, its release into the environment, can cause adverse ecological effects. When using enantiopure amines such as (R)- and (S)-1-phenylethan-1-amine the corresponding chiral amides were obtained (entries **3j** and **3k**, Table 6). Consequently, the rapidity of the conversion achieved through the developed protocol enabled to avoid the necessity of employing HOBt, enhancing the overall sustainability of the process.

Table 6. *Synthesis of amides in phenylacetic acid-based RDES*

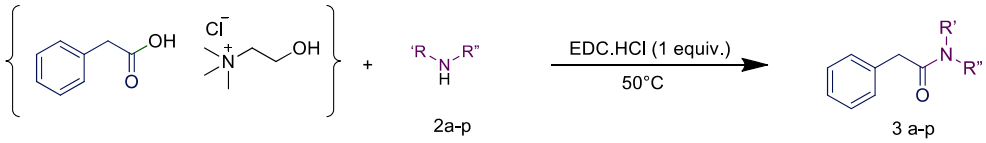

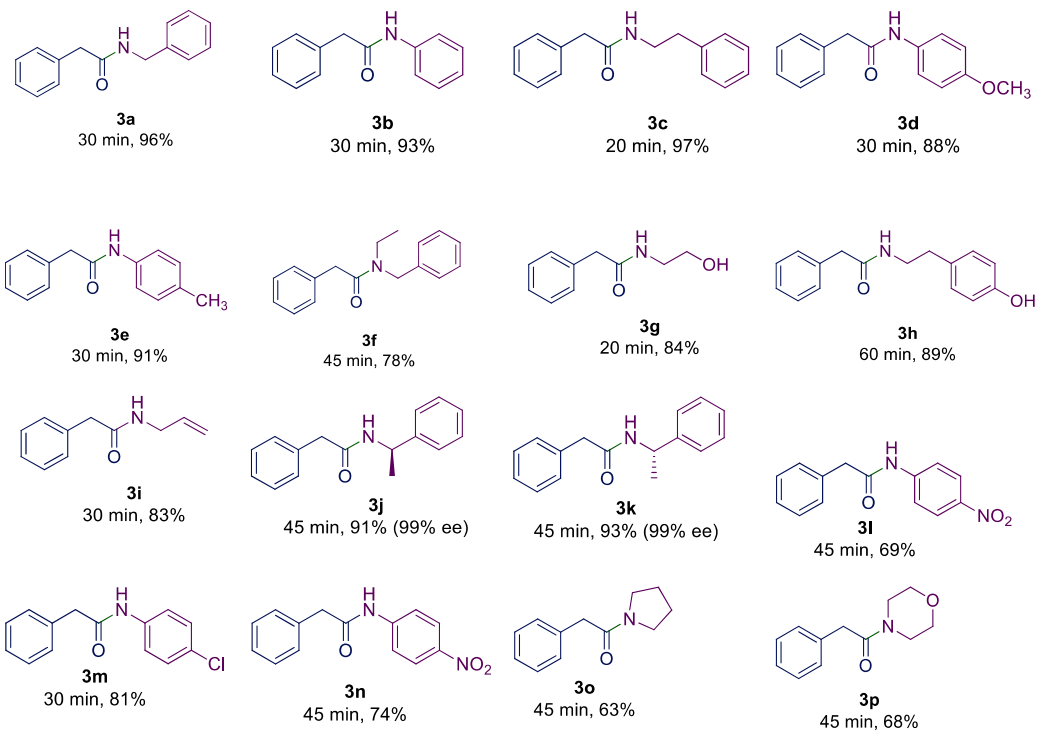

[a]Reaction conditions: the coupling reagent, (1 equiv.) was added in RDES (1 equiv.) and stirred for 10 min at different temperatures. Successively, the amine (1 equiv.) was added and stirred for the time reported above. d determined by chiral HPLC (see Supporting Information for details).

In order to highlight the generality of the process, some of the same amine moieties were used to perform coupling reactions with the other two RDESs prepared. The results showed that even changing the acidic component in the RDES, the performance of the systems was comparable with the first one, confirming and widening the scope of the protocol developed. The benzoic acid-based RDES reacted with aromatic and primary and secondary amines with acceptable yields (Table 7).

Table 7. Synthesis of amides in benzoic acid-based RDES[a].

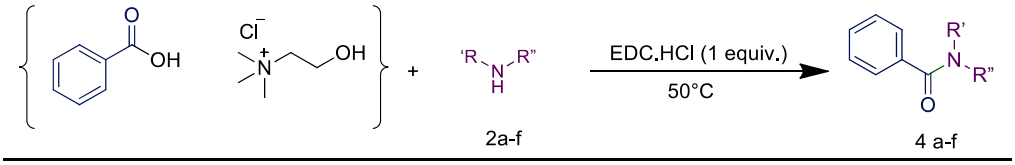

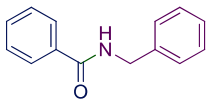

4a
30 min, 81%

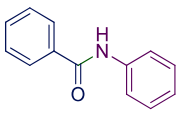

4b
30 min, 76%

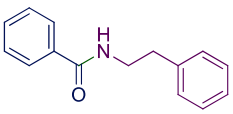

4c
30 min, 83%

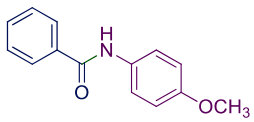

4d
60 min, 74%

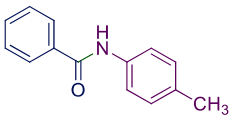

4e
45 min, 88%

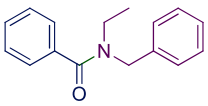

4f
60 min, 56%

[a]Reaction conditions: the coupling reagent, (1 equiv.) was added in benzoic acid-based RDES (1 equiv.) and stirred for 10 min at different temperatures. Successively, the amine (1 equiv.) was added and stirred for the time reported above

p-Hydroxyphenylacetic acid-based RDES was also evaluated as a substrate. A slight drop in the yield was observed and the corresponding amides were isolated in fair to good yields (Table 8).

Table 8. Synthesis of amides in 4-hydroxyphenylacetic acid-based RDES.

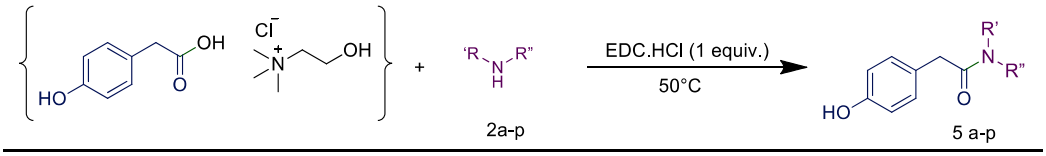

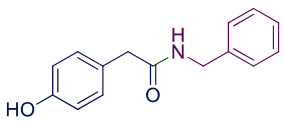

5a
30 min, 80%

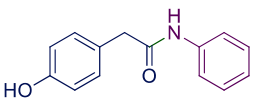

5b
30 min, 74%

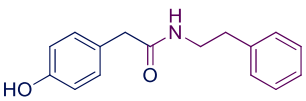

5c
30 min, 61%

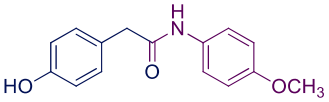

5d
45 min, 74%

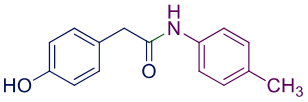

5e
45 min, 58%

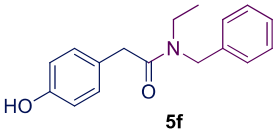

5f
60 min, 34%

[a]Reaction conditions: the coupling reagent, (1 equiv.) was added in 4-hydroxyphenilacetic acid-based RDES (1 equiv.) and stirred for 10 min at different temperatures. Successively, the amine (1 equiv.) was added and stirred for the time reported above

In order to investigate the utility of the developed methodology in the pharmaceutical industry, the optimized reaction conditions were applied to synthesize 4-hydroxyphenylacetamide, a key synthetic intermediate in the industrial production of atenolol. Atenolol represents one of the top-five bestselling drugs in the world, today used to treat angina, hypertension and to reduce the risk of death after a heart attack[163]. In this regard, the synthesis of 4-hydroxyphenylacetamide represents the first step in the atenolol industrial production. From the reaction between ammonium chloride and 4-hydroxyphenylacetic acid-based RDES, the desired amide was recovered in 94% yield, using EDC·HCl as the coupling reagent (Scheme 8).

Scheme 8. Proposed N-amidation mechanism in RDES.

Is important to emphasize that one of the advantages of the developed method is that for all these amidations, the devised workup procedure gave the pure amide product without the requirement for chromatography purification or extraction using VOC solvents.

By considering the possibility of adopting the developed synthetic route for the industrial synthesis of amides, the gram-scale synthesis of *N*-phenethyl-2-phenylacetamide was carried out. By water quenching to the reaction mixture at the end of the coupling reactions the precipitated product was successfully recovered in high yields and purity by simply filtration, without needs of chromatographic procedures.

In order to demonstrate the environmental benefits of the developed approach, we calculated the green chemistry metrics for the synthesis of the pilot reaction. The method resulted highly efficient to produce the desired amide in 97% yield (on gram scale) with PMI (Process Mass Intensity) greater when compared to the conventional industrial method (Figure 11).

$$PMI = \frac{Total\ amount\ of\ imputs}{Amount\ of\ product}$$

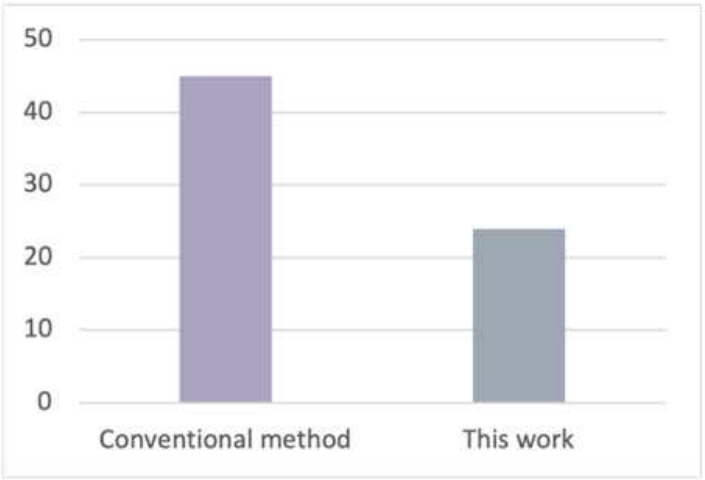

Figure 11. Comparison of PMI data with conventional industrial method.

On the basis of previous literature results and our experiments, a plausible mechanism for amidation reaction in presence of RDES is shown in the following Scheme 9.

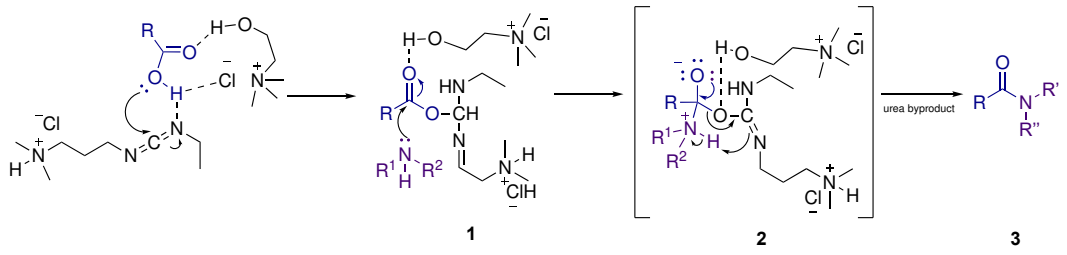

Scheme 9. Proposed *N*-amidation mechanism in RDES.

In a first reaction step, the proton transfer from the carboxylic acid to the weakly basic nitrogen atom on the EDC was facilitated by hydrogen bond interactions between the RDES and the coupling reagent causing the nucleophilic attack of the resulting carboxylate anion to led to the formation of the O-Acylisourea intermediate (1). Then, the same hydrogen bond interactions allowed the aminolysis step (2). Finally, the anchimeric assistance guided the formation of the amide product (3), along with the production of urea as byproduct.

C1.4 Conclusions

Based on these previous results, the following conclusions have been drawn from this chapter:

- The RDESs have been successfully used as both reaction medium and reagents for the direct *N*-amidation of amines with carboxylic acid;
- The exploitation of RDESs overcome the use of hazardous solvents and additives, significantly reducing the environmental footprint of amide synthesis;
- RDES-mediated amide synthesis proves excellent efficiency, allowing for the formation of amide bonds with high purity and yield. Moreover, the method is versatile and tuneable for a broad range of substrates, both aliphatic and aromatic, including chiral compounds, without any observed racemization;
- The innovative approach is not confined to laboratory-scale applications but can be easily scaled up for industrial manufacturing;
- This sustainable approach aligns with the principles of green chemistry, contributing to a cleaner and more responsible pharmaceutical industry.

In summary, the successful application of RDESs in *N*-amidation offers a promising and environmentally friendly alternative for amide synthesis. Features such as efficiency, versatility, scalability, and alignment with green chemistry principles make this novel method a valuable contribution to advancing sustainable practices in the pharmaceutical industry.

CHAPTER II
Visible-Light-Mediated Amide Synthesis in DESs

C2.1 Antecedents

As discussed in the general introduction, DESs have been employed to perform traditional and novel reactions, including organo-catalysed processes, as well as transition-metal mediated transformations. Another important aspect to improve the sustainability of an industrial process is the development of efficient catalytic systems. Particularly, photoredox catalysis has stood up in recent years, due to the possibility of employing (solar)light to facilitate a given reaction[164]. However, photoredox processes generally demand the use of inert conditions and a narrow range of VOC solvents. Although the spectacular synthetic achievements of the use of DES as reaction media during the last 20 years, their combination with photocatalytic process remained mostly elusive. In this sense, a seminal work by Capriati *et al.* described an enzymatic photosynthetic process using DESs as solvents in 2017,[165] paving the way for further research. However, so far only a handful of reports can be found in the literature regarding the use of DESs as solvents and different types of photoirradiation, which include resveratrol isomerization,[166] the study of pyrene fluorescence dissolved in reline,[167] and very recently, the thiolene click reaction in ChCl:glycerol[168]. However, the implementation of recent photocatalyzed processes[169] in these neoteric solvents is still uncharted territory. The possible light absorption of some DES components, the presence of cations and anions which can interact with the photocatalyst excited state, or the non-homogeneous character of the DES 3D-network based on hydrogen bonds may be some of the reasons that could explain why these processes have remained out of reach in the field of DESs.

On this matter, photoredox catalysed amide synthesis offers several advantages, such as the ability to activate organic substrates under mild reaction conditions, as well as the capability of exhibiting higher selectivity than those found in traditional methods[170,171]. Among the most effective acyl sources, thioacids proved to play an essential role in the formation of amide bonds, through their capability of forming thioacid radicals[172]. As a result of visible light irradiation, thioacids can be activated to generate active intermediates that may act in situ as mild acylating reagents in

the presence of amines, allowing the synthesis of amides of industrial significance and biologically meaningful peptides. In this scenario, Tan's research group employed Tris(bipyridine)ruthenium(II) chloride ($Ru(bpy)_3Cl_2$) as a photocatalyst to generate disulfide intermediates from thioacid potassium salts in order to produce amides (Figure 12a)[173]. Later, the group of Biswas reported the efficient successful synthesis of amides from thioacids by using CdS nanoparticles as heterogeneous photocatalysts (Figure 12b)[174]. Finally, it is worth mentioning that Song and co-workers reported the oxidative amidation of thioacids by using an organic dye as photocatalyst and air as an oxidant (Figure 12c)[172].

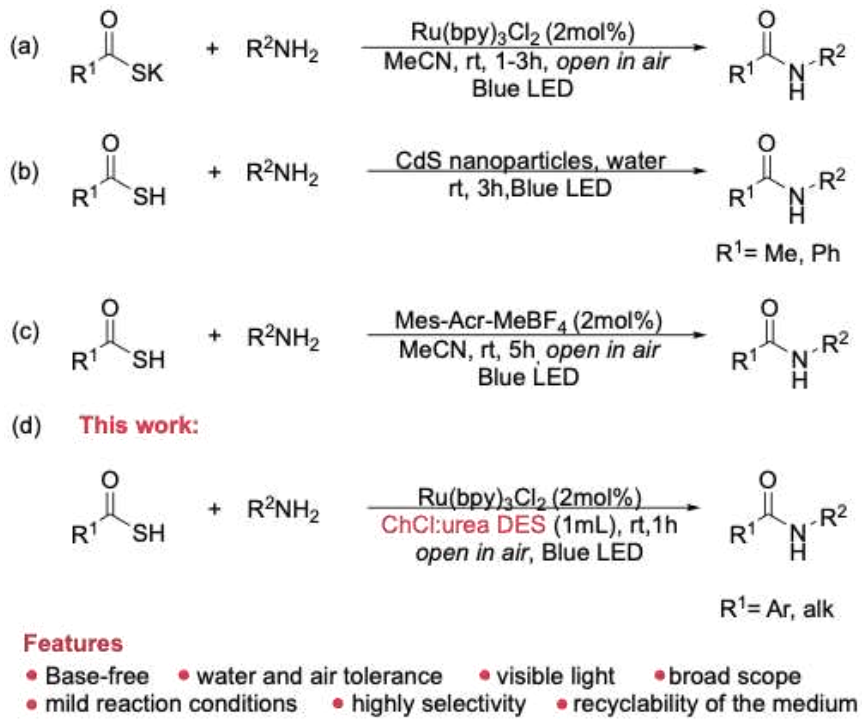

Figure 12. Approaches for amide bond formation.

C.2.2 Objectives

The previously mentioned studies highlight the potential of thioacids as a significant resource for photocatalytic amidation. However, there are notable challenges that need to be addressed for these procedures to be applicable in

industrial settings, including the use of hazardous organic solvents. Traditional photocatalytic amidation processes often employ inert conditions and a narrow range of VOC solvents. On this matter, despite considerable progress in employing DESs across various applications in the past two decades, the combination of DESs with photocatalytic processes has not been extensively explored.

In light of these findings and driven by the valuable characteristics of DESs, the research has outlined the following objectives:

- To synthesize amides from thioacids using visible light in DES: the research aims to pioneer the synthesis of amides from thioacids using visible light under mild conditions within deep eutectic solvents as reaction media;
- To investigate synergies between DES and photocatalysis: the objective is to explore and exploit the synergies between deep eutectic solvents and photocatalytic processes, with a focus on mitigating the challenges associated with hazardous organic solvents in the context of amide synthesis;
- To evaluate environmental and operational benefits of the developed method: by replacing hazardous organic solvents with DES, the research aims to contribute to a greener and more sustainable approach, aligning with the principles of green chemistry. Moreover, the use of visible light under mild conditions further emphasizes the potential for operational benefits, making the process more energy-efficient and environmentally friendly.

In summary, the research objectives are centered around unlocking the untapped potential of deep eutectic solvents in combination with photocatalytic processes, specifically in the context of synthesizing amides from thioacids. The goal is to provide a safer and more sustainable alternative to traditional, hazardous organic solvents in industrial processes.

C2.3 Results and discussion

The study started by testing the amide formation merging thioacetic acid **1a** and aniline **2a**, catalyzed by visible light photosensitizer $Ru(bpy)_3Cl_2$[175] (Table 9, entry

1), using the mixture K_2CO_3:glycerol (1:4) as solvent. After exposure to a blue light-emitting diode (LED) (450 nm) irradiation for 5 h, the two substrates were converted to the corresponding amide product **3a** in moderate efficiency (71% yield). In an attempt to optimize the reaction conditions, we decided to explore the contributing factors such as DES systems, photocatalysts, substrate and catalyst loadings, that could facilitate this transformation (Table 9). Regarding the DESs systems, the best results were obtained with the eutectic mixture ChCl:urea without the need of an external base. Among the factors that can explain the better performance of this solvent, are the basic character of the system, which can deprotonate the thioacid facilitating the course of the reaction, in addition to the lower viscosity of ChCl:urea compared with other DESs[176]. Considering that the DES could work as both the reaction medium and the base, such photoredox catalytic amide formation could be achieved without the extra addition of an inorganic salt or base, compared with the previous reported protocols, thus reducing the chemical waste of the process. Concerning the efficiency of the photocatalysts, the best results were obtained with $Ru(bpy)_3Cl_2$, affording the desired product in 91% yield when it was used in combination with ChCl:urea (Table 9, entry **6**). When the same reaction was performed for 1 h, the amide was obtained in quantitative yield (Table 9, entry **23**). This is probably due to degradation processes that could occur by extending the reaction time. Interestingly, increasing the catalyst loading to 3–5mol% resulted in a decrease of the yield (Table 9, entries **21** and **22**), while a using equimolar amounts of amine and thioacid or using the thioacid as limiting reagent (Table 9, entries **24**-**25**) caused a yield drop. Finally, it was observed a sharp decrease of the yield when the reaction was performed in darkness with or without a catalyst (Table 9, entries **26** and **27**), supporting the photoredox catalysis-based mechanism. Interestingly, other photocatalysts gave similar results (entries **6**-**10**), which is an important aspect for its implementation in further photocatalyzed processes in DES media.

Table 9. Optimization of the reaction conditions[a]

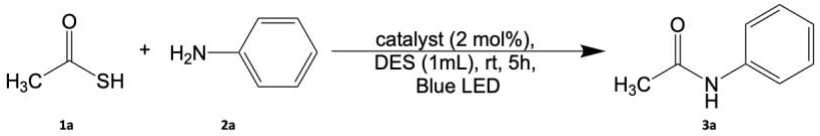

Entry	DES systems	Catalyst (mol%)	Yield (%)
1	K_2CO_3: Gly (1:4)	$Ru(bpy)_3Cl_2$ (2mol%)	71
2	K_2CO_3: Gly (1:4)	Mes-Acr-ClO_4 (2mol%)	91
3	K_2CO_3: Gly (1:4)	Fluoresceine (2mol%)	74
4	K_2CO_3: Gly (1:4)	Riboflavin (2mol%)	63
5	K_2CO_3: Gly (1:4)	$[Ir(ppy)_3]$ (2mol%)	81
6	ChCl:urea (1:2)	$Ru(bpy)_3Cl_2$ (2mol%)	91
7	ChCl:urea (1:2)	Mes-Acr-ClO_4 (2mol%)	87
8	ChCl:urea (1:2)	Fluoresceine (2mol%)	83
9	ChCl:urea (1:2)	Riboflavin (2mol%)	77
10	ChCl:urea (1:2)	$[Ir(ppy)_3]$ (2mol%)	86
11	ChCh:glycerol (1:2)	$Ru(bpy)_3Cl_2$ (2mol%)	78
12	ChCh:glycerol (1:2)	Mes-Acr-ClO_4 (2mol%)	79
13	ChCh:glycerol (1:2)	Fluoresceine (2mol%)	65
14	ChCh:glycerol (1:2)	Riboflavin (2mol%)	73
15	ChCh:glycerol (1:2)	$[Ir(ppy)_3]$ (2mol%)	85
16	Bet:HFIP (1:2)	$Ru(bpy)_3Cl_2$ (2mol%)	89
17	Bet:HFIP (1:2)	Mes-Acr-ClO_4 (2mol%)	61
18	Bet:HFIP (1:2)	Fluoresceine (2mol%)	65
19	Bet:HFIP (1:2)	Riboflavin (2mol%)	71
20	Bet:HFIP (1:2)	$[Ir(ppy)_3]$ (2mol%)	87
21	ChCl:urea (1:2)	$Ru(bpy)_3Cl_3$ (3 mol%)	93
22	ChCl:urea (1:2)	$Ru(bpy)_3Cl_2$ (5 mol%)	89
23[c]	**ChCl:urea (1:2)**	**$Ru(bpy)_3Cl_2$ (2 mol%)**	**>99**
24[d]	ChCl:urea (1:2)	$Ru(bpy)_3Cl_2$ (2mol%)	46
25[e]	ChCl:urea (1:2)	$Ru(bpy)_3Cl_2$ (2mol%)	78
26[f]	ChCl:urea (1:2)	$Ru(bpy)_3Cl_2$ (2mol%)	27
27[g]	ChCl:urea (1:2)	-	19

[a]Reaction conditions: **1a** (0.4 mmol), **2a** (0.2 mmol), catalyst (1–3 mol%) at rt in 1 mL of DES. [b]Yield determined by ^{1}H NMR using 1,2,4,5-tetramethylbenzene as internal standard. [c]The reaction was performed in 1 h. [d]**1a** (0.4 mmol), **2a** (0.4 mmol), catalyst (3 mol%) at rt in 1 mL of DES. [e]**1a** (0.4 mmol), **2a** (0.8 mmol), catalyst (3 mol%) at rt in 1 mL of DES, [f]The reaction was performed in darkness. [g]The reaction was performed without the photocatalyst and in darkness.

With the optimized conditions in hand, the substrate scope and versatility of this methodology were assessed. As shown in Table 10, upon exposure of structurally variable aromatic aniline derivatives (**3 b-3 k**) to the standard conditions, the amide products were isolated in a highly efficient manner, with yields ranging from 68% to 96%. The electronic effect of the substituents in the amine structure did not seem to have relevant effect for this transformation, since aniline derivatives decorated with electron-withdrawing or electron-donating substituents afforded similar results. Namely, the reaction yields obtained for electron-donating *p*-methylphenyl (**3b**) and *p*-methoxyphenyl (**3c**) products were comparable to those of electron-deficient *p*-chlorophenyl (**3f**) and *p*-bromophenyl (**3i**) ones. In addition to the para-substituted anilines, the corresponding *m*- and *o*-methylanilines (**3d** and **3e**) or chloroanilines (**3g** and **3h**) were also smoothly transformed into the corresponding amides in reasonable yields. Furthermore, a superior selectivity toward the acylation of the amine motif to the free hydroxyl group was also proven using p-aminophenol as substrate leading to the amide **3j** bearing a phenolic group, without any ester detected as by-product. Finally, *N*-(naphthalen-1-yl) acetamide (**3n**) was achieved from 1-naphthylamine with 63% yield. It can be inferred that steric issues on the amine are more relevant in this transformation, as slightly lower yields were obtained when *ortho*-substituted anilines were employed (**3e**, **3h, 3n**). It is worth noting that aliphatic amines (**3m**-**3o**) were also tolerated under the same reaction conditions, affording the desired amide products in moderate to excellent yields (73%).

Table 10. Reaction scope of visible light-mediated *N*-acylation reaction.

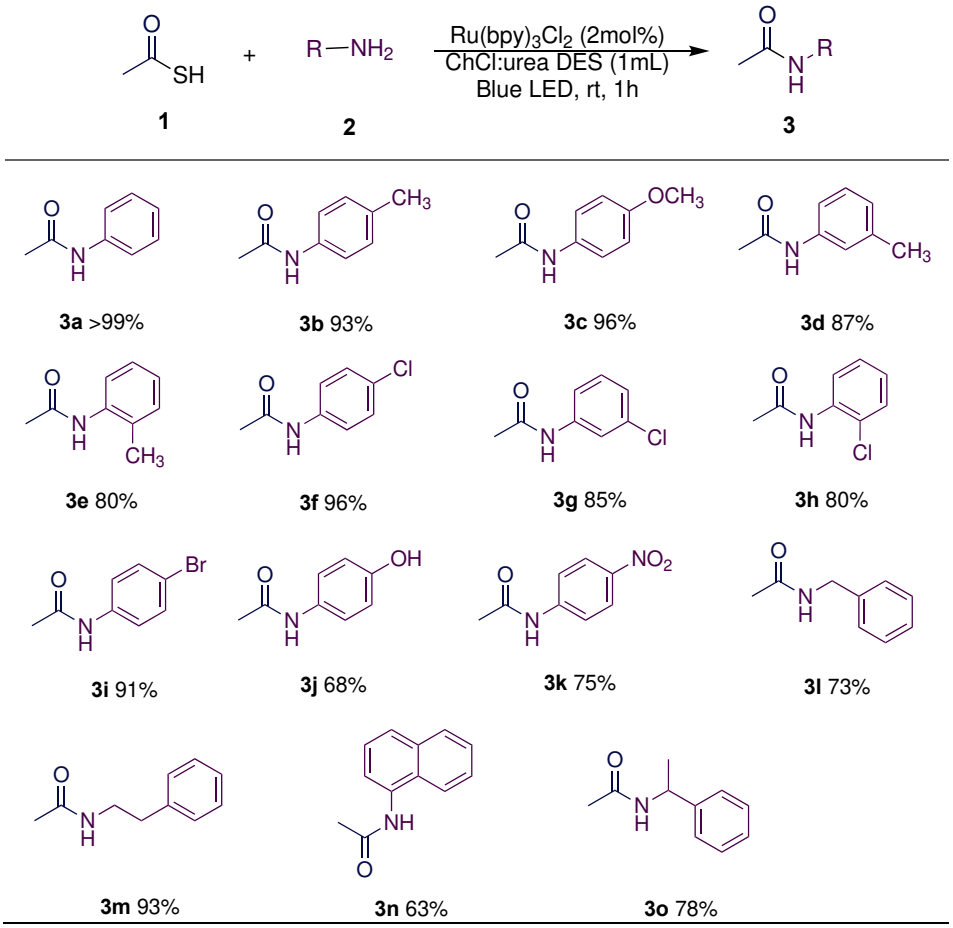

Reaction conditions: **1a** (2.0equiv.), **2** (1.0equiv.), $Ru(bpy)_3Cl_2$ (2 mol %), DES (1 mL), rt for 1 h. Yield of the isolated product.

As shown in Table 11, aniline and *p*-toluidine could react with thiobenzoic acid to afford **3p** and **3q** in high yields (96% and 91% respectively). For alkyl thioacids, good yields were obtained in the case of cyclohexyl, tert-butyl, n-pentyl, and n-heptyl substrates (**3r**-**3y**). Even terminal alkene moieties, a typical scavenger of radical intermediates, were tolerated, since undec-10-enoic thioacid could be efficiently employed as coupling partner with aniline and *p*-toluidine (**3z** and **3ba**), without observing any side reaction.

Table 11. Scope of thioacids substrates

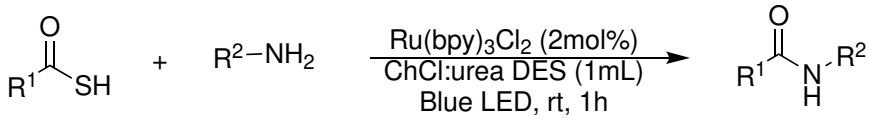

1 **2** **3**

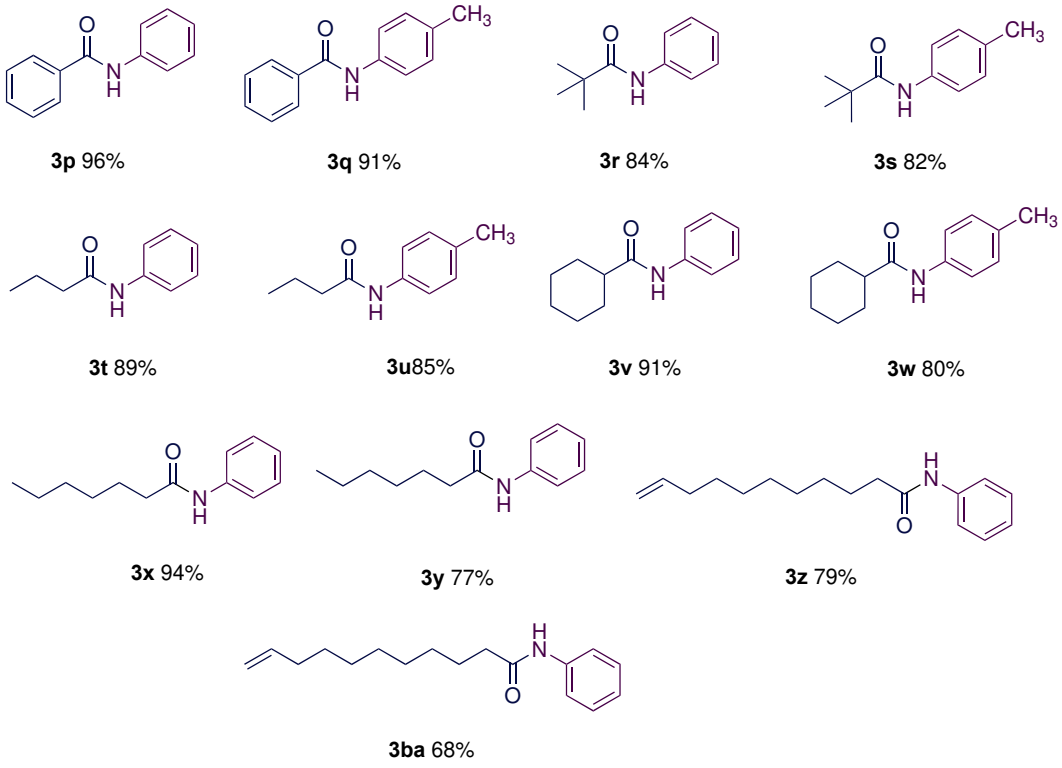

Reaction conditions: 1 (2.0 equiv.), 2 (1.0 equiv.), Ru(bpy)3Cl2 (2 mol %), DES (1 mL), rt for 1 h. Yields of the isolated products.

In order to shed light on the potential reaction pathway, mechanistic experiments were conducted, as summarized in Scheme 8. The results obtained are in line with the previously reported works. In this sense, when 2.0 equiv. of 2,2,6,6-tetramethylpiperidin 1-oxyl (TEMPO) was added to the mixture of thioacetic acid (**1a**) and aniline (**2a**), the corresponding amide (**3a**) was obtained only in trace amounts (Scheme 10a). Therefore, a mechanism involving the thioacid radical was suggested. To gain a deep insight into the reaction associated with the isolation of active intermediates, thiobenzoic acid **4a** was exposed to visible light for 30 minutes

and yielded an instructive disulfide intermediate with almost 57% yield (Scheme 10b). An orthogonal experiment using thioacetic acid 1a and disulfide intermediate **5** was set up under standard conditions (Scheme 10c). A mixture of **3** a and **4** a was obtained, which clearly demonstrated that disulfide intermediate **5** would be involved in the mechanism.

Finally, the involvement of atmospheric oxygen was evaluated by performing the model reaction under argon atmosphere. Thus, a much lower reaction rate was observed, obtaining only 46% yield of **3** a after 2h instead of the 99% yield observed under aerobic conditions.

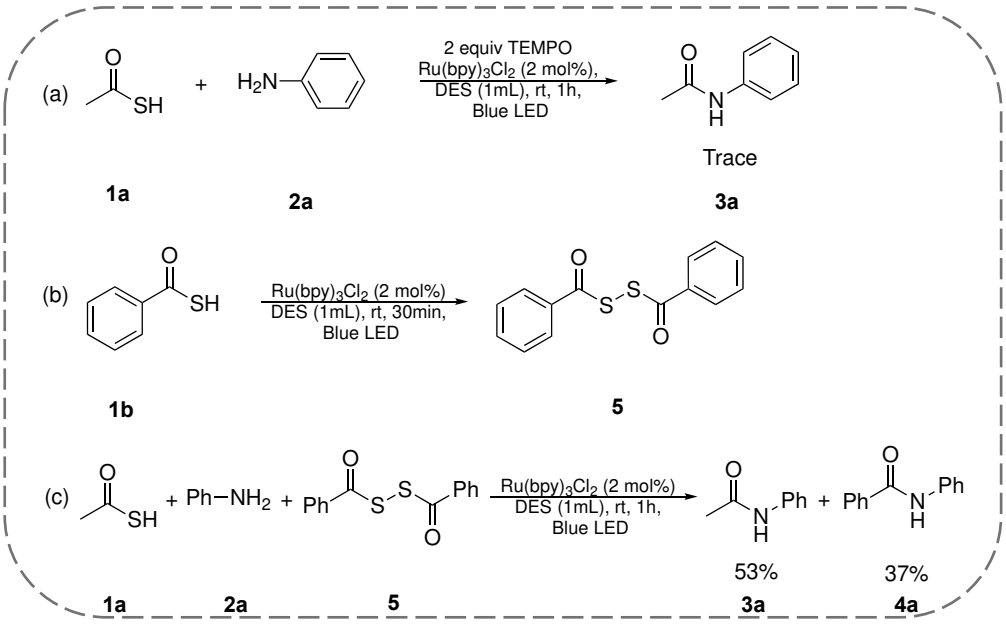

Scheme 10. Experimental probes on reaction mechanism.

Based on the results of the above-mentioned studies, a plausible mechanism is proposed for the synthesis of amides (Scheme 11). Initially, thioacid **1** was deprotonated by the DES to form the intermediate A, although the role of the starting amine should not be ruled out. The blue LED should photoexcite the Ru^{2+} to generate excited Ru_2^{+*}, which was subsequently reduced to Ru^{1+} by the electron-rich thioacetic anion. Then, the involvement of atmospheric oxygen[177] converting

Ru^{1+} back to Ru^{2+} catalyst, closed the whole catalytic process. This single-electron transfer (SET) resulted in the generation of thioacetic acid radical **B**, which was transformed to the disulfide intermediate **5** by diradical coupling reaction and then induced the amide formation by means of a nucleophilic attack of amine **2** to afford the amide **3**. At the same time, intermediate **4** could further generate amide 3 through aminolysis.

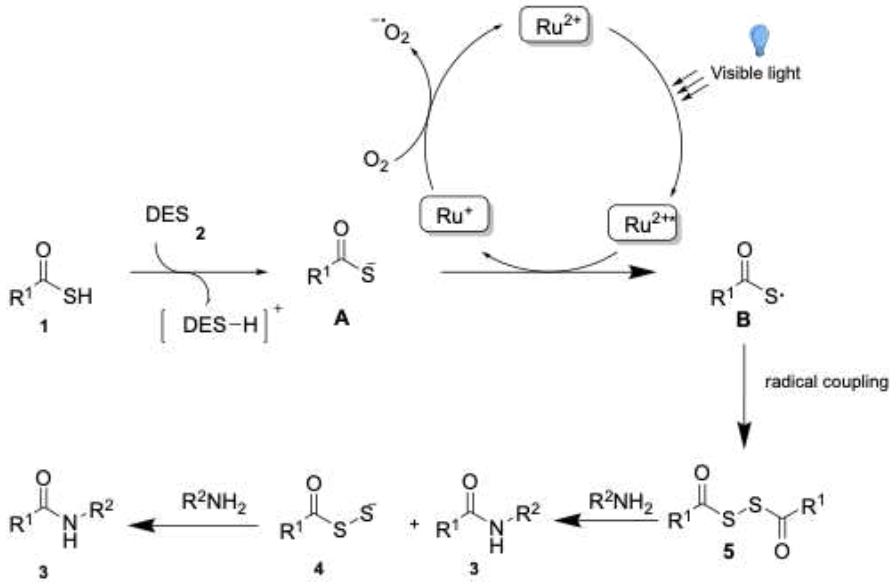

Scheme 11. Proposed mechanism for photocatalytic amide synthesis.

Since the recycling of the DES and the catalyst is a crucial point for the sustainability of the process from the industrial point of view, we also evaluated the possibility to recover the DES-catalyst system and reuse it. Therefore, the extraction of the organic compounds using different immiscible organic solvents was performed. The best results were obtained when ethyl acetate was employed. The mixture of DES and photocatalyst was reused, after being vacuum dried, performing a new reaction cycle under the same reaction conditions. It was possible to recycle the DES and catalyst for up to three cycles, even though a decrease in the reaction yield was observed after the third cycle (Figure 13). ICP-MS analysis showed that only 0.2% of the initial Ru loading was extracted with EtOAc. Therefore, most of the photocatalyst remains in the DES phase and the lost in activity should be attributed

to other factors such as the cumulative presence of different salts that could affect and modified the DES structure.

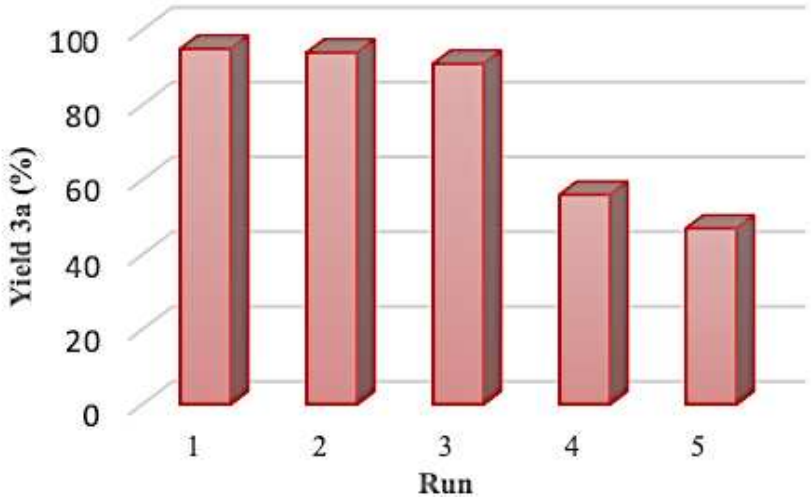

Figure 13. Recyclability of the system.

To assess the efficiency of the developed method, some green metrics were analysed and compared with the previously reported photoredox amide synthesis from amines and thioacids. In this regard, a semiquantitative analysis which takes into account the quality of a protocol based on reaction yield, cost, safety and ease of purification known as EcoScale[13,178] was determined. Thus, the EcoScale value of the present protocol performed in DES was 64, with values ranging from 50 to 75 being classified as acceptable. This fact is particularly relevant when compared with the values of those reports performed with the same catalyst but using acetonitrile (MeCN) as the solvent[173] or those using 9-Mesityl-10-methylacridinium tetrafluoroborate ($MesAcrBF_4$)[172] or Cds[174] as the catalyst, with values of 53, 57 and 52, respectively. Regarding the atom economy[179] for the synthesis of **3a**, a value of 79.9% was obtained for the methods that make use of thioacetic acid, while a lower value of 65.2% is observed when potassium thioacetate is employed as a reactant.

C2.4 Conclusions

Based on the previous results, the following conclusion have been drawn from this chapter:

- A visible-light-promoted photo-redox catalytic amide formation in an eco-friendly and biodegradable DES based on the ChCl:urea mixture was disclosed;
- The developed method features operational simplicity, excellent functional selectivity, short reaction time, broad substrate and photocatalyst scope and high yields (up to 99%);
- The recyclability of the DES and its synergistic effect on the reaction outcome has also been demonstrated, highlighting the possibility to reuse the system for at least three consecutive cycles without a significant decrease in the reaction yield;
- The protocol proves the possibility of performing photoredox catalysis using DESs as reaction media, thus combining the use of sustainable solvents and a mild and efficient photo-induce activation process, which can open the gates to further studies in this field.

CHAPTER III

A Brønsted Acidic Deep Eutectic Solvent for *N*-Boc Deprotection

C3.1 Antecedents

In 2015, the ACS Green Chemistry Institute® Pharmaceutical Roundtable (GCIPR) (Washington, DC, USA)[9] issued a Reagent Guide heading for providing information and to guide chemists in the selection of environmentally friendly reagents for diverse chemical transformations. On this matter, the development of general methods for the removal of the Boc protecting group has been identified as one of the priority research areas for the pharmaceutical sector (Figure 14). Boc is a widely used amino protecting group due to its resistance to catalytic hydrogenolysis, induction of favourable solubility characteristics, and resistance to hydrolysis under basic conditions and nucleophilic reagents. This makes it useful when conditions of orthogonality between protective groups are required[145,180]. Given these advantageous characteristics, several amines, amino acids, and peptide synthons supplied to the pharmaceutical industry are sold *Boc*-protected[181].

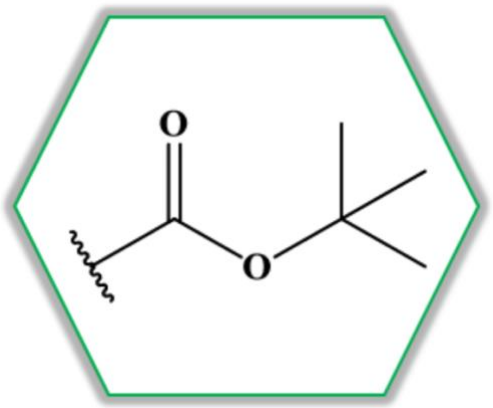

Figure 14. Chemical structure of Boc protecting group.

Several experimental procedures for Boc deprotection have been developed over the years, typically involving the use of strong acids such as phosphoric acid[182,183], HCl[184,185], H_2SO_4[186], Lewis acids[187–189], or even some special basic conditions[190,191]. However, most of these methods exhibit several disadvantages, including high acidity, the use of expensive reagents, excessive amounts of catalysts and organic solvents, low chemoselectivity, high temperatures, and challenges in catalyst

recovery[192]. On this matter, trifluoroacetic acid (TFA) remains the reagent of choice for Boc group removal; however, this approach has its drawbacks as TFA is toxic, volatile, and environmentally unfriendly[193]. Furthermore, it is an extremely corrosive and relatively expensive compound, particularly when employed in solid-phase peptide synthesis, which necessitates large quantities of this material. Therefore, the main "Green Criteria" requires the replacement of conventional solvents and reagents that present important safety as well as the reduction in hazardous waste to a minimum[194–196]. Thus, the development of an environmentally benign, atom-economic, and sustainable method in the Boc-deprotection still remains a contemporary challenge in synthetic chemistry and the chemical industry.

In this regard, G. Wang *et al.* described the use of supercritical water under pressure as a medium for the *N*-Boc deprotection of both aromatic and aliphatic *N*-Boc amines[197,198]. However, the methodology was characterized by long reaction times and showed incompatibility with the ester functionality. Additionally, an ionic liquid has been proposed as a reaction medium for the *N*-Boc deprotection strategy[199]. Nevertheless, the addition of a water–dioxane mixture to solubilize the substrates, as well as high reaction temperatures, were required. More recently, Mandal *et al.* reported a $FeCl_3$-mediated Boc-deprotection strategy for peptide synthesis both in the solution and in a solid phase[188,189]. However, the protocol used dichloromethane (DCM) as the medium and presented limitations related to the recovery step of the Boc cleaved product.

In this panorama, the emergence of DESs as greener alternatives to conventional solvents, coupled with their excellent tunability, opens up possibilities for the development of environmentally friendly protocols in deprotection reactions. This fact could hold significant importance in the realm of sustainable development chemistry.

On this matter, in choosing the best synthetic route for Boc deprotection that meets the criteria required by Green Chemistry, the Pharmaceutical Roundtable of the ACS Green Chemistry Institute has furnished a Guide to Reagents with the aim of

guiding the researcher to use more sustainable reagents[145]. The choice of the most suitable reagent for Boc-deprotection was summarized in a Venn Diagram (Figure 15), in which each circle represented a criterion, namely: 'Scalability', 'Greenness,' and 'Wide utility'.

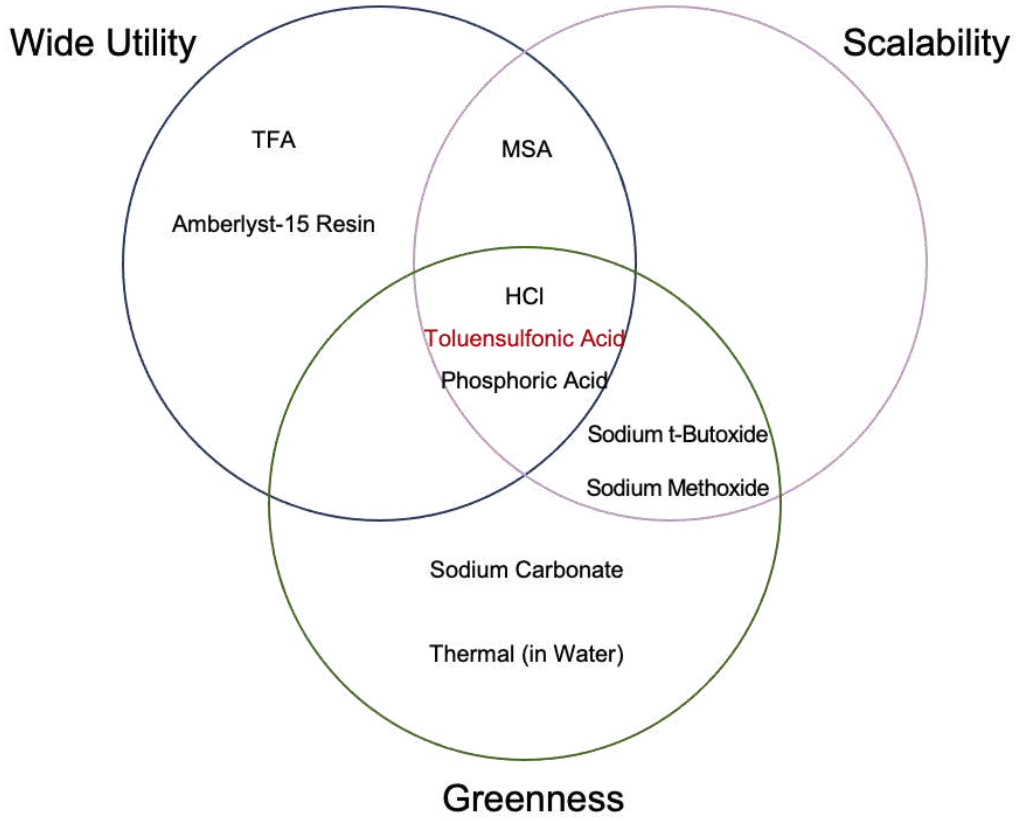

Figure 15. Venn diagram for *N*-Boc-deprotection.

The ideal reagent should have all three characteristics, and therefore, should be located in the center, between the intersections of the circles. According to this reagent guide, *p*-toluenesulfonic acid (pTSA) represents the best alternative to TFA for an eco-friendly Boc-deprotection procedure as it is cheap, readily available, and also biodegradable. It is a Brønsted acid catalyst largely investigated for several reactions, given its strong acidity[200–202].

C.3.2 Objectives

Based on the previous informations, the following objectives has been established:

- To explore the feasibility of RDESs for Boc-cleavage: the research aims to investigate the feasibility of employing RDESs for the development of a straightforward Boc-cleavage method;
- To investigate the catalytic efficiency of a DES composed of *p*-toluenesulfonic acid monohydrate (pTSA) and choline chloride (ChCl), with the DES serving both as a reaction medium and catalyst simultaneously;
- To evaluate and compare the catalytic efficiency of the pTSA-ChCl DES with other acidic DESs to understand its relative effectiveness;
- To assess the "greenness" of the developed method: this involves a comprehensive evaluation comparing the environmental impact of the RDES-based approach with other conventional methods

In summary, this research initiative is driven by the overarching goal of developing an efficient and practical Boc-cleavage method, leveraging the unique properties of Reactive DESs. The specific focus on the pTSA-ChCl DES and its comparison with other acidic DESs aims to identify the most effective catalytic system for the targeted cleavage reactions. Additionally, the utilization of *p*-toluenesulfonic acid in DES form addresses specific challenges associated with its traditional use, contributing to the overall feasibility and sustainability of the cleavage method.

C3.3 Results and discussion

The main goal the following study was to present a simple and cost-effective approach to the deprotection of protected *N*-Boc derivatives that leads to the corresponding deprotected products with high purities and high yields without the need to apply post-reaction purification. Since the selective deprotection of the Boc group is conducted under mildly acidic conditions, we tested the catalytic behaviour of different Brønsted acid and Lewis acid-type DESs. In particular, the quaternary ammonium salt choline chloride has been used as HBA since it is an economic, biodegradable, nontoxic, and even edible quaternary salt that can be extracted from

biomass or easily synthesized from fossil reserves[83], whereas pTSA, oxalic acid, citric acid, malonic acid, succinic acid, and $FeCl_3$ were chosen as HBDs and catalysts (Table 11).

All RDESs have been prepared by using the previously protocol based on mixing the components in a defined molar ratio and then heating at 60-80 °C for 2 h, under constant stirring in a round bottom flask, until a stable homogeneous colourless liquid phase was formed[176]. After the preparation, the DESs were cooled to room temperature and kept closed at room temperature. All the prepared RDESs were tested on the deprotection of *N*-Boc-benzylamine (**1a**), selected as a model substrate, and the reaction progress was followed by the TLC and GC/MS analysis of crude reaction mixtures. The results of the development and optimization of the deprotection studies are displayed in Table 1. For a systematic study of the action of the investigated systems, all reactions were conducted at room temperature, except in the case of the DES, which was prepared using citric acid and required a temperature of 50 ◦C due to its high viscosity that limited the application as a reaction medium. The times shown in the table were referred to the respective points of maximum conversion in the substrate, as verified by GC/MS. Surprisingly, the treatment of *N*-Boc benzylamine (1 mmol) with 1 mL of ChCl: pTSA (1:1) at room temperature, led to the deprotection after only 10 min in a 98% yield, and the free amine was detected by GC-MS after aqueous work-up (Table 12, entry **1**). Otherwise, when the model reaction was screened in the other Brønsted acid and Lewis acid type DESs, **2a** was produced in lower yields (entries **2-6**, Table 12). More specifically, by performing the same procedure in oxalic acid-based DES (entry **2**, Table 12), the deprotection of the amine was achieved in a 58% yield after 30 min. At the same time, using other DESs based on Brønsted acids (entries **3-5**, Table 12), a drastic decrease in yield was observed, even when increasing the reaction time. This is probably related to the lower acidic character of the acids used compared to the first mentioned. In the case of the citric acid-based DES, the poor yields observed were probably justified by the highly viscous medium, which did not allow an easy handle of the compound. When the deprotection process was

performed in $FeCl_3$-based Lewis acid DES (entry **6**, Table 12), amine deprotection was obtained in a 62% yield after 15 min, confirming the already present literature data that demonstrate its suitability as a catalyst in this transformation, also because it is economic and sustainable[189]. However, as previously reported, the employment of $FeCl_3$ makes the work-up procedures more complicated, as a large amount of the deprotected compound went into the water with iron during the work-up. An example of the Boc-deprotection protocol carried out with *p*-Toluensulfonic acid was reported by Stone et al.[203]. Nevertheless, N-deprotection occurred after 60 min in a mixture of dichloromethane/tetrahydrofuran (DCM/THF), and the purification procedures were very difficult.

Table 12. Optimization of conditions for the cleavage of ***N***-protecting group.

1a **2a**

Entry	DES	T (°C)	Time[b] (min)	Yield (%)
1	ChCl: pTSA (1:1)	25	10	98
2	ChCl: oxalic acid (1:1)	25	30	58
3	ChCl: citric acid (1:1)	50[a]	30	15
4	ChCl: malonic acid (1:1)	25	60	26
5	ChCl: succinic acid (1:1)	25	60	20
6	ChCl: $FeCl_3$ (1:1)	25	15	62

[a]Reaction performed at 50 °C due to the high viscosity of the investigated DES; [b] Times refer to the respective points of maximum conversion of the substrate, according to GC/MS.

Encouraged by these preliminary results, the scope and limitations of the optimised method on a variety of aliphatic and aromatic *N*-tertbutylcarbamates were assessed. The broad applicability of the procedure is shown in Table 13, exhibiting the efficient deprotection of various classes of nitrogen-containing functional groups (primary and secondary amines, anilines, etc.). All substrates display quantitative isolated yields after reaction times varying from 10 to 30 min.

In particular, *N*-Boc-protected 2-phenylethylamine (**1b**) easily undergoes deprotection under the selected reaction conditions to afford the desired amine in an excellent yield (entry **1**, Table 13). The removal of the Boc group works well even in the case of *N*-Boc-aniline (**1c**) and its substituted derivatives (entries **2–6**, Table 13). More specifically, the deprotection reaction of **1c** proceeded in 10 min, unlike its derivatives like N-Boc toluidine (**1d**) and *N*-Boc anisidine (**1e**), which required shorter reaction times (both 8 min), probably for the effect of the electron-donating substituents present in para position to the amino function. *N*-Boc 3-nitroaniline (**1f**) underwent deprotection within 20 min, probably due to the presence of the nitro electron withdrawing group, which reduced the reactivity of the molecule. Next, the method was also successfully applied to the deprotection of several *N*-Boc-protected aliphatic amines. As shown in the Table, cyclic and aliphatic primary amines (entries **7–12**, Table 13) can be fully deprotected within 10–20 min. At the same time, when the protocol was applied to secondary Boc-protected amines (entries **14–15**, Table 13), the free amines were obtained in excellent yields after 30 min. The secondary heterocyclic amine, such as *N*-Boc piperidine (**2h**), underwent deprotection in 15 min in an almost quantitative yield. The deprotection of *N*-Boc 4pyridin-4-amine (**2f**) required a longer reaction time, about 20 min, and this behaviour could be explained by the fact that the nitrogen of the heterocyclic ring was protonated by the DES, also leading to a decrease in the yield. *N*-Boc ethylbenzylamine (**1n**) afforded the unmasked amine in 30 min and with a 70% yield, while the presence of the isopropyl group in the secondary amine *N*-Boc isopropyl benzylamine (**1o**) led to a reduction in the yield (56%), probably due to the steric hindrance that the isopropyl group obtains from the molecule.

Table 13. Reaction scope for *N*-Boc deprotection of amines.

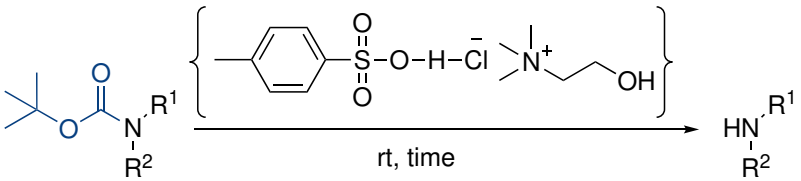

1a **2a**

Entry	N-Boc-amine	Product	Time (min)	Yield (%)[b]
1	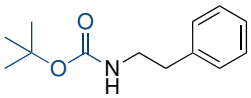 **1b**	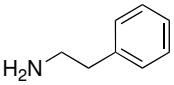 **2b**	10	>98
2	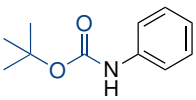 **1c**	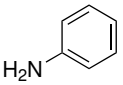 **2c**	10	>98
3	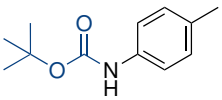 **1d**	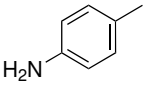 **2d**	15	>98
4	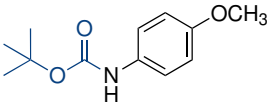 **1e**	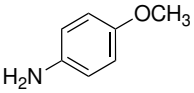 **2e**	15	>98
5	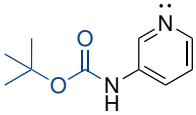 **1f**	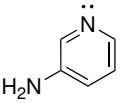 **2f**	20	90
6	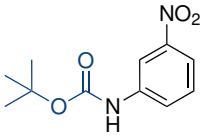 **1g**	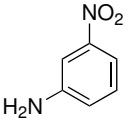 **2g**	20	86
7	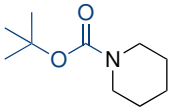 **1h**	 **2h**	15	>98

Table 13. Continuation

8	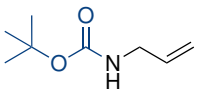 **1i**	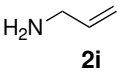 **2i**	10	>98
9	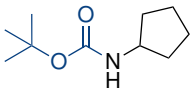 **1j**	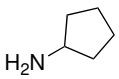 **2j**	10	>98
10	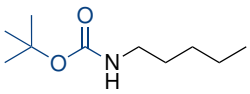 **1k**	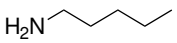 **2k**	10	>98
11	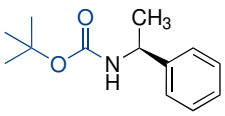 **1l**	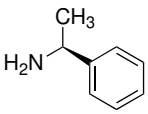 **2l**	20	>98
12	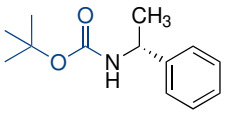 **1m**	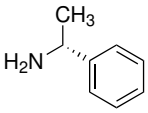 **2m**	20	>98
13	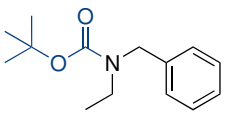 **1n**	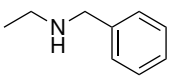 **2n**	25	70
14	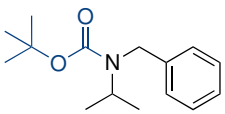 **1o**	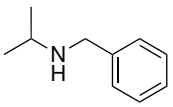 **2o**	30	56

[a] Reaction conditions: all reactions were carried out by using 1 mmol of N-Boc amine in 1 mL of ChCl: pTSA at rt for the time reported above. b Isolated yields after work-up.

An important advantage of the protocol is the simplicity of the reaction products recovery. The deprotected substrates can be isolated directly from the reaction mixture as tosylate salts just by washing them with water, followed by

recrystallization from ethyl acetate (AcOEt). Free substrates were instead obtained by a simple workup that involved the addition of an aqueous solution of sodium bicarbonate $NaHCO_3$ (5%). The crude material was then extracted with AcOEt (3 x 5 mL). In both cases, no tedious chromatographic purification was required. All the known compounds had spectroscopic data identical to those reported in the literature[190,195].

Considering the great scientific and industrial value of N-Boc protection in peptide synthesis, the *N*-Boc deprotection of different amino acid derivatives was also investigated. For this purpose, some methyl esters of amino acids have been preliminarily protected on the α-amino function with the protecting group Boc. As shown in Table 14, methyl esters of amino acids have aliphatic side chains such as L-Alanine methyl ester and D-Alanine methyl ester, which underwent deprotection in just 10 min and both with yields greater than 98% (entry **1,2**, Table 14). Esters are compatible with the reaction conditions (entries **1-5** and **7**, Table 14). In each example, no product resulting from the degradation of methyl esters was observed. The selectivity of deprotection was confirmed in the ^1H NMR spectrum of the crude mixtureby the presence of a methyl ester group signal at about 3.70 ppm. Branched-chain amino acid methyl esters, such as *N*-Boc L-Leucine and *N*-Boc Valine, required longer deprotection times, of about 25 min, with lower yields with respect to amino acids with aliphatic side chains; in particular, leucine was obtained with a yield of 68%, and valine with a yield of 63%, probably both due to the steric hindrance of their side chains (entries **3–4**, Table 14).

Table 14. DES-catalysed deprotection of *N*-Boc amino acid derivatives and *N*-Boc dipeptide[a].

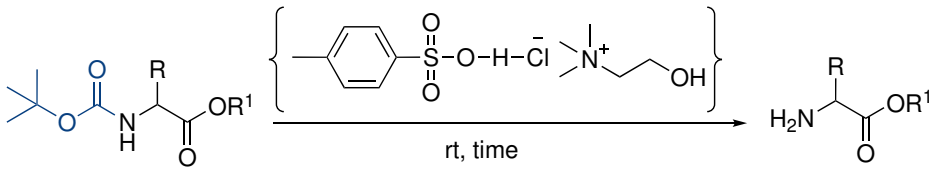

1 **2**

Entry	*N*-Boc-amino acid	Product[c]	Time (min)	Yield (%)[b]
1	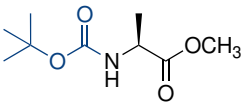 **1p**	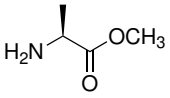 **2p**	10	>98[d]
2	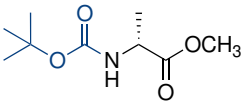 **1q**	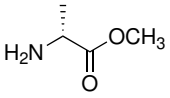 **2q**	10	>98[d]
3	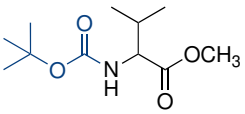 **1r**	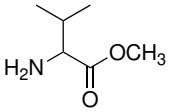 **2r**	20	63
4	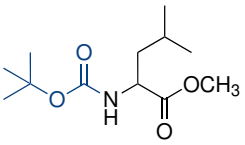 **1s**	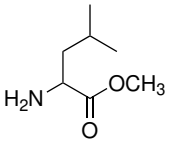 **2s**	15	68
5	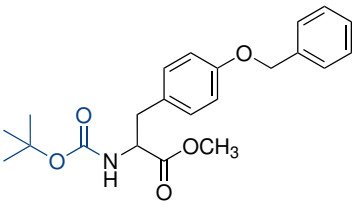 **1t**	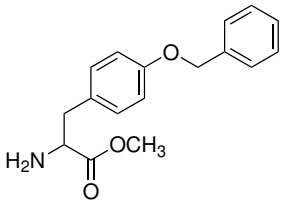 **2t**	35	>98

Table 14. Continuation

6	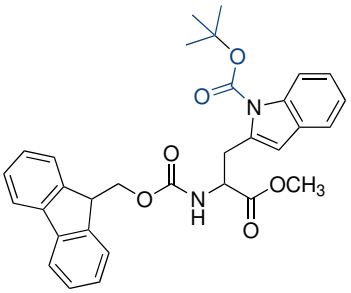 **1u**	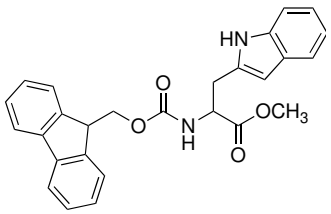 **2u**	40	90
7	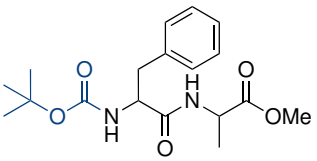 **1v**	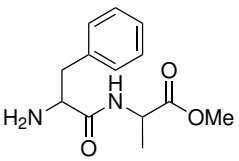 **2v**	15	>98

[a]Reaction conditions: all reactions were carried out using 1 mmol of *N*-Boc-amine in 1 mL of ChCl: the pTSA at rt for the time reported above. [b] Isolated yields after work-up. [c]MS and NMR were used to verify the exact mass and structure of the prepared product. [d]To verify enantiomeric purity, chiral HPLC was performed and compared with the commercially available racemic mixture. A single peak was observed at the corresponding retention time, while the racemic mixture provided two.

It was important, at this point, to verify whether the reaction conditions adopted could make the strategy orthogonal, that is, without affecting other protecting groups present in the side chains of the amino acids. Substrates bearing acid-labile protecting groups, such as benzyl ether, remained stable under our conditions. In this regard, we have chosen as substrate the O-Benzyl-L-tyrosine methyl ester since the Boc/Bn strategy, where the Boc group was used as a temporary protecting group of the amino function and Bn (benzyl) of the side chains of the amino acids, is one of the most widely used protection strategies in peptide synthesis. In particular, the α-amino function of the O-benzyl-tyrosine methyl ester was protected with the Boc protecting group, and subsequently, its deprotection was carried out in DES ChCl:pTSA (entry **5**, Table 14). In this case, the Boc-group was removed selectively without affecting the O-benzyl ether protection, as proven by the GC/MS and NMR analysis. The Fluorenylmethyloxycarbonyl (Fmoc) and Boc protecting groups are widely used in peptide synthesis, and therefore, it is of great importance to developing conditions that successfully remove the Boc protecting group while

leaving the Fmoc protection unchanged[204–206]. To this aim, the stability of the Fmoc group present in the tryptophan side chain was evaluated (entry **6**, Table 14), and it was shown that Fmoc was well tolerated under the reaction conditions adopted. Finally, the preparation of the dipeptide *N*-Boc-L-Phenylalanyl-L-Alanine methyl ester allowed us to explore the possible extension of the protocol for the deprotection of the amino function of a dipeptide. The dipeptide under consideration underwent the deprotection reaction in Brønsted acidic DES ChCl:pTSA within 15 min (entry **8**, Table 14). The removal of the Boc protecting group was monitored by TLC and GC/MS analysis from which it was shown that cleavage occurred in the yields demonstrating the high advantage of the DES in this protocol. Even in the case of deprotection reactions carried out on amino acid systems and the dipeptide, the final products were recovered by a simple work-up operation without the need for any chromatographic purification. To obtain the amino acid or dipeptide not charged and neutralized, a saturated aqueous solution of $NaHCO_3$ was added and extracted with ethyl acetate and was subsequently washed with brine. The combined organic layers were dried on magnesium sulphate ($MgSO_4$), filtered, and vacuum-evaporated to provide the raw product in quantitative yield. All the compounds obtained have been characterized by GC/MS and NMR and show spectroscopic data comparable to those reported in the literature[194,195]

Based on the previously reported literature[107,204], a plausible mechanistic pathway for Boc-cleavage has been hypothesized (Scheme 12). At first, the Bronsted acidic site of the CHCl: *p*TSA DES activated the carbamate oxygen by protonation, therefore, weakening and breaking the C=O bond causing the loss of the t-butyl carbocation. The reversible hydrogen bonding between the DES and the substrate made it so that the resultant carbamic acid underwent proton transfer followed by decarboxylation to provide the deprotected amine salt. The final basic workup affords the free amine.

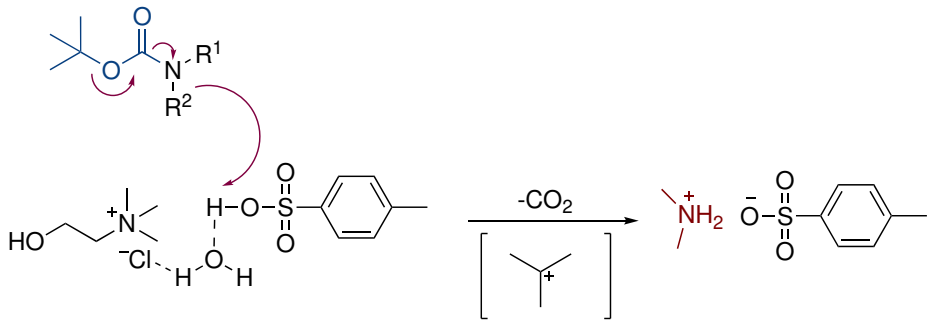

Scheme 12. Proposed mechanism for Boc-deprotection in RDES.

Finally, the feasibility of the developed method was evaluated for a somewhat scaled-up (on the gram scale) experiment with the model substrate N-Boc benzylamine. Even in this case, the reaction proceeded smoothly, affording the desired free amine in 94% of yields, almost similar in all respects to the 1 mmol scale entry (Table 11, entry **1**). These results highlighted the efficiency of the RDES for large-scale production as well.

In order to understand the efficiency of the developed protocol with respect to conventional methods already reported in the literature for the deprotection of the Boc group, the PMI and E-factor were calculated. Table 15 shows the two metrics calculated for our procedure and compares them with those of other reported methodologies. The PMI and E-factor for our procedure were calculated as 68 and 67, respectively, whereas those for the other procedures were found to be higher. Nevertheless, the ideal E factor is 0, and higher E factors are relatively less amenable. However, it matters what kind of wastes are produced because, in our protocol, choline chloride and *p*-toluensulfonic acid may be of little concern compared to toxic organic volatile solvents and corrosive acids. Therefore, these data indicate the feasibility, greenness, and sustainability of our process.

Table 15. Calculated green metrics percentage yield, PMI, and E-Factor for our Boc deprotection procedure and for already re-ported methods.

Entry	Reaction conditions	Yield (%)	PMI	E-factor	Ref.
1	THF, aqueous H_3PO_4	94	91	90	[164]
2	DCM, aqueous H_3PO_4	91	96	95	[165]
3	DCM, H_2SO_4	93	383	382	[168]
4	DCM, TFA	98	92	91	[169]
5	ChCl:pTSA	98	68	67	Our work

C3.4 Conclusions

Based on the previous results, the following conclusion have been drawn from this chapter:

- A highly efficient protocol for the deprotection of Boc protecting group has been developed using pTSA-based RDESs. This innovative approach involves the RDES both as a reaction medium and catalyst, enabling the selective deprotection of a wide variety of N-Boc derivatives in high yields with excellent purities. The simplicity of the workup process further enhances the practicality of the method;
- The developed strategy demonstrates a broad substrate scope, accommodating structurally diverse amines, amino acids, and dipeptides. This versatility allows for the selective deprotection of various N-Boc derivatives under mild reaction conditions. The applicability of the method to different substrates underscores its potential utility in diverse chemical contexts.

In summary, the chapter presents a novel and highly efficient approach for Boc deprotection using pTSA-based RDES. The method's versatility, ease of operation, and environmentally friendly characteristics position it as a promising alternative for selective deprotection of N-Boc derivatives across a range of substrates.

CHAPTER IV

Synthesis of Atenolol in DES: A Sustainable Approach

C4.1 Antecedents

Aryloxy propanolamines represent chemically noteworthy compounds with significant medicinal implications. A considerable number within this class serve as robust antagonists of β-adrenergic receptors, commonly referred to as β-blockers. Noteworthy pharmaceuticals such as atenolol, propranolol, and metoprolol fall under this category, playing pivotal roles in medical prescriptions[207].

Racemic atenolol is currently among the top five best-selling drugs in the World, and manufactured under the names Tenormin®, Mylan® and others[208]. First introduced in 1976 as a substitute for propranolol, atenolol is widely used for the treatment of hypertension, myocardial infarction, arrhythmias, angina, as well as conditions due to reduced blood circulation and vasoconstriction, including migraine[209]. Atenolol belongs to the class of ß-blockers, and, as such, is a selective antagonist of ß1 receptors[208,210]. It hinders the activity of substances present in the body, such as adrenaline, at the level of the heart and blood vessels, causing a consequent reduction in heart rate and blood pressure as well as cardiac stress[211].

In 2022, the sales market for atenolol was more than USD 11 billion and it is estimated to reach USD 28 billion by the end of 2035. This growth is attributable to a worldwide increase in hypertension among people, along with increased awareness of the risks associated with it[212].

The initial patented chemical routes for the synthesis of atenolol used DL-4-hydroxyphenylglycine or 4-hydroxyphenylacetic acid as starting reagents to prepare 2-(4-hydroxyphenyl)acetamide (Scheme 1) which further reacted in some subsequent steps to afford atenolol[213]. Currently, the industrial procedure is simplified by the commercial availability of the 2-(4-hydroxyphenyl)acetamide, which reacts with a large excess of epichlorohydrin in the presence of piperidine to give 2-(4-(oxiran-2-ylmethoxy)phenyl)acetamide. The latter compound further reacts with excess isopropylamine (IPA) to give atenolol [208,214].

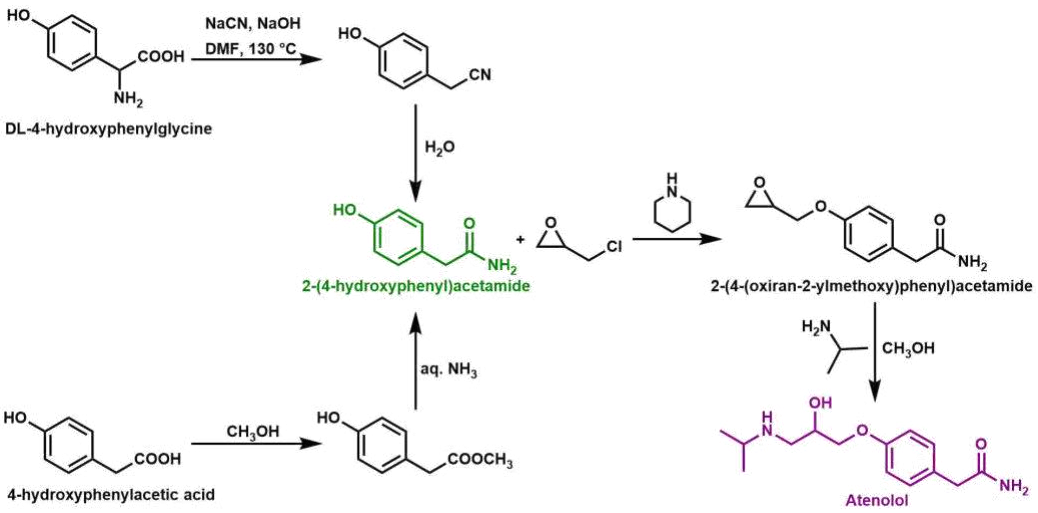

Scheme 1. Industrial synthesis of atenolol.

The industrial processes, however, suffer from severe drawbacks in terms of sustainability as they generate substantial quantities of waste and other by-products that must be appropriately disposed of[214]. Various synthetic strategies for the synthesis of atenolol and related compounds have been reported over the years, nevertheless none of them are very promising from the green chemistry perspective.

Most of these methods rely on the use of toxic or expensive unusual catalysts [215-219], VOC-based harmful solvents[215-218], as well as high reaction temperatures[220], harsh reaction conditions, long reaction times[221] and solubility issues[222], which can hamper the efficiency and scalability of the synthesis. On the other hand, various strategies have been proposed for the enzymatic kinetic resolution of racemic atenolol as well as for the enantioselective synthesis of the (S)-enantiomer to which the maximum β1-blocking activity is attributed[223-227]. Although efficient methods that lead to formation of enantiomerically pure (S)-Atenolol can be of interest to the pharmaceutical industry and academia, the proposed routes use multistep procedures with low overall yield thus not aligning with current environmental challenges[224-226]. A recent approach suggests the use of glycerol as an eco-friendly reaction medium for the last step of atenolol synthesis[228]. Consequently, the development of a more efficient and practical green route to Atenolol API remains an important synthetic goal for numerous academic and

industrial researchers in order to minimize the environmental impact of such pharmaceutical processes.

C4.2 Objectives

Based on the provided informations, the following objectives has been established:

- To address and reduce the environmental impact associated with atenolol synthesis by utilizing DES as a more eco-friendly reaction medium, and streamlining the synthetic process;
- To propose and implement a one-pot, two-step synthesis of atenolol within DES to establish a sustainable and environmentally conscious alternative to conventional industrial synthetic routes;
- To ensure the proposed synthesis adheres to the principles of green chemistry, contributing to a sustainable and environmentally responsible manufacturing process for atenolol, by comparing the overall efficiency of the developed method with the industrial classical method.

C4.3 Results and discussion

Given that DESs have proven valuable for the ring opening of various epoxides using a variety of nucleophiles, leading to products with favourable chemo-, regio-, and stereoselectivities[229-231], we considered using the first reported choline-based DES, formed by naturally available components such as choline chloride (ChCl) and urea (1:2) for the optimization of the first step of the industrial production of atenolol (Scheme 14).

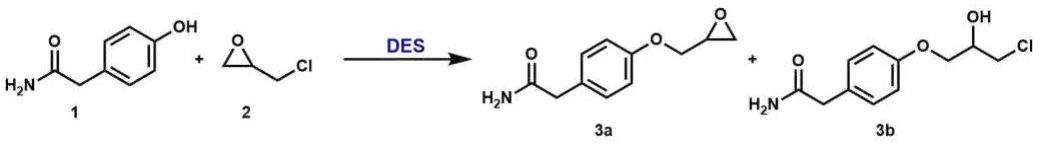

Scheme 14. First reaction step for the formation of atenolol

This DES, also named reline, is widely studied as it is biodegradable and non-toxic in the environment[232,233]. ChCl alone had no catalytic effect being scarcely soluble in epichlorohydrin within 8 h (entry 1, Table 16). Therefore, our investigation proceeded by suspending p-hydroxyphenylacetamide **1** in 1g of the eutectic mixture ChCl:urea (1:2) and magnetically stirring the resulting mixture at 40 °C. After 15 minutes, epichlorohydrin (1 equiv.) was added dropwise and the mixture was further stirred at room temperature (rt, 25 °C) without any additional solvents. After 15 hours of reaction time, only a 54% conversion of **1** occurred (entry 2, Table 16). After removing the unreacted epichlorohydrin by evaporation under reduced pressure conditions, the addition of water resulted in precipitation of the reaction product from the DES mixture. The final characterization of the resulting precipitate confirmed that the reaction led to the formation of a mixture of the corresponding glycidyl ether (**3a**) and the halohydrin (**3b**) in 80% and 20% yield, respectively, calculated by GC/MS. The conversion percentage did not significantly improve even when the experiment was conducted at 40°C, with extended reaction times and/or increased equivalents of epichlorohydrin used (entries 3 and 4, Table 16).

Table 16. Optimization data for the formation of intermediate 3 and 4 in the synthesis of Atenolol

Entry	DES	T (°C)	t (h)	Conversion (%)[c]	Selectivity[c] (%)	
					3a	3b
1[a]	ChCl	rt	8	No conversion	-	-
2[a]	ChCl:U (1:2)	rt	15	54	80	20
3[b]	ChCl:U (1:2)	rt	24	61	80	20
4[b]	ChCl:U (1:2)	40	24	68	85	15
5[b]	ChCl:gly (1:2)	rt	24	73	90	10
6[b]	ChCl:gly (1:2)	40	24	80	90	10
7[b]	ChCl:EG (1:2)	rt	24	85	95	5
8[b]	ChCl:EG (1:2)	40	6	>99[d]	95	5

Table 16. Continuation

9[a]	ChCl:EG (1:2)	40	6	65	93	7
10[b]	EG	40	24	No conversion	-	-

[a] The reaction was performed by using *p*-hydroxyphenylacetamide: epychloridrin in 1:1 molar ratio. [b] The reaction was performed by using p-hydroxyphenylacetamide: epychloridrin in 1:1.5 molar ratio. [c]The conversion percentage and the selectivity were assessed by GC-MS analysis. [d] The DES was recovered and successfully reused for up to 3 cycles. No changes in yields were observed.

At this point, we wondered if ChCl:glycerol (glyceline) and ChCl:ethylene glycol (ethaline) DESs that are efficiently applied in the ring opening of epoxides as well as in nucleophilic bimolecular substitutions could perform better. Notably, the effectiveness of the desired transformation increased when using ChCl: glycerol (gly) (1:2) DES as the reaction medium. The conversion percentage of *p*-hydroxyphenylacetamide (**1**) was 73%, with products yields for **3a** and **3b** calculated by GC/MS at 90% and 10%, respectively (entry 5, Table 16). The conversion percentage of **1** reached 80% when the experiment was conducted at 40°C (entry 6, Table 16). Remarkably, the efficiency of this transformation improved upon switching to ChCl: ethylene glycol (EG) (1:2) as the reaction medium. In this regard, it is worth noting that a rapid and complete solubilization of the starting p-hydroxyphenylacetamide was observed. A very good selectivity for the formation of **3a** was afforded by stirring the reaction at room temperature for 24 hours. The resulting conversion reached 85% (entry 7, Table 16). The best conversion (99%) was achieved in only 6 h when the reaction was performed at 40 °C (entry 8, Table 16). No improved result was obtained carrying out the experiment using a 1:1 molar ratio between the starting compounds (entry 9, Table 16). Furthermore, ethylene glycol used alone (entry 10, Table 16) was ineffective even after 24 h.

Remarkably, the DES used went beyond the role of solvent medium for the reaction, showing a catalytic effect too. Indeed, based on the data previously reported in the literature we hypothesized a plausible mechanism for the reaction of epichlorohydrin with p-hydroxyphenylacetamide catalyzed by ChCl:EG DES

(Scheme 15). Initially, epichlorohydrin (**2**) is activated via the establishment of a hydrogen bonding between the ethylene glycol OH proton and the oxygen of the epoxide ring. This molecular arrangement enables the epoxide ring to open. Then, the HBA component of the DES assists the epoxide ring opening: during this step, the chloride ion acts as a nucleophile, and attacks the epoxide methylene term, forming the intermediate 1,3-dichloro-2-propanol (**A**).

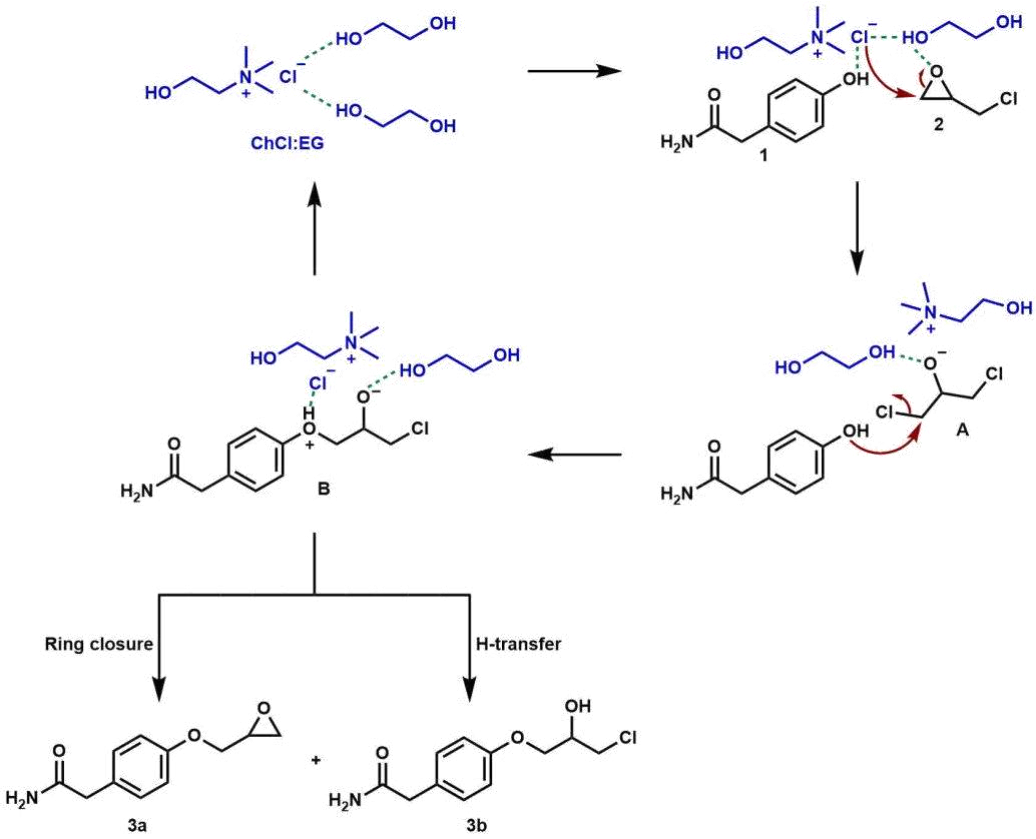

Scheme 15. Hypothesized reaction mechanism for the DES-catalyzed formation of intermediates **3** and **4**.

This hypothesis was confirmed by the results obtained from the GC/MS analysis of an aliquot of the crude reaction mixture, performed after 1 h (Figure 16). The chromatogram showed a peak with a retention time of 7.49 min, whose mass spectrum confirmed the formation of 1,3-dichloro-2-propanol. Successively, the nucleophilic attack of the phenol function of p-hydroxyphenylacetamide (**1**) on 1,3-

dichloro-2-propanol (**A**) generates another intermediate (**B**), that in turn cyclizes to give the glycidyl ether product **3a** through the chloride elimination. The non-quantitative yields in **3a** were attributed to the formation of a secondary product, the chlorohydrin open-chain **3b** through a proton transfer (Scheme 15).

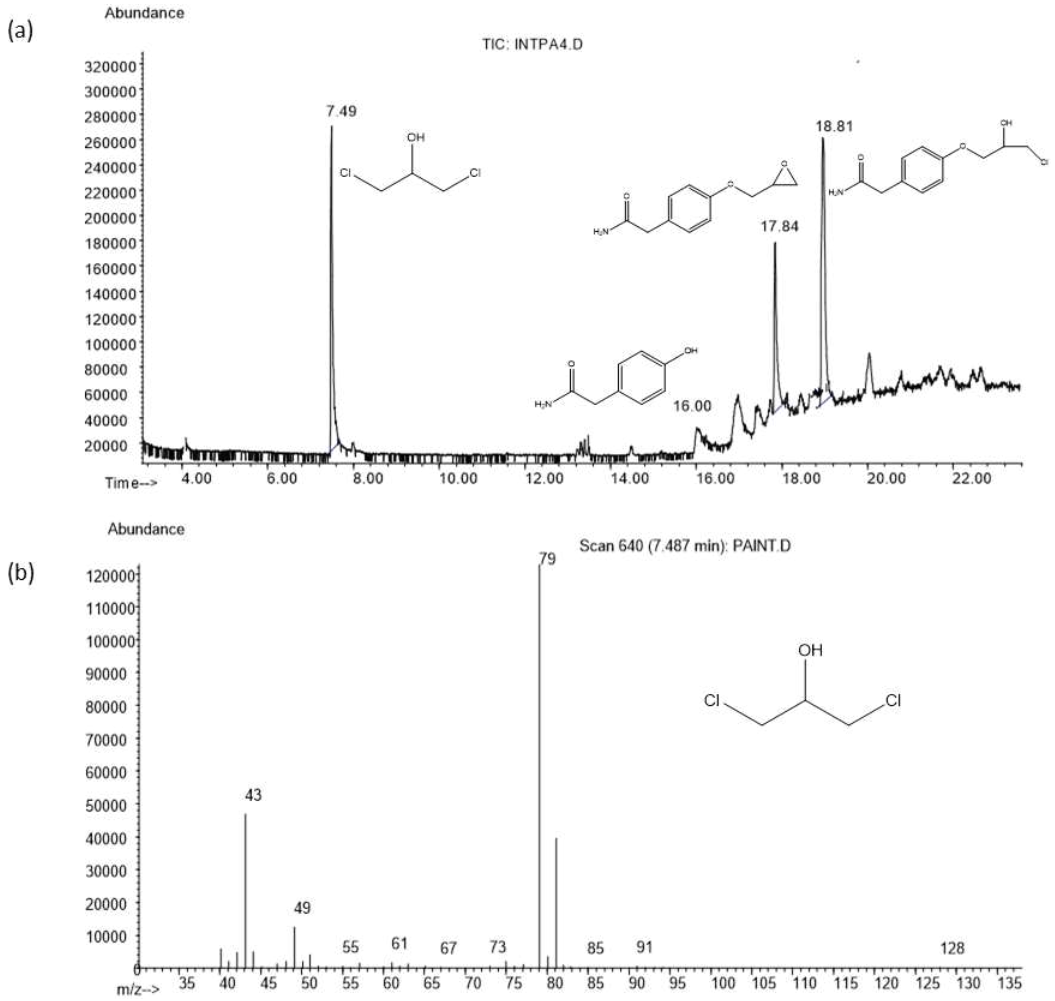

Figure 16. (a) GC spectrum of a crude mixture; (b) MS spectrum of intermediate **3**.

A notable benefit of conducting the reaction in DES was the direct precipitation of compounds **3a** and **3b** as a mixture upon adding water to the reaction mixture. Water competes for interactions with DES anions, disrupting their ability to dissolve the intermediates leading to their precipitation from DES-water mixtures. This

process eliminated the need for laborious work-up procedures or column chromatographic purification.

In order to provide additional support for our proposed mechanism, we conducted an in-depth high-resolution NMR analysis, adopting advanced mono- and two-dimensional homonuclear techniques (Figure 17). The objective was to elucidate the structure of the key intermediate in the synthesis process of atenolol.

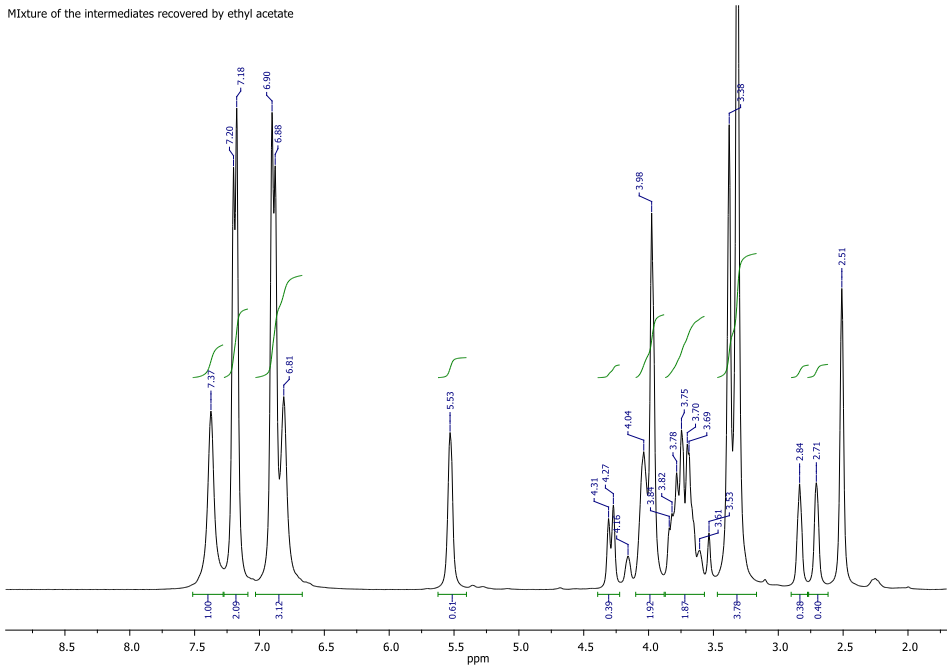

Figure 17. ^{1}H-NMR spectrum of an aliquot of the crude product from reaction (entry 8, Table 16) was obtained. The signal at 2.51 ppm corresponds to the solvent used for the NMR analysis, and it serves as the reference for spectrum calibration

The ^{1}H NMR spectrum displays clearly distinguishable and resolved signals that correlate with the oxyranic structure alone (**3a**). All spectral windows highlight the signals of the proton resonances of each of the proton spin systems of the molecular structure, together with a set of signals not generated by the protons of the oxyranic intermediate, but which can be easily attributed to residues of DES present in the sample and deriving from the extraction with the organic solvent. Starting from the

spectral window of the shielded proton resonances, the pair of signals at 2.71 and 2.84 ppm attributable to the methylene diastereotopic protons of the oxyranic ring is evident. The remaining proton of the three-membered heterocyclic ring generates a fairly deshielded resonance signal centred at 4.29 ppm; the same zone contains the signals attributable to the diastereotopic protons of the oxygen-bound methylene group of the aromatic ring. Aromatic protons generate resonances whose signals are detectable in the spectrum in the form of a pair of apparent doublets at 6.89 and 7.19 ppm. The pair of methylene protons in the α position to the amide carbonyl resonate in the form of a singlet centred at 3.98 ppm, while the two chemically non-equivalent protons of the NH_2 group provide the two signals at 6.81 and 7.37 ppm.

To attribute the remaining resonance signals not generated by protons of the molecular structure of **3a** and hypothesized to be due to the protons of the pair of components of DES, a proton spectrum of an aliquot of the freshly prepared DES was recorded. Finally, the absence of signals attributable to the hypothetical structure of a chlorohydrin open-chain intermediate (**3b**), at least within the limits of sensitivity of the NMR instrumental techniques used, would confirm the formation of oxirane as the only key intermediate during the process under consideration. The chemical shift value of the resonance signal generated by the methylene proton resonance of the oxyranic ring can corroborate the hypothesis. In fact, this value (4.29 ppm) is not common for structurally simple oxyranes, as it is significantly downfield shifted due to the transfer of electron density to the oxygen atom which is supposed to be involved in hydrogen bond networks with the OH group of ethylene glycol. On the other hand, this conclusion is in total agreement with the results obtained from the GC-MS analysis performed on the same raw sample subjected to the spectroscopic investigation. To further confirm the hypothesis, a two-dimensional homonuclear NOESY correlation spectrum was recorded on the same sample for which the spectrum of the oxyranic intermediate was acquired in the presence of DES (Figure 18).

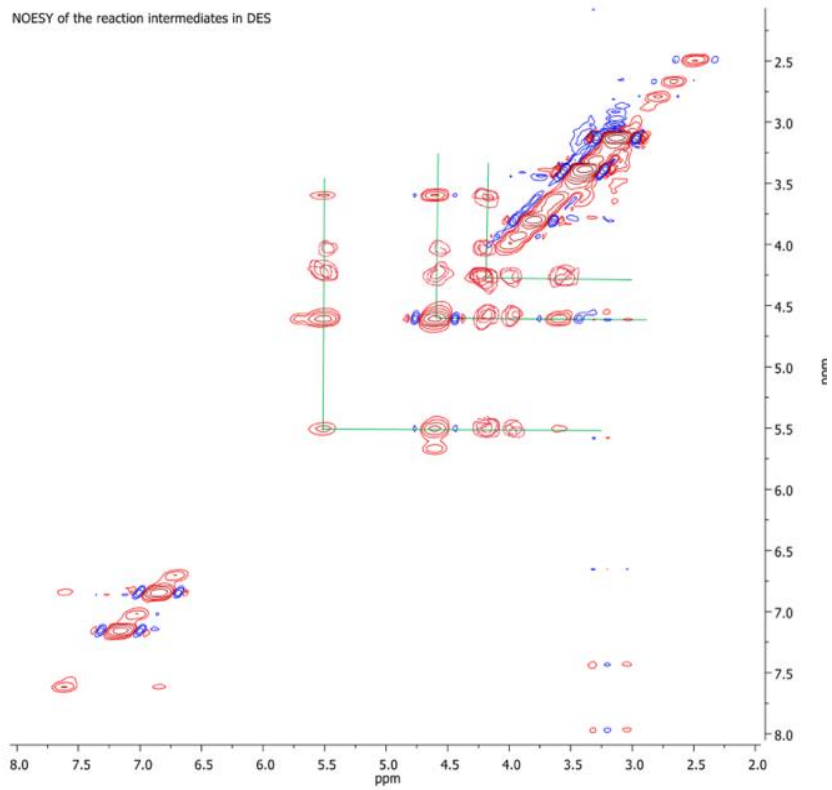

Figure 18. ^{1}H,1H-2D-Homonuclear NOESY spectrum recorded on a sample containing the oxyranic intermediate, in the presence of the DES.

The plot of the two-dimensional homonuclear spectrum clearly highlights the spatial correlations between the choline OH proton (5.50 ppm), the ethylene glycol OH (4.52 and 4.04 ppm), the oxyrane CH proton (4.19 ppm), and the glycol and choline methylene systems (range between 3.50 and 3.80 ppm), confirming the installation of a network of hydrogen bonds whose main partners are the oxyranic ring (via its oxygen atom) and the ethylene glycol. The same downfield shift due to the OH-O interaction would also be operative on the methylene proton pair of the three-terminus ring, thus determining the activation of the CH_2 group at the nucleophilic attack that completes the synthesis of Atenolol.

With this data in hand, and considering that also the final step of the industrial production of Atenolol API (see scheme 13) involves a ring-opening reaction, we

envisaged the feasibility of performing a one-pot, two-step synthesis of atenolol in ChCl:EG DES. A tool to reduce waste during chemical reactions is the one-pot synthesis approach that avoids the purification and isolation of intermediates, thereby reducing the amount of solvents used.9 As a result, one-pot synthesis holds promise for addressing various challenges encountered in pharmaceutical and synthetic laboratories, including reduced exposure time and simplified procedures.

To demonstrate this, we replicated the experiment involving the reaction between p-hydroxyphenylacetamide **1** and epichlorohydrin **2** in DES to yield the corresponding glycidyl ether **3a** and chlorohydrin **3b** intermediates. Excess epichlorohydrin was removed under vacuum, and isopropylamine (IPA, 3 equiv.) was directly added to the reaction mixture, which was further stirred at 40 °C (Scheme 16).

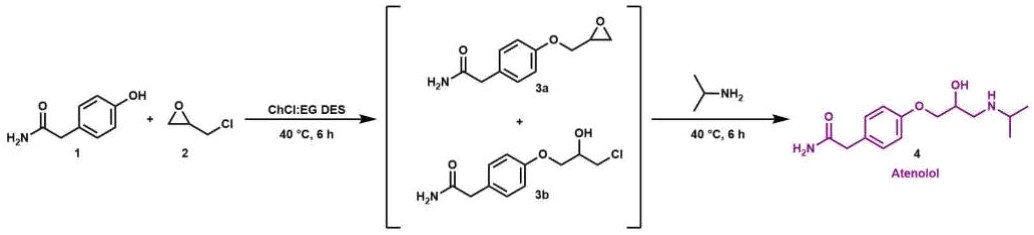

Scheme 16. Second step in the DES-based synthesis of atenolol.

As expected, the reaction proceeded smoothly in 6 hours, and upon completion, the excess IPA was removed via vacuum evaporation. Quenching with an aqueous solution of $NaHCO_3$, at this point, caused the formation of a suspension. The addition of tert-butylmethyl ether resulted in the precipitation of a white solid, which was subsequently filtered, washed with water, and dried to give the corresponding atenolol (**4**) with an overall yield of 95%. Characterization of Atenolol was performed using NMR spectroscopy. Even in this final step, the ring opening of epoxide in the intermediate **3a**, assisted by isopropylamine, was conceivably aided by the hydrogen bond network formed by the components of the DES. Consequently, isopropylamine attacked the less hindered side of the epoxide, yielding the desired

Atenolol **4**). Atenolol was successfully isolated and recovered without the need for chromatographic purification.

Given the estimated growth of Atenolol market and its relevance as an antihypertensive drug, the potential applicability for large-scale manufacturing of the developed method has subsequently been evaluated. On this matter, the robustness of this transformation in the mentioned DES was confirmed through a scale-up investigation. From an industrial perspective, evaluating the results of gram-scale production is crucial. In this regard, the entire process was successfully scaled up to 1g of p-hydroxyphenylacetamide (**1**) (6.62 mmol) using 3 mL of ChCl:EG DES. Following the detailed procedure outlined above, atenolol was obtained with a yield of 95%. Further scaling up the reaction to 10 g of **1** (66.2 mmol) in 30 mL of DES resulted in Atenolol being recovered with excellent yield, indicating the potential switch to industrial-scale production using the developed method.

Furthermore, from an industrial perspective, the recovery and reuse of DES play a significant role in addressing both economic and environmental concerns within chemical processes. The assessment of DES reusability is detailed in Table 16 (entry 8). Following completion of the reaction, water was introduced to the reaction mixture, vigorously shaken, and the solid product filtered off. The ChCl:EG deep eutectic solvent was then recovered from the filtrate by evaporating the water phase under vacuum at 80°C, allowing for its reuse with minimal loss of activity.

In line with the first principle of green chemistry, we proceeded to evaluate the E-factor of the proposed procedure. By incorporating this metric into our analysis, we aimed to provide a comprehensive understanding of the environmental impact of our synthetic approach, thereby contributing to the advancement of sustainable manufacturing practices in the pharmaceutical industry. In this regard, the green advance of our work is the lack of purification of the product by chromatography and the reduction of the waste generated compared with the two-step traditional synthesis. Specifically, we found an E-factor of **3** for the first step. The cumulative E factor extends the concept of the E-factor to consider the entire synthetic route,

including all intermediate steps. A cumulative E-factor of 22 was calculated for this process. Moving beyond the use of the E-factor, a deep insight evaluation of the greenness of our method using the First Pass CHEM21 Metrics Toolkit[12.13] was performed enabling the comparison of these values (whenever possible) with the conventional industrial routes[234,235] to Atenolol in order to ensure a truly holistic approach. Table 17 details the values calculated for the main green metrics including atom economy (AE), reaction mass efficiency (RME), optimum efficiency (OE), mass intensity (MI), and process mass intensity (PMI) metrics, with a breakdown of the latter for "chemicals" (reactants, reagents, and catalyst) (PMI RRC), chemical and reaction solvents (PMI Solv).

Entry	Ideal Values	Our work	Jang *et al.* [234]	Kitaori *et al.* [235]
AE (%)	100	88	88	88
RME (%)	100	54	6	14
OE (%)	100	61.6	7.1	15.5
PMI	1	3.9	25.2	10.8
PMI_{RRC}	1	1.8	16.0	7.5
PMI_{Solv}	1	2	9.2	3.3
Solvents (First Pass)				
Catalyst/enzyme (First Pass)				
Energy (First pass)				
Work-up				

Tabella 17. Comparison of the green metrics of the developed method with the available procedures published for the synthesis of atenol.

Most of the parameters evaluated proved the greenness of our work among the others. Specifically, RME value of this methodology was 54%, in contrast to 6% and 14% obtained for the other procedures. Consequently, the OE value (61.6%), calculated as the ratio of RME and AE, resulted in a better percentage rather than the others (7.1% and 15.5%, respectively). Additionally, a notable difference in the case of the PMI values was observed. PMI is defined as the total mass of reactants used to produce a specified mass of product, including solvents, work-up and purification steps, additives and catalysts. It represents the most important metric for pharmaceutical companies in evaluating the greenness of a chemical process. On this matter, an ideal process should have a PMI value close to 0; higher values of PMI mean a greater negative environmental impact of the method. In our case PMI, PMI_{RRC} and PMI_{Solv} values were 3.9, 1.8 and 2.0, respectively. The same parameters were also evaluated for the patented routes taken into account, resulting in higher values. Therefore, from a green chemistry perspective, it is clear that the DES-based one-pot synthesis of Atenolol offers the best route with respect to the classical procedures.

Likewise, the overall qualitative evaluation further highlights the greenness of the developed method. Qualitative parameters play a pivotal role, particularly in their assessment of the intrinsic safety of utilized materials and the efficiency of energy. These parameters are systematically classified into three categories: green, amber, and red flags, indicating the desirability of preferred conditions, acceptability with certain concerns, and the avoidance of undesirable situations, respectively. More specifically, the flags assigned to reagents and work-up tabs align with the results obtained in the mass metrics. Both patented procedures raised concerns, marked by a red flag regarding solvents and catalyst/enzyme usage. Additionally, concerning energy consumption, an amber flag was noted for Jang *et al.* while Kitaori *et al.* received a green flag. Nevertheless, in an overall view, our approach outperforms in terms of all the parameters considered, making this approach more desirable.

C4.4 Conclusions

Based on the previous results, the following conclusion have been drawn from this chapter:

- The developed method allowed for a one-pot, two-steps synthesis of atenolol in ChCl:ethylene glycol DES, demonstrating the versatility of the system;
- The proposed mechanism suggested the involvement of hydrogen bonds between the DES components and the starting materials used, facilitating the epoxide ring opening and the consecutive formation of atenolol. The role of both components (hydrogen bond acceptor and donor) of the DES resulted crucial for the reaction success;
- The scalability of the process to gram-scale production was successfully demonstrated, emphasizing its potential for industrial applications. Furthermore, the recovery and reuse of DES for the first step were explored, showing minimal loss of activity after several cycles;
- The 'greenness' evaluation using the First Pass CHEM21 Metrics Toolkit highlighted the superior atom economy, reaction mass efficiency, and overall process mass intensity of the DES-based synthesis compared to the already existing methods.

In summary, the study presented a robust, environmentally friendly, and economically viable method for the synthesis of atenolol, showcasing the potential of deep eutectic solvents in industrial processes.

CHAPTER V

DESs for improving the solubilization and delivery of APIs

C5.1 Antecedents

As mentioned in the general introduction, a key challenge in drug manufacturing and development is the need to improve the permeability and bioavailability of poorly water-soluble drugs. Solubility, as a fundamental characteristic, is one of the most important physicochemical phenomena in pharmaceutical sciences and pharmaceutical industry. The efficiency of a drug can be severely limited by its low aqueous solubility. Moreover, the reactivity, stability, and bioavailability of an API are profoundly impacted by its capacity to dissolve in a specific solvent[236].

On this matter, investigations into solubility, that encompass both equilibrium and kinetic methodologies, play a pivotal role across various critical domains, including advancing liquid dosage, improving bioavailability, facilitating crystallization, assisting in pre-formulation and enabling thermodynamic modeling[237]. Consequently, it can be readily inferred that solvents play an exceedingly important role in the pharmaceutical industry, potentially constituting up to 90% of all chemicals utilized in this sector[25].

Given the substantial quantity of solvents utilised, it is imperative to focus not only on their efficacy in dissolving desired compounds but also on their environmental impact. Traditional organic solvents, commonly employed to enhance solubility, present challenges in pharmaceutical applications due to factors such as toxicity and unpleasant odour or taste. Hence, there is a growing demand for new solvents or media capable of providing higher drug solubility while ensuring environmental and health safety.

Over the last few years, several methods for increasing the solubility of hydrophobic drugs have been developed, such as solid dispersions, soluble cyclodextrin complexes, self-emulsifying drug delivery systems, nanocrystals, ordered mesoporous silica, nanonization, cosolvency.

In this context, DESs have recently gained significant interest as alternative vehicles for the preparation of pharmaceutical formulations. Their adoption is seen as a promising strategy to address solubility challenges while concurrently adhering to safety and environmental requirements in drug development[137].

C5.1.1 Solubility concerns of Dapsone

Dapsone (DAP) or 4,4'-diaminodiphenylsulfone, is a derivative of aniline belonging to the group of synthetic sulfones (Figure 19). It is a promising therapeutic agent for a wide range of dermatological diseases, since it combines antimicrobial and anti-inflammatory activities[238]. Its first use dates back to 1940 for the treatment of leprosy. It was later tested for skin disorders such as acne or dermatitis herpetiformis[239]. Furthermore, its use as an antimalarial and antileishmanial drug has also been described[240]. Even today, after half a century, dapsone represents a drug widely used in the treatment of acne.

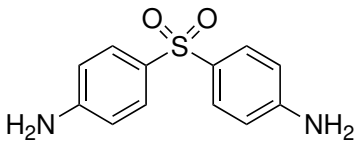

Figure 19. Chemical structure of dapsone.

In light of the Biopharmaceutics Classification System (BCS), dapsone is classified as class IV, which reflects its limited water solubility as well as its reduced permeability[241,242], leading to a low therapeutic index[243]. Because of the above features, the transdermal delivery route, instead of the oral one, is the preferred way of administering this drug[244,245]. These limitations were the inspiration for various strategies aimed at resolving the poor aqueous solubility and low bioavailability of DAP[246,147]. For example, new dapsone salts, such as chloride, bromide, and nitrate salts, were prepared and subsequently fully characterized using X-ray diffraction techniques (single and powder), spectroscopic methods (FT-IR) and thermal analyses (DSC and TGA)[248]. X-ray results revealed that dapsone chloride and bromide are isomorphic compounds. The equilibrium solubility of dapsone salts was

compared to that of free dapsone in three aqueous media: HCl buffer pH 1.2, acetate buffer pH 4.5, and phosphate buffer pH 6.8. Higher solubility values were observed in acidic media, and dapsone bromide was found to be slightly more soluble than free dapsone. However, this strategy cannot be employed for dermatological preparations due to the acidic nature of the medium where increased solubility of salts is observed. Additionally, the dapsone salts decompose without melting and exhibit lower thermal stability compared to pure DAP.

In general, from various studies reported in the literature, it is evident that the solubilization of DAP requires an increase in temperature, a pH variation, or the use of solvents not well-suited for dermatological applications. For this reason, there is a current need for new solubilization strategies for the mentioned drug, which could potentially be a breakthrough, especially for topical preparations.

C5.1.2 Solubility theme of Mesalazine

Mesalazine (Figure 20), also known as mesalamine or 5-aminosalicylic acid (5-ASA), is a derivative of salicylic acid, belonging to the class of non-steroidal anti-inflammatory drugs (NSAIDs). It is used for the treatment of inflammatory bowel diseases such as indeterminate inflammatory bowel disease (IBDU), ulcerative colitis, and Crohn's disease[249]. Mesalazine is classified in the biopharmaceutics classification scheme as a class IV drug, since it has low permeability and low solubility in water[250].

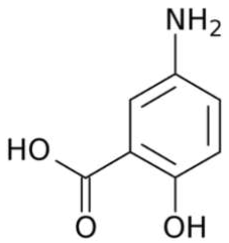

Figure 20. Chemical structure of Mesalazine.

In recent years, several controlled release systems have been developed to ensure appropriate release at the colon level to improve the treatment of IBD. Various studies regard on increasing the solubility of mesalazine by using different

techniques, including salt formation, particle size reduction, pH adjustments, and the use of solubility enhancers such as cosolvents, complexing agents, and prodrugs[251]. Commercially available mesalazine represents the active component of prodrugs such as sulfasalazine or balsalazide, which, undergoing hepatic metabolism, release the same and, respectively, sulfapyridine and 4-aminobenzoic acid as secondary metabolites. The use of prodrugs aims to improve the physicochemical properties (solubility, permeability, and stability) of active ingredients or to direct their release to a specific site[252]. Prodrugs are prepared by linking the active ingredient to a non-toxic chemical agent, which, due to pH and/or enzyme action in the colon, allows the release of 5-ASA in this region. However, the major problem with the use of prodrugs is the dosing regimen, which leads to more pronounced side effects. For this reason, the use of an alternative administration method should reduce the frequency and doses, minimizing dose-related side effects.

Other strategy used to improve the solubility of 5-ASA involve a pH-dependent or time-dependent approach. This relies on the use of a carrier that does not dissolve in the stomach pH but begins to dissolve and release the active ingredient in the terminal ileum[253]. The latter is based on the use of carriers that delay the release time of the active ingredient, ensuring release when the formulation reaches the target site.

Among other approaches, the use of nanoparticles, particularly polysaccharide nanoparticles, is of particular interest due to their renewable, biodegradable, and cost-effective nature. These nanoparticles are designed in a wide variety of shapes and tend to enhance the solubility and permeability of the drug[254,255].

Finally, another approach for improving the solubilization of mesalazine is the use of cosolvents, which represents the most commonly used technique in the pharmaceutical industry. Specifically, the solubilization profile of mesalazine has been tested in various aqueous cosolvent systems, including ethanol, propylene

glycol, 2-propanol, and different solvents such as ethanol, methanol, tetrahydrofuran; revealing the "preference" of mesalazine to dissolve in apolar systems rather than polar ones[256–258].

C5.2 Objectives

Based on these informations, the following objectives have been established:

- To investigate the potential of DESs in increasing the solubility profile of the reported drugs: it involves experimental work to determine the solubility of the drugs in various DES formulations. Increased solubility is desirable as it can enhance the drug's bioavailability and efficiency;
- To deep insight into drug-DES molecular interactions: by employing advanced analytical techniques such as Differential Scanning Calorimetry (DSC), Nuclear Magnetic Resonance (NMR), and Fourier Transform Infrared Spectroscopy (FT-IR) to study the molecular interactions between the drugs and the DES components;
- To evaluated the release profile of the drug dissolved in DES: it involves the study of the release kinetics and mechanisms, providing valuable information on the sustained release properties of the drug-DES formulation. This is important for designing drug delivery systems that control and extend the release of the drug, potentially improving therapeutic outcomes and minimizing side effects.

In summary, these objectives collectively aim to comprehensively investigate the use of Deep Eutectic Solvents in enhancing drug solubility, understand the molecular interactions involved, and assess the release profile of drugs dissolved in these solvents. The findings from these investigations can contribute to the development of more effective and controlled drug delivery systems.

C5.3 Results and discussion

C5.3.1 Solubility enhancement of Dapsone

The investigation started with the selection and preparation of DESs for the solubilization of dapsone. Among the various possible types of DES, over the years, THEDES, a new type of DES in which at least one of the components is an active ingredient, has been developed. As already mentioned, this class of DESs has a great potential as dissolution enhancer in the development of novel and more effective drug delivery system. DAP is structurally characterized by the presence of groups that can act as donors and acceptors, resulting in a possible ideal component for the formation of THEDES. This strategy allows to overcome important challenges related to drugs and APIs, such as polymorphism, as well as increasing the solubility and bioavailability of the target API which leads to greater bioavailability. Based on these considerations, 1:1 and 1:2 molar ratios between choline chloride and DAP were tested, in order to obtain a stable and useful eutectic mixture for the intended purpose. However, none of the molar ratio tested lead to the formation of a DES led to a liquid mixture. Specifically, the mixture of the two components in a 1:1 molar ratio lead to the formation of a viscous liquid that quickly solidifies at room temperature. At the same time, the mixing of components in a 1:2 ratio leads to a mixture that remained solid. These observations were corroborated by POM images where the presence of crystals were observed (Table 18).

Thus, the investigation continued by preparing DESs for the direct solubilization of dapsone. On this matter, choline chloride was chosen as the hydrogen bond acceptor, while an organic acid, such as ascorbic acid, and a polyalcohol, like propylene glycol, were selected as hydrogen bonds donors. As already mentioned in general introduction, choline chloride is a complex B vitamin that plays a vital role in cellular metabolism, commonly used as a food additive. At the same time, ascorbic acid, known as ascorbate or vitamin C, can promote collagen biosynthesis, provide photoprotection, improve immunity, and reduce melanin production[259]. On the other hand, the use of DES based on choline chloride and ascorbic acid at 2:1

molar ration has already been reported as an exciting possibility as solubilizing vehicle of APIs[260]. Moreover, as an alternative to the DES based on the use of organic acid as a donor, it was also decided to study the possibility of using a DES composed of choline chloride and a polyol as a donor[261]. The choice fell on propylene glycol, often used as HBD, as it is a viscous liquid and a safer option to ethylene glycol, recognized in the pharmacopoeia as an excipient for the formulation of dermatological preparations. In addition, it is used as a non-toxic polyol in food-processing and for production of polymers. Therefore, the DESs resulting by their combinations can be considered harmless, non-toxic, and advantageous for their applications such as drug delivery systems, given their natural and therapeutic properties and high biodegradability and biocompatibility.

DESs	HBA	HBD	HBA/HBD molar ratio	Aspect	POM images
ChCl:AA	ChCl	AA	2:1	Viscous yellow liquid	
ChCl:PG	ChCl	PG	1:3	Transparent liquid	
ChCl:DAP	ChCl	DAP	1:1	Viscous liquid that rapidly solified at rt	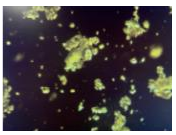
			1:2	Solid	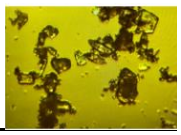

Table 18. POM analysis of the prepared DESs and THEDESs.

The potential of the prepared DESs in increasing the solubility of DAP was explored. The shake flask method represents a typical method for determining the solubility of pharmaceuticals in solvents[262]. In this process, an excess amount of the

drug is added to a given volume of solvent, and the sample is placed under constant stirring at room temperature for a sufficient time to reach equilibrium. After equilibrium, the undissolved solid is separated from the solution, and the concentration of the dissolved drug is measured by an appropriate method. DAP presents a water solubility of 380 mg/L. The results showed that the solubility of DAP was largely increased in the considered DESs, compared to its solubility in water. In particular, the solubility of DAP in DES consisting of ChCl and AA amounts to ~150 mg/mL; a greater solubility of the same drug was found in the DES consisting of CC and PG, which turns out to be 500 mg/mL. Since propylene glycol is liquid at room temperature, it was interesting to verify whether this component could dissolve the drug. Therefore, the solubility of DAP in propylene alone was tested at the concentration of 500 mg/mL. Interestingly, it was observed that the addition of this quantity of dapsone led to the formation of a very turbid mixture, even after 48 h under constant stirring at rt. This result further confirmed the important solvent power of the DES considered, improving drug solubility. The successful dissolution of the drug in the DES systems was confirmed by POM images, since no crystal-like structures (black images) were observed when compared with drug in propylene glycol.

ChCl:AA is characterized by high viscosity, given the extensive hydrogen bonds between the DES components. This can be a limiting factor affecting homogenization/solubilization[263]. The addition of water to the DES is generally used to reduce viscosity, modifying hydrogens bonds in DES, thereby facilitating mass transfer from the solute to the solution[264]. More importantly, the dissolving capacity of DES can be adjusted by varying the water content. Therefore, formulations containing 10% and 20% by volume of water in the DES-water mixture were tested to dissolve the model drug. Higher percentages showed to cause the DES solubilization by breaking up the hydrogen interactions among the components and promoting hydrogen interactions between the water molecules themselves, reducing the ability of the DES in enhancing dissolution. Although the addition of water greatly reduced viscosity, this did not significantly improve the solubility of the

model drug in DES, reaching a maximum of 200 mg/mL in the DES with the 20% water content.

The increase in solubility of DAP in the DESs can be justified by the formation of hydrogen bonds between DAP and DES components. In order to detect intermolecular interactions between DAP and the DESs' components, the DSC, FIT-IR, and NMR analysis were performed on the pure drug, the single DESs, and the drug-DES mixtures. In particular, the investigation mainly concerned the CC:PG DES, given its highest solvation power.

DSC analysis of the pure DAP, the ChCl:PG DES, and the drug-DES mixture was adopted as an efficient technique to track thermal and crystallographic changes of the resulted mixtures. Generally, the thermogram of ChCl presents an endothermic peak at 81 °C which is ascribed to a crystallographic arrangement during its transition phase[265,266]. On the other side, the thermogram of PG is dominated by an endothermic peak at −59 °C, which corroborated previous results in the literature. Like all eutectic binary mixtures, the DSC thermogram of the ChCl:PG DES represents a complex formed by strong hydrogen bonding between the starting components. This was corroborated by the absence of the melting endotherms of propylene glycol and choline chloride peaks (Figure 21, thermogram 3). As a consequence, a strong depression on the melting points occurs.

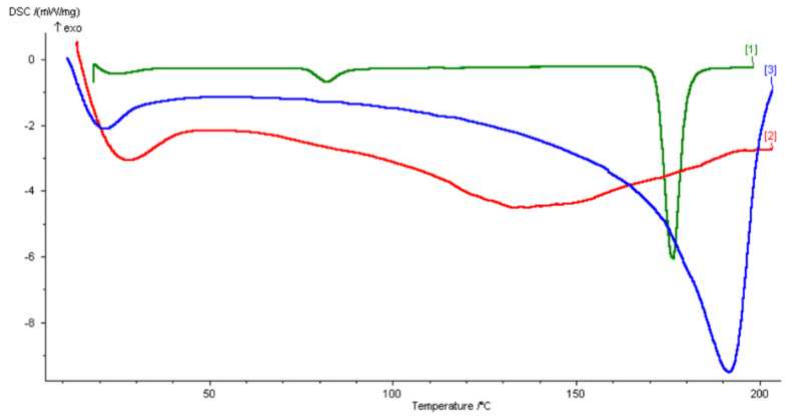

Figure 21. DSC thermograms of (1) dapsone, (2) drug-DES mixture, and (3) CC:PG DES.

The addition of the drug in the eutectic mixture did not significantly affect the main crystallization and melting peaks of the DES (Figure 21, thermogram 2). However, the melting endotherm of DAP at 176.7 °C (Figure 21, thermogram 1) no longer existed. The absence of the melting point of the drug in the thermogram of the drug-DES mixture highlighted the ability of the DES to maintain the drug in the soluble state up to temperature that is lower than its melting point.

In order to gain deep insight into the intermolecular interactions between DAP and the ChCl:PG DES components, the infrared spectra of pure DAPs as well as DES and the drug-DES system have been performed and analysed. Changes in the structure can be seen from the widening or merging of the peaks involving hydroxyl and amino groups, the shift of carbonyl peak of acids, or loss of the representative group peak of pure substances. FT-IR spectrum of pure dapsone (Figure 22a) is characterized by a band at 3300 to 3400 cm^{-1}, corresponding to the stretching of the amino group, and peaks between 1590 and 1550 cm^{-1}, corresponding to the bending vibration of -NH_2 groups. Other bands at 1143 and 1180 cm^{-1} are ascribed to the symmetric and asymmetric vibrations of the sulfone group (-SO_2). Finally, the bending (out-of-plane) vibration of *p*-disubstituted aromatic ring can be found at 831 cm^{-1}. As shown in Figure 22c, the FTIR spectrum of the DAP-DES mixture was nothing more than a combination of the single DAP and DES spectra. In fact, all the previous bands are clearly observed in the spectrum of drug-DES system, with no radicle change related to the major vibrations of the single spectra. The most obvious differences were observed in the 3200–3600 cm^{-1} region, related to the elongation vibrations of hydroxyl groups (-OH) of the DES components and the stretching of the amino group (N-H) of the DAP, and in the 1140 and 1190 cm^{-1} region, ascribed to the symmetric and asymmetric vibrations of the sulfone group of DAP. The enlargement and shifting of such bands, respectively, are attributed to the formation of hydrogen bonds between the components. In all spectra analysed, the appearance or disappearance of IR bands were not observed, suggesting that the drug preserved its chemical structure when it interacts with DES components

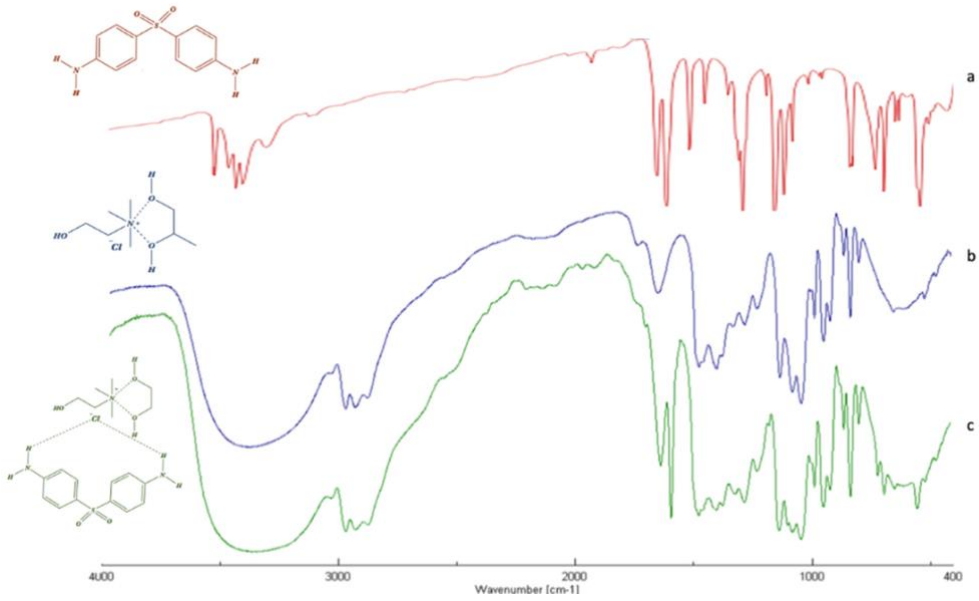

Figure 22. FT-IR of dapsone (red) (a), CC:PG DES (blue) (b) and drug-DES mixture (green) (c).

The NMR spectra recorded on samples of choline chloride and DAP, dissolved with no pre-treatment in exadeuterated dimethylsulfoxide (DMSO-d_6) as the solvent, showed the respective chemical structural features and the appropriate signal intensities (Figure 23, spectra A and B). DMSO-d_6 was used as the solvent due to CC and DAP good solubility herein, and its weak effect on the interaction with the other components in DES. All proton resonances were attributed and confirmed comparing the experimental chemical shifts with those already reported in literature for the same compounds. Contrariwise, all proton signals of propylene glycol (PG) were attributed according to the literature.

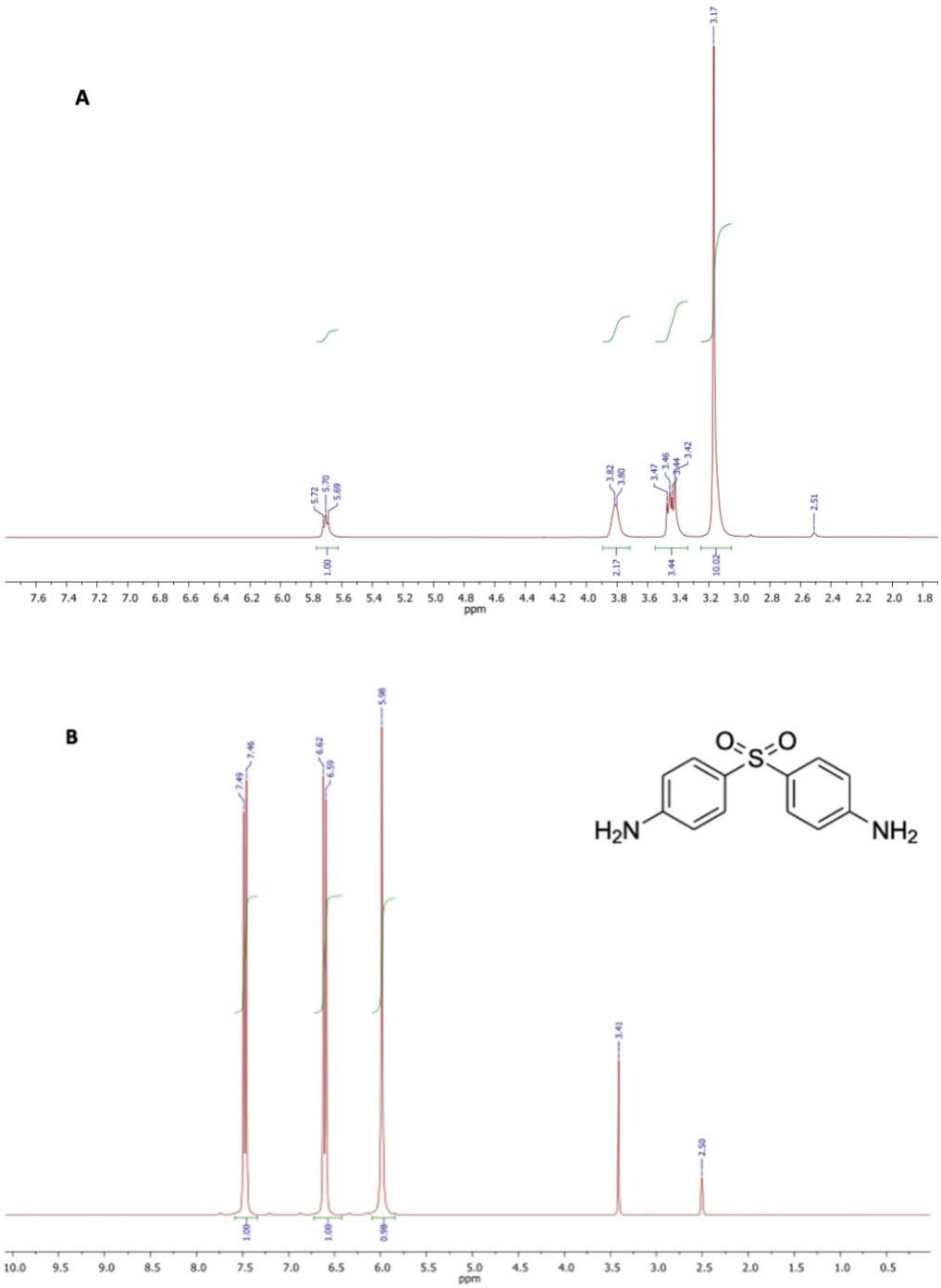

Figure 23. ^{1}H NMR spectra of choline chloride (ChCl) (**A**), and Dapsone (**B**).

The proton spectrum depicted in Figure 24 A, showed the characteristic singlet generated by the three methyl groups of the choline structure, centered at 3.17 ppm. Two multiplets at 3.38-3.49 ppm and 3.75-3.83 ppm were attributed to the protons of methylene groups bound to the quaternary nitrogen and the hydroxyl function, respectively. The triplet appearing at 5.70 ppm was generated by the OH proton resonance. The spectrum of DAP (Figure 24 B) showed three signals: a singlet at 5.98 attributable to the four protons of the amino groups, and two doublets centered at 6.61 and 7.48 ppm attributable to the resonances of the aromatic protons in the ortho position with respect to the amino and sulphonic groups, respectively. The singlet at 3.41 was due to impurities.

The chemical structure and purity of the DES, and the DES-DAP system were likely confirmed by proton and carbon NMR spectroscopy. The proton spectra are displayed in Figure 24. In that case, the ^{1}H NMR analysis was useful to confirm the existence of molecular interactions between the components of DES, on the basis of the chemical shift variations observed for some spin systems. With reference to the spectrum A in Figure 24, the DES showed all the expected proton resonance signals. In particular, signals appearing at 5.55 (triplet), 4.57 (triplet), and 4.51 (doublet) ppm, were due to the resonances of OH protons of CC and PG. The signal centered at 3.82 ppm, and the signal appearing between 3.40 and 3.50 ppm were respectively attributed to the CH_2O and CH_2N methylene protons of CC structure, while the well-defined signals centered at 3.24 and 3.56 ppm were generated by the CH_2 protons of PG. The intense singlet at 3.15 ppm is referred to as the nine methyl protons of CC, and this signal overlaps the multiplet generated by the methine proton in the PG structure. Finally, the doublet at 0.99 ppm was attributed to the CH_3 protons of PG. Integral values of all signals in the spectrum were found to be consistent with the molecular composition of the DES. No other signals were observed in the spectrum, indicating the DES purity. Comparing with the spectra of pure CC and PG, the chemical shift of OH of ChCl moved to upfield, and the OH protons of PG moved to downfield in the binary system CC-PG. It is likely that the intramolecular hydrogen bonds in ChCl were broken, and new intermolecular

hydrogen bonds formed between ChCl and PG. After DAP was loaded into ChCl-PG DES, all the active hydrogen signals of each component in the formed ternary mixture were clearly distinguishable and attributable (Figure 24, spectrum B).

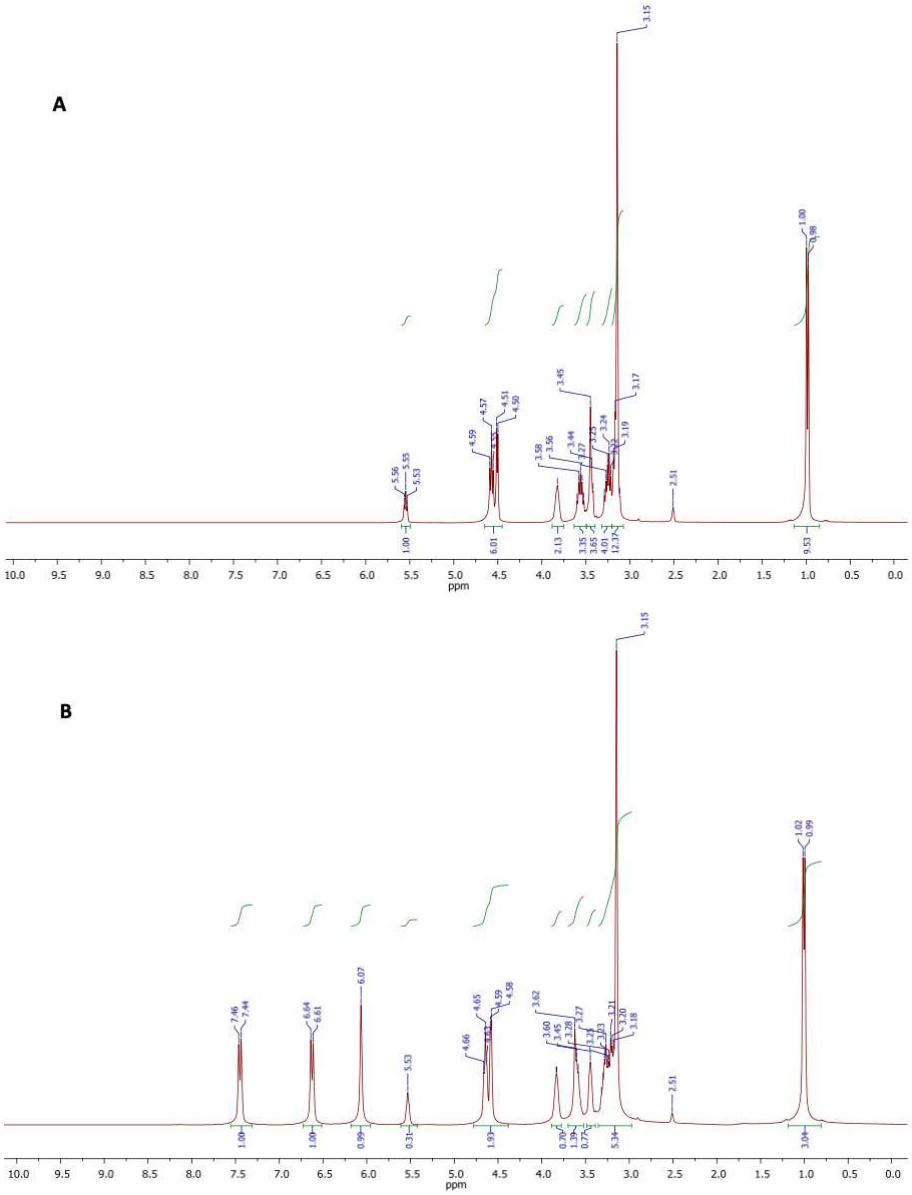

Figure 24. ^{1}H NMR spectra of the ChCL:PG DES (A), and DES-DAP ternary system (B).

The spectral region between 5.75 and 7.75 ppm showed all signals attributable to the resonance of the dap protons. The signals of all C-H protons in the structures of ChCl and PG were found in the spectral region between 0.80 and 4.00 ppm.

Furthermore, the ^{1}H NMR spectrum of the DES-DAP system could infer the presence of interactions between DAP and the DES components. In fact, it is important to note the chemical shift variations of resonances attributed to NH and OH protons. In particular, the NH_2 protons of DAP resonated at 6.07 ppm, showed a significant downfield shift with respect to the signal featured by the spectrum recorded for the sample of standard DAP (5.98 ppm), and suggesting the NH_2 groups might be involved in the formation of H-bonding networks with the DES components.

5.3.2 Dapsone Release

To evaluate the suitability of the DES for dapsone release, in vitro studies were performed at different time intervals (15, 30, 60, 90, and 120 min) and at a pH 7.4 and 34 °C, with the aim to simulate physiological conditions. The drug release profile was determined by UV-Vis spectrometry and expressed as a cumulative percentage of the released drug as a function of time (=0.908, =293 nm). Data analysis showed a total and massive release of the drug in the first two hours while no release was observed in the following hours (Figure 25).

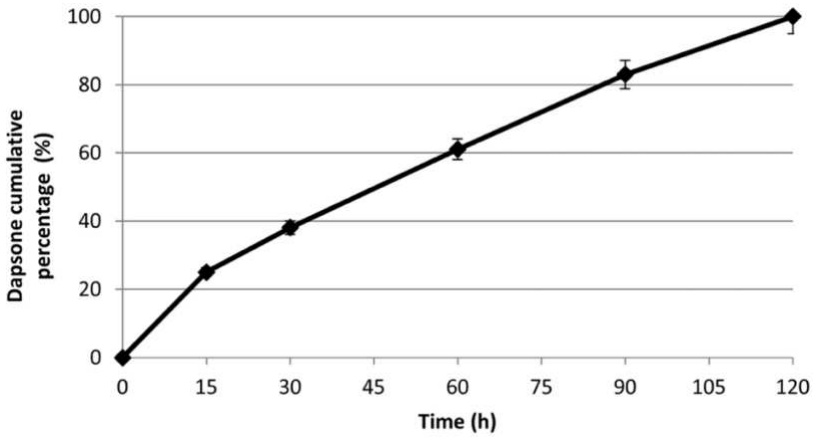

Figure 25. The in vitro cumulative release of Dapsone from the DES in pH 7.4 at 34 ◦C

This release profile can be considered very advantageous and useful for obtain the desired therapeutic effect. In particular, the complete release of the loaded drug within 2h results quite satisfactory

5.3.3 Solubility enhancement of Mesalazine

At first, the objective of this study was to prepare a Therapeutic Deep Eutectic Solvent where mesalazine would serve as a direct component of the DES. Mesalazine is a monohydroxybenzoic acid, meaning salicylic acid substituted with an amino group at position 5. Structurally, it contains different functional groups (amino, carboxylic, and hydroxyl) that make it a potential hydrogen bond acceptor and/or donor in DES formation. For this purpose, mesalazine was combined with various components commonly used in the formation of THEDES, such as betaine, menthol, lactic acid, etc.. Nevertheless, as shown in Table 19, the formation of a THEDES was not achieved in any case. Specifically, when mesalazine was used in combination with choline chloride, betaine, lactic acid, and arginine, the mixture remained solid at all tested molar ratios (Table 19, entries 1, 3, 4, 5). Similarly, heating a mixture of mesalazine and menthol at various molar ratios resulted in the formation of an opalescent viscous liquid that rapidly solidified at room temperature (Table 19, entry 2).

Entry	HBA	HBA:5-ASA molar ratio	T (°C)	Time (min)	Aspect
1	ChCl	1:1	80	120	Solid
		1:2			Solid
		1:3			Solid
		1:4			Solid
2	(+)-Menthol	2:1	50	60-120	Opalescent viscous liquid that rapidly solified at rt
		3:1			Opalescent viscous liquid that rapidly solified at rt
		6:1			Opalescent viscous liquid that rapidly solified at rt
3	Betaine	1:1	80	120	Solid

Table 19. Continuation

4	Lactic acid	2:1	80	120	Solid
5	L-Arginine	1:1	80	180	Solid

Table 19. HBA:5-ASA Molar ratio tested for the formation of THEDES.

An additional investigated strategy involved the preparation of a Deep Eutectic Solvent capable of enhancing the solubility of 5-ASA. As previously mentioned, various studies report that the solubility of API can be significantly increased in DES systems compared to their solubility in water. Therefore, they may play a crucial role as solvents and co-solvents in drug delivery applications. Most studies in this regard have employed DES based on choline chloride in association with various hydrogen bond donors of natural origin. The chemical structure of DES components and their molar ratio significantly influence solvation properties, potentially altering polarity and pH and introducing new intermolecular interactions.

Based on the above-mentioned considerations, several Deep Eutectic Solvents were prepared in this study, using choline chloride in combination with various HBDs such as urea, ethylene glycol, glycerol, ascorbic acid, oxalic acid, and lactic acid, mixed at different molar ratios (Table 20). All the components used are known to be safe and non-toxic; therefore, the resulting DESs pose no toxicity issues for humans.

Entry	HBD	ChCl:HBD Molar ratio
1	Urea	1:2
2	Ascorbic Acid	2:1
3	Glycerol	1:1
4	Lactic Acid	1:10
5	Ethylene glycol	1:2
6	Oxalic acid	1:1

Table 20. DESs considered for the solubilization of 5-ASA.

The solubility of 5-ASA was initially qualitatively assessed using polarized optical microscopy (POM) with incremental addition of the drug to 1 ml of each considered DES. Among these, the DES formed by choline chloride and lactic acid exhibited the strongest ability to enhance the solubility of mesalazine, as no crystalline structures were observed below 35 mg 5-ASA/ml of DES (Table 21). Simultaneously, POM images captured the presence of crystals for the same amount of drug in water. On the other hand, the presence of fully formed crystals was observed at higher concentrations, namely 50 and 65 mg/mL. These findings support the visual observation of the mixture, where solid aggregates were visible to the naked eye at the bottom of the vials.

Solvent	Quantity of 5-ASA (mg)/mL	POM images
ChCl:LA (1:10)	35	
	50	
	65	
Water	35	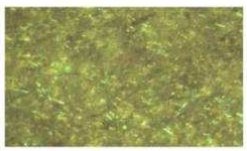

Table 21. POM analysis of 5-ASA in DES and in water.

The solubility profile of 5-ASA was successively quantitatively determined using the shake-flask method. For this purpose, an excess amount of the API was added

to 1 mL of the DES, and the mixture was then agitated and maintained at a constant temperature for a sufficiently long period to reach saturation equilibrium (approximately 24 hours). Once equilibrium was attained, the undissolved solid was separated through a PTFE syringe filter with a 0.45µm membrane. Subsequently, the liquid phase was diluted in methanol, and the amount of dissolved 5-ASA was determined using a validated UV method on a UV spectrophotometer (UV-530 JASCO). The absorbance of the solutions was measured at the maximum absorption wavelength of 5-ASA (300 nm). The analysis results demonstrate that mesalazine exhibits a solubility of 30 mg/mL in the considered DES, a value significantly higher when compared to its solubility in water or other binary solvent mixtures reported in the literature.

The increase in solubility in the DES can be attributed to the formation of hydrogen bonds between mesalazine and the components of the DES. To verify the various intermolecular interactions between mesalazine and the DES components, several analyses were conducted, including FT-IR and ^{1}H-NMR of the individual pure compounds, the specific DES under consideration, and the 5-ASA-DES mixture, as done in the case of dapsone.

Initially, the infrared spectra of the pure compounds, as well as the DES and the mesalazine-DES system, were obtained and analysed. Changes in the structure are typically associated with the broadening or merging of peaks involving hydroxyl groups, the shifting of the carbonyl peak of acids, or the loss of characteristic groups of pure substances.

The FT-IR spectrum of choline chloride shows a strong and broad hydroxyl peak in the range of 3650-3200 cm^{-1}, along with additional peaks indicating the presence of a specific quaternary ammonium compound group in the range of 900 to 980 cm^{-1} (Figure 26a).

Characteristic peaks of lactic acid are related to the alcoholic and acid hydroxyl groups, appearing in the spectrum as a broad single peak covering a range from 2500 to 3550 cm^{-1}, in addition to the carbonyl group peak typically present at a wavelength of 1700 cm^{-1} (Figure 26b).

In the FT-IR spectrum of the formed DES (Figure 27c), it can be observed that the hydroxyl peak of lactic acid is shifting and broadening, indicating the formation of hydrogen bonds in the DES.

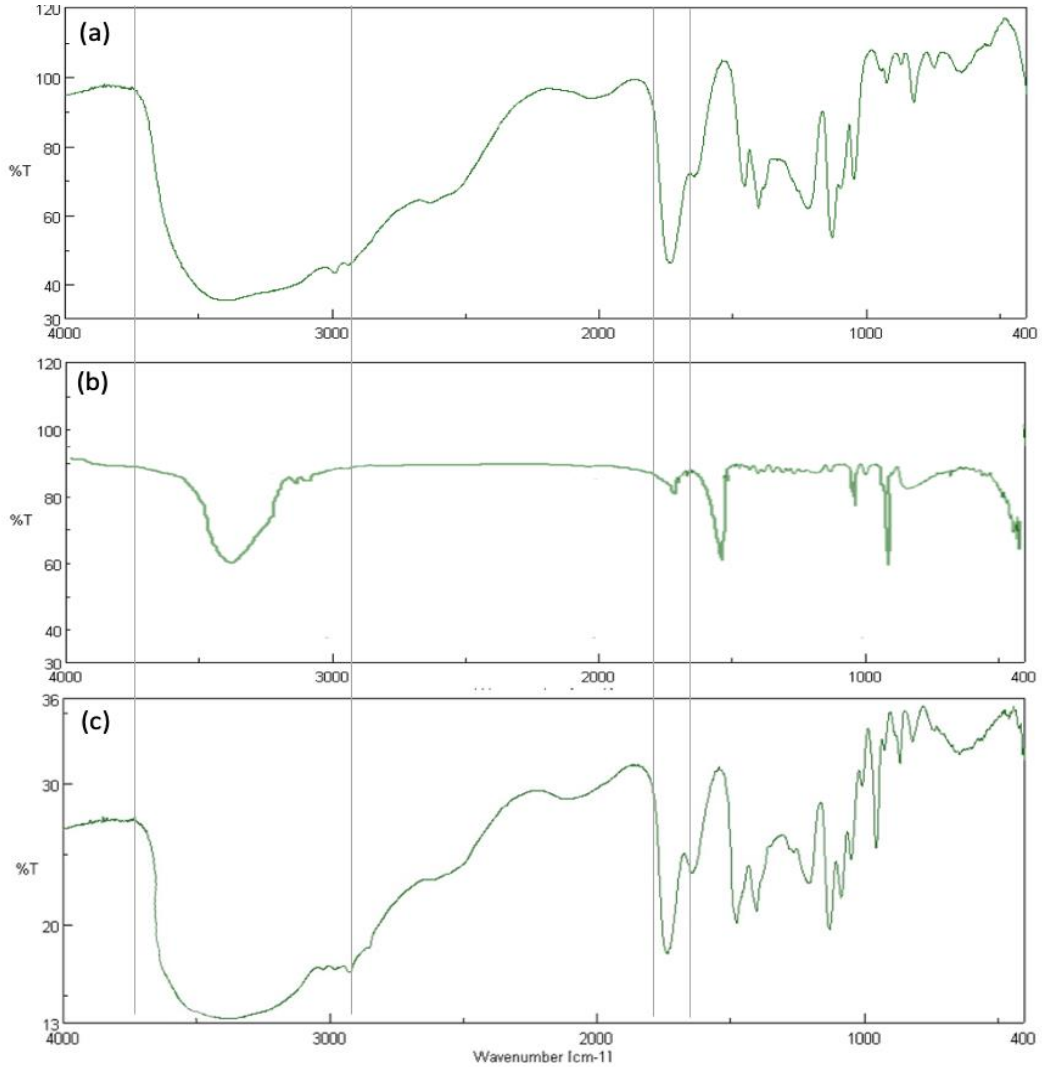

Figura 26. FT-IR spectra of (a) Lactic acid, (b) ChCl and (c) DES ChCl:LA (1:10).

The FT-IR spectrum of the DES was then compared with that of mesalazine and the mesalazine-DES system (Figure 27). The spectrum of pure mesalazine (Figure 27a) shows peaks for the bending of the hydroxyl group in the range of 1350-1260 cm^{-1}. Additionally, the presence of the amino group is denoted at 150-159 cm^{-1}. Comparing this spectrum with the spectra of the DES and the mesalazine-DES system (Figure 27c), it was possible to observe that the peaks of the DES are almost diminished or merged together, appearing as broad peaks. These experimental findings confirm the formation of strong interactions between the components of the DES and mesalazine.

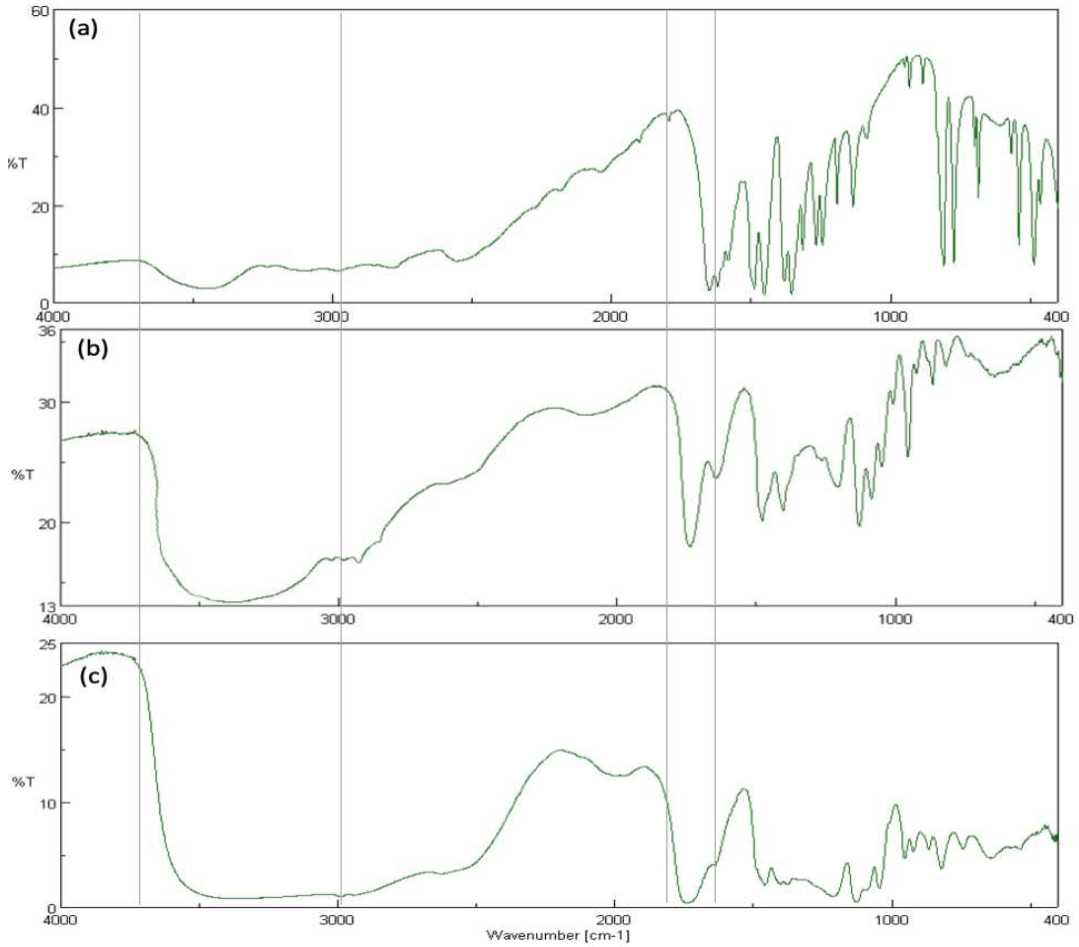

Figure 27. FT-IR spectra of (a) Mesalazine, (b) DES ChCl:LA (1:10) and (c) Mesalazine-DES system.

In order to verify the molecular arrangement of the components of the examined DES, a comprehensive NMR analysis was performed. Proton high-resolution nuclear magnetic resonance spectroscopy was initially applied to choline chloride and lactic acid in search for their structural characterizing resonance signals. In particular, the spectra recorded for a sample of commercially available lactic acid, clearly showed its purity grade. The main signals are indicated by arrows, while some minor resonances are present. However, there were attributed to secondary materials that, as it will be demonstrated, did not participate or interfere in forming the DES molecular aggregate. Specifically, the spectra recorded for a commercially available sample of lactic acid clearly highlighted its purity level (Figure 28a). The main signals are indicated by arrows, and there are some minor resonances present. Furthermore, the spectra recorded for a commercially available sample of choline chloride clearly demonstrated its purity level. The main signals are indicated by arrows, and some minor resonances are visible.

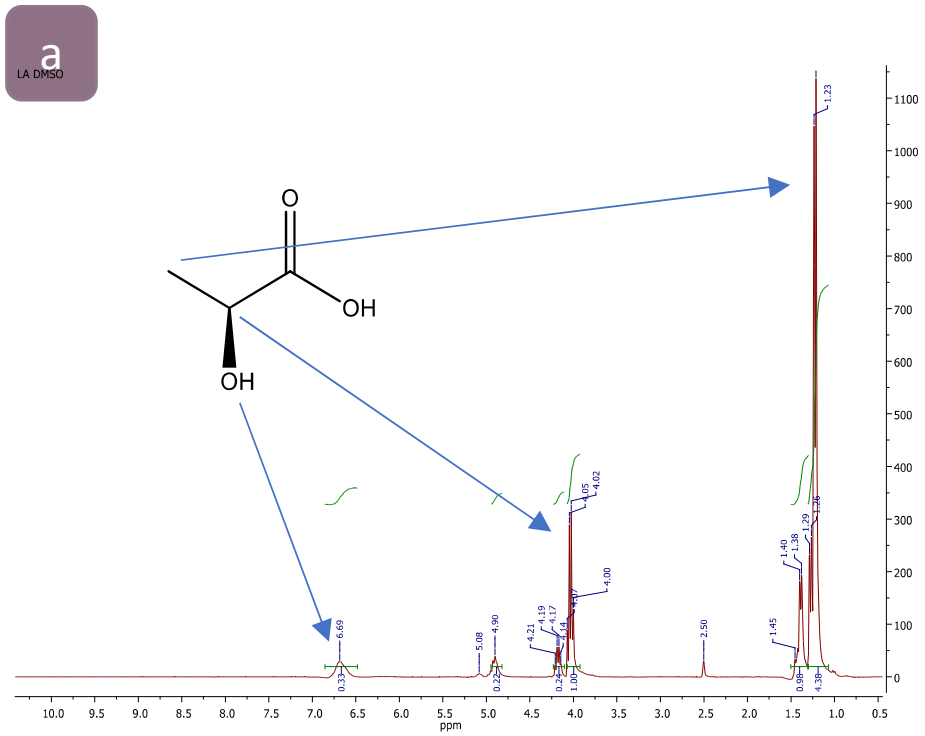

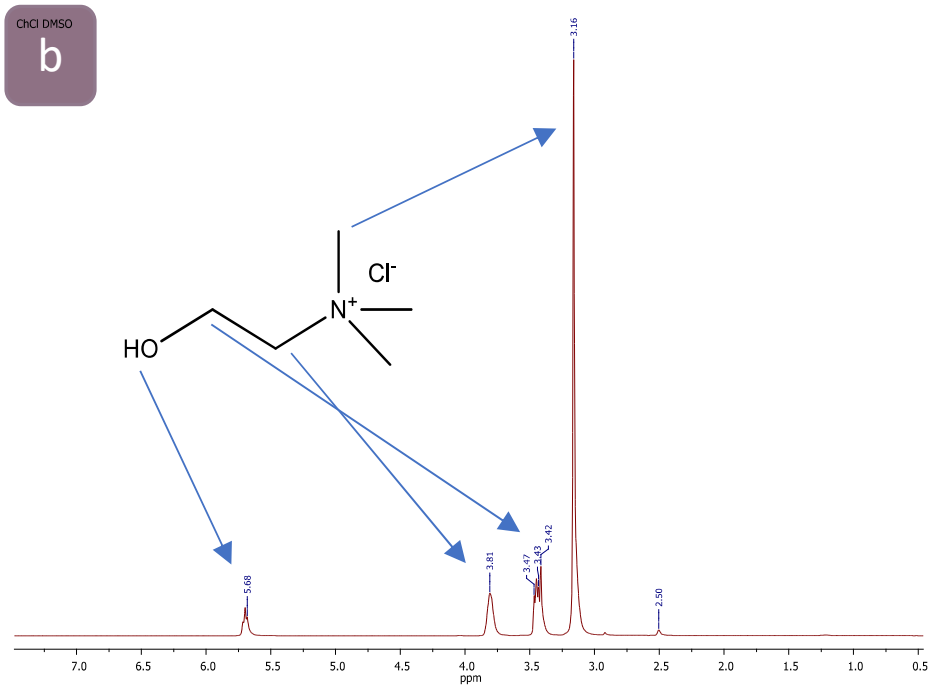

Figure 28. HNMR spectra of pure (a) Lactic acid and (b) choline chloride.

The same former analysis was also done on a sample of pure 5-ASA (Figure 29). In this case, the proton spectrum enabled the attribution of signals to the corresponding aromatic proton, based on their observable multiplicities and coupling constants.

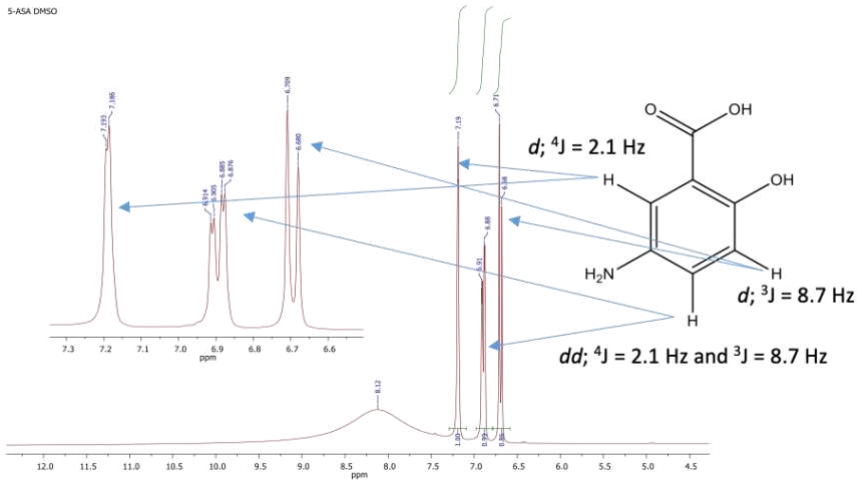

Figure 29. ^{1}H NMR of an aliquot of pure of mesalazine.

A fully mono-dimensional NMR analysis was applied in order to characterize the freshly prepared DES. No noticeable differences where observed between the chemical shift values of the single components and those of the DES molecular aggregate (Figure 30).

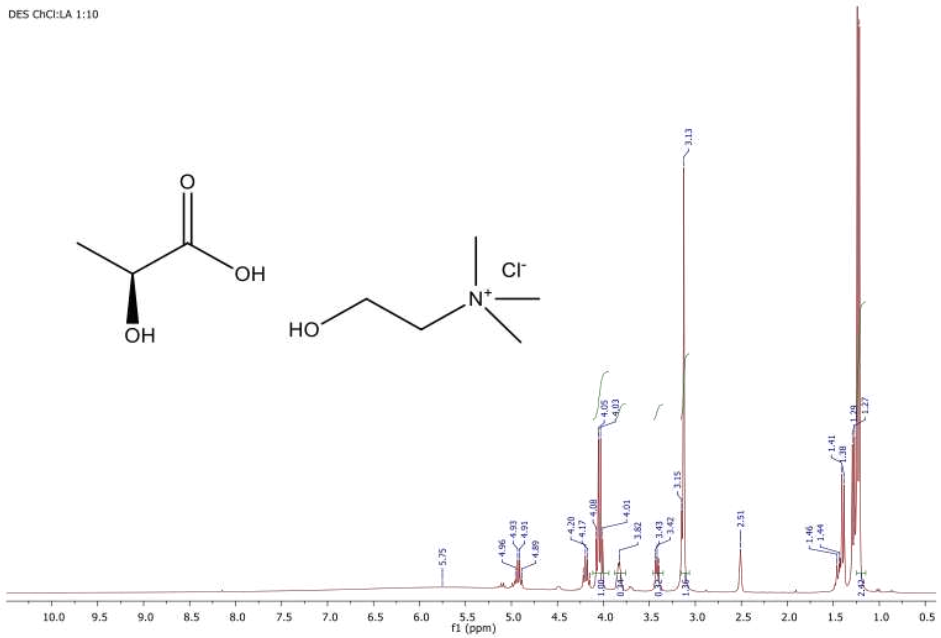

Figure 30. Mono-dimensional NMR analysis of the freshly prepared DES.

Then, a mono-dimensional NMR investigation of the DES after 5-ASA inclusion was performed (Figure 31). Proton chemical shifts of choline chloride and lactic acid remained quite the same with respect to the corresponding single component analysis. Notwithstanding, it is relevant the downfield shift of the peak attributable to all heteroatom protons (from 5.90 ppm ca. for DES, to 6.95 ppm ca. for the DES + 5-ASA sample). This shift was rationally attributed to the formation of a complex H-bond network involving the DES components, as well as the polar functions of 5-ASA. Aromatic protons of 5-ASA presented their respective peaks as shoulders of the intense peak centered at 6.95 ppm. However, their resonances remain distinguishable.

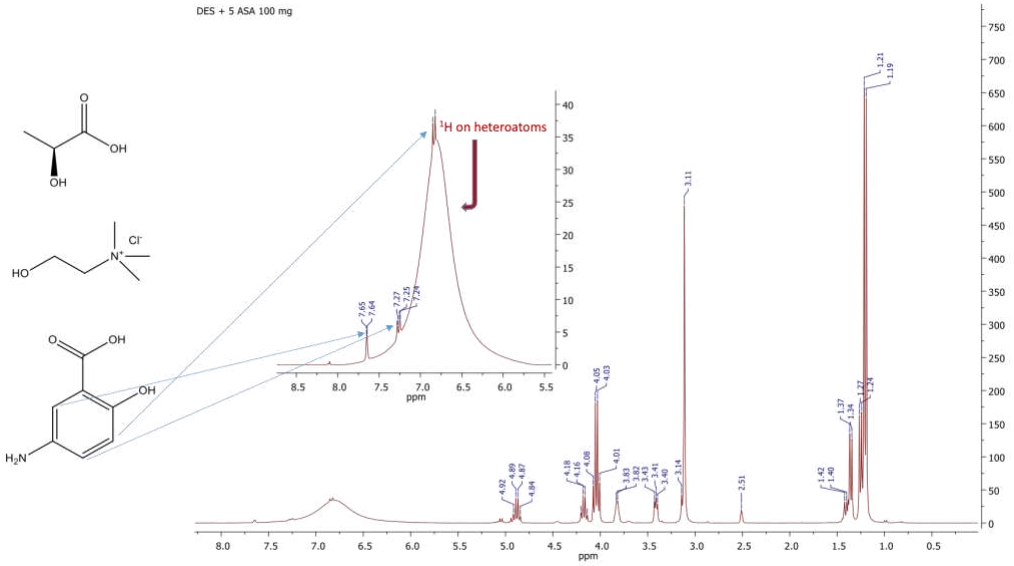

Figure 31. Proton spectrum of a sample of 5-ASA solubilized in DES.

All molecular through-the-space interactions involved in the 5-ASA inclusion in the DES structure, were definitively assessed by the extensive application of 2D-NOESY analysis, which was performed on DES and DES+5-ASA samples, under the same instrumental conditions. All spectra were recorded in DMSO-d_6 and at 25 ± 0.1 °C. The 2D-NOESY spectrum of DES showed strong spatial interactions between the CH_3 in lactic acid and the CH_2O methylene protons (Figure 32).

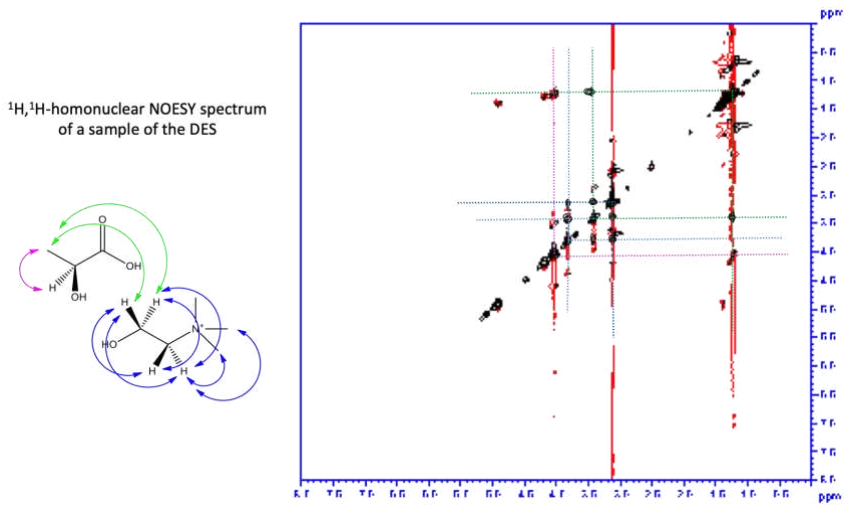

Figure 33. 2D-NOESY spectrum of a sample of the DES

The 2D-NOESY cross-correlations detected for the aromatic proton at 6.80 ppm with the CH and CH_3 group of lactic acid, together with the cross-peaks generated by the NOE effect between the same aromatic proton and the CH_2N^+ methylene protons of the choline frame, unambiguously defined the molecular spatial arrangement of all components in the DES and 5-ASA structure (Figure 33). Finally, all spectra evidences, together with the behaviour of the 5-ASA C-OH, as it is and after its inclusion in the DES, also suggested the existence of a H-bond network involving the COOH and OH groups of 5-ASA and the same counterparts in lactic acid.

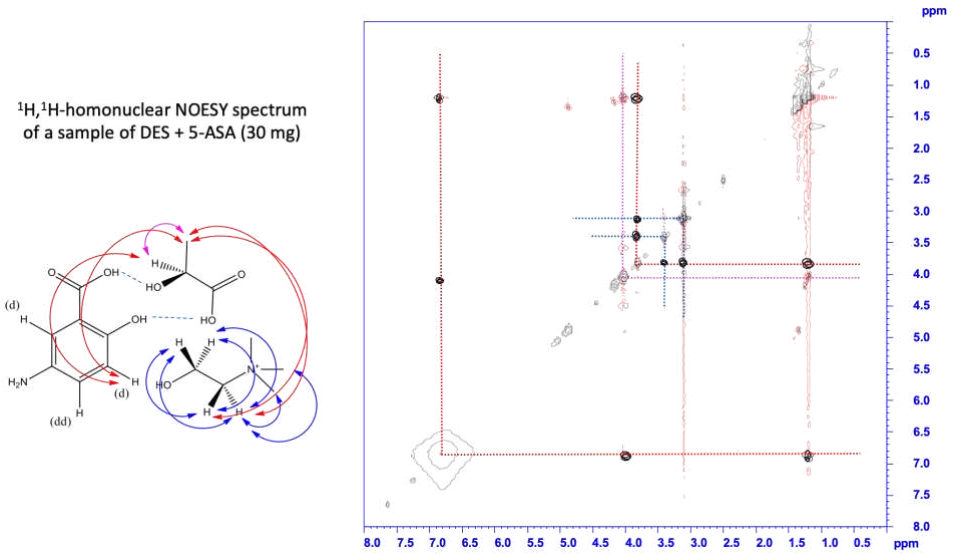

Figure 33. 2D-NOY spectrum of a sample of DES + 5-ASA

5.3.4 Mesalazine in vitro release studies

Encouraged by the excellent solubility results, the research aimed to investigate how this particular DES system could enhance the release of mesalazine. Mesalazine release experiments were conducted at two different pH values (6.8 and 7.4), simulating conditions in the intestinal environment. Samples of the solution were collected at various time intervals (30 minutes, 45 minutes, 1 hour, 2 hours, 4 hours, 6 hours, and 24 hours), and the release was monitored using UV-Vis spectrophotometry. The findings revealed that the DES gradually released

mesalazine at pH 6.8 over a 24-hour period, whereas at pH 7.4, a higher release of the substance occurred within the initial 6 hours (as depicted in Figure 34).

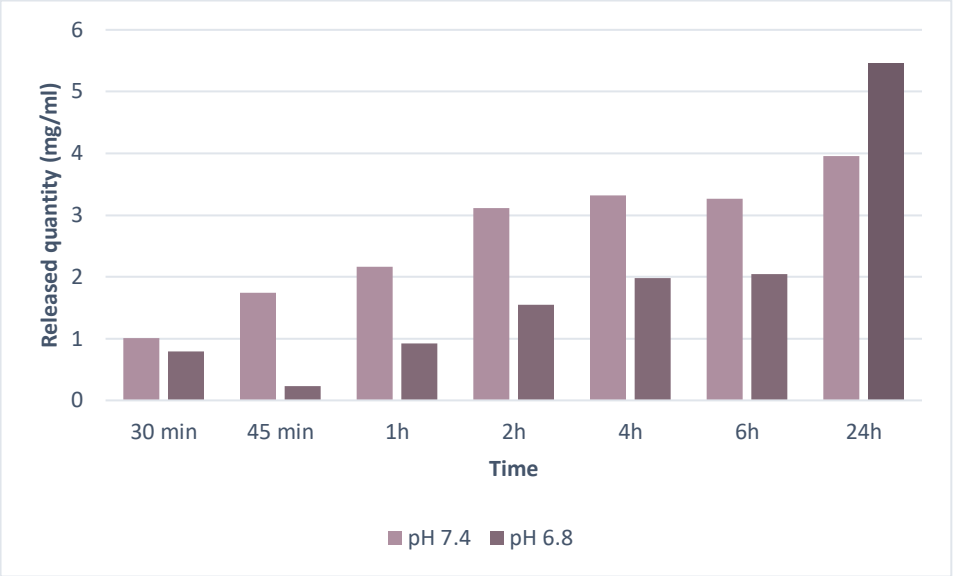

Figura 34. Release studies of mesalazine at pH 6.8 and pH 7.4.

Consequently, these results suggest the potential for oral administration and advocate for the use of the DES as a carrier for mesalazine in the intestine.

5.4 Conclusions

Based on the previous results, the following conclusion have been drawn from this chapter:

- The research further outlined the potential of DESs in increasing the solubility profile of water-insoluble drugs , with a specific focus on API such as mesalazine and dapsone. The increased solubility observed in these systems holds promise for improving the bioavailability and efficiency of mesalazine and dapsone, addressing a key challenge in their pharmaceutical use;
- The use of advanced analytical techniques, including Differential Scanning Calorimetry (DSC), Nuclear Magnetic Resonance (NMR), and Fourier Transform Infrared Spectroscopy (FT-IR), provides valuable insights into the

molecular interactions between the drugs considered and the DES components. Understanding these interactions is pivotal for optimizing DES systems tailored to the unique properties of these drugs, ensuring stability and efficacy;

- Finally, the assessment of the release profile of mesalazine and dapsone dissolved in DESs contributes significant information on sustained release properties. This is crucial for designing drug delivery systems that control and extend the release of these drugs. The potential improvements in therapeutic outcomes and the minimization of side effects are particularly relevant in the context of the anti-inflammatory effects of mesalazine and the possible use of dapsone in various dermatological conditions.

In summary, the research objectives provide a framework for a thorough exploration of DESs as a means to enhance the solubility, understand molecular interactions, and assess release profiles of mesalazine and dapsone. The outcomes of these investigations contribute valuable knowledge to the broader field of pharmaceutical research, offering potential solutions to enhance the effectiveness and application of these important therapeutic agents.

Experimental section

E.1 Detailed experimental protocols

E.1.1 Chapter 1

General procedure for the preparation of RDESs

The different RDESs were prepared by mixing choline chloride and the carboxylic acid (benzoic, phenyl acetic or 4-hydroxyphenylacetic acid) in a round-bottom flask under inert atmosphere in a 1:1 molar ratio. The resulting mixture was magnetically stirred at 60-80 °C, until a clear liquid was observed. The obtained DESs were directly used without further purification.

General procedure: amide synthesis in RDES

In a typical procedure, 1mmol of the coupling reagent was added to a ChCl: carboxylic acid (1:1)-based RDES. After stirring at 50°C for 10- 15 minutes, the amine was added in equimolar ratio and the resulting mixture was vigorously stirred at the given temperature for an additional time (30-60 min). The progress of the reaction was monitored by TLC and GC/MS analysis. Upon completion, 2 mL of H2O were added. The resulting aqueous suspension was then extracted with ethyl acetate (3 × 2 mL). The organic phases were dried over sodium sulphate, followed by evaporation under reduced pressure to give the corresponding amides. The reaction conversions were determined by GC/MS analysis. Spectral data were in accordance with the literature.

E.1.2 Chapter 2

General Procedure for the Preparation of DESs

A mixture of hydrogen-bond donor and hydrogen-bond acceptor compound, with the previously specified molar ratio, was added in a round bottom flask under an inert atmosphere. The mixture was stirred for 30 minutes in a T range between 65 and 80 °C obtaining the corresponding DES.

General procedure for the preparation of thioacid substrates

All thioacids employed in the present study, except thioacetic acid and thiobenzoic acid, were prepared from the corresponding acyl chloride and

thioacetamide according to the literature with slight modification. To a round-bottom flask containing thioacetamide (10 mmol, 1 equiv.) in DCM (20 mL), acyl chloride (10 mmol, 1 equiv.) was added dropwise. The mixture was kept under stirring for 3 h at 30 °C. Then, NaOH (10% m/m) was added, and the resulted liquid-liquid two phase system was kept under stirring for 30 minutes at r.t. Then, the reaction was acidified with HCl (1N). The organic phase was washed with brine, dried over $MgSO_4$ and concentrated in vacuo. The crude thioacid was obtained as a yellow oil and was used to the visible-light induced reactions without further purification.

General Procedure for the Synthesis of Amides

To a vial containing $Ru(bpy)_3Cl_2$ (2.6 mg, 2 mol%) in DES (1 mL), the thioacid (0.4 mmol, 2 equiv.) and the amine (0.2 mmol, 1 equiv.) were added. The mixture was stirred under blue LED at rt for 1 h. Then, the mixture was quenched with water (2 mL) and extracted with EtOAc (3×4 mL). The organic phase was washed with brine and dried over $MgSO_4$. The crude organic phase was concentrated in vacuo and purified by preparative thin layer chromatography on silica gel (usually with hexane/EtOAc=5:1) to afford the pure product.

General Procedure for the Recycling Experiments

The reaction was performed according to the general procedure. Once the reaction was completed, the formed product was extracted with a small amount of EtOAc (3×3 mL). The resulting biphasic mixture was stirred at room temperature for 10 min, and the upper phase was separated by decantation. Then, the residual eutectic mixture (bottom phase) was dried under vacuum and re-charged with fresh reagents, repeating the process.

Mechanistic Investigations

To a vial containing aniline (34 mg, 0.2 mmol, 1 equiv.) in DES (1 mL) and $Ru(bpy)_3Cl_2$ (2.6 mg, 2 mol%), thioacetic acid (30 mg, 0.4 mmol, 2 equiv.) and TEMPO (62 mg, 0.4 mmol, 2 equiv.) were added. The mixture was stirred under

blue LED irradiation at r.t. for 1 h. The mixture was analysed by ^{1}H NMR obtaining a complex spectrum with no evidence of product.

To a vial containing $Ru(bpy)_3Cl_2$ (2.6 mg) in DES (1 mL) was added thiobenzoic acid (55 mg, 0.4 mmol, 2 equiv.). The mixture was stirred under blue LED at rt for 20 minutes. The mixture was quenched with water (2 mL) and then extracted with EtOAc (3×4 mL). The organic phase was washed by brine, dried over $MgSO_4$ and concentrated in vacuo. The mixture was purified with flash column chromatography (using Hex:EtOAc 10/1 as eluent) to give the pure product as a white solid.

Controlled experiment without photocatalyst

To a vial containing aniline (19 mg, 0.2 mmol, 1 equiv.) in 1 mL of DES, thioacetic acid (30 mg, 0.4 mmol, 2 equiv.) was added under air atmosphere. The mixture was stirred under blue LED at rt for 1 h. Then, the mixture was quenched with water (2 mL) and then extracted with EtOAc (3×4 mL). The organic phase was washed with brine, dried over $MgSO_4$ and concentrated in vacuo. The mixture was purified according to the general 2 procedure to give the pure product 3a (13 mg, 34%) as a white solid.

E.1.3 Chapter 3

Preparation of DESs

DESs were prepared following the heating method [58]. First, choline chloride was dried in a high vacuum pump at 50 °C for 1 day, while the hydrogen bond donors (pTSA, oxalic acid, citric acid, malonic acid, succinic acid, and $FeCl_3$) were used without any further purification. The hydrogen bond acceptor (HBA) and hydrogen bond donors (HBDs) at a proper molar ratio (1:1) were placed in a glass screw cap vial and were heated to 60–70 °C under a constant stirring speed of 100 rpm by using a heating plate (Bibby Scientific Limited, Beacon Road, Stone, Staffordshire, UK) until a homogeneous clear liquid was formed.

General procedure for the synthesis of *N*-Boc amines and amino acid derivatives

A 50 mL round-bottom flask containing 10 mL of dichloromethane (DCM) was charged with the starting amine or amino acid derivative (1 equiv) and triethylamine (TEA) (1.5 equiv). Di-tert-butyl dicarbonate ($(Boc)_2O$) (1 equiv) was then added to the former solution and the resulting mixture was stirred at r.t. The reaction was monitored by TLC and was complete in 3-4 h. The reaction mixture was acidified with an aqueous solution of HCl 1N and then extracted with DCM (3 x 10 mL). The combined organic layers were dried over Na_2SO_4. The filtrate was concentrated in vacuo under reduced pressure to obtain the pure N-Boc protected amines or amino acid derivatives without need of further purification. All N-Boc-protected starting materials were characterized by GC-MS, ^{1}H-NMR and ^{13}C-NMR before their use. Spectral data are consistent with those already reported in the literature.

General Procedure for the *N*-Boc Deprotection of Amines and Amino Acid Derivatives

In a 10 mL round-bottomed flask, 1 mL of DES (ChCl:*p*TSA) was maintained under stirring, and an N-Boc-protected amine or N-Boc-protected amino acid derivative (1 mmoL) was added. The mixture was allowed to stir at room temperature. TLC and GC/MS were used to monitor the reaction. Upon completion of the reaction, an aqueous solution of sodium bicarbonate $NaHCO_3$ (5%) was added. The crude material was then extracted with AcOEt (3 x 5 mL). The organic layer was dried over anhydrous Na_2SO_4, filtered, and finally concentrated under a low vacuum using a rotary evaporator to yield the pure deprotected amine. Spectroscopic data (GC-MS, ^{1}H-NMR e ^{13}C-NMR) were compared to those of the pure products. The obtained spectroscopic data are in agreement with the literature data.

E.1.4 Chapter 4

Experimental procedure for the preparation of DES

The DESs used were prepared following literature-reported procedures, using heating and stirring method. Specifically, all DESs were prepared by employing choline chloride as the hydrogen bond acceptor (HBA) and urea, glycerol, and ethylene glycol as hydrogen bond donors (HBD) in a 1:2 molar ratio, respectively. The components were placed in a heated glass flask at approximately 60°C and continuously stirred using a heating plate equipped with a magnetic stirrer, for 2 hours. The obtained DESs were used without any further purification.

Experimental procedure for the one-pot, two steps synthesis of atenolol

In a 25 mL round-bottom flask containing 0.6 mL of ChCl:EG DES, *p*-hydroxyphenylacetamide (200 mg, 1 equiv.) was introduced, and the mixture was stirred magnetically at 50 °C. Following the immediate solubilization of the amide, epichlorohydrin (0.184 g, 1.5 equiv.) was added dropwise, and the reaction mixture was further stirred at a temperature of 50 °C for 6 hours. The reaction progress was monitored by TLC and GC/MS. Upon completion, unreacted epichlorohydrin was removed by evaporation under reduced pressure. After removing the excess epichlorohydrin, the reaction mixture was subjected again to magnetic stirring and heated to a temperature of 50 °C. Subsequently, isopropylamine (0.235g, 3 equiv.) was added dropwise. The reaction progress was continually monitored via TLC and GC/MS. Upon completion after 6 hours, the excess isopropylamine was removed by evaporation under reduced pressure. Atenolol recovery was performed by adding an aqueous solution of $NaHCO_3$, followed by extraction with ethyl acetate (5 mL x 3). Next, the organic phase was dehydrated with Na_2SO_4, filtered, and then subjected to evaporation under reduced pressure. The obtained solid was washed with a mixture of hexane (5 mL) and tert-butyl methyl ether (1 mL), further with hexane (5 mL x 2), and finally subjected to evaporation under reduced pressure. The obtained atenolol was characterized through NMR analysis.

Scale-up procedure for the one-pot, two steps synthesis of atenolol (1g)

In a 25 mL round-bottom flask containing 3mL of ChCl:EG DES, *p*-hydroxyphenylacetamide (1g, 1 equiv.) was introduced, and the mixture was stirred magnetically at 50 °C. Following the immediate solubilization of the amide, epichlorohydrin (0.918 g, 1.5 equiv.) was added dropwise, and the reaction mixture was further stirred at a temperature of 50 °C for 6 hours. The reaction progress was monitored by TLC and GC/MS. Upon completion, unreacted epichlorohydrin was removed by evaporation under reduced pressure. After removing the excess epichlorohydrin, the reaction mixture was subjected again to magnetic stirring and heated to a temperature of 50 °C. Subsequently, isopropylamine (1.173 g, 3 equiv.) was added dropwise. The reaction progress was continually monitored via TLC and GC/MS. Upon completion after 6 hours, the excess isopropylamine was removed by evaporation under reduced pressure. Atenolol recovery was performed by adding an aqueous solution of $NaHCO_3$, followed by extraction with ethyl acetate (5 mL x 3). Next, the organic phase was dehydrated with Na_2SO_4, filtered, and then subjected to evaporation under reduced pressure. The obtained solid was washed with a mixture of hexane (5 mL) and tert-butyl methyl ether (1 mL), further with hexane (5 mL x 2), and finally subjected to evaporation under reduced pressure. The obtained atenolol was characterized through NMR analysis.

Scale-up procedure for the one-pot, two steps synthesis of atenolol (10g)

In a 25 mL round-bottom flask containing 30mL of ChCl:EG DES, *p*-hydroxyphenylacetamide (10g, 1 equiv.) was introduced, and the mixture was stirred magnetically at 50 °C. Following the immediate solubilization of the amide, epichlorohydrin (9.181 g, 1.5 equiv.) was added dropwise, and the reaction mixture was further stirred at a temperature of 50 °C for 6 hours. The reaction progress was monitored by TLC and GC/MS. Upon completion, unreacted epichlorohydrin was removed by evaporation under reduced pressure. After removing the excess epichlorohydrin, the reaction mixture was subjected again to magnetic stirring and

heated to a temperature of 50 °C. Subsequently, isopropylamine (11.731 g, 3 equiv.) was added dropwise. The reaction progress was continually monitored via TLC and GC/MS. Upon completion after 6 hours, the excess isopropylamine was removed by evaporation under reduced pressure. Atenolol recovery was performed by adding an aqueous solution of $NaHCO_3$, followed by extraction with ethyl acetate (15 mL x 3). Next, the organic phase was dehydrated with Na_2SO_4, filtered, and then subjected to evaporation under reduced pressure. The obtained solid was washed with a mixture of hexane (15 mL) and tert-butyl methyl ether (3 mL), further with hexane (15 mL x 2), and finally subjected to evaporation under reduced pressure. The obtained atenolol was characterized through NMR analysis.

E.1.5 Chapter 5

Polarized Optical Microscopy (POM) analysis

A small droplet of DESs with an incremental amount of the drug were deposited on a microscopic slide for observation at a magnification of 10x. The polarized light image was observed at room temperature and captured using a Nikon ECLIPSE LV100N polarizing microscope (Nikon Corporation, Japan) coupled with Nikon DS-Fi2 camera. When there is no presence of solid crystalline structure, the polarized light image is uniformly black.

DES solubility measurement

In order to determine the solubility of the drugs in the prepared DESs, its excess amount was added to ~1mL of the eutectic mixtures which were then kept under constant stirring for 24 h, in order to reach equilibrium conditions at room temperature. After the saturation, the samples were filtered with PTFE syringe filter with a 0.45 µm membrane, to separate the macroscopic solid from the liquid phase. Then, the liquid phase was diluted in methanol, and the amount of the dissolved drug was determined by using a validated UV method on a UV spectrophotometer (UV-530 JASCO). The absorbance of the solutions was measured at the API maximum absorption wavelength. The concentration of drugs

was based on a calibration curve obtained by dissolving pre-weighed amounts of the drug in methanol and measuring their absorbance in the function of concentration, expressed as mass of the drug dissolved in mL of the solvent (mg/mL).

Differential Scanning Calorimetry (DSC) analysis

The DSC experiments were performed for the different samples. Briefly, 5–9 mg of the DESs, solid drug or the drug dissolved in DESs were placed in hermetic closed sample pans prior to thermal analysis using the DSC instrument (DSC 200 PC Netzsch). The thermograms were collected from 20 to 200 °C at a rate of 5 °C min^{-1}, in order to detect all the transitions, melting points and Tg of the substances.

In vitro skin permeation of DAP

Permeation study (n = 3) was performed on the excised skin of sacrificed rabbit (New Zealand rabbits of 2.9–3.1 kg), which was obtained from a local slaughter's house, using Franz Diffusion cells. The skin was allowed to equilibrate with dissolution medium (pH 7.4 buffer solution) for 12 h before using it for permeation studies and was mounted on Franz Diffusion cells. The receptor compartment was filled with pH 7.4 buffer solution as diffusion medium (37 ± 0.5 °C). Skin was saturated with dissolution medium for 1 h before the application of sample. Dapsone-loaded DES were placed on the stratum corneum side of the skin, and the donor compartment was covered with laboratory film (Parafilm®). At specific intervals (1, 2, 3, 4, 6, and 24 h), 100 µL of receiver solution was withdrawn from the receiver compartment and replaced with fresh buffer. The dapsone concentration in the receiver solution samples was assayed by UV–Vis spectrophotometry. All experiments were per-formed in triplicate (n = 3).

In vitro release studies of Mesalazine

In vitro release studies of mesalazine from the DES were conducted over a 24-hour period at two pH values that mimic conditions in the intestinal environment: pH 6.8 and pH 7.4. Specifically, the mesalazine-containing DES (6 mg/mL) was

placed in a cellulose acetate membrane in contact with the aforementioned fluids at 37°C under agitation. At regular time intervals (30 minutes, 45 minutes, 1 hour, 2 hours, 4 hours, 6 hours, and 24 hours), 2 mL of the solutions were sampled, and the medium was replaced with fresh solution to maintain the same total volume during the study. The concentration of released mesalazine was monitored using UV-Vis spectrophotometry at a wavelength of 300 nm.

E.2 Spectral data of all compounds

E.2.1 Chapter 1

All products described were obtained pure from the crude reaction mixture.

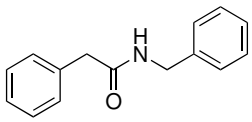	***N*-Benzyl-2-phenylacetamide:** White solid, yield 96%; ^{1}H NMR (300 MHz, $CDCl_3$) δ 7.56-7.01 (m, 9H), 5.82 (s, 1H), 4.37 (d, J = 5.8 Hz, 2H), 3.59 (s, 1H) ppm; ^{13}C NMR (75 MHz, $CDCl_3$) 171.1, 138.1, 135.6, 130.0, 129.5, 128.7, 127.5, 127.4, 43.8, 43.6 ppm. EIMS m/z (%): 225 ($M^{+\cdot}$, 30), 91 (100), 77 (5), 65 (15).
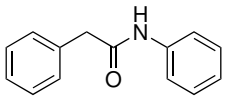	***N*,2-Diphenylacetamide:** White solid, yield 93%; ^{1}H NMR (300 MHz, $CDCl_3$) δ 7.82 (s, 1H), 7.63 – 6.78 (m, 10H), 3.67 (d, J = 6.7 Hz, 2H) ppm. ^{13}C NMR (75 MHz, $CDCl_3$) 169.6, 137.9, 134.7, 129.7, 129.3, 129.1, 128.9, 127.7, 127.3, 120.4, 44.6 ppm. EIMS m/z (%): 211 ($M^{+\cdot}$, 80%), 119 (1), 93 (100), 77 (14), 65 (36).
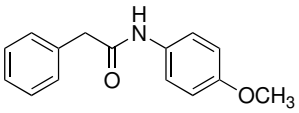	***N*-(4-Methoxyphenyl)-2-phenylacetamide:** White solid, yield 88%; ^{1}H NMR (300 MHz, $CDCl_3$) δ 7.48 – 7.21 (m, 7H), 7.04 (s, 1H), 6.90-6.71 (m, 2H), 3.79 (d, J = 1.2 Hz, 3H), 3.75 (s, 2H) ppm. ^{13}C NMR (75 MHz, $CDCl_3$) 168.9, 156.6, 134.6, 130.7, 129.2, 128.6, 127.6, 117.0, 114.9, 56.6, 44.7 ppm. EIMS m/z (%): 241 (M+., 82), 149 (10), 123 (100), 108 (57), 91 (50), 80 (7), 65 (16).
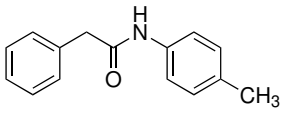	**2-Phenyl-*N*-(p-tolyl)acetamide:** White solid, yield 91%; ^{1}H NMR (300 MHz, $CDCl_3$) δ 7.91 (s, 1H), 7.35 (td, J = 7.4, 3.8 Hz, 7H), 7.09 (d, J = 8.0 Hz, 2H), 3.67 (d, J = 2.4 Hz, 2H), 2.32 (s, 3H) ppm. ^{13}C NMR (75 MHz, $CDCl_3$) 169.6, 135.2, 134.0, 129.7, 129.4, 128.8, 127.6, 127.2, 120.6, 44.8, 20.9 ppm. EIMS m/z (%): 225 ($M^{+\cdot}$).
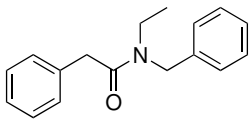	***N*-Benzyl-*N*-ethyl-2-phenylacetamide:** White solid, yield 78%; ^{1}H NMR (300 MHz, $CDCl_3$) δ 7.48 – 6.96 (m, 20H), 4.60 &4.46 (2 singlets, rotamers, 2H), 3.77 & 3.67 (2 singlets, rotamers, 2H), 3.41 & 3.25 (2 quadruplets, rotamers, J = 7.2 Hz, 2H), 1.17 – 0.95 (m, rotamers, 3H) ppm. ^{13}C NMR (101 MHz, $CDCl_3$, mixture of two rotamers 1:1) δ 171.1, 170.9, 137.8, 136.9, 135.2, 129.0, 128.9, 128.7, 127.6, 127.9, 127.4, 127.1, 126.7, 47.9, 46.7, 43.5, 42.2, 14.8, 14.7 ppm. EIMS m/z (%): 253 ($M^{+\cdot}$, 39), 162 (4), 106 (12), 91 (100), 65 (13).
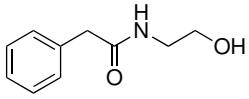	***N*-(2-Hydroxyethyl)-2-phenylacetamide:** White solid, yield 84%; ^{1}H NMR (300 MHz, $CDCl_3$) δ 7.52 – 7.11 (m, 5H), 5.54 (s, 1H), 4.25 – 4.01 (m, 1H), 3.55 – 3.40 (m, 2H) ppm. ^{13}C NMR (75 MHz, $CDCl_3$) 171.6, 129.4, 129.2, 129.0, 127.4, 63.3, 43.7, 38.7 ppm. EIMS m/z (%): 162 ($M^{+\cdot}$, 16%), 118 (28), 91 (100), 77 (5), 65 (13).

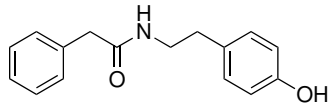	***N*-(4-Hydroxyphenethyl)-2-phenylacetamide**: White solid, yield 89%; ^{1}H NMR (300 MHz, $CDCl_3$) δ 9.18 (s, 1H), 8.05 (s, 1H) 7.28-7.23 (m, 5H), 6.96-6.93 (m, 2H), 6.67-6.64 (m, 2H), 3.51-3.32 (m, 17H) 3.21-3.19 (m, 2H), 2.6-2.50 (m, 2H) ppm. ^{13}C NMR (75 MHz, $CDCl_3$) 170.1, 156.6, 137.5, 131.3, 130.6, 129.0, 127.4, 116.7, 116.1, 43.5, 39.7, 35.3 ppm. EIMS m/z (%): 255 ($M^{+\cdot}$, 2%), 136 (13), 120 (100), 105 (20), 91 (48), 77 (12), 65 (10), 51 (4).
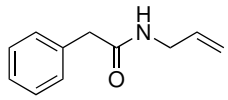	***N*-Allyl-2-phenylacetamide:** White solid, yield 83%; ^{1}H NMR (300 MHz, $CDCl_3$) δ 7.44 – 7.21 (m, 5H), 5.78 (ddt, J = 16.8, 10.8, 5.5 Hz, 1H), 5.54 (s, 1H), 5.10 – 4.99 (m, 2H), 3.86 (tt, J = 5.6, 1.6 Hz, 2H), 3.62 (s, 2H) ppm. ^{13}C NMR (75 MHz, $CDCl_3$) 170.8, 138.6, 134.8, 134.0, 129.6, 127.5, 116.9, 43.8, 43.4 ppm. EIMS m/z (%): 175 ($M^{+\cdot}$, 18%), 118 (5), 91 (100), 84 (13), 77 (2), 65 (25), 57 (24), 51 (5), 41 (43).
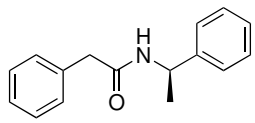	**(R)-2-Phenyl-*N*-(1-phenylethyl)acetamide:** White solid, yield 91%; ^{1}H NMR (300 MHz, $CDCl_3$) δ 7.48 – 7.04 (m, 10H), 5.62 (s, 1H), 5.14 (p, J = 7.1 Hz, 1H), 3.61 (s, 2H), 1.42 (dd, J = 6.9, 0.6 Hz, 3H) ppm. ^{13}C NMR (75 MHz, $CDCl_3$) 170.0, 143.0, 135.7, 129.4, 128.6, 127.4, 127.3, 125.9, 53.8, 46.1, 21.8 ppm. EIMS m/z (%): 239 ($M^{+\cdot}$, 34%), 224 (2), 120 (5), 105 (100), 91 (24), 77 (13), 65 (9), 51 (5).
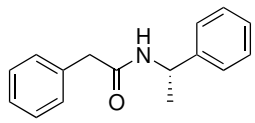	**(S)-2-phenyl-*N*-(1-phenylethyl)acetamide**: White solid, yield 93%. ^{1}H NMR (300 MHz, $CDCl_3$) δ 7.48 – 7.00 (m, 10H), 5.67 (s, 1H), 5.14 (p, J = 7.1 Hz, 1H), 3.59 (s, 2H), 1.42 (dd, J = 6.9, 0.6 Hz, 3H) ppm.13C NMR (75 MHz, $CDCl_3$) 170.0, 143.0, 134.9, 129.3, 129.0, 128.6, 127.4, 125.9, 48.7, 43.9, 21.7 ppm. EIMS m/z (%): 239 ($M^{+\cdot}$, 34%), 224 (3), 120 (7), 105 (100), 91 (21), 77 (13), 65 (10), 51 (5).
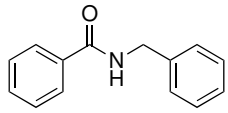	***N*-Benzylbenzamide:** White solid, yield 81%; ^{1}H NMR (300 MHz, $CDCl_3$): δ 7.84 – 7.68 (m, 2H), 7.52 – 7.18 (m, 8H), 6.68 (s, 1H), 4.59 (d, J = 5.6 Hz, 2H) ppm. ^{13}C NMR (300 MHz, $CDCl_3$): 167.5, 137.8, 134.3, 131.8, 128.8, 128.1, 127.5, 126.6 ppm. EIMS m/z (%): 211 ($M^{+\cdot}$, 69%), 105 (100), 91 (14), 77 (62), 65 (10), 51 (23).
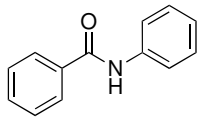	***N*-Phenylbenzamide:** White solid, yield 76%; ^{1}H NMR (400 MHz, $CDCl_3$) δ 8.07 (s, 1H), 7.91 – 7.80 (m, 2H), 7.53 (t, J = 7.7 Hz, 3H), 7.45 (t, J = 7.2 Hz, 2H), 7.16 (d, J = 8.0 Hz, 2H), 2.35 (s, 3H) ppm. ^{13}C NMR (300 MHz, $CDCl_3$) δ 165.85, 137.94, 135.00, 131.85, 129.11, 128.79, 127.05, 124.60, 120.28 ppm. EIMS m/z (%): 197 ($M^{+\cdot}$, 39), 105 (100), 77 (63).
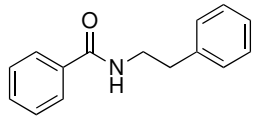	***N*-Phenethylbenzamide:** White solid, yield 83%; ^{1}H NMR (300 MHz, $CDCl_3$) δ 7.69 (d, J = 7.5 Hz, 2H), 7.44 (t, J = 7.3 Hz, 1H), 7.37 (d, J = 7.3 Hz, 2H), 7.28 (d, J = 7.1 Hz, 2H), 7.21 (d, J = 15.9 Hz, 3H), 6.51 (t, J = 6.2 Hz, 1H), 3.66 (q, J = 6.6 Hz, 2H), 2.89 (t, J = 7.0 Hz, 2H) ppm. ^{13}C NMR (75 MHz, $CDCl_3$): δ 167.6, 138.9,

	134.6, 131.2, 128.9, 128.8, 127.9, 127.7, 126.5 ppm. EIMS m/z (%): 225 ($M^{+\cdot}$, 41%), 134 (15), 105 (100), 91 (7), 77 (46), 65 (5), 51(12).
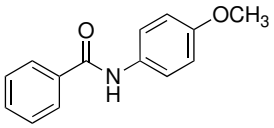	***N*-(4-Methoxyphenyl)benzamide:** White solid, yield 74%; ^{1}H NMR (300 MHz, $CDCl_3$) δ 7.82 (d, J = 7.4 Hz, 2H), 7.73 (s, 1H), 7.47 (dd, J = 16.7, 8.0 Hz, 5H), 6.96 – 6.76 (m, 2H), 3.77 (d, J = 2.3 Hz, 3H) ppm. ^{13}C NMR (75 MHz, $CDCl_3$): δ 165.6, 158.6, 135.0, 131.5, 128.6, 127.4, 122.5, 121.9, 114.3, 55.9 ppm. EIMS m/z (%): 227 ($M^{+\cdot}$, 60%), 105 (100), 77 (53), 65 (1), 51 (10).
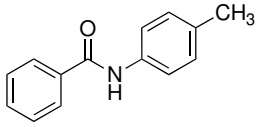	***N*-(*p*-Tolyl)benzamide:** White solid, yield 88%; ^{1}H NMR (400 MHz, $CDCl_3$) δ 8.07 (s, 1H), 7.91 – 7.80 (m, 2H), 7.53 (t, J = 7.7 Hz, 3H), 7.45 (t, J = 7.2 Hz, 2H), 7.16 (d, J = 8.0 Hz, 2H), 2.35 (s, 3H) ppm. ^{13}C NMR (300 MHz, $CDCl_3$) δ 165.89, 135.41, 135.05, 134.47, 134.22, 131.70, 129.55, 129.04, 128.70, 128.16, 127.09, 120.48, 29.73, 20.95. MS (70 eV, EI): m/z (%): 211 (M+, 41), 105 (100), 77 (45) ppm. EIMS m/z (%): 211 ($M^{+\cdot}$, 44%), 105 (100), 77 (57), 65 (1), 51 (13).
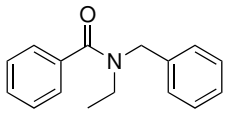	***N*-Benzyl-*N*-ethylbenzamide:** White solid, yield 56%; ^{1}H NMR (300 MHz, $CDCl_3$) δ 7.32 (ddt, J = 26.3, 12.6, 5.9 Hz, 20H), 4.87 – 4.24 (2 singlets, rotamers 2H), 3.76 – 3.65 & 3-26 & 3.05 (2 multiplets, rotamers 2H), 1.21 – 1.00 (m, rotamers. 3H) ppm. EIMS m/z (%): 329 ($M^{+\cdot}$, 41%), 105 (100), 91 (16), 77 (40).
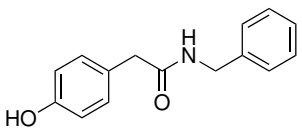	***N*-Benzyl-2-(4-hydroxyphenyl)acetamide:** White solid, yield 80%; ^{1}H NMR (300 MHz, DMSO-d_6) δ 9.22 (s, 1H), 7.22 (d, J = 7.9 Hz, 4H), 7.10 – 7.02 (m, 3H), 6.71 – 6.65 (m, 2H), 4.26 (d, J = 5.6 Hz, 3H), 3.51 (d, J = 8.9 Hz, 2H) ppm. ^{13}C NMR (75 MHz, DMSO-d_6) δ 168.8, 156.3, 168.8, 130.9, 129.6, 128.8, 128.6, 127.7, 121.8, 115.5, 42.6, 42.0 ppm. EIMS m/z (%): 241 ($M^{+\cdot}$, 33%), 147 (4), 107 (100), 91 (56), 77 (22), 65 (9), 51 (6).
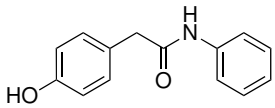	**2-(4-Hydroxyphenyl)-*N*-phenylacetamide:** White solid, yield 74%; ^{1}H NMR (300 MHz, $CDCl_3$) δ 7.38 (d, J = 8.2 Hz, 2H), 7.33 – 7.18 (m, 4H), 7.19 – 7.08 (m, 2H), 6.78 (dd, J = 8.3, 3.8 Hz, 2H), 3.60 (d, J = 11.4 Hz, 2H) ppm. ^{13}C NMR (75 MHz, $CDCl_3$) δ 168.9, 157.3, 138.7, 130.8, 128.7, 128.1, 124.6, 120.1, 116.7, 43.9 ppm. EIMS m/z (%): 227 ($M^{+\cdot}$, 52), 134 (43), 107 (100), 93 (67), 77 (44), 51 (13).
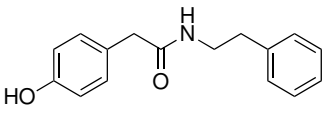	**2-(4-Hydroxyphenyl)-*N*-phenethylacetamide:** White solid, yield 61%; ^{1}H NMR (300 MHz, $CDCl_3$) δ 7.31 – 7.17 (m, 4H), 7.10 – 7.02 (m, 2H), 6.98 (d, J = 8.3 Hz, 2H), 6.85 (d, J = 8.4 Hz, 2H), 5.76 (d, J = 6.0 Hz, 1H), 3.47 (d, J = 6.0 Hz, 4H), 2.73 (t, J = 6.9 Hz, 2H) ppm. ^{13}C NMR (75 MHz, $CDCl_3$) δ 172.8, 156.4, 138.4, 131.4, 128.8, 128.7, 127.4, 126.5, 116.8, 42.8, 40.9, 35.4 ppm. EIMS m/z (%): 255 ($M^{+\cdot}$, 29), 207 (3), 151(16), 136 (14), 107 (100), 91 (15), 77 (19), 51 (5).

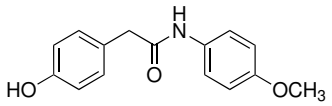	**2-(4-Hydroxyphenyl)-*N*-(4-methoxyphenyl)acetamide:** White solid, yield 74%; ^{1}H NMR (300 MHz, DMSO-d_6) δ 10.04 (s, 1H), 9.93 (s, 2H), 9.29 (s, 3H), 7.51 (d, J = 8.5 Hz, 7H), 7.17 – 6.98 (m, 13H), 6.87 (d, J = 8.5 Hz, 6H), 6.74 (dd, J = 12.7, 8.1 Hz, 9H), 3.98 (s, 2H), 3.81 (s, 5H), 3.71 (s, 12H), 3.60 (d, J = 12.4 Hz, 5H), 3.47 (s, 7H) ppm. ^{13}C NMR (75 MHz, DMSO-d_6) δ 169.6, 156.9, 156.5, 131.3, 130.4, 129.6, 122.3, 116.1, 114.1, 55.8, 44.7 ppm. EIMS m/z (%): 257 ($M^{+\cdot}$, 66%), 207 (3), 149 (13), 123 (100), 107 (72), 92 (7), 77 (25), 52 (10).
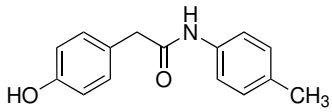	**2-(4-Hydroxyphenyl)-*N*-(p-tolyl)acetamide:** White solid, yield 58%; ^{1}H NMR (300 MHz, DMSO-d_6) δ 9.95 (s, 1H), 9.24 (s, 1H), 7.48 (d, J = 8.0 Hz, 3H), 7.21 – 6.98 (m, 6H), 6.74 (t, J = 10.4 Hz, 3H), 3.49 (s, 3H), 2.24 (s, 4H) ppm. ^{13}C NMR (75 MHz, DMSO-d_6) δ 169.8, 156.9, 137.3, 134.1, 131.3, 129.5, 128.7, 121.9, 116.1, 43.8, 20.9 ppm. EIMS m/z (%): 241 ($M^{+\cdot}$, 66%), 242 (100), 108 (54), 104 (65).
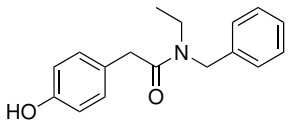	***N*-Benzyl-*N*-ethyl-2-(4-hydroxyphenyl)acetamide:** White solid; yield 54%; ^{1}H NMR (300 MHz, DMSO-d_6) δ 9.24 (s, 1H), 7.36 – 6.59 (m, 9H), 4.54 & 4.52 (2 singlets, rotamers, 2H) 3.59 & 3.49 (2 singlets, rotamers, 2H) 3.41 (m,, 2H), 0.99 (m, rotamers, 3H) ppm. ^{13}C NMR (75 MHz, DMSO-d_6) δ 171.1, 156.3, 136.4, 130.3, 128.9, 127.9, 127.8, 127.2, 126.4, 115.6, 47.5, 42.2, 40.8, 12.8 ppm. EIMS m/z (%): 269 ($M^{+\cdot}$, 33%), 162 (3), 107 (49), 91 (100), 77 (12), 51 (3).

E.2.2 Chapter 2

All products described were obtained pure from the crude reaction mixture.

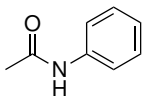

***N*-phenylacetamide:** White solid (26.7 mg, 100%). m.p. = 114-115 °C. ^{1}H NMR (300 MHz, $CDCl_3$) δ 8.28 (s, 1H), 7.57-7.50 (m, 2H), 7.35-7.27 (m, 2H), 7.15-7.08 (m, 1H), 2.16 (s, 3H). ^{13}C NMR (101 MHz, $CDCl_3$) δ 169.2, 138.1, 128.9, 124.3, 120.3, 24.4. MS (70 eV, EI): m/z (%): 135 ($M^{+\cdot}$, 39%), 93 (100), 66 (12), 43 (22). IR (ATR): ν = 3190, 3062, 1658, 1597, 1435, 1257, 906, 748, 694 cm^{-1}.

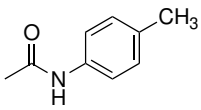

***N*-(p-tolyl)acetamide:** White solid (27,8 mg, 93%). m.p. = 152-153 °C.^{1}H NMR (400 MHz, $CDCl_3$) δ 7.76 (s, 1H), 7.38 (d, J = 8.0 Hz, 2H), 7.13 (d, J = 8.0 Hz, 2H), 2.32 (s, 3H), 2.20 (s, 3H). ^{13}C NMR (101 MHz, $CDCl_3$) δ 168.82, 135.11, 134.23, 129.48, 120.29, 24.26, 20.87. MS (70 eV, EI): m/z (%):149 (M^{+} 54 %), 107 (100), 106 (92), 77 (14). IR (ATR): ν = 3190, 3062, 1658, 1597, 1435, 1257, 906, 748, 694 cm^{-1}; IR (ATR): ν = 3186, 3066, 2920, 1658, 1604, 1546, 1508, 1261, 818 cm^{-1}.

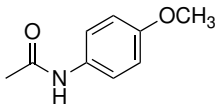

***N*-(4-methoxyphenyl)acetamide:** White solid (31.7 mg, 96%). m.p. = 130-131°C. ^{1}H NMR (400 MHz, $CDCl_3$) δ 7.85 (s, 1H), 7.40-7.35 (m, 2H), 6.86-6.80 (m, 2H), 3.77 (s, 3H), 2.13 (s, 3H). ^{13}C NMR (101 MHz, $CDCl_3$) δ 169.0, 156.7, 131.0, 122.3, 114.2, 55.6, 24.2. MS (70 eV, EI): m/z (%): 165 ($M^{+\cdot}$, 69%), 123 (67%), 108 (100), 95 (80), 43 (37). IR (ATR): ν = 3190,3074, 3005, 2839, 1647, 1604, 1508, 1242, 1026, 833, 771 cm^{-1}.

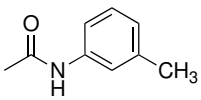

***N*-(m-tolyl)acetamide:** White solid (26.0 mg, 87%). m.p. = 64-65 °C. ^{1}H NMR (400 MHz, $CDCl_3$) δ 8.50 (s, 1H), 7.38 (s, 1H), 7.33 (d, J = 8.1 Hz, 1H), 7.17 (t, J = 7.8 Hz, 1H), 6.91 (d, J = 7.5 Hz, 1H), 2.29 (s, 3H), 2.15 (s, 3H). ^{13}C NMR (101 MHz, $CDCl_3$) δ 169.4, 138.7, 138.0, 128.7, 125.2, 121.0, 117.4, 24.3, 21.4. MS (70 eV, EI): m/z (%): 149 ($M^{+\cdot}$, 51%), 107 (100), 106 (54). IR (ATR): ν =3289, 2919, 2364, 2333, 1658, 1612, 1484, 1319, 1261, 1033, 879, 752 cm^{-1}.

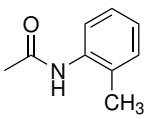

***N*-(o-tolyl)acetamide:** White solid (24.0 mg, 80%). m.p. = 110-111 °C. ^{1}H NMR (400 MHz, $CDCl_3$) δ 7.69 (d, J = 7.9 Hz, 1H), 7.25-7.15 (m, 3H), 7.08 (t, J = 7.7 Hz, 1H), 2.24 (s, 3H), 2.20 (s, 3H). ^{13}C NMR (101 MHz, $CDCl_3$) δ 168.8, 135.6, 130.6, 129.8, 126.8, 125.6, 123.8, 24.2, 17.9. MS (70 eV, EI): m/z (%): 149 ($M^{+\cdot}$, 52%), 107 (100), 106 (80). IR (ATR): ν = 3290, 3032, 2981, 1647, 1523, 1269, 756 cm^{-1}.

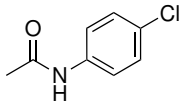

***N*-(4-chlorophenyl)acetamide:** White solid (39.0 mg, 96%). m.p. = 130- 178-179 °C. ^{1}H NMR (400 MHz, $CDCl_3$) δ 7.53 – 7.43 (m, 2H), 7.39 (br s, 1H), 7.29-7-24 (m, 2H), 2.17 (s, 3H). ^{13}C NMR (101 MHz, $CDCl_3$) δ 168.6, 136.6, 129.4, 129.1, 121.2, 24.7. MS (70 eV, EI): m/z (%): 169 ($M^{+\cdot}$, 27%), 129 (33), 127 (100), 92 (67), 65 (58), 43 (32). IR (ATR): ν = 3190,3074, 3005, 2839, 1647, 1604, 1508, 1242, 1026, 833, 771 cm-1; IR (ATR): ν = 3159, 3128, 1662, 1601, 1535, 1485, 1261, 1092, 825 cm^{-1}.

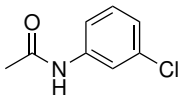

***N*-(3-chlorophenyl)acetamide:** White solid (34.3 mg, 85%). m.p. = 78- 79 °C. ^{1}H NMR (400 MHz, $CDCl_3$) δ 8.13 (s, 1H), 7.65 (t, J = 2.0 Hz, 1H), 7.44 – 7.31 (m, 1H), 7.21 (t, J = 8.0 Hz, 1H), 7.07 (dd, J = 7.9, 2.0 Hz, 1H), 2.19 (s, 3H). ^{13}C NMR (101 MHz, $CDCl_3$) δ 169.2, 139.1, 134.5, 129.9, 124.4, 120.2, 118.0, 24.5. MS (70 eV, EI): m/z (%): 169 ($M^{+\cdot}$, 23%), 129 (32), 127 (100), 92 (83). IR (ATR): ν = 3198, 1666, 1593, 1535, 1415, 1277, 1092, 902, 868, 779, 701 cm^{-1}.

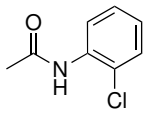

***N*-(2-chlorophenyl)acetamide:** White solid (32.5 mg, 80%). m.p. = 87-88 °C. ^{1}H NMR (400 MHz, $CDCl_3$) δ 8.37 (d, J = 8.3 Hz, 1H), 7.65 (s, 1H), 7.38 (dd, J = 8.0, 1.5 Hz, 1H), 7.29 (td, J = 7.9, 1.5 Hz, 1H), 7.06 (td, J = 7.7, 1.5 Hz, 1H), 2.26 (s, 3H). ^{13}C NMR (101 MHz, CDCl3) δ 168.3, 134.6, 129.0, 127.8, 124.6, 122.5, 121.7, 24.9. MS (70 eV, EI): m/z (%): 169 ($M^{+\cdot}$, 16%), 129 (33), 127 (100), 92 (73). IR (ATR): ν = 3240, 3047, 2924, 2854, 2364, 2333, 1654, 1585, 1435, 1369, 1257, 1060, 1033, 752, 721, 698 cm^{-1}.

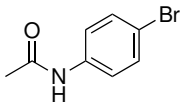

***N*-(4-bromophenyl)acetamide:** White solid (39.0 mg, 91%). m.p. = 167- 169 °C. ^{1}H NMR (400 MHz, $CDCl_3$) δ 7.54 (s, 1H), 7.42 (m, 4H), 2.19 (s, 3H). ^{13}C NMR (101 MHz, $CDCl_3$) δ 168.6, 136.9, 132.0, 121.5, 117.0, 77.3, 29.7, 24.6. MS (70 eV, EI): m/z (%): 213 ($M^{+\cdot}$, 21%), 171 (73), 92 (41), 65 (37), 43 (100). IR (ATR): ν = 3298, 3059, 2924, 1662, 1597, 1539, 1257, 1072, 818 cm^{-1}.

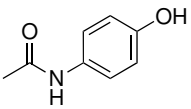

***N*-(4-hydroxyphenyl)acetamide:** White solid (20.3 mg, 68%). m.p. = 169-170 °C. ^{1}H NMR (400 MHz, acetone-d_6) δ 9.01 (s, 1H), 8.26 (s, 1H), 7.48 – 7.38 (m, 2H), 6.80 – 6.71 (m, 2H), 2.04 (s, 3H). ^{13}C NMR (101 MHz, acetone-d_6) δ 168.4, 154.3, 132.6, 121.7, 115.9, 24.0. MS (70 eV, EI): m/z (%): 151 ($M^{+\cdot}$, 40%), 109 (100), 80 (22). IR (ATR): ν = 3325 (brs), 3205, 1655, 1554, 1508, 1450, 1238, 833 cm^{-1}.

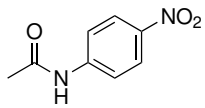

***N*-(*p*-nitrophenyl)acetamide:** White solid (26,8 mg, 75%). m.p. = 216- 217 °C. ^{1}H NMR (300 MHz, DMSO-d_6) δ 10.54 (s, 1H), 8.18 (d, J = 9.1 Hz, 1H), 7.80 (d, J = 9.1 Hz, 1H), 2.11 (s, 2H). ^{13}C NMR (75 MHz, DMSO-d_6) δ 169.3, 145.5, 142.0, 124.9, 118.5, 24.2. MS (70 eV, EI): m/z (%):180 ($M^{+\cdot}$, 26%), 138 (100), 108 (28), 92 (23). IR (ATR): ν = 3275, 3093, 2920, 1678, 1496, 1331, 1261, 849 cm^{-1}.

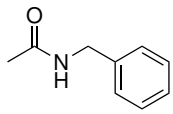

***N*-benzylacetamide:** White solid (21.6 mg, 73%). m.p. = 60-62 °C. ^{1}H NMR (400 MHz, $CDCl_3$) δ 7.36 – 7.24 (m, 5H), 6.32 (br s, 1H), 4.40 (d, J = 5.6 Hz, 2H), 2.00 (s, 3H). ^{13}C NMR (101 MHz, $CDCl_3$) δ 170.3, 138.3, 128.7, 127.9, 127.6, 43.8, 23.2. MS (70 eV, EI): m/z (%): 149 ($M^{+\cdot}$, 96), 106 (100), 91 (29). IR (ATR): ν = 3182, 3089, 2919, 2850, 1635, 1550, 1442, 1230, 748, 694 cm^{-1}.

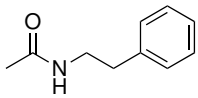

***N*-phenethylacetamide:** White solid (30.4 mg, 93%). m.p. = 38-39 °C. ^{1}H NMR (400 MHz, $CDCl_3$) δ 7.35 – 7.26 (m, 2H), 7.25 – 7.16 (m, 3H), 5.87 (s, 1H), 3.51 (q, J = 6.8 Hz, 2H), 2.82 (t, J = 6.8 Hz, 2H) 1.96 (s, 3H). ^{13}C NMR (101 MHz, $CDCl_3$) δ 170.5, 138.9, 128.9, 128.8, 126.7, 40.9, 35.7, 23.3. MS (70 eV, EI): m/z (%): 163 ($M^{+\cdot}$, 29%), 104 (100), 72 (11). IR (ATR): ν = 3286, 3086, 2931, 1639, 1547, 1303, 744, 701cm^{-1}.

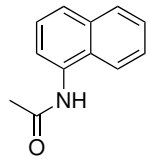

1-Acetamidonaphtalene: White solid (23.0 mg,63%). ^{1}H NMR (300 MHz, $CDCl_3$) δ 7.97-7.79 (m, 3H), 7.74 (d, J = 7.4 Hz, 1H), 7.67 (d, J = 8.2 Hz, 1H), 7.52-7.35 (m, 3H), 2.22 (s, 3H). ^{13}C NMR (101 MHz, $CDCl_3$) δ 169.5, 134.1, 132.5, 128.7, 127.7, 126.2, 126.1, 126.0, 125.7, 121.8, 121.3, 24.1. MS (70 eV, EI): m/z (%): 185 ($M^{+\cdot}$, 33%), 143 (100), 115 (25). IR (ATR): ν = 3167, 3051, 2924, 1651, 1539, 1276, 771, 721cm^{-1}.

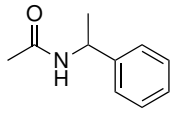

***N*-(1-phenylethyl)acetamide:** White solid (25.3 mg,78%). m.p. = 72-73 °C. ^{1}H NMR (300 MHz, $CDCl_3$) δ 7.33 – 7.15 (m, 5H), 6.15 (br s, 1H), 5.11 – 5.00 (m, 1H), 1.90 (s, 3H), 1.42 (d, J = 7.0 Hz, 3H). ^{13}C NMR (75 MHz, $CDCl_3$) δ 169.3, 143.4, 128.7, 127.4, 126.3, 48.9, 23.4, 21.8. MS (70 eV, EI): m/z (%): 163 ($M^{+\cdot}$, 51), 148 (29), 120 (37), 106 (100). IR (ATR): ν = 3265, 3065, 2971,1640,1552, 1432,1176,1137, 700 cm^{-1}.

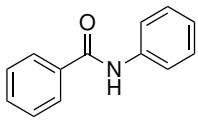

***N*-phenylbenzamide:** White solid (38.0 mg, 96%). m.p. = 162-163 °C. ^{1}H NMR (400 MHz, $CDCl_3$) δ 7.93 (s, 1H), 7.89 – 7.84 (m, 2H), 7.67 – 7.62 (m, 2H), 7.57 – 7.51 (m, 1H), 7.50 – 7.44 (m, 2H), 7.40 – 7.33 (m, 2H), 7.18 – 7.12 (m, 1H). ^{13}C NMR (101 MHz, $CDCl_3$) δ 166.0, 138.1, 135.1, 132.0, 129.2, 128.9, 127.2, 124.7, 120.4. MS (70 eV, EI): m/z (%): 197 ($M^{+\cdot}$, 56), 105 (100). IR (ATR): ν = 3344, 3051, 1655, 1527, 1439, 1319, 1253, 906, 748, 748, 687 cm^{-1}.

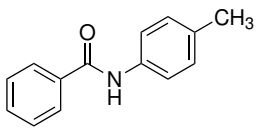

***N*-(4-methylphenyl)benzamide**: White solid (38.5 mg, 91%). m.p. = 158-159 °C. ^{1}H NMR (400 MHz, $CDCl_3$) δ 8.05 (br s, 1H), 7.84 (d, J = 7.1 Hz, 2H), 7.51 (t, J = 7.8 Hz, 3H), 7.43 (t, J = 7.2 Hz, 2H), 7.14 (d, J = 8.0 Hz, 2H), 2.33 (s, 3H). ^{13}C NMR (101 MHz, $CDCl_3$) δ 166.0, 135.5, 135.1, 134.3, 131.8, 129.6, 128.8, 127.2, 120.5, 21.0. MS (70 eV, EI): m/z (%): 211 ($M^{+\cdot}$, 41), 105 (100), 77 (45). IR (ATR): ν = 3309 2364, 2333, 1647, 1600, 1515, 1400, 1315, 1260, 809 cm^{-1}.

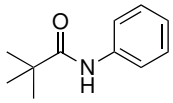

***N*-phenylpivalamide:** White solid (29.6 mg, 84%). m.p. = 131-132 °C. ^{1}H NMR (400 MHz, $CDCl_3$) δ 7.56 – 7.49 (m, 2H), 7.36 – 7.29 (m, 3H), 7.10 (ddt, J = 7.5, 5.9, 1.1 Hz, 1H), 1.32 (s, 9H). ^{13}C NMR (101 MHz, $CDCl_3$) δ 176.7, 138.1, 129.1, 124.3, 120.1, 39.7, 27.8. MS (70 eV, EI): m/z (%): 177 ($M^{+\cdot}$, 39), 93 (71), 77 (10), 65 (11), 57 (100). IR (ATR): ν = 3305, 2965, 1651, 1587, 1531, 1400, 1369, 1315, 1241, 902, 752, 698 cm^{-1}.

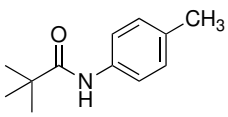

***N*-(*p*-tolyl)pivalamide**: White solid (31.3 mg, 82%). m.p. = 102-103 °C. ^{1}H NMR (400 MHz, $CDCl_3$) δ 7.44 – 7.37 (m, 2H), 7.30 (br s, 1H), 7.15 – 7.04 (m, 2H), 2.30 (s, 3H), 1.30 (s, 9H). ^{13}C NMR (101 MHz, $CDCl_3$) δ 176.6, 135.5, 133.9, 129.6, 120.2, 39.6, 27.8, 21.0. MS (70 eV, EI): m/z (%): 191 ($M^{+\cdot}$, 50%), 132 (8), 107 (70), 77 (8), 57 (100). IR (ATR): ν = 3294, 2966, 2924, 1651, 1600, 1515, 1400, 1315, 1241, 810 cm^{-1}.

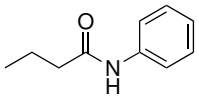

***N*-phenylbutanamide:** White solid (28.8 mg, 89%). m.p. = 97-98 °C. ^{1}H NMR (400 MHz, $CDCl_3$) δ 7.58-7.45 (m, 3H), 7.30 (t, J = 7.7 Hz, 2H), 7.09 (t, J = 7.4 Hz, 1H), 2.34 (t, J = 7.5 Hz, 2H), 1.76 (h, J = 7.4 Hz, 2H), 1.00 (t, J = 7.4 Hz, 3H). ^{13}C NMR (101 MHz, $CDCl_3$) δ 171.8, 138.0, 129.1, 124.4, 120.1, 39.7, 19.2, 13.9. MS (70 eV, EI): m/z (%): 163 ($M^{+\cdot}$, 27%), 93 (100). IR (ATR): ν = 3255, 2962, 2923, 1600, 1543, 1496, 1438, 1250, 748 690, 640 cm^{-1}.

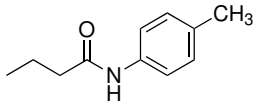

***N*-(*p*-tolyl)butanamide**. White solid (30.1 mg, 85%). m.p. = 73-74°C. ^{1}H NMR (400 MHz, $CDCl_3$) δ 7.58 (br s, 1H), 7.40 (d, J = 7.7 Hz, 2H), 7.10 (d, J = 6.6 Hz, 2H), 2.38-2.26 (m, 5H), 1.75 (q, J = 7.1 Hz, 2H), 0.99 (t, J = 6.8 Hz, 3H). ^{13}C NMR (101 MHz, $CDCl_3$) δ 171.7, 135.4, 134.0, 129.5, 120.3, 39.7, 21.0, 19.3, 13.9. MS (70 eV, EI): m/z (%): 177 ($M^{+\cdot}$, 30), 107 (100), 77 (4), 43 (7). IR (ATR): ν = 3297, 2962, 2364, 1654, 1604, 1538, 1511, 1246, 813, 737 cm^{-1}.

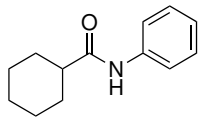

***N*-phenylcyclohexanecarboxamide:** White solid (36.9 mg, 91%). m.p. = 131-132 °C. ^{1}H NMR (400 MHz, $CDCl_3$) δ 7.61 (br s, 1H), 7.59 – 7.52 (m, 2H), 7.38 – 7.23 (m, 2H), 7.14 – 7.04 (m, 1H), 2.27 (tt, J = 11.8, 3.5 Hz, 1H), 1.95 (dtd, J = 14.9, 3.5, 1.7 Hz, 2H), 1.84 (dq, J = 13.6, 3.7 Hz, 2H), 1.75 – 1.65 (m, 1H), 1.63 – 1.48 (m, 2H), 1.37 – 1.17 (m, 3H). ^{13}C NMR (101 MHz, $CDCl_3$) δ 174.8, 138.2, 129.0, 124.2, 120.0, 46.5, 29.7, 25.7. MS (70 eV, EI): m/z (%): 203 ($M^{+\cdot}$, 25%). IR (ATR): ν = 3313, 3062, 2924, 2854, 1658, 1600, 1531, 1439, 1250, 732, 683 cm^{-1}.

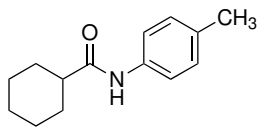

***N*-(*p*-tolyl)cyclohexanecarboxamide:** White solid (40.8 mg, 80%). m.p. = 153-155 °C. ^{1}H NMR (400 MHz, $CDCl_3$) δ 7.45 – 7.39 (m, 2H), 7.34 (s, 1H), 7.12 (d, J = 8.1 Hz, 2H), 2.32 (s, 3H), 2.28 – 2.17 (m, 1H), 2.02 – 1.90 (m, 2H), 1.90 – 1.79 (m, 2H), 1.72 (ddd, J = 5.6, 3.5, 1.6 Hz, 1H), 1.55 (qd, J = 12.1, 3.3 Hz, 2H), 1.37 – 1.20 (m, 3H). ^{13}C NMR (101 MHz, $CDCl_3$) δ 174.5, 135.6, 133.8, 129.5, 120.0, 46.6, 29.8, 25.8, 21.0. MS (70 eV, EI): m/z (%): 217 ($M^{+\cdot}$, 7%), 107 (100) 91 (5), 91 (5), 83 (27), 55 (23). IR (ATR): ν = 3244, 2927, 2854, 1655, 1600, 1516, 1446, 1319, 1253, 809 cm^{-1}.

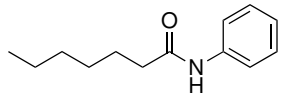

***N*-phenyleptanamide:** White solid (38.5 mg, 94%). m.p. = 64- 65 °C. ^{1}H NMR (400 MHz, $CDCl_3$) δ 7.56 (s, 1H), 7.51 (d, J = 7.9 Hz, 2H), 7.30 (t, J = 7.9 Hz, 2H), 7.10 (t, J = 7.4 Hz, 1H), 2.37 (t, J = 7.6 Hz, 2H), 1.72 (p, J = 7.5 Hz, 2H), 1.41 – 1.23 (m, 6H), 0.93 – 0.81 (m, 3H). ^{13}C NMR (101 MHz, $CDCl_3$) δ 172.0, 138.0, 129.1, 124.4, 120.1, 37.8, 31.7, 29.1, 25.8, 22.6, 14.2. MS (70 eV, EI): m/z (%): 205 ($M^{+\cdot}$, 6%), 135 (10), 93 (100), 77 (8), 43 (21). IR (ATR): ν = 3251, 2924, 2854, 1655, 1531, 1469, 1254, 2927, 2858, 1655, 721 cm^{-1}.

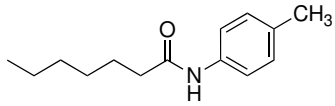

***N*-(*p*-tolyl)eptanamide:** White solid (33.7 mg, 77%). m.p. = 79-80 °C. ^{1}H NMR (400 MHz, $CDCl_3$) δ 7.44 – 7.39 (m, 2H), 7.37 (s, 1H), 7.12 (d, J = 8.1 Hz, 2H), 2.36 (d, J = 7.5 Hz, 2H), 2.32 (d, J = 2.0 Hz, 3H), 1.73 (p, J = 7.4 Hz, 2H), 1.43 – 1.25 (m, 6H), 0.94 – 0.87 (m, 3H). ^{13}C NMR (101 MHz, $CDCl_3$) δ 171.6, 135.5, 133.9, 129.5, 120.1, 37.9, 31.7, 29.1, 25.8, 22.6, 21.0, 14.2. MS (70 eV, EI): m/z (%): 233 ($M^{+\cdot}$, 9%), 149 (10), 107 (100), 91 (3), 57 (4). IR (ATR): ν = 3313, 2927, 2858, 1655, 1527, 1466, 1250, 813, 721 cm^{-1}.

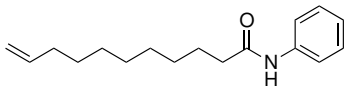

***N*-phenyl-10-undecenamide:** White solid (79%). m.p. = 65-66 °C. ^{1}H NMR (400 MHz, $CDCl_3$) δ 7.64 – 7.49 (m, 2H), 7.32 (t, J = 7.9 Hz, 2H), 7.11 (t, J = 7.4 Hz, 1H), 5.82 (ddt, J = 16.9, 10.2, 6.7 Hz, 1H), 5.09 – 4.86 (m, 2H), 2.36 (t, J = 7.6 Hz, 2H), 2.13 – 1.97 (m, 2H), 1.80 – 1.60 (m, 2H), 1.47 – 1.18 (m, 10H). ^{13}C NMR (101 MHz, $CDCl_3$) δ 171.7, 139.2, 138.0, 129.0, 124.2, 119.9, 114.2, 37.8, 37.4, 33.8, 29.3, 29.3, 29.1, 29.0, 28.9, 25.7, 25.1, 24.4. MS (70 eV, EI): m/z (%): 259 ($M^{+\cdot}$, 24 %), 148 (16), 135 (100), 120 (15). IR (ATR): ν = 3301, 2924, 2850, 1662, 1604, 1547, 1496, 1439, 1319, 1250, 1002, 914, 756, 721, 690 cm^{-1}.

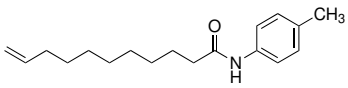

***N*-(4-Methylphenyl)-10-undecenamide:** White solid (30.7 mg, 68%). m.p. = 67-69 °C. ^{1}H NMR (400 MHz, $CDCl_3$) δ 7.66 (s, 1H), 7.43 – 7.35 (m, 2H), 7.11 (d, J = 8.1 Hz, 2H), 5.82 (ddtd, J = 16.9, 10.2, 6.7, 1.9 Hz, 1H), 5.09 – 4.86 (m, 2H), 2.38 – 2.33 (m, 2H), 2.32 (d, J = 4.1 Hz, 3H), 2.10 – 1.95 (m, 2H), 1.69 (dt, J = 18.3, 9.0 Hz, 2H), 1.41 – 1.24 (m, 10H). ^{13}C NMR (101 MHz, $CDCl_3$) δ 171.9, 139.2, 135.5, 133.9, 129.5, 120.2, 114.3, 37.7, 33.9, 29.4, 29.4, 29.2, 29.1, 29.0, 25.8, 20.9. MS (70 eV, EI): m/z (%): 273 ($M^{+\cdot}$, 18%), 149 15), 107 (100). IR (ATR): ν = 3305, 2920, 2850, 1527, 1461, 1246, 910, 814 cm^{-1}.

E.2.3 Chapter 3

All products described were obtained pure from the crude reaction mixture.

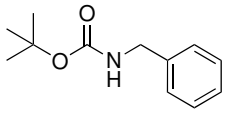

***N*-Boc-Benzylamine:** White solid. ^{1}H NMR (300 MHz, $CDCl_3$) δ = 7.39- 7.20 (m, 5H, ArH), 4.97 (br s, 1H, NH), 4.28 (s, 2H, CH_2), 1.43 (s, 9H, tbu) ppm. ^{13}C NMR (75 MHz, $CDCl_3$): δ 155.9, 139.0, 128.7, 128.5, 127.4, 79.4, 44.7, 28.4. GC/MS (EI): m/z 207 (M^{+}, 4%), 151 (90), 150 (100), 133 (7), 106 (49), 91 (73), 77 (15), 65 (11), 57 (91), 51 (9), 41 (27).

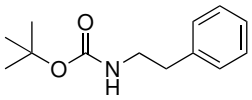

***N*-Boc-2-Phenylethylamine:** White solid. ^{1}H NMR (300 MHz, $CDCl_3$) δ 7.30-7.15 (m, 5 H, ArH), 4.54 (br s, 1H, NH), 3.50-3.47 (m, 2H, CH_2), 2.77 (t, 2H, J= 7.0 Hz, CH_2), 1.48 (s, 9H, tbu) ppm. ^{13}C NMR (75 MHz, $CDCl_3$) δ 155.9, 139.0, 128.8, 128.5, 126.5, 80.5, 41.8, 36.2, 28.4. GC/MS (EI): m/z 221 (M^{+}·, 3%), 165 (48), 104 (29), 92, 24), 91 (30), 77 (8), 65 (10), 57 (100), 41 (20), 30 (27).

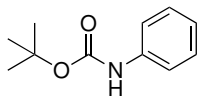

***N*-Boc-Aniline:** White solid. ^{1}H NMR (300 MHz, $CDCl_3$) δ 7.39-7.20 (m, 4H, ArH), 6.99 (t, 1H, J=.7.2 Hz ArH), 6.42 (s, 1H, NH), 1.49 (s, 9H, tBu) ppm. ^{13}C NMR (75 MHz, $CDCl_3$): δ 153.80, 138.3, 129.1, 123.0, 118.4, 80.5, 28.8. GC/MS (EI): m/z 193 ($M^{\cdot+}$, 9 %), 137 (46), 119 (5), 93 (69), 77 (7), 65 (15), 57 (100), 51 (4), 41 (32).

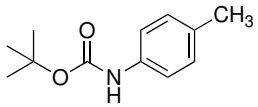

***N*-Boc *p*-Toluidine:** White solid. ^{1}H NMR (300 MHz, $CDCl_3$) δ = 7.39-7.20 (m, 4H, ArH), 6.99 (t, 1H, J=.7.2 Hz ArH), 6.42 (s, 1H, NH), 1.49 (s, 9H, tBu) ppm. ^{13}C NMR (75 MHz, $CDCl_3$): δ= 153.80, 138.3, 129.1, 123.0, 118.4, 80.5, 28.8. GC/MS (EI): m/z 193 (M^{+}·, 9%), 137 (46), 119 (5), 93 (69), 77 (7), 65 (15), 57 (100), 51 (4), 41 (32).

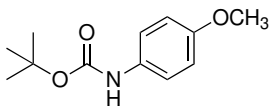

***N*-Boc *p*-Anisidine:** Off white solid. ^{1}H NMR (300 MHz, $CDCl_3$) δ 7.23 (d, J = 8.7 Hz, 2H, ArH), 6.79 (d, J = 8.7 Hz, 2H, ArH), 6.48 (br s, 1H, NH), 3.73 (s, 3H, OCH_3), 1.51 (s, 9H, tBu) ppm. ^{13}C NMR (75 MHz, $CDCl_3$) δ 155.6, 153.3, 131.5, 114.1, 80.2, 55.9, 28.4. GC/MS (EI): m/z 223 (M^{+}**·**,14%), 167 (100), 149 (9), 134 (5), 123 (34), 108 (65), 95 (7), 80 (9), 57 (74), 41 (28).

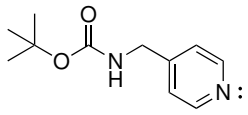

***N*-Boc Pyridin-4-methylamine:** White solid. ^{1}H NMR (300 MHz, $CDCl_3$) δ 8.90 (d, 2H, J= 4.5 Hz, ArH), 7.08 (2H, J= 4.5, ArH), 5.64 (brs, 1H, NH), 4.20 (m, 2H, CH_2), 1.43 (s, 9H, tbu) ppm. ^{13}C NMR (75 MHz, $CDCl_3$) δ 156.1, 150.3, 149.8, 121.9, 79.7, 43.4, 28.3. GC/MS (EI): m/z 208 ($M^{+\cdot}$, 4%), 152 (56), 153 (54), 135 (30), 107 (14), 92 (30), 79 (17), 65 (9), 57 (100), 51 (9), 41 (24).

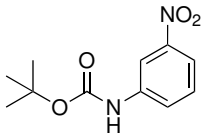

***N*-Boc 3-Nitroaniline:** Yellow solid. ^{1}H NMR (300 MHz, $CDCl_3$) δ 8.32 (s, 1H, ArH), 7.89 (d, 1H, J = 8.1 Hz, ArH), 7.70 (d, 1H, J= 8.1 Hz, ArH), 7.46 (t, 1H, J = 8.1 Hz, ArH), 6.78 (br s, 1H, NH), 1.51 (s, 9H, tbu) ppm. ^{13}C NMR (75 MHz, $CDCl_3$) δ 152.3, 148.1, 139.7, 123.5, 116.8, 113.3, 81.6, 28.3. GC/MS (EI): m/z 238 ($M^{+\cdot}$, 5%), 182 (7), 138 (15), 92 (6), 65 (7), 57 (100), 41 (22).

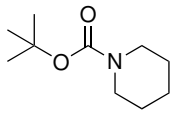

***N*-Boc Piperidine:** White solid. ^{1}H NMR: (300 MHz, $CDCl_3$) δ 3.40–3.30 (m, 2H, NCH_2), 3.19 3.09 (m, 2H, NCH_2), 1.52 (s, 9H, tbu), 1.47–1.40 [m, 6H, $NCH_2(CH_2)_3$] ppm. ^{13}C NMR: (75 MHz, $CDCl_3$). GC/MS (EI): m/z 185 ($M^{+\cdot}$, 10%), 129 (47), 112 (30), 84 (65), 69 (13), 57 (100), 41 (41).

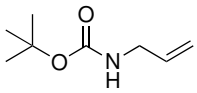

***N*-Boc Allylamine:** White solid. ^{1}H NMR (300 MHz, $CDCl_3$) δ 5.76 (m, 1H, CH), 5.14-5.02 (m, 2H, CH_2CH), 4.66 (br, s, 1H, NH), 3.68 (s, 2H, CH_2NH), 1.43 (2, 9H, tbu) ppm. ^{13}C NMR (75 MHz, $CDCl_3$, 25 °C): δ= 155.8, 134.9, 115.6, 79.3, 43.0, 28.4. GC/MS (EI): m/z 157 ($M^{+\cdot}$, 3%), 101 (72), 59 (47), 57 (100), 41 (49).

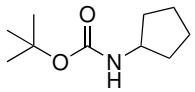

***N*-Boc Cyclopentylamine:** White solid. ^{1}H NMR (300 MHz, $CDCl_3$) δ 4.49 (br s, 1H, NH), 3.93 (br s, 1H, CH), 2.01-1.84 (m, 2H, CH_2), 1.78-1.53 (m, 6H, $CH_2CH_2CH_2$), 1.42 (s, 9H, tbu) ppm. GC/MS (EI): m/z 185 ($M^{+\cdot}$, 3%), 170 (3), 130 (26), 129 (25), 100 (13), 85 (3), 69 (9), 62 (10), 59 (32), 57 (100) , 56 (42), 41 (34).

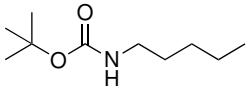

***N*-Boc Pentylamine:** White solid. ^{1}H NMR (300 MHz, $CDCl_3$) δ 4.54 (br s, 1H, NH), 3.019 (t, 2H, J= 6.8 Hz, $NHCH_2$), 1.39 (s, 9H, tBu), 1.41-1.44 (m, 2H, CH_2), 1.21-1.23 (m, 4H, CH_2CH_2), 0.82 (t, J = 6.7 Hz, 3H, CH_3) ppm. ^{13}C NMR (75 MHz, $CDCl_3$) δ 156.0, 78.9, 40.7, 29.7, 28.9, 28.4, 22.3, 13.9. GC/MS (EI): m/z 187 ($M^{+\cdot}$, 3%), 132 (21), 131 (19), 87 (10), 74 (5), 57 (100), 41 (26), 30 (18).

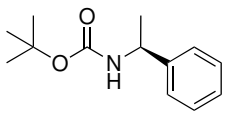

***N*-Boc (R)-1-phenylethylamine:** White solid. ^{1}H NMR (300 MHz, $CDCl_3$) δ 7.40-7.20 (m, 5H, ArH), 4.93 (br s 1H, NH), 4.78 (m, 1H, CH), 1.38 (s, 12H, tbu and CH3) ppm. ^{13}C NMR (75 MHz, $CDCl_3$) δ 155.1, 141.6, 128.6, 127.1, 125.9, 79.3, 50.2, 28.4, 22.7. GC/MS (EI): m/z 221 ($M^{+\cdot}$, 2%), 165 (64), 150 (93), 132 (6), 120 (16), 106 (64), 105 (70), 91 (3), 77 (23), 57 (100), 51 (7), 41 (23).

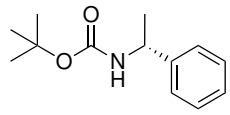

***N*-Boc (S)-1-phenylethylamine:** White solid. ^{1}H NMR (300 MHz, $CDCl_3$) δ 7.39-7.11 (m, 5H, ArH), 4.90-4.68 (m, 2H, NH, CH),1.35 (s, 12H, tbu and CH_3) ppm. ^{13}C NMR (75 MHz, $CDCl_3$) δ 155.6, 143.6, 128.7, 127.2, 126.0, 79.4, 55.1, 28.4, 22.7. GC/MS (EI): m/z 221 (M^{+}·, 2%), 165 (64), 150 (100), 132 (6), 120 (16), 105 (70),106 (62), 91(3), 77 (23), 57 (87), 51 (7), 41 (23).

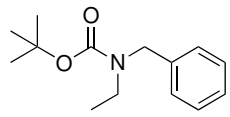

***N*-Boc *N*-Ethylbenzylamine:** White solid. ^{1}H NMR (300 MHz, $CDCl_3$) δ 7.40-7.20 (m, 5H, ArH), 4.42 (s, 2H, CH_2Ph), 3.40-3.12 (m, 2H, CH_2CH_3), 1.52 (s, 9H, tbu), 1.06 (m, 3H, CH_2CH_3) ppm. ^{13}C NMR (75 MHz, $CDCl_3$) δ 154.2, 137.2, 128.5, 128.3, 127.1, 79.5, 50.6, 41.3, 28.5, 13.3. GC/MS (EI): m/z 235 (M^{+}·, 3%), 220 (3), 179 (82), 164 (12), 150 (5), 134 (13), 120 (38), 106 (5), 92 (25), 91 (100), 77 (5), 65 (10), 57 (80), 41 (20).

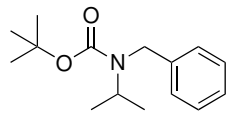

***N*-Boc *N*-Isopropylbenzylamine:** White solid. ^{1}H NMR (300 MHz, $CDCl_3$) δ 7.29-7.15 (m, 5H, ArH), 4.32-4.10 (m, 2H, NH, CH), 1.43 (s, 9H, tbu), 0.861 (d, 6H, J= 6Hz, $CH(CH_3)_2$) ppm. ^{13}C NMR (75 MHz, $CDCl_3$, 25 °C) δ 139.0, 128.1, 127.3, 126.6, 79.5, 57.3, 47.1, 28.4, 20.8. GC/MS (EI): m/z 249 (M^{+}·, 3%), 234 (3), 193 (45), 178 (32), 150 (10), 134 (38), 106 (7), 92 (7), 91 (100), 77 (5), 65 (10), 57 (80), 41 (24).

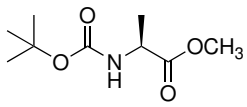

***N*-Boc L-Alanine methyl ester:** White solid. ^{1}H NMR (300 MHz, $CDCl_3$) δ 5.05 (brs, 1H NH), 4.32 (m, 1H, α-CH), 3.75 (s, 3H, OMe), 1.44 (s, 9H, tbu), 1.38 (d, J = 7.2 Hz, 3H, CH_3) ppm. ^{13}C NMR (150 MHz, $CDCl_3$) δ 173.8, 154.2, 79.8, 54.4, 49.1, 28.3, 18.6 .GC/MS (EI): m/z 203 (M^{+}·, 3%), 188 (3), 144 (36), 130 (7), 116 (5), 102 (18), 88 (28), 70 (7), 59 (30), 57 (100).

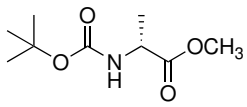

***N*-Boc D-Alanine methyl ester:** White solid. ^{1}H NMR (300 MHz, $CDCl_3$) δ 5.05 (br s, 1H, NH), 4.32 (m, 1H, α-CH), 3.75 (s, 3H, OMe), 1.44 (s, 9H, tbu), 1.38 (d, J = 7.2 Hz, 3H, CH_3) ppm. ^{13}C NMR (150 MHz, $CDCl_3$) δ 173.8, 154.2, 79.8, 54.4, 49.1, 28.3, 18.6. GC/MS (EI): m/z 203 (M^{+}·, 3%), 144 (36), 130 (7), 116 (5), 102 (18), 88 (28), 70 (7), 57 (100).

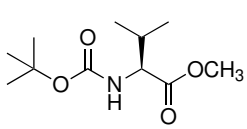

***N*-Boc -L-Valine methyl ester:** White solid. ^{1}H NMR (300 MHz, $CDCl_3$) δ 5.04 (d, 1H, J=6.9 Hz, NH), 4.17 (m, 1H, α-CH), 3.70 (s, 3H, OMe), 2.07 (m, 1H, $CH(CH_3)_3$), 1.42 (s, 9H, tbu), 0.92 (d, 3H, J= 6.6 Hz, CH_3), 0.86 (d, 3H, J= 6.9 Hz, CH_3) ppm. ^{13}C NMR (150 MHz, $CDCl_3$) δ172.8, 155.6, 79.6, 53,1, 51.5, 30.4, 28.3, 18.4. GC/MS (EI): m/z (%) 231 (M^{+}·, 3%), 172 (22), 158 (5), 130 (19), 116 (52), 98 (10), 88 (12), 72 (65), 57 (100).

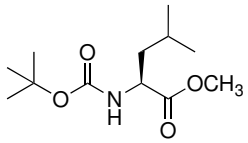

***N*-Boc L-Leucine methyl ester:** White solid. ^{1}H NMR (300 MHz, $CDCl_3$) δ 5.10 (d, 1H, J= 8.1 Hz, NH), 4.18 (m, 1H, α-CH), 3.56 (s, 3H, OMe), 1.58 (m, 1H, CH_2), 1. 47 (m, 2H, CH_2, $CH(CH_3)_2$), 1.38 (s, 9H, tbu), 0.81 (d, 6H, J= 6.3 $(CH_3)_2$) ppm. ^{13}C NMR (150 MHz, $CDCl_3$) δ 173.8, 155.9, 79.5, 53.6, 52.8, 41.6, 28.3, 24.5, 22.7. GC/MS (EI): m/z 230 ($M^{+\cdot}$, 15%), 186 (20), 172 (3), 144 (13), 130 (65), 86 (72), 57 (100).

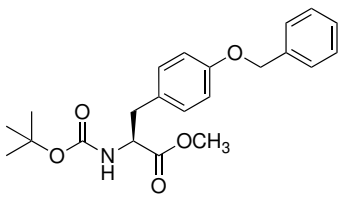

***N*-Boc O-Benzyl-L-Tyrosine methyl ester:** White solid. ^{1}H NMR (300 MHz, $CDCl_3$) δ 7.49-7.31 (m, 5H, ArH), 7.06 (d, 2H, J=7.2 Hz, ArH), 6.93 (d, 2H, J=7.2 Hz, ArH), 5.08 (s, 2H, OCH_2), 4.53 (m, 1H, α-CH), 3.71 (s, 3H, OMe), 3.13-2.99 (m, 2H, CH_2Ph), 1.42 (s,9H, tbu) ppm. ^{13}C NMR (75 MHz, $CDCl_3$) δ 172.4, 155.1, 146.7, 137.1, 129.5, 128.7, 128.4, 127.3, 114.9, 79.8, 70.0, 54.6, 51.9, 37.5, 28.3.

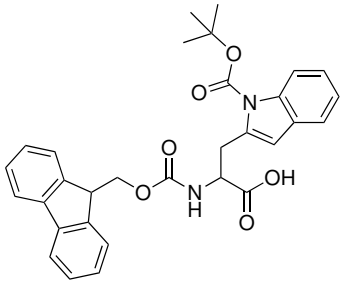

***Nα*-Fmoc-N(in)-Boc-L-tryptophan:** White solid. ^{1}H NMR (300 MHz, $CDCl_3$) δ 8.08 (d, 1H, J = 7.5 Hz, NH), 7.73-7.71 (m, 3H, ArH), 7.56–7.16 (m, 10 H), 5.44 (d, 1H, J= 7.5 Hz, α-CH), 4.76 (m, 1H), 4.78 (m, 1H, CH-Fmoc), 4.35 (m, 2H, CH_2-Fmoc), 3.31-3.14 (m, 2H, CH_2-Trp), 3.49 (s, 1H), 1.62 (s, 9H, tBu) ppm. ^{13}C NMR (150 MHz, $CDCl_3$) δ 175.6, 143.7, 141.3, 135.3, 130.2, 127.6, 127.2, 125.2, 124.8, 120.5, 119.9, 118.8, 114.9, 110.9, 83.9, 67.3, 59.4, 47.0, 28.16.

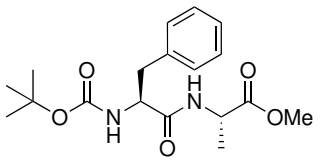

***N*-Boc L-Phe-LAlaOMe:** White solid. ^{1}H NMR (300 MHz, $CDCl_3$) 7.23–7.15 (m, 5H, ArH), 6.70 (br s, 1H, OCONH), 5.14 (d, 1H, J = 8.2 Hz, $NHCHCH_3$), 4.47 (m, 1H, α-CHAla); 4.38 (m, 1H, α-CHPhe), 3.66 (s, 3H, OMe), 3.09–2.92 (m, 2H, CH_2Ph), 1.31 (s, 9H, tBu), 1.18-1.14 (d, 3H, $CHCH_3$) ppm. ^{13}C NMR (75 MHz, $CDCl_3$) 172.9, 171.0, 155.4, 136.6, 129.4, 128.5, 126.6, 80.1, 55.7, 52.1, 47.9, 38.3, 28.2, 17.8. GC/MS (EI): m/z 350 ($M^{+\cdot}$, 2%), 294 (9), 277 (5), 263 (4), 233 (14), 174 (12), 164 (37), 159 (21), 120 (90), 91 (19), 77 (4), 57 (100).

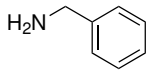

Benzylamine: Transparent liquid. ^{1}H NMR (300 MHz, DMSO-d_6) δ 9.01 (brs, 2H). 7.43-7.20 (m, 5H), 5.13 (s, 2H). ^{13}C NMR (75 MHz, DMSO-d_6) 144.6, 129.2, 126.9, 126.5, 45.6 ppm. GC/MS (EI): m/z 107 ($M^{+\cdot}$, 100%), 91 (14), 79 (43), 65 (7), 51 (17).

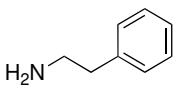

2-phenylethylamine: Transparent liquid. ^{1}H NMR (300 MHz, DMSO-d_6) δ 7.53 (m, 2H), 7.31-7.26 (m, 3H), 5.42 (brs, 2H), 2.99-2.95 (m, 2H), 2.85-2.81 (m, 2H). ^{13}C NMR (75 MHz, DMSO-d_6) δ 139.5, 128.8, 124.8, 41.7, 38.7 ppm. GC/MS (EI): m/z 121 ($M^{+\cdot}$, 23%), 91 (100), 77 (19), 65 (48), 51 (25).

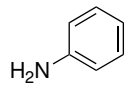	**Aniline:** Yellow liquid. ^{1}H NMR (300 MHz, DMSO-d_6) δ 7.24-7.18 (m, 2H), 6.94-6.72 (m, 1H), 6.61-6-41 (m, 2H), 6.32 (brs, 1H). ^{13}C NMR (75 MHz, DMSO-d_6) δ 152.3, 128.7, 122.3, 115.7 ppm. GC/MS (EI): m/z 93 ($M^{+\cdot}$, 100%), 66 (42).
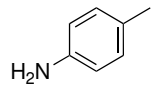	***p*-toluidine:** white solid. ^{1}H NMR (300 MHz, DMSO-d_6) δ 7.01-6.95 (m, 2H), 6.53-6.48 (m, 2H), 6.27 (brs, 2H), 2.38 (s, 3H). ^{13}C NMR (75 MHz, DMSO-d_6) δ 146.3, 131.6, 129.5, 115.3 ppm. GC/MS (EI): m/z 107 ($M^{+\cdot}$, 100), 77 (18), 52 (8), 41 (4).
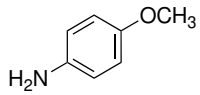	***p*-anisidine:** White solid. ^{1}H NMR (300 MHz, DMSO-d_6) δ 6.76-6.72 (m, 2H), 6.68-6.64 (M, 2H), 6.24 (brs, 2H), 3.78 (s, 3H). ^{13}C NMR (75 MHz, DMSO-d_6) δ 153.8, 141.3, 115.7, 115.3, 50.4 ppm. GC/MS (EI): m/z 123 ($M^{+\cdot}$, 63%), 108 (100), 95 (4), 80 (48), 65 (8), 53 (19), 41 (4).
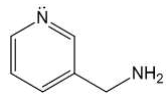	**4-pycolilamine:** ^{1}H NMR (300 MHz, DMSO-d_6) δ 8.92 (brs, 2H), 8.63-8.54 (m, 2H), 7.37-7.21 (m, 2H), 4.36 (s, 2H). ^{13}C NMR (75 MHz, DMSO-d_6) δ150.4, 147.3, 123.2, 40.3 ppm. GC/MS (EI): m/z 108 ($M^{+\cdot}$, 24), 80 (100), 51 (16) inserire metilene
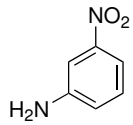	**3-nitroaniline:** Yellow solid. ^{1}H NMR (300 MHz, DMSO-d_6) δ 7.68-7.64 (m, 2H), 7.55-7.32 (m, 2), 6.25 (brs, 2H). ^{13}C NMR (75 MHz, DMSO-d_6) δ 150.2, 148.9, 131.5, 121.1, 114.3, 109.6 ppm. GC/MS (EI): m/z 138 ($M^{+\cdot}$, 74%), 122 (13), 92 (100)
	**Pyperidine:** Transparent liquid. ^{1}H NMR (300 MHz, DMSO-d_6) δ 2.83-2.72 (m, 5H), 1.54-1.46 (m, 6H). ^{13}C NMR (75 MHz, DMSO-d_6) δ 48.3, 25.4, 22.1 ppm. GC/MS (EI): m/z 85 ($M^{+\cdot}$, 100%), 70 (12), 56 (49). 44 (25).
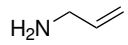	**Allylamine:** Transparent liquid. ^{1}H NMR (300 MHz, DMSO-d_6) δ 5.98-5.74 (m, 1H), 5.30-5.16 (m, 2H), 3.43-4.37 (m, 2H), 1.76 (brs, 2H). ^{13}C NMR (75 MHz, DMSO-d_6) δ 133.5, 112.9, 43.2 ppm.
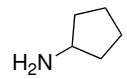	**Cyclopentylamine:** Transparent liquid. ^{1}H NMR (300 MHz, DMSO-d_6) δ 5.81 (brs, 2H), 3.22-2.65 (m, 1H), 1.88-1.44 (m, 8H). ^{13}C NMR (75 MHz, DMSO-d_6) δ 50.4, 33.4, 23.5 ppm. GC/MS (EI): m/z 85 ($M^{+\cdot}$, 12%), 56 (100), 43 (9).
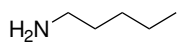	**Pentylamine:** Transparent liquid. ^{1}H NMR (300 MHz, DMSO-d_6) δ 5.12 (brs, 2H), 2.70-2.58 (m, 2H), 1.60-1.30 (m, 4H), 1.07-0.93 (m, 3H). ^{13}C NMR (75 MHz, DMSO-d_6) δ 42.5, 35.6, 21.5, 14.1 ppm. GC/MS (EI): m/z 87 ($M^{+\cdot}$, 100%), 69 (9), 55 (23), 41 (86)

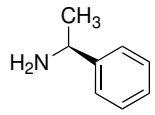	**(S)-1-Phenyl ethylamine:** Transparent liquid. ^{1}H NMR (300 MHz, DMSO-d_6) δ 7.52-7.41 (m, 2H), 7.30-7.26 (m, 3H), 5.23 (brs, 2H) 4.22-4.05 (m, 1H), 1.30-1.26 (m, 3H). ^{13}C NMR (75 MHz, DMSO-d_6) δ 148.3, 127.5, 16.9, 125.9, 52.4, 25.8 ppm. GC/MS (EI): m/z 121 ($M^{+\cdot}$, 6%), 106 (100), 79 (29), 51 (9).
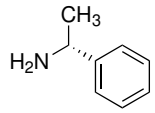	**(R)-1-Phenyl ethylamine:** Transparent liquid. ^{1}H NMR (300 MHz, DMSO-d_6) δ 7.64-7.58 (m, 2H), 7.28-7.21 (m, 3H), 5.29 (brs, 2H) 4.23-4.05 (m, 1H), 1.45-1.32 (m, 3H). ^{13}C NMR (75 MHz, DMSO-d_6) δ 142.3, 129.5, 128.9, 122.7, 53.9, 25.2 ppm. GC/MS (EI): m/z 121 ($M^{+\cdot}$, 8%), 106 (100), 79 (25), 51 (13).
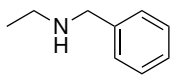	***N*-ethyl benzylamine**. White solid. ^{1}H NMR (300 MHz, DMSO-d_6) δ 7.43-7.18 (m, 5H), 4.86 (brs, 1H), 3.54 (s, 2H), 2.65-2.48 (m, 2H), 1.02 (t, 3H). ^{13}C NMR (75 MHz, DMSO-d_6) δ 142.3, 128.4, 127.5, 127.0, 56.3, 44.3, 18.2 ppm. GC/MS (EI): m/z 135 ($M^{+\cdot}$, 13%),120 (31), 91 (100), 79 (6), 65 (12), 58 (14)
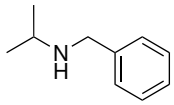	***N*-isopropryl benzylamine.** White solid. ^{1}H NMR (300 MHz, DMSO-d_6) δ 7.42-7.22 (m, 5H), 4.81 (brs, 1H), 3.77 (s, 2H), 3.23-2.82 (m, 1H), 1.34-1.03 (m, 6H). ^{13}C NMR (75 MHz, DMSO-d_6) δ 141.3, 129.6, 127.5, 127.01, 53.4, 51.4, 27.1. GC/MS (EI): m/z 149 ($M^{+\cdot}$, 4%), 134 (43), 106 (4), 91 (100), 77 (4), 65 (10), 41 (4).
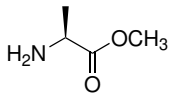	**D-Ala-OMe.** White solid. ^{1}H NMR (300 MHz, DMSO-d_6) δ 5.24 (brs, 2H), 6.70-3.60 (M, 4H), 1.34-1.28 (m, 3H). ^{13}C NMR (75 MHz, DMSO-d_6) δ 173.1, 53.4, 49.7, 18.4 ppm.
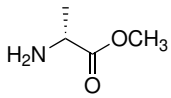	**L-Ala-OMe.** White solid. ^{1}H NMR (300 MHz, DMSO-d_6) δ 5.24 (brs, 2H), 6.78-3.63 (M, 4H), 1.38-1.22 (m, 3H). ^{13}C NMR (75 MHz, DMSO-d_6) δ 173.5, 54.4, 49.7, 18.1 ppm.
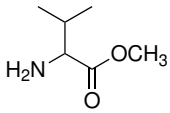	**Val-OMe.** White solid. ^{1}H NMR (300 MHz, DMSO-d_6) δ 5.11 (brs, 2H), 4.54-4.23 (M, 1H), 3.54 (s, 3H), 2.96-2.74 (m, 1H), 0.90 (d, 6H). ^{13}C NMR (75 MHz, DMSO-d_6) δ 171.8, 61.3, 52.9, 42.6, 20.1 ppm.
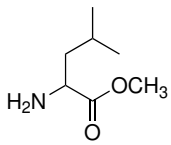	**Leu-OMe:** White solid. ^{1}H NMR (300 MHz, DMSO-d_6) δ 5.17 (brs, 2H), 3.41 (s, 3H), 3.21 (t, 1H), 1.88 (t, 2H), 1.54-1.37 (M, 1H), 0.91 (d, 6H). ^{13}C NMR (75 MHz, DMSO-d_6) δ 176.3, 53.4, 52.8, 43.2, 25.6, 22.6 ppm.

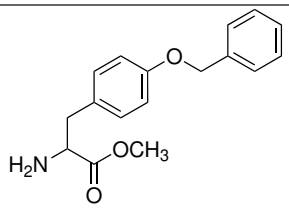	**O-Benzyl-L-Tyrosine methyl ester:** White solid. ^{1}H NMR (300 MHz, DMSO-d_6) δ 7-55-7.33 (m, 5H), 7-28-7.13 (m, 2H), 6.98-6.54 (m, 2H), 5.21 (s, 2H), 5.17 (brs, 2H), 4.67-4.43 (m, 1H), 3.66 (s, 3H), 3.54-3.29 (m, 2H). ^{13}C NMR (75 MHz, DMSO-d_6) δ 173.4, 156.4, 137.2, 128.7, 127.3, 115.3, 71.8, 55.2, 51.9, 37.2 ppm.
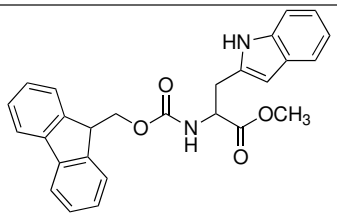	***N*-Fmoc-Tryptophan:** White solid. ^{1}H NMR (300 MHz, DMSO-d_6) δ 8.03 (s, 1H), 7.91-7.87 (m, 2H), 7.63-7.54 (m, 2H), 7.38-7.28 (m, 5H), 7.10-6.98 (m, 3H), 6.02 (s, 1H), 4.74-4.67 (m, 3H), 4.46-4.38 (m, 1H), 3.70 (s, 3H), 3.33-3.08 (m, 2H) ppm. ^{13}C NMR (75 MHz, DMSO-d_6) δ 172.3, 160.1, 144.3, 143.8, 138.3, 133.7, 128.5, 127.3, 126.5, 121.7, 120.5, 119.7, 111.3, 98.7, 67.5, 60.7, 46.5, 29.8 ppm.
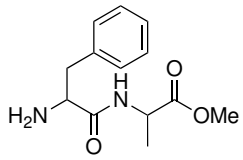	**Phe-Ala:** White solid. ^{1}H NMR (300 MHz, DMSO-d_6) δ 8.03 (s, 1H), 7.43-7.39 (m, 2H), 5.32-5-29 (m, 2H), 4.47-4.39 (m, 1H), 4.28-3.95 (m, 1H), 3.72 (s, 3H), 3.43-3.22 (m, 2H), 1.52-1.49 (m, 3H) ppm. ^{13}C NMR (75 MHz, DMSO-d_6) δ 173.2, 171.8, 136.7, 127.9, 123.7, 56.3, 51.8, 51.5, 39.1, 23.1 ppm.

E.2.4 Chapter 4

All products described were obtained pure from the crude reaction mixture

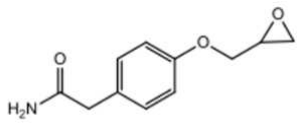	**Intermediate 5:** White solid. ^{1}H NMR (300MHz, DMSO-d6) 7.37 (br s, 1H, NH), 7.19 (d, 2H, ArH), 6.89 (d, 2H, ArH), 6.81 (s, 1H, NH), 4.29 (m, 1H, CH ossiranic), 3.98 (s, 2H, CH_2CONH_2), 3.82-3.69 (m, 2H, OCH_2), 2.84 (s, 1H, CH_2 ossiranic diast), 2.71 (s, 1H, CH_2 ossiranic diast) ppm. ^{13}C NMR; EI (MS) 207 (43, $M^{+\cdot}$), 191 (2), 163 (100), 133 (10), 107 (99), 89 (12), 77 (20), 57 (26), 44 (22) ppm.
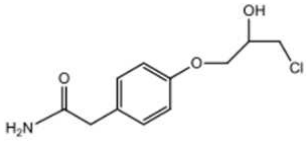	**Intermediate 6:** White solid. EI (MS) 243/245 ($M^{+\cdot}$, 20/7%), 199/201 (49/17), 131 (9), 107 (100), 89 (10), 77 (13), 57 (6), 44 (12).
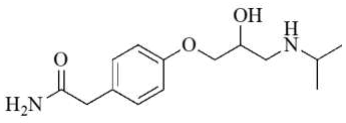	**Atenolol:** White solid. ^{1}H NMR (300 MHz, DMSO-d6) δ 7.39 (s, 1H, NH_2), 7.16 (m, 2H, ArH), 6.86 (d, 3H, ArH, NH_2), 4.97 (br s, 1H, OH), 3.95-3.83 (m, 3H, CHOH, CH_2CHOH), 3.29 (s, 2H, CH_2CONH_2), 2.76-2.66 (m, 2H, CH_2NH), 2.57 (m, 1H, $CH(CH_3)_2$), 1.51 (br s, 1H, NH), 0.98-95 (m, 6H, $CH(CH_3)_2$); ^{13}C NMR (75 MHz, DMSO-d_6) δ 173.6, 158.0, 130.7, 129.8, 114.9, 80.0, 68.5, 50.7, 48.9, 42.1, 23.4, 22.6 ppm.

General Conclusions

In conclusion, deep eutectic solvents (DESs) have been found to be truly sustainable alternatives for hazardous and toxic solvents for pharmaceutical purposes, such as those exposed in this doctoral thesis:

- Reactive DESs (RDESs) have been successfully employed as both reaction media and reagents for direct *N*-amidation of amines with carboxylic acids, showing a promising and eco-friendly alternative for amide synthesis;
- A significant breakthrough in visible-light-promoted photo-redox catalytic amide formation within an eco-friendly and biodegradable DES based on the ChCl:urea mixture has been described. This protocol not only demonstrates the feasibility of photoredox catalysis using DESs as reaction media but also emphasizes the combination of sustainable solvents and a mild, efficient photo-induced activation process. The potential of this breakthrough is underscored as it may open new avenues for further exploration and studies in this field;
- Furthermore, a novel and highly efficient approach for *N*-Boc deprotection using pTSA-based RDES has been developed. The method versatility, ease of operation, and environmentally friendly characteristics position it as a promising alternative for the selective deprotection of N-Boc derivatives across a range of substrates;
- In the realm of pharmaceutical synthesis, a robust, environmentally friendly, and economically viable method for synthesizing atenolol has been disclosed. This method involves a one-pot, two-step synthesis of atenolol in ChCl: ethylene glycol DES, showcasing the versatility and environmentally friendly nature of the system;
- Finally, the research also delves into the potential of DESs to enhance the solubility profile of water-insoluble drugs, focusing specifically on mesalazine and dapsone. The observed increase in solubility in these formulations holds promise for improving the bioavailability and efficiency of mesalazine and dapsone, addressing a key challenge in their pharmaceutical use. In summary, these findings contribute significantly to advancing sustainable and environmentally friendly practices within the pharmaceutical industry.

Future Perspectives

The results obtained from the present doctoral thesis underscore the promising role of Deep Eutectic Solvents as viable alternatives to conventional solvents in synthetic methodologies. Continued research and development in this area will contribute to advancing sustainable and environmentally friendly synthetic protocols using DES, aligning with the principles of green chemistry. Moreover, the unique properties of DESs in enhancing the solubility and delivery of poorly water-soluble drugs offer promising opportunities to optimize drug release profiles, stability, and targeting capabilities. However, comprehensive evaluation of the toxicity profile of DESs is imperative to ensure their safe and responsible application in pharmaceutical formulations. Future studies should prioritize assessing the toxicity, understanding the metabolic pathways of DESs, and investigating potential long-term effects to facilitate their integration into drug development and delivery systems.

In summuary, the findings from this doctoral thesis pave the way for further exploration and development of DES as innovative solvents in pharmaceutical applications. Continued research efforts will be essential in advancing our understanding of DES properties as alternative reaction media, their safety profiles, and their full potential in revolutionizing the overall pharmaceutical industrial processes.

Acknowledgments

I would like to express my sincere gratitude to the esteemed institutions whose financial support has enabled the realization of this research endeavor. I acknowledge the invaluable financial assistance provided by the Ministero dell'Università e della Ricerca (MUR) and the University of Calabria, whose contributions have significantly propelled the advancement of this study. Furthermore, I extend my appreciation to the University of Alicante (VIGROB-316FI), the Spanish Ministerio de Ciencia e Innovación (PID2021-127332NB-I00), and the Valencian Department of Innovation, Universities, Science, and Digital Society (APOSTD/2020/235 and AICO/2021/013) for their generous support. Their contributions have played a crucial role in fostering the progression of this research initiative.

Bibliography

(1) Fauzi, R. T.; Lavoie, P.; Sorelli, L.; Heidari, M. D.; Amor, B. Exploring the Current Challenges and Opportunities of Life Cycle Sustainability Assessment. *Sustainability* **2019**, *11* (3), 636;

(2) Sijtsema, S. J.; Snoek, H. M.; van Haaster-de Winter, M. A.; Dagevos, H. Let's Talk about Circular Economy: A Qualitative Exploration of Consumer Perceptions. *Sustainability* **2019**, *12* (1), 286;

(3) Sadhukhan, J.; Dugmore, T. I. J.; Matharu, A.; Martinez-Hernandez, E.; Aburto, J.; Rahman, P. K. S. M.; Lynch, J. Perspectives on "Game Changer" Global Challenges for Sustainable 21st Century: Plant-Based Diet, Unavoidable Food Waste Biorefining, and Circular Economy. *Sustainability* **2020**, *12* (5), 1976;

(4) Costanza, R.; Fioramonti, L.; Kubiszewski, I. The UN Sustainable Development Goals and the Dynamics of Well-Being. *Front. Ecol. Environ.* **2016**, *14*, 59;

(5) Anastas, P. T.; Warner, J. C. *Green Chemistry*; Oxford University PressOxford, **2000**;

(6) Tang, S. L. Y.; Smith, R. L.; Poliakoff, M. Principles of Green Chemistry: productively. *Green Chemistry* **2005**, *7* (11), 761;

(7) Sheldon, R. A. Fundamentals of Green Chemistry: Efficiency in Reaction Design. *Chem. Soc. Rev.* **2012**, *41* (4), 1437–1451;

(8) Anastas, P.; Eghbali, N. Green Chemistry: Principles and Practice. *Chem. Soc. Rev.* **2010**, *39* (1), 301–312;

(9) Simon, M.-O.; Li, C.-J. Green Chemistry Oriented Organic Synthesis in Water. *Chem. Soc. Rev.* **2012**, *41* (4), 1415–1427;

(10) Sheldon, R. A.; Bode, M. L.; Akakios, S. G. Metrics of Green Chemistry: Waste Minimization. *Curr Opin Green Sustain. Chem.* **2022**, *33*, 100569;

(11) Sheldon, R. A. The E Factor 25 Years on: The Rise of Green Chemistry and Sustainability. *Green Chem.* **2017**, *19* (1), 18–43;

(12) Monteith, E. R.; Mampuys, P.; Summerton, L.; Clark, J. H.; Maes, B. U. W.; McElroy, C. R. Why We Might Be Misusing Process Mass Intensity (PMI) and a Methodology to Apply It Effectively as a Discovery Level Metric. *Green Chem.* **2020**, *22* (1), 123–135;

(13) McElroy, C. R.; Constantinou, A.; Jones, L. C.; Summerton, L.; Clark, J. H. Towards a Holistic Approach to Metrics for the 21st Century Pharmaceutical Industry. *Green Chem.* **2015**, *17* (5), 3111–3121;

(14) L. Summerton; H. F. Sneddon; L. C. Jones; J. H. Clark. Green and Sustainable Medicinal Chemistry: Methods, Tools and Strategies for the 21st Century Pharmaceutical Industry. *RSC* **2016**;

(15) Dicks, A. P.; Hent, A. Atom Economy and Reaction Mass Efficiency In: Green Chemistry Metrics. SpringerBriefs in Molecular Science. Springer, Cham. **2015**, 17–44;

(16) Trost, B. The Atom Economy—A Search for Synthetic Efficiency. *Science* **1991**, *254* (5037), 1471–1477;

(17) Dicks, A. P.; Hent, A. The E Factor and Process Mass Intensity; In: Green Chemistry Metrics. SpringerBriefs in Molecular Science. Springer, Cham.**2015**, 45–67;

(18) Jimenez-Gonzalez, C.; Ponder, C. S.; Broxterman, Q. B.; Manley, J. B. Using the Right Green Yardstick: Why Process Mass Intensity Is Used in the Pharmaceutical Industry To Drive More Sustainable Processes. *Org Process Res Dev* **2011**, *15* (4), 912–917;

(19) L. Summerton; A. Constantinou, in Green and Sustainable Medicinal Chemistry for the 21st Century Pharmaceutical Industry, ed. L. Jones, L. Summerton, H. Sneddon and J. Clark, RSC, Cambridge, **2024** (submitted);

(20) Gupta, P.; Mahajan, A. Green Chemistry Approaches as Sustainable Alternatives to Conventional Strategies in the Pharmaceutical Industry. *RSC Adv* **2015**, *5* (34), 26686–26705;

(21) Byrne, F. P.; Jin, S.; Paggiola, G.; Petchey, T. H. M.; Clark, J. H.; Farmer, T. J.; Hunt, A. J.; Robert McElroy, C.; Sherwood, J. Tools and Techniques for Solvent Selection: Green Solvent Selection Guides. *Sustainable Chemical Processes* **2016**, *4* (1), 7;

(22) Zhou, X.; Zhou, X.; Wang, C.; Zhou, H. Environmental and Human Health Impacts of Volatile Organic Compounds: A Perspective Review. *Chemosphere* **2023**, *313*, 137489;

(23) Yaseen, G.; Ahmad, M.; Zafar, M.; Akram, A.; Sultana, S.; Kilic, O.; Sonmez, G. D. Current Status of Solvents Used in the Pharmaceutical Industry. In *Green Sustainable Process for Chemical and Environmental Engineering and Science*; Elsevier, **2021**, 195–219;

(24) Constable, D. J. C.; Jimenez-Gonzalez, C.; Henderson, R. K. Perspective on Solvent Use in the Pharmaceutical Industry. *Org Process Res Dev* **2007**, *11* (1), 133–137;

(25) Henderson, R. K.; Jiménez-González, C.; Constable, D. J. C.; Alston, S. R.; Inglis, G. G. A.; Fisher, G.; Sherwood, J.; Binks, S. P.; Curzons, A. D. Expanding GSK's Solvent Selection Guide – Embedding Sustainability into Solvent Selection Starting at Medicinal Chemistry. *Green Chemistry* **2011**, *13* (4), 854;

(26) Prat, D.; Hayler, J.; Wells, A. A Survey of Solvent Selection Guides. *Green Chem.* **2014**, *16* (10), 4546–4551;

(27) Prat, D.; Wells, A.; Hayler, J.; Sneddon, H.; McElroy, C. R.; Abou-Shehada, S.; Dunn, P. J. CHEM21 Selection Guide of Classical- and Less Classical-Solvents. *Green Chem.* **2016**, *18* (1), 288–296;

(28) Gawande, M. B.; Bonifácio, V. D. B.; Luque, R.; Branco, P. S.; Varma, R. S. Solvent-Free and Catalysts-Free Chemistry: A Benign Pathway to Sustainability. *ChemSusChem* **2014**, *7* (1), 24–44;

(29) Zangade, S.; Patil, P. A Review on Solvent-Free Methods in Organic Synthesis. *Curr Org Chem* **2020**, *23* (21), 2295–2318;

(30) Cseri, L.; Razali, M.; Pogany, P.; Szekely, G. Organic Solvents in Sustainable Synthesis and Engineering. In *Green Chemistry*; Elsevier, **2018**,513–553.

(31) Sperry, J.; García-Álvarez, J. Special Issue: "Organic Reactions in Green Solvents." *Molecules* **2016**, *21* (11), 1527;

(32) Häckl, K.; Kunz, W. Some Aspects of Green Solvents. *C. R. Chim.* **2018**, *21* (6), 572–580;

(33) Capello, C.; Fischer, U.; Hungerbühler, K. What Is a Green Solvent? A Comprehensive Framework for the Environmental Assessment of Solvents. *Green Chem.* **2007**, *9* (9), 927;

(34) Dunn, P. Water as a Green Solvent for Pharmaceutical Applications. In *Handbook of Green Chemistry*; Wiley, **2010**, 363–383;

(35) Hartonen, K.; Riekkola, M.-L. Water as the First Choice Green Solvent. In *The Application of Green Solvents in Separation Processes*; Elsevier, **2017**, 19–55;

(36) Zhou, F.; Hearne, Z.; Li, C.-J. Water—the Greenest Solvent Overall. *Curr Opin Green Sustain Chem* **2019**, *18*, 118–123;

(37) Calvo-Flores, F. G.; Monteagudo-Arrebola, M. J.; Dobado, J. A.; Isac-García, J. Green and Bio-Based Solvents. *Top Curr Chem* **2018**, *376* (3), 18;

(38) Gu, Y.; Jérôme, F. Bio-Based Solvents: An Emerging Generation of Fluids for the Design of Eco-Efficient Processes in Catalysis and Organic Chemistry. *Chem Soc Rev* **2013**, *42* (24), 9550;

(39)Sheldon, R. A. Green Solvents for Sustainable Organic Synthesis: State of the Art. *Green Chem.* **2005**, *7* (5), 267;

(40) Horváth, I. T.; Mehdi, H.; Fábos, V.; Boda, L.; Mika, L. T. γ-Valerolactone—a Sustainable Liquid for Energy and Carbon-Based Chemicals. *Green Chem.* **2008**, *10* (2), 238–242;

(41) Sherwood, J.; De bruyn, M.; Constantinou, A.; Moity, L.; McElroy, C. R.; Farmer, T. J.; Duncan, T.; Raverty, W.; Hunt, A. J.; Clark, J. H. Dihydrolevoglucosenone (Cyrene) as a Bio-Based Alternative for Dipolar Aprotic Solvents. *Chem. Commun.* **2014**, *50* (68), 9650–9652;

(42) Onyekere, P. F.; Nnamani, D. O.; Peculiar-Onyekere, C. O.; Uzor, P. F. Limonene. In *Green Sustainable Process for Chemical and Environmental Engineering and Science*; Elsevier, **2021**, 219–227;

(43) Pace, V.; Hoyos, P.; Castoldi, L.; Domínguez de María, P.; Alcántara, A. R. 2-Methyltetrahydrofuran (2-MeTHF): A Biomass-Derived Solvent with Broad Application in Organic Chemistry. *ChemSusChem* **2012**, *5* (8), 1369–1379;

(44) Noyori, R. Supercritical Fluids: Introduction. *Chem Rev* **1999**, *99* (2), 353–354;

(45) Oakes, R. S.; Clifford, A. A.; Rayner, C. M. The Use of Supercritical Fluids in Synthetic Organic Chemistry. *J Chem Soc Perkin 1* **2001**, No. 9, 917–941;

(46) Alekseev, E. S.; Alentiev, A. Yu.; Belova, A. S.; Bogdan, V. I.; Bogdan, T. V.; Bystrova, A. V.; Gafarova, E. R.; Golubeva, E. N.; Grebenik, E. A.; Gromov, O. I.; Davankov, V. A.; Zlotin, S. G.; Kiselev, M. G.; Koklin, A. E.; Kononevich, Y. N.; Lazhko, A. E.; Lunin, V. V.; Lyubimov, S. E.; Martyanov, O. N.; Mishanin, I. I.; Muzafarov, A. M.; Nesterov, N. S.; Nikolaev, A. Yu.; Oparin, R. D.; Parenago, O. O.; Parenago, O. P.; Pokusaeva, Y. A.; Ronova, I. A.; Solovieva, A. B.; Temnikov, M. N.; Timashev, P. S.; Turova, O. V.; Filatova, E. V.; Philippov, A. A.; Chibiryaev, A. M.; Shalygin, A. S. Supercritical Fluids in Chemistry. *Russ. Chem. Rev*. **2020**, *89* (12), 1337–1427;

(47) Maul, J. J.; Ostrowski, P. J.; Ublacker, G. A.; Linclau, B.; Curran, D. P. Benzotrifluoride and Derivatives: Useful Solvents for Organic Synthesis and Fluorous Synthesis; **1999**, 79–105;

(48) Sugiishi, T.; Matsugi, M.; Hamamoto, H.; Amii, H. Enhancement of Stereoselectivities in Asymmetric Synthesis Using Fluorinated Solvents, Auxiliaries, and Catalysts. *RSC Adv* **2015**, *5* (22), 17269–17282;

(49) Mishra, R.; Mishra, S.; Chaubey, S. A.; Barot, Y. B. Ionic Liquids as Alternative Greener Solvents and Catalysts in Organic Transformations. In *Handbook of Greener Synthesis of Nanomaterials and Compounds*; Elsevier, **2021**, 359–404;

(50) Kianfar, E.; Mafi, Sajjad. Ionic Liquids: Properties, Application, and Synthesis. *Fine Chemical Engineering* **2020**, 22–31;

(51) Singh, S. K.; Savoy, A. W. Ionic Liquids Synthesis and Applications: An Overview. *J Mol Liq* **2020**, *297*, 112038;

(52) de Jesus, S. S.; Maciel Filho, R. Are Ionic Liquids Eco-Friendly? *Renewable and Sustainable Energy Reviews* **2022**, *157*, 112039;

(53) Chen, Y.; Mu, T. Revisiting Greenness of Ionic Liquids and Deep Eutectic Solvents. *GreenChE* **2021**, *2* (2), 174–186;

(54) Smith, E. L.; Abbott, A. P.; Ryder, K. S. Deep Eutectic Solvents (DESs) and Their Applications. *Chem Rev* **2014**, *114* (21), 11060–11082;

(55) Florindo, C.; Lima, F.; Ribeiro, B. D.; Marrucho, I. M. Deep Eutectic Solvents: Overcoming 21st Century Challenges. *Curr Opin Green Sustain Chem* **2019**, *18*, 31–36;

(56) Perna, F. M.; Vitale, P.; Capriati, V. Deep Eutectic Solvents and Their Applications as Green Solvents. *Curr Opin Green Sustain Chem* **2020**, *21*, 27–33;

(57) El Achkar, T.; Greige-Gerges, H.; Fourmentin, S. Basics and Properties of Deep Eutectic Solvents: A Review. *Environ Chem Lett* **2021**, *19* (4), 3397–3408;

(58)Tang, B.; Row, K. H. Recent Developments in Deep Eutectic Solvents in Chemical Sciences. *Monatshefte für Chemie - Chemical Monthly* **2013**, *144* (10), 1427–1454;

(59) Abbott, A. P.; Barron, J. C.; Ryder, K. S.; Wilson, D. Eutectic-Based Ionic Liquids with Metal-Containing Anions and Cations. *Chemistry – A European Journal* **2007**, *13* (22), 6495–6501;

(60) Scientific Opinion on Safety and Efficacy of Choline Chloride as a Feed Additive for All Animal Species. *EFSA Journal* **2011**, *9* (9);

(61) Paiva, A.; Craveiro, R.; Aroso, I.; Martins, M.; Reis, R. L.; Duarte, A. R. C. Natural Deep Eutectic Solvents – Solvents for the 21st Century. *ACS Sustain Chem Eng* **2014**, *2* (5);

(62) Liu, Y.; Friesen, J. B.; McAlpine, J. B.; Lankin, D. C.; Chen, S.-N.; Pauli, G. F. Natural Deep Eutectic Solvents: Properties, Applications, and Perspectives. *J Nat Prod* **2018**, *81* (3), 679–690;

(63) Rahman, M. S.; Roy, R.; Jadhav, B.; Hossain, M. N.; Halim, M. A.; Raynie, D. E. Formulation, Structure, and Applications of Therapeutic and Amino Acid-Based Deep Eutectic Solvents: An Overview. *J Mol Liq* **2021**, *321*, 114745;

(64) Duarte, A. R. C.; Ferreira, A. S. D.; Barreiros, S.; Cabrita, E.; Reis, R. L.; Paiva, A. A Comparison between Pure Active Pharmaceutical Ingredients and Therapeutic Deep Eutectic Solvents: Solubility and Permeability Studies. *Eur. J. Pharm. Biopharm.* **2017**, *114*, 296–304;

(65) Zaib, Q.; Eckelman, M. J.; Yang, Y.; Kyung, D. Are Deep Eutectic Solvents Really Green? : A Life-Cycle Perspective. *Green Chem.* **2022**, *24* (20), 7924–7930;

(66) Gurkan, B.; Squire, H.; Pentzer, E. Metal-Free Deep Eutectic Solvents: Preparation, Physical Properties, and Significance. *J Phys Chem Lett* **2019**, *10* (24), 7956–7964;

(67) Rodriguez Rodriguez, N.; van den Bruinhorst, A.; Kollau, L. J. B. M.; Kroon, M. C.; Binnemans, K. Degradation of Deep-Eutectic Solvents Based on Choline Chloride and Carboxylic Acids. *ACS Sustain Chem Eng* **2019**, *7* (13), 11521–11528;

(68) Płotka-Wasylka, J.; de la Guardia, M.; Andruch, V.; Vilková, M. Deep Eutectic Solvents vs Ionic Liquids: Similarities and Differences. *Microchem. J.* **2020**, *159*, 105539;

(69) Gutiérrez, M. C.; Ferrer, M. L.; Mateo, C. R.; del Monte, F. Freeze-Drying of Aqueous Solutions of Deep Eutectic Solvents: A Suitable Approach to Deep Eutectic Suspensions of Self-Assembled Structures. *Langmuir* **2009**, *25* (10), 5509–5515;

(70) Dai, Y.; van Spronsen, J.; Witkamp, G.-J.; Verpoorte, R.; Choi, Y. H. Natural Deep Eutectic Solvents as New Potential Media for Green Technology. *Anal Chim Acta* **2013**, *766*, 61–68;

(71) Santana, A. P. R.; Mora-Vargas, J. A.; Guimarães, T. G. S.; Amaral, C. D. B.; Oliveira, A.; Gonzalez, M. H. Sustainable Synthesis of Natural Deep Eutectic Solvents (NADES) by Different M,ethods. *J Mol Liq* **2019**, *293*, 111452;

(72) Bajkacz, S.; Adamek, J. Development of a Method Based on Natural Deep Eutectic Solvents for Extraction of Flavonoids from Food Samples. *Food Anal Methods* **2018**, *11* (5), 1330–1344. https://doi.org/10.1007/s12161-017-1118-5.

(73) Omar, K. A.; Sadeghi, R. Physicochemical Properties of Deep Eutectic Solvents: A Review. *J Mol Liq* **2022**, *360*, 119524;

(74) Ijardar, S. P.; Singh, V.; Gardas, R. L. Revisiting the Physicochemical Properties and Applications of Deep Eutectic Solvents. *Molecules* **2022**, *27* (4), 1368;

(75) Zhang, Q.; De Oliveira Vigier, K.; Royer, S.; Jérôme, F. Deep Eutectic Solvents: Syntheses, Properties and Applications. *Chem Soc Rev* **2012**, *41* (21), 7108;

(76) Shahbaz, K.; Mjalli, F. S.; Hashim, M. A.; AlNashef, I. M. Prediction of Deep Eutectic Solvents Densities at Different Temperatures. *Thermochim Acta* **2011**, *515* (1–2), 67–72;

(77) Abbott, A. P.; Barron, J. C.; Ryder, K. S.; Wilson, D. Eutectic-Based Ionic Liquids with Metal-Containing Anions and Cations. *Chemistry – A European Journal* **2007**, *13* (22), 6495–6501;

(78) García, G.; Aparicio, S.; Ullah, R.; Atilhan, M. Deep Eutectic Solvents: Physicochemical Properties and Gas Separation Applications. *Energy & Fuels* **2015**, *29* (4), 2616–2644;

(79) Gajardo-Parra, N. F.; Cotroneo-Figueroa, V. P.; Aravena, P.; Vesovic, V.; Canales, R. I. Viscosity of Choline Chloride-Based Deep Eutectic Solvents: Experiments and Modeling. *J Chem Eng Data* **2020**, *65* (11), 5581–5592;

(80) Gautam, R. K.; Seth, D. Thermal Conductivity of Deep Eutectic Solvents. *J Therm Anal Calorim* **2020**, *140* (6), 2633–2640;

(81) van Osch, D. J. G. P.; Zubeir, L. F.; van den Bruinhorst, A.; Rocha, M. A. A.; Kroon, M. C. Hydrophobic Deep Eutectic Solvents as Water-Immiscible Extractants. *Green Chem.* **2015**, *17* (9), 4518–4521;

(82) Zhang, Q.; De Oliveira Vigier, K.; Royer, S.; Jérôme, F. Deep Eutectic Solvents: Syntheses, Properties and Applications. *Chem Soc Rev* **2012**, *41* (21), 7108;

(83) Abbott, A. P.; McKenzie, K. J.; Ryder, K. S. Electropolishing and Electroplating of Metals Using Ionic Liquids Based on Choline Chloride *ACS Symposium Series*. **2007**, *975*,186–197;

(84) You, Y. H.; Gu, C. D.; Wang, X. L.; Tu, J. P. Electrodeposition of Ni–Co Alloys from a Deep Eutectic Solvent. *Surf Coat Technol* **2012**, *206* (17), 3632–3638;

(85) Abbott, A. P.; Capper, G.; McKenzie, K. J.; Ryder, K. S. Electrodeposition of Zinc–Tin Alloys from Deep Eutectic Solvents Based on Choline Chloride. *JEAC* **2007**, *599* (2), 288–294;

(86) Fernández, M. de los Á.; Boiteux, J.; Espino, M.; Gomez, F. J. V.; Silva, M. F. Natural Deep Eutectic Solvents-Mediated Extractions: The Way Forward for Sustainable Analytical Developments. *Anal Chim Acta* **2018**, *1038*, 1–10;

(87) Cunha, S. C.; Fernandes, J. O. Extraction Techniques with Deep Eutectic Solvents. *TrAC Trends in Analytical Chemistry* **2018**, *105*, 225–239;

(88) Chen, C.-C.; Huang, Y.-H.; Fang, J.-Y. Hydrophobic Deep Eutectic Solvents as Green Absorbents for Hydrophilic VOC Elimination. *J Hazard Mater* **2022**, *424*, 127366;

(89) Li, C.; Li, D.; Zou, S.; Li, Z.; Yin, J.; Wang, A.; Cui, Y.; Yao, Z.; Zhao, Q. Extraction Desulfurization Process of Fuels with Ammonium-Based Deep Eutectic Solvents. *Green Chem.* **2013**, *15* (10), 2793;

(90) Hansen, B. B.; Spittle, S.; Chen, B.; Poe, D.; Zhang, Y.; Klein, J. M.; Horton, A.; Adhikari, L.; Zelovich, T.; Doherty, B. W.; Gurkan, B.; Maginn, E. J.; Ragauskas, A.; Dadmun, M.; Zawodzinski, T. A.; Baker, G. A.; Tuckerman, M. E.; Savinell, R. F.; Sangoro, J. R. Deep Eutectic Solvents: A Review of Fundamentals and Applications. *Chem Rev* **2021**, *121* (3), 1232–1285;

(91) Li, X.; Hou, M.; Han, B.; Wang, X.; Zou, L. Solubility of CO_2 in a Choline Chloride + Urea Eutectic Mixture. *J Chem Eng Data* **2008**, *53* (2), 548–550;

(92) Najaf-Abadi, M. K.; Ghobadian, B.; Dehghani-Soufi, M. A Review on Application of Deep Eutectic Solvents as Green Catalysts and Co-Solvents in Biodiesel Production and Purification Processes. *Biomass Conv. Bioref.* **2024**, *14*, 3117–3134;

(93) Emami, S.; Shayanfar, A. Deep Eutectic Solvents for Pharmaceutical Formulation and Drug Delivery Applications. *Pharm Dev Technol* **2020**, *25* (7), 779–796;

(94) Zainal-Abidin, M. H.; Hayyan, M.; Ngoh, G. C.; Wong, W. F.; Looi, C. Y. Emerging Frontiers of Deep Eutectic Solvents in Drug Discovery and Drug Delivery Systems. *JCR* **2019**, *316*, 168–195;

(95) Pedro, S. N.; Freire, M. G.; Freire, C. S. R.; Silvestre, A. J. D. Deep Eutectic Solvents Comprising Active Pharmaceutical Ingredients in the Development of Drug Delivery Systems. *Expert Opin Drug Deliv* **2019**, *16* (5), 497–506;

(96) Mustafa, N.; Spelbos, V.; Witkamp, G.-J.; Verpoorte, R.; Choi, Y. Solubility and Stability of Some Pharmaceuticals in Natural Deep Eutectic Solvents-Based Formulations. *Molecules* **2021**, *26* (9), 2645;

(97) Lu, C.; Cao, J.; Wang, N.; Su, E. Significantly Improving the Solubility of Non-Steroidal Anti-Inflammatory Drugs in Deep Eutectic Solvents for Potential Non-Aqueous Liquid Administration. *Medchemcomm* **2016**, *7* (5), 955–959;

(98) Pedro, S. N.; Mendes, M. S. M.; Neves, B. M.; Almeida, I. F.; Costa, P.; Correia-Sá, I.; Vilela, C.; Freire, M. G.; Silvestre, A. J. D.; Freire, C. S. R. Deep Eutectic Solvent Formulations and Alginate-Based Hydrogels as a New Partnership for the Transdermal Administration of Anti-Inflammatory Drugs. *Pharmaceutics* **2022**, *14* (4), 827;

(99) Banerjee, A.; Ibsen, K.; Iwao, Y.; Zakrewsky, M.; Mitragotri, S. Transdermal Protein Delivery Using Choline and Geranate (CAGE) Deep Eutectic Solvent. *Adv Healthc Mater* **2017**, *6* (15);

(100) Długosz, O. Natural Deep Eutectic Solvents in the Synthesis of Inorganic Nanoparticles. *Materials* **2023**, *16* (2), 627;

(101) Pradeepkumar, P.; Rajan, M.; Almoallim, H. S.; Alharbi, S. A. Targeted Delivery of Doxorubicin in HeLa Cells Using Self-Assembled Polymeric Nanocarriers Guided by Deep Eutectic Solvents. *ChemistrySelect* **2021**, *6* (28), 7232–7241;

(102) Juneidi, I.; Hayyan, M.; Hashim, M. A. Intensification of Biotransformations Using Deep Eutectic Solvents: Overview and Outlook. *Process Biochemistry* **2018**, *66*, 33–60;

(103) Yang, Z.; Wen, Q. Deep Eutectic Solvents as a New Reaction Medium for Biotransformations. In *Ionic Liquid-Based Surfactant Science*; Wiley, **2015**, 517–531;

(104) Jablonský, M.; Škulcová, A.; Šima, J. Use of Deep Eutectic Solvents in Polymer Chemistry–A Review. *Molecules* **2019**, *24* (21), 3978;

(105) Alonso, D. A.; Baeza, A.; Chinchilla, R.; Guillena, G.; Pastor, I. M.; Ramón, D. J. Deep Eutectic Solvents: The Organic Reaction Medium of the Century. *European J Org Chem* **2016**, *2016* (4), 612–632;

(106) Khandelwal, S.; Tailor, Y. K.; Kumar, M. Deep Eutectic Solvents (DESs) as Eco-Friendly and Sustainable Solvent/Catalyst Systems in Organic Transformations. *J Mol Liq* **2016**, *215*, 345–386;

(107) Liu, P.; Hao, J.-W.; Mo, L.-P.; Zhang, Z.-H. Recent Advances in the Application of Deep Eutectic Solvents as Sustainable Media as Well as Catalysts in Organic Reactions. *RSC Adv* **2015**, *5* (60), 48675–48704;

(108) Ünlü, A. E.; Arıkaya, A.; Takaç, S. Use of Deep Eutectic Solvents as Catalyst: A Mini-Review. *Green Processing and Synthesis* **2019**, *8* (1), 355–372;

(109) Abbott, A. P.; Capper, G.; Davies, D. L.; Rasheed, R. K.; Tambyrajah, V. Quaternary Ammonium Zinc- or Tin-Containing Ionic Liquids: Water Insensitive, Recyclable Catalysts for Diels–Alder Reactions. *Green Chem.* **2002**, *4* (1), 24–26;

(110) Patil, U. B.; Singh, A. S.; Nagarkar, J. M. Choline Chloride Based Eutectic Solvent: An Efficient and Reusable Solvent System for the Synthesis of Primary Amides from Aldehydes and from Nitriles. *RSC Adv.* **2014**, *4* (3), 1102–1106;

(111) Tran, P. H.; Nguyen, H. T.; Hansen, P. E.; Le, T. N. An Efficient and Green Method for Regio- and Chemo-Selective Friedel–Crafts Acylations Using a Deep Eutectic Solvent ([CholineCl][$ZnCl_2$]$_3$). *RSC Adv* **2016**, *6* (43), 37031–37038;

(112) Calderon Morales, R.; Tambyrajah, V.; Jenkins, P. R.; Davies, D. L.; Abbott, A. P. The Regiospecific Fischer Indole Reaction in Choline Chloride·2$ZnCl_2$ with Product Isolation by Direct Sublimation from the Ionic Liquid. *Chem. Commun.* **2004**, 2, 158–159;

(113) Sunitha, S.; Kanjilal, S.; Reddy, P. S.; Prasad, R. B. N. Liquid–Liquid Biphasic Synthesis of Long Chain Wax Esters Using the Lewis Acidic Ionic Liquid Choline Chloride·2ZnCl2. *Tetrahedron Lett* **2007**, *48* (39), 6962–6965;

(114) Wang, A.; Xing, P.; Zheng, X.; Cao, H.; Yang, G.; Zheng, X. Deep Eutectic Solvent Catalyzed Friedel–Crafts Alkylation of Electron-Rich Arenes with Aldehydes. *RSC Adv* **2015**, *5* (73), 59022–59026;

(115) Keshavarzipour, F.; Tavakol, H. Deep Eutectic Solvent as a Recyclable Catalyst for Three-Component Synthesis of β-Amino Carbonyls. *Catal Letters* **2015**, *145* (4), 1062–1066;

(116) Abbott, A. P.; Bell, T. J.; Handa, S.; Stoddart, B. O-Acetylation of Cellulose and Monosaccharides Using a Zinc Based Ionic Liquid. *Green Chem.* **2005**, *7* (10), 705;

(117) Azizi, N.; Batebi, E. Highly Efficient Deep Eutectic Solvent Catalyzed Ring Opening of Epoxides. *Catal Sci Technol* **2012**, *2* (12), 2445;

(118) Liu, W.; Wang, F. *p*-Toluenesulfonic Acid-Based Deep Eutectic Solvent as Transesterification Catalyst for Biodiesel Production. *J Oleo Sci* **2018**, *67* (9), 1163–1169;

(119) Wang, L.; Zhou, M.; Chen, Q.; He, M.-Y. Brønsted Acidic Deep Eutectic Solvent Catalysed the One-Pot Synthesis of 2 *H* -Indazolo[2,1-*b*]Phthalazine-Triones. *J Chem Res* **2013**, *37* (10), 598–600;

(120) Pawar, P. M.; Jarag, K. J.; Shankarling, G. S. Environmentally Benign and Energy Efficient Methodology for Condensation: An Interesting Facet to the Classical Perkin Reaction. *Green Chem.* **2011**, *13* (8), 2130;

(121) Sonawane, Y. A.; Phadtare, S. B.; Borse, B. N.; Jagtap, A. R.; Shankarling, G. S. Synthesis of Diphenylamine-Based Novel Fluorescent Styryl Colorants by Knoevenagel Condensation Using a Conventional Method, Biocatalyst, and Deep Eutectic Solvent. *Org Lett* **2010**, *12* (7), 1456–1459;

(122) Handy, S.; Lavender, K. Organic Synthesis in Deep Eutectic Solvents: Paal–Knorr Reactions. *Tetrahedron Lett* **2013**, *54* (33), 4377–4379;

(123) Azizi, N.; Dezfooli, S.; Khajeh, M.; Hashemi, M. M. Efficient Deep Eutectic Solvents Catalyzed Synthesis of Pyran and Benzopyran Derivatives. *J Mol Liq* **2013**, *186*, 76–80;

(124) Azizi, N.; Alipour, M. Eco-Efficiency and Scalable Synthesis of Bisamides in Deep Eutectic Solvent. *J Mol Liq* **2015**, *206*, 268–271;

(125) Gore, S.; Baskaran, S.; Koenig, B. Efficient Synthesis of 3,4-Dihydropyrimidin-2-Ones in Low Melting Tartaric Acid–Urea Mixtures. *Green Chem.* **2011**, *13* (4), 1009;

(126) Di Gioia, M. L.; Cassano, R.; Costanzo, P.; Herrera Cano, N.; Maiuolo, L.; Nardi, M.; Nicoletta, F. P.; Oliverio, M.; Procopio, A. Green Synthesis of Privileged Benzimidazole Scaffolds Using Active Deep Eutectic Solvent. *Molecules* **2019**, *24* (16), 2885;

(127) Göke, K.; Lorenz, T.; Repanas, A.; Schneider, F.; Steiner, D.; Baumann, K.; Bunjes, H.; Dietzel, A.; Finke, J. H.; Glasmacher, B.; Kwade, A. Novel Strategies for the Formulation and Processing of Poorly Water-Soluble Drugs. *Eur. J. Pharm. Biopharm.* **2018**, *126*, 40–56;

(128) Fourmentin, S., Costa Gomes, M., Lichtfouse, E., Eds. Deep Eutectic Solvents for Medicine, Gas Solubilization and Extraction of Natural Substances; Springer International Publishing: Cham, **2021**, Vol. 56;

(129) Emami, S.; Shayanfar, A. Deep Eutectic Solvents for Pharmaceutical Formulation and Drug Delivery Applications. *Pharm Dev Technol* **2020**, *25* (7), 779–796;

(130) Rahman, M. S.; Roy, R.; Jadhav, B.; Hossain, M. N.; Halim, M. A.; Raynie, D. E. Formulation, Structure, and Applications of Therapeutic and Amino Acid-Based Deep Eutectic Solvents: An Overview. *J Mol Liq* **2021**, *321*, 114745;

(131) Pedro, S. N.; Freire, C. S. R.; Silvestre, A. J. D.; Freire, M. G. Deep Eutectic Solvents and Pharmaceuticals. *Encyclopedia* **2021**, *1* (3), 942–963;

(132) Lu, C.; Cao, J.; Wang, N.; Su, E. Significantly Improving the Solubility of Non-Steroidal Anti-Inflammatory Drugs in Deep Eutectic Solvents for Potential Non-Aqueous Liquid Administration. *Medchemcomm* **2016**, *7* (5), 955–959;

(133) Silva, J. M.; Reis, R. L.; Paiva, A.; Duarte, A. R. C. Design of Functional Therapeutic Deep Eutectic Solvents Based on Choline Chloride and Ascorbic Acid. *ACS Sustain Chem Eng* **2018**, *6* (8), 10355–10363;

(134) Halder, A. K.; Cordeiro, M. N. D. S. Probing the Environmental Toxicity of Deep Eutectic Solvents and Their Components: An In Silico Modeling Approach. *ACS Sustain Chem Eng* **2019**, *7* (12), 10649–10660;

(135) Dai, Y.; van Spronsen, J.; Witkamp, G.-J.; Verpoorte, R.; Choi, Y. H. Natural Deep Eutectic Solvents as New Potential Media for Green Technology. *Anal Chim Acta* **2013**, *766*, 61–68;

(136) Pedro, S. N.; Freire, M. G.; Freire, C. S. R.; Silvestre, A. J. D. Deep Eutectic Solvents Comprising Active Pharmaceutical Ingredients in the Development of Drug Delivery Systems. *Expert Opin Drug Deliv* **2019**, *16* (5), 497–506;

(137) Phaechamud, T.; Tuntarawongsa, S.; Charoensuksai, P. Evaporation Behavior and Characterization of Eutectic Solvent and Ibuprofen Eutectic Solution. *AAPS PharmSciTech* **2016**, *17* (5), 1213–1220;

(138) Aroso, I. M.; Craveiro, R.; Rocha, Â.; Dionísio, M.; Barreiros, S.; Reis, R. L.; Paiva, A.; Duarte, A. R. C. Design of Controlled Release Systems for THEDES—Therapeutic Deep Eutectic Solvents, Using Supercritical Fluid Technology. *Int J Pharm* **2015**, *492* (1–2), 73–79. https://doi.org/10.1016/j.ijpharm.2015.06.038.

(139) Abbott, A. P.; Ahmed, E. I.; Prasad, K.; Qader, I. B.; Ryder, K. S. Liquid Pharmaceuticals Formulation by Eutectic Formation. *Fluid Phase Equilib* **2017**, *448*;

(140) Tarate, B.; Bansal, A. K. Characterization of CoQ 10-Lauric Acid Eutectic System. *Thermochim Acta* **2015**, *605*, 100–106;

(141) Stott, P. Transdermal Delivery from Eutectic Systems: Enhanced Permeation of a Model Drug, Ibuprofen. *Journal of Controlled Release* **1998**, *50* (1–3), 297–308;

(142) Mota-Morales, J. D.; Gutiérrez, M. C.; Ferrer, M. L.; Sanchez, I. C.; Elizalde-Peña, E. A.; Pojman, J. A.; Monte, F. Del; Luna-Bárcenas, G. Deep Eutectic Solvents as Both Active Fillers and Monomers for Frontal Polymerization. *J Polym Sci A Polym Chem* **2013**, *51* (8), 1767–1773;

(143) Roughley, S. D.; Jordan, A. M. The Medicinal Chemist's Toolbox: An Analysis of Reactions Used in the Pursuit of Drug Candidates. *J Med Chem* **2011**, *54* (10), 3451–3479;

(144) Bryan, M. C.; Dunn, P. J.; Entwistle, D.; Gallou, F.; Koenig, S. G.; Hayler, J. D.; Hickey, M. R.; Hughes, S.; Kopach, M. E.; Moine, G.; Richardson, P.; Roschangar, F.; Steven, A.; Weiberth, F. J. Key Green Chemistry Research Areas from a Pharmaceutical Manufacturers' Perspective Revisited. *Green Chem.* **2018**, *20* (22), 5082–5103;

(145) Albericio, F.; El-Faham, A. Choosing the Right Coupling Reagent for Peptides: A Twenty-Five-Year Journey. *Org Process Res Dev* **2018**, *22* (7), 760–772;

(146) Massolo, E.; Pirola, M.; Benaglia, M. Amide Bond Formation Strategies: Latest Advances on a Dateless Transformation. *European J Org Chem* **2020**, *2020* (30), 4641–4651;

(147) Sherwood, J. European Restrictions on 1,2-Dichloroethane: C−H Activation Research and Development Should Be Liberated and Not Limited. *Angewandte Chemie International Edition* **2018**, *57* (43), 14286–14290;

(148) Fail, P. A.; George, J. D.; Grizzle, T. B.; Heindel, J. J. Formamide and Dimethylformamide: Reproductive Assessment by Continuous Breeding in Mice. *Reproductive Toxicology* **1998**, *12* (3), 317–332;

(149) Procopio, D.; Siciliano, C.; Trombino, S.; Dumitrescu, D. E.; Suciu, F.; Di Gioia, M. L. Green Solvents for the Formation of Amide Linkages. *Org Biomol Chem* **2022**, *20* (6), 1137–1149;

(150) Cortes-Clerget, M.; Berthon, J.-Y.; Krolikiewicz-Renimel, I.; Chaisemartin, L.; Lipshutz, B. H. Tandem Deprotection/Coupling for Peptide Synthesis in Water at Room Temperature. *Green Chem.* **2017**, *19* (18), 4263–4267;

(151) Gallou, F.; Guo, P.; Parmentier, M.; Zhou, J. A General and Practical Alternative to Polar Aprotic Solvents Exemplified on an Amide Bond Formation. *Org Process Res Dev* **2016**, *20* (7), 1388–1391;

(152) Petchey, T. H. M.; Comerford, J. W.; Farmer, T. J.; Macquarrie, D. J.; Sherwood, J.; Clark, J. H. Optimization of Amidation Reactions Using Predictive Tools for the Replacement of Regulated Solvents with Safer Biobased Alternatives. *ACS Sustain Chem Eng* **2018**, *6* (2), 1550–1554;

(153) Bousfield, T. W.; Pearce, K. P. R.; Nyamini, S. B.; Angelis-Dimakis, A.; Camp, J. E. Synthesis of Amides from Acid Chlorides and Amines in the Bio-Based Solvent Cyrene™. *Green Chem.* **2019**, *21* (13), 3675–3681;

(154) Jad, Y. E.; Acosta, G. A.; Khattab, S. N.; de la Torre, B. G.; Govender, T.; Kruger, H. G.; El-Faham, A.; Albericio, F. 2-Methyltetrahydrofuran and Cyclopentyl Methyl Ether for Green Solid-Phase Peptide Synthesis. *Amino Acids* **2016**, *48* (2), 419–426:

(155) Konwar, M.; Khupse, N. D.; Saikia, P. J.; Sarma, D. A Potential Greener Protocol for Peptide Coupling Reactions Using Recyclable/Reusable Ionic Liquid [C_4-DABCO] [$N(CN)_2$]. *Chem. Sci. J.* **2018**, *130* (5), 53;

(156)Galy, N.; Mazières, M.-R.; Plaquevent, J.-C. Toward Waste-Free Peptide Synthesis Using Ionic Reagents and Ionic Liquids as Solvents. *Tetrahedron Lett* **2013**, *54* (21), 2703–2705. https://doi.org/10.1016/j.tetlet.2013.03.072.

(157) Azizi, N.; Gholibeglo, E.; Babapour, M.; Ghafuri, H.; Bolourtchian, S. M. Deep Eutectic Solvent Promoted Highly Efficient Synthesis of N, N'-Diarylamidines and Formamides. *Comptes Rendus Chimie* **2012**, *15* (9), 768–773. https://doi.org/10.1016/j.crci.2012.06.011.

(158) Messa, F.; Perrone, S.; Capua, M.; Tolomeo, F.; Troisi, L.; Capriati, V.; Salomone, A. Towards a Sustainable Synthesis of Amides: Chemoselective Palladium-Catalysed Aminocarbonylation of Aryl Iodides in Deep Eutectic Solvents. *Chem. Comm.* **2018**, *54* (58), 8100–8103;

(159) Dunetz, J. R.; Magano, J.; Weisenburger, G. A. Large-Scale Applications of Amide Coupling Reagents for the Synthesis of Pharmaceuticals. *Org Process Res Dev* **2016**, *20* (2), 140–177;

(160) Isidro-Llobet, A.; Kenworthy, M. N.; Mukherjee, S.; Kopach, M. E.; Wegner, K.; Gallou, F.; Smith, A. G.; Roschangar, F. Sustainability Challenges in Peptide Synthesis and Purification: From R&D to Production. *J Org Chem* **2019**, *84* (8), 4615–4628;

(161) *https://echa.europa.eu/it/substance-information//substanceinfo/100.018.173*.

(162) Carlberg, B.; Samuelsson, O.; Lindholm, L. H. Atenolol in Hypertension: Is It a Wise Choice? *The Lancet* **2004**, *364* (9446), 1684–1689;

(163) Romero, N. A.; Nicewicz, D. A. Organic Photoredox Catalysis. *Chem Rev* **2016**, *116* (17), 10075–10166;

(164) Milano, F.; Giotta, L.; Guascito, M. R.; Agostiano, A.; Sblendorio, S.; Valli, L.; Perna, F. M.; Cicco, L.; Trotta, M.; Capriati, V. Functional Enzymes in Nonaqueous Environment: The Case of Photosynthetic Reaction Centers in Deep Eutectic Solvents. *ACS Sustain Chem Eng* **2017**, *5* (9), 7768–7776;

(165) Mattioli, R.; Di Risola, D.; Federico, R.; Ciogli, A.; Gasparrini, F.; Villani, C.; Fontana, M.; Maggiore, A.; d'Erme, M.; Mosca, L.; Francioso, A. Effect of Natural Deep Eutectic Solvents on Trans-Resveratrol Photo-Chemical Induced Isomerization and 2,4,6-Trihydroxyphenanthrene Electro-Cyclic Formation. *Molecules* **2022**, *27* (7), 2348;

(166) Dhingra, D.; Bhawna; Pandey, A.; Pandey, S. Pyrene Fluorescence To Probe a Lithium Chloride-Added (Choline Chloride + Urea) Deep Eutectic Solvent. *J Phys Chem B* **2019**, *123* (14), 3103–3111;

(167) Nolan, M. D.; Mezzetta, A.; Guazzelli, L.; Scanlan, E. M. Radical-Mediated Thiol–Ene 'Click' Reactions in Deep Eutectic Solvents for Bioconjugation. *Green Chem.* **2022**, *24* (4), 1456–1462;

(168) Yoon, T. P.; Ischay, M. A.; Du, J. Visible Light Photocatalysis as a Greener Approach to Photochemical Synthesis. *Nat Chem* **2010**, *2* (7), 527–532;

(169) Chan, C.-M.; Chow, Y.-C.; Yu, W.-Y. Recent Advances in Photocatalytic C–N Bond Coupling Reactions. *Synthesis (Stuttg)* **2020**;

(170) Xuan, J.; Zhang, Z.; Xiao, W. Visible-Light-Induced Decarboxylative Functionalization of Carboxylic Acids and Their Derivatives. *Angewandte Chemie International Edition* **2015**, *54* (52), 15632–15641;

(171) Song, W.; Dong, K.; Li, M. Visible Light-Induced Amide Bond Formation. *Org Lett* **2020**, *22* (2), 371–375;

(172) Liu, H.; Zhao, L.; Yuan, Y.; Xu, Z.; Chen, K.; Qiu, S.; Tan, H. Potassium Thioacids Mediated Selective Amide and Peptide Constructions Enabled by Visible Light Photoredox Catalysis. *ACS Catal* **2016**, *6* (3), 1732–1736;

(173) Das, S.; Ray, S.; Ghosh, A. B.; Samanta, P. K.; Samanta, S.; Adhikary, B.; Biswas, P. Visible Light Driven Amide Synthesis in Water at Room Temperature from Thioacid and Amine Using CdS Nanoparticles as Heterogeneous Photocatalyst. *Appl Organomet Chem* **2018**, *32* (3);

(174) Tyson, E. L.; Niemeyer, Z. L.; Yoon, T. P. Redox Mediators in Visible Light Photocatalysis: Photocatalytic Radical Thiol–Ene Additions. *J Org Chem* **2014**, *79* (3), 1427–1436;

(175) El Achkar, T.; Greige-Gerges, H.; Fourmentin, S. Basics and Properties of Deep Eutectic Solvents: A Review. *Environ Chem Lett* **2021**, *19* (4), 3397–3408;

(176) Khaksar, S.; Fattahi, E.; Fattahi, E. Organocatalytic Synthesis of Amides from Nitriles via the Ritter Reaction. *Tetrahedron Lett* **2011**, *52* (45), 5943–5946;

(177) Van Aken, K.; Strekowski, L.; Patiny, L. EcoScale, a Semi-Quantitative Tool to Select an Organic Preparation Based on Economical and Ecological Parameters. *Beilstein J. Org. Chem.* **2006**, *2*;

(178) Link for EcoScale calculator: The EcoScale (cheminfo.org);

(179) Margetić, D.; Đud, M. Solvent-Free Mechanochemical Deprotection of *N*-Boc Group. *Int J Org Chem (Irvine)* **2017**, *07* (02), 140–144;

(180) Di Gioia, M. L.; Barattucci, A.; Bonaccorsi, P.; Leggio, A.; Minuti, L.; Romio, E.; Temperini, A.; Siciliano, C. Deprotection/Reprotection of the Amino Group in α-Amino Acids and Peptides. A One-Pot Procedure in [Bmim][BF_4] Ionic Liquid. *RSC Adv.* **2014**, *4* (6), 2678–2686;

(181) Li, B.; Berliner, M.; Buzon, R.; Chiu, C. K.-F.; Colgan, S. T.; Kaneko, T.; Keene, N.; Kissel, W.; Le, T.; Leeman, K. R.; Marquez, B.; Morris, R.; Newell, L.; Wunderwald, S.; Witt,

M.; Weaver, J.; Zhang, Z.; Zhang, Z. Aqueous Phosphoric Acid as a Mild Reagent for Deprotection of *Tert* -Butyl Carbamates, Esters, and Ethers. *J Org Chem* **2006**, *71* (24), 9045–9050;

(182) Li, B.; Bemish, R.; Buzon, R. A.; Chiu, C. K.-F.; Colgan, S. T.; Kissel, W.; Le, T.; Leeman, K. R.; Newell, L.; Roth, J. Aqueous Phosphoric Acid as a Mild Reagent for Deprotection of the T-Butoxycarbonyl Group. *Tetrahedron Lett* **2003**, *44* (44), 8113–8115;

(183) Coffey, D. S.; Hawk, M. K. N.; Steven W. Pedersen; Ghera, S. J.; Marler, P. G.; Dodson, P. N.; Lytle, M. L. Large Scale Deprotection of a *Tert* -Butoxycarbonyl (Boc) Group Using Aqueous HCl and Acetone. *Org Process Res Dev* **2004**, *8* (6), 945–947;

(184) Han, G.; Tamaki, M.; Hruby, V. J. Fast, Efficient and Selective Deprotection of the *Tert* -butoxycarbonyl (Boc) Group Using HCl/Dioxane (4 M). *Journ. of Pept. Res.* **2001**, *58* (4), 338–341;

(185) Strazzolini, P.; Misuri, N.; Polese, P. Efficient Cleavage of Carboxylic Tert-Butyl and 1-Adamantyl Esters, and N-Boc-Amines Using H_2SO_4 in CH_2Cl_2. *Tetrahedron Lett* **2005**, *46* (12), 2075–2078;

(186) Subhas Bose, D.; Kiran Kumar, K.; Narsimha Reddy, A. V. A New Protocol for Selective Deprotection of *N*-Tert -Butoxycarbonyl Protective Group (*t*-Boc) with $Sn(OTf)_2$. *Synth Commun* **2003**, *33* (3), 445–450;

(187) López-Soria, J. M.; Pérez, S. J.; Hernández, J. N.; Ramírez, M. A.; Martín, V. S.; Padrón, J. I. A Practical, Catalytic and Selective Deprotection of a Boc Group in N,N′-Diprotected Amines Using Iron (III)-Catalysis. *RSC Adv* **2015**, *5* (9), 6647–6651;

(188) Giri, R. S.; Roy, S.; Dolai, G.; Manne, S. R.; Mandal, B. $FeCl_3$ -Mediated Boc Deprotection: Mild Facile Boc-Chemistry in Solution and on Resin. *ChemistrySelect* **2020**, *5* (6), 2050–2056;

(189) Chakrabarty, M.; Kundu, T.; Harigaya, Y. Mild Deprotection of *Tert* -Butyl Carbamates of NH-Heteroarenes under Basic Conditions. *Synth Commun* **2006**, *36* (14), 2069–2077;

(190) Tom, N. J.; Simon, W. M.; Frost, H. N.; Ewing, M. Deprotection of a Primary Boc Group under Basic Conditions. *Tetrahedron Lett* **2004**, *45* (5), 905–906;

(191) Cheraiet, Z.; Ouarna, S.; Hessainia, S.; Berredjem, M.; Aouf, N.-E. *N-Tert* -Butoxycarbonylation of Structurally Diverse Amines and Sulfamides under Water-Mediated Catalyst-Free Conditions. *ISRN Org Chem* **2012**, *2012*, 1–8;

(192) Srinivasan, N.; Yurek-George, A.; Ganesan, A. Rapid Deprotection of N-Boc Amines by TFA Combined with Freebase Generation Using Basic Ion-Exchange Resins. *Mol Divers* **2005**, *9* (4), 291–293;

(193) George, N.; Ofori, S.; Parkin, S.; Awuah, S. G. Mild Deprotection of the *N-Tert* -Butyloxycarbonyl (*N* -Boc) Group Using Oxalyl Chloride. *RSC Adv* **2020**, *10* (40), 24017–24026;

(194) Verschueren, R. H.; Gilles, P.; Van Mileghem, S.; De Borggraeve, W. M. Solvent-Free *N* -Boc Deprotection by *Ex Situ* Generation of Hydrogen Chloride Gas. *Org Biomol Chem* **2021**, *19* (26), 5782–5787;

(195) Zinelaabidine, C.; Souad, O.; Zoubir, J.; Malika, B.; Nour-Eddine, A. A Simple and Efficient Green Method for the Deprotection of N-Boc in Various Structurally Diverse Amines under Water-Mediated Catalyst-Free Conditions. *Int J Chem* **2012**, *4* (3);

(196) Wang, J.; Liang, Y.-L.; Qu, J. Boiling Water-Catalyzed Neutral and Selective N-Boc Deprotection. *Chem. Comm.* **2009**, 4, 5144;

(197) Wang, G.; Li, C.; Li, J.; Jia, X. Catalyst-Free Water-Mediated N-Boc Deprotection. *Tetrahedron Lett* **2009**, *50* (13), 1438–1440;

(198) Majumdar, S.; De, J.; Chakraborty, A.; Roy, D.; Maiti, D. K. A Protic Ionic Liquid Catalyzed Strategy for Selective Hydrolytic Cleavage of Tert-Butyloxycarbonyl Amine (N-Boc). *RSC Adv* **2015**, *5* (5), 3200–3205;

(199) Boddula, R.; Srinivasan, P. Emeraldine Base Form of Polyaniline Nanofibers as New, Economical, Green, and Efficient Catalyst for Synthesis of *Z* -Aldoximes. *J. Catal.* **2014**, *2014*, 1–6;

(200) Palaniappan, S.; Rajender, B.; Umashankar, M. Controllable Stereoselective Synthesis of Cis or Trans Pyrano and Furano Tetrahydroquinolines: Polyaniline-p-Toluenesulfonate Salt Catalyzed One-Pot Aza-Diels–Alder Reactions. *J Mol Catal A Chem* **2012**, *352*, 70–74;

(201) Palaniappan, S.; Rajender, B. A Novel Polyaniline-Silver Nitrate- *p* -Toluenesulfonic Acid Salt as Recyclable Catalyst in the Stereoselective Synthesis of B-Amino Ketones: “One-Pot” Synthesis in Water Medium. *Adv Synth Catal* **2010**, *352* (14–15), 2507–2514;

(202) Brinkman, H. R.; Landi, J. J.; Paterson, J. B.; Stone, P. J. The Use of P-Toluenesulfonic Acid for Removal of the N-T-Butoxy-Carbonyl Protecting Group in Solid Phase Peptide Synthesis. *Synth Commun* **1991**, *21* (3), 459–465;

(203) Jahani, F.; Tajbakhsh, M.; Khaksar, S.; Azizi, M. R. An Efficient and Highly Chemoselective N-Boc Protection of Amines, Amino Acids, and Peptides under Heterogeneous Conditions. *Monatshefte für Chemie - Chemical Monthly* **2011**, *142* (10), 1035–1043;

(204) Azizi, N.; Shirdel, F. Sustainable and Chemoselective N-Boc Protection of Amines in Biodegradable Deep Eutectic Solvent. *Monatshefte für Chemie - Chemical Monthly* **2017**, *148* (6), 1069–1074;

(205) Di Gioia, M. L.; Gagliardi, A.; Leggio, A.; Leotta, V.; Romio, E.; Liguori, A. N-Urethane Protection of Amines and Amino Acids in an Ionic Liquid. *RSC Adv* **2015**, *5* (78), 63407–63420;

(206) Gaillard, P.; Carrupt, P.-A.; Testa, B.; Schambel, P. Binding of Arylpiperazines, (Aryloxy)Propanolamines, and Tetrahydropyridylindoles to the 5-HT_{1A} Receptor: Contribution of the Molecular Lipophilicity Potential to Three-Dimensional Quantitative Structure−Affinity Relationship Models. *J Med Chem* **1996**, *39* (1), 126–134;

(207) Yadav, J. S.; Reddy, A. R.; Narsaiah, A. V.; Reddy, B. V. S. An Efficient Protocol for Regioselective Ring Opening of Epoxides Using Samarium Triflate: Synthesis of Propranolol, Atenolol and RO363. *J Mol Catal A Chem* **2007**, *261* (2), 207–212;

(208) 1. Shrivastava, A.; Rathor, P. Optimization and Validation of GC Method for Determination of Methanol as Organic Volatile Impurity in Atenolol Bulk Drug. Wld. *J. Anal. Chem.* **2013**, *1* (4), 54-58

(209) Sarrafi, A. H. M.; Konoz, E.; Feyzbakhsh, A. Chemometrics-Assisted Simultaneous Determination of Atenolol and Furosemide in Synthetic Binary Mixtures and Combined Tablet Preparations. *E-J. Chem.* **2010**, *7* (3), 997–1002;

(210) Carlberg, B.; Samuelsson, O.; Lindholm, L. H. Atenolol in hypertension: is it a wise choice?. *The lancet* **2004**, *6*,1684-9;

(211) 4. Reddy, A. V. B.; Yusop, Z.; Jaafar, J.; Bin Aris, A.; Abdul Majid, Z. A Simple, Selective, and Sensitive Gas Chromatography–Mass Spectrometry Method for the Analysis of Five Process-related Impurities in Atenolol Bulk Drug and Capsule Formulations. *J. Sep. Sci.* **2017**, *40* (15), 3086–3093;

(212) Gupta R.; Bhutani S. Global Market Size, Forecast, and Trend Highlights Over 2023-2035. Research Nester 2023. https://www.researchnester.com/reports/atenolol-market/4076;

(213) Kleemann, A.; Engel, J.; Kutscher, B.; Reichert, D. Syntheses, Patents and Applications of the most relevant APIs in: Pharmaceutical Substances. *Thieme*, 5th edition, **2009**;

(214) Nandini, P. R.; Suhas, P. S. Green Chemical Route for Process Development of Atenolol Intermediate. *RJPT*, **2014**, *1* (7), 44-47;

(215) Cepanec, I.; Litvić, M.; Mikuldaš, H.; Bartolinčić A.; Vinković, V. Calcium trifluoromethanesulfonate-catalysed aminolysis of epoxides Tetrahedron, 2003, 59, 2435–2439;

(216) Ollevier, T.; Lavie-Compin, G. Bismuth triflate-catalyzed mild and efficient epoxide opening by aromatic amines under aqueous conditions. Tetrahedron Lett., 2004, 45, 49–52;

(217) Yadav, J. S.; Reddy, A. R.; Narsaiah A. V.; Reddy, B. V. S. An efficient protocol for regioselective ring opening of epoxides using samarium triflate: Synthesis of propranolol, atenolol and RO363. J. Mol. Catal. A. Chem., 2007, 261, 207–212;

(218) Chini, M.; Crotti, P.; Macchia, F. Regioalternating Selectivity in the Metal Salt Catalyzed Aminolysis of Styrene Oxide. J. Org. Chem. 1991, 56 (20), 5939–5942;

(219) Shivani; Pujala, B.; Chakraborti, A. K. Zinc(II) Perchlorate Hexahydrate Catalyzed Opening of Epoxide Ring by Amines: Applications to Synthesis of (RS)/(R)-Propranolols and (RS)/(R)/(S)-Naftopidils. J. Org. Chem. 2007, 72 (10), 3713–3722;

(220) Apparu, M.; Tiba, Y. Ben; Léo, P.-M.; Hamman, S.; Coulombeau, C. Determination of the Enantiomeric Purity and the Configuration of β-Aminoalcohols Using (R)-2-Fluorophenylacetic Acid (AFPA) and Fluorine-19 NMR: Application to β-Blockers. *Tetrahedron Asymm.* **2000**, *11* (14), 2885–2898;

(221) Azizi, N.; Saidi, M. R. Highly chemoselective addition of amines to epoxides in water *Org. Lett.*, **2005**, *7*, 3649–3651; 39;

(222) Abaee, M. S.; Hamidi, V.; Mojtahedi, M. M. Ultrasound promoted aminolysis of epoxides in aqueous media: A rapid procedure with no pH adjustment for additive-free synthesis of β-aminoalcohols. Ultrason. Sonochem., 2008, 15, 823–827;

(223)Dwivedee, B.; Ghosh, S.; Bhaumik, J.; Banoth, L.; Banerjee, U. C. Lipase catalyzed Green Synthesis of Enantiopure Atenolol. *RSC Adv.*, **2015**, *5*, 15850-15860;

(224) Hansen, M.B.; Tennfjord, A.L.; Blindheim, F.H.; Bocquin, L.H.Y.; Jacobsen, E.E. Synthesis of Enantiopure (S)-Atenolol by Utilization of Lipase-Catalyzed Kinetic Resolution of a Key Intermediate. *Int. J. Mol. Sci.* **2024**, *25*, 3497;

(225) Agustian, J.; Kamaruddin, A.H.; Aboul-Enein, H.Y. Enantio-conversion and -selectivity of racemic atenolol kinetic resolution using free Pseudomonas fluorescens lipase (Amano) conducted via ransesterification reaction. *Rsc. Adv.* **2016**, *6*, 26077-26085;

(226) Sikora, A.; Chalupka, J.; Marszall, M.P. The Use of Ion Liquids as a Trojan Horse Strategy in Enzyme-Catalyzed Biotransformation of (R,S)-Atenolol. *Catalysts*, **2020**, *10*, 787;

(227) Chalupka, J.; Sikora, A.; Marszall, M.P. The Utilization of Two-Phase Catalytic System in Enantioselective Biotransformation of Racemic Atenolol. *Catalysts* **2022**, *12*, 1068;

(228) Saquib, M.; Khan, M. F.; Singh, J.; Khan, B.; Priti; Kumar, P.; Hussain, M. K. Operationally Simple, Scalable Synthesis of Aryloxy Propanolamines Using Glycerol as a Green Promoting Media: Practical Eco-Friendly Access to Propranolol and Atenolol. *Sustain. Chem. Pharm.* **2022**, *30*, 100860;

(229) Vagnoni, M.; Samorì, C.; Galletti, P. Choline-based eutectic mixtures as catalysts for effective synthesis of cyclic carbonates from epoxides and CO2. J. CO2 Util., 2020, 42, 101302;

(230) Zhang, Z.; Taoyuan L. Applications of Green Deep Eutectic Solvents (DESs) in Synthetic Transformations. Green Solvents in Organic Synthesis, 2024, 199-236;

(231) Azizi, N.; Batebi, E. Highly efficient deep eutectic solvents catalysed ring opening of epoxides. Catal. Sci. Technol. 2012, 2 (12), 2445;

(232) Tang, B.; Row, K.H. Recent developments in deep eutectic solvents in chemical sciences. Monatsh. Chem. 2013, 144, 1427–1454 (2013);

(233) Wen, Q.; Chen, J.-X.; Tang,Y. L.; Wang, J.; Yang, Z. Assessing the toxicity and biodegradability of deep eutectic solvents. Chemosphere 2015, 132, 63-69;

(234) Kitaori, K.; Takehira, Y.; Furukawa, Y.; Yoshimoto, H.; Otera, J. Convenient Preparation of Enantiopure Atenolol by Means of Preferential Crystallization. Chem. Pharm. Bull. (Tokyo) 1998, 46 (3), 505–507;

(235) Abbott, A.P.; Boothby D.; Capper G.; Davies D. L.; Rasheed R. K. Deep eutectic solvents formed between choline chloride and carboxylic acids: versatile alternatives to ionic liquids. J. Am. Chem. Soc.. 2004, 126 (29), 9142-9147;

(236) Zhang, X.; Xing, H.; Zhao, Y.; Ma, Z. Pharmaceutical Dispersion Techniques for Dissolution and Bioavailability Enhancement of Poorly Water-Soluble Drugs. *Pharmaceutics* **2018**, *10* (3), 74;

(237) Kalam, M. A.; Alshamsan, A.; Alkholief, M.; Alsarra, I. A.; Ali, R.; Haq, N.; Anwer, M. K.; Shakeel, F. Solubility Measurement and Various Solubility Parameters of Glipizide in Different Neat Solvents. *ACS Omega* **2020**, *5* (3), 1708–1716;

(238) Mahore, J. G.; Suryawanshi, S. D.; Shirolkar, S. V.; Deshkar, S. S. Enhancement of Percutaneous Delivery of Dapsone by Microemulsion Gel. *Journal of Young Pharmacists* **2017**, *9* (4), 507–512;

(239) Wozel, G.; Blasum, C. Dapsone in Dermatology and Beyond. *Arch Dermatol Res* **2014**, *306* (2), 103–124;

(240) Moreno, E.; Calvo, A.; Schwartz, J.; Navarro-Blasco, I.; González-Peñas, E.; Sanmartín, C.; Irache, J.; Espuelas, S. Evaluation of Skin Permeation and Retention of

Topical Dapsone in Murine Cutaneous Leishmaniasis Lesions. *Pharmaceutics* **2019**, *11* (11), 607;

(241) Martins, M. H.; Calderini, A.; Pessine, F. B. T. Host–Guest Interactions between Dapsone and β-Cyclodextrin (Part II): Thermal Analysis, Spectroscopic Characterization, and Solubility Studies. *J Incl Phenom Macrocycl Chem* **2012**, *74* (1–4), 109–116;

(242) Linderstrøm-lang, C.; Naylor, R. 4,4′-Diaminodiphenyl Sulphone: Solubility and Distribution in Blood. *Biochem J.* **1962**, *83* (3), 417–420;

(243) Chougule, M.; Padhi, B.; Misra, A. Development of Spray Dried Liposomal Dry Powder Inhaler of Dapsone. *AAPS PharmSciTech* **2008**, *9* (1), 47–53;

(244) Cha, Y. S.; Kim, H.; Kim, J.; Kim, Oh. H.; Kim, H. Il; Cha, K.; Lee, K. H.; Hwang, S. O. Incidence and Patterns of Hemolytic Anemia in Acute Dapsone Overdose. *Am J Emerg Med* **2016**, *34* (3), 366–369;

(245) Schneider-Rauber, G.; Argenta, D. F.; Caon, T. Emerging Technologies to Target Drug Delivery to the Skin – the Role of Crystals and Carrier-Based Systems in the Case Study of Dapsone. *Pharm Res* **2020**, *37* (12), 240;

(246) Mahore, J.; Shelar, A.; Deshkar, S.; More, G. Conceptual Design and Optimization of Self Microemulsifying Drug Delivery Systems for Dapsone by Using Box-Behnken Design. *J. Res. Pharm.* **2021**, *25(2)*, 179–195;

(247) Wu, Y.; Hao, X.; Li, J.; Guan, A.; Zhou, Z.; Guo, F. New Insight into Improving the Solubility of Poorly Soluble Drugs by Preventing the Formation of Their Hydrogen-Bonds: A Case of Dapsone Salts with Camphorsulfonic and 5-Sulfosalicylic Acid. *CrystEngComm* **2021**, *23* (35), 6191–6198;

(248) de Melo, C. C.; Bitencourt, M.; Corrêa, C. C.; Doriguetto, A. C. Investigating the Solubilities of the Nitrate and Isomorphous Bromide and Chloride Salts of Dapsone. *Cryst Growth Des* **2020**, *20* (4), 2313–2320;

(249) Mazaher Haji Agha, E.; Barzegar-Jalali, M.; Adibkia, K.; Hemmati, S.; Kuentz, M.; Martinez, F.; Jouyban, A. Solubility of Mesalazine in {1-Propanol/Water} Mixtures at Different Temperatures. *J Mol Liq* **2020**, *301*, 112436;

(250) Zarghampour, A.; Moradi, M.; Martinez, F.; Hemmati, S.; Rahimpour, E.; Jouyban, A. Solubility Study of Mesalazine in the Aqueous Mixtures of a Deep-Eutectic Solvent at Different Temperatures. *J Mol Liq* **2021**, *336*, 116300;

(251) Mohammadian, E.; Foroumadi, A.; Hasanvand, Z.; Rahimpour, E.; Zhao, H.; Jouyban, A. Simulation of Mesalazine Solubility in the Binary Solvents at Various Temperatures. *J Mol Liq* **2022**, *357*, 119160;

(252) Shahdadi Sardo, H.; Saremnejad, F.; Bagheri, S.; Akhgari, A.; Afrasiabi Garekani, H.; Sadeghi, F. A Review on 5-Aminosalicylic Acid Colon-Targeted Oral Drug Delivery Systems. *Int J Pharm* **2019**, *558*, 367–379;

(253) Takahashi, K.; Bamba, S.; Morita, Y.; Nishida, A.; Kawahara, M.; Inatomi, O.; Sugimoto, M.; Sasaki, M.; Andoh, A. pH-Dependent 5-Aminosalicylates Releasing Preparations Do Not Affect Thiopurine Metabolism. *Digestion* **2019**, *100* (4), 238–246;

(254) Meneguin, A. B.; Sábio, R. M.; de Souza, M. P. C.; Fernandes, R. P.; de Oliveira, A. G.; Chorilli, M. Cellulose Nanofibers Improve the Performance of Retrograded Starch/Pectin Microparticles for Colon-Specific Delivery of 5-ASA. *Pharmaceutics* **2021**, *13* (9), 1515;

(255) Tang, H.; Xiang, D.; Wang, F.; Mao, J.; Tan, X.; Wang, Y. 5-ASA-Loaded SiO_2 Nanoparticles-a Novel Drug Delivery System Targeting Therapy on Ulcerative Colitis in Mice. *Mol Med Rep* **2017**, *15* (3), 1117–1122;

(256) Mohammadian, E.; Foroumadi, A.; Hasanvand, Z.; Rahimpour, E.; Zhao, H.; Jouyban, A. Simulation of Mesalazine Solubility in the Binary Solvents at Various Temperatures. *J Mol Liq* **2022**, *357*, 119160;

(257) Jafari, P.; Barzegar-Jalali, M.; Jouyban, A. Solubility of Mesalazine in Aqueous Solutions of Two Betaine-Based Deep Eutectic Solvents at Different Temperatures: Data Correlation and Thermodynamic Analysis. *J Mol Liq* **2022**, *366*, 120306;

(258) Armani, E.; Jafari, P.; Hemmati, S.; Rahimpour, E.; Barzegar-Jalali, M.; Jouyban, A. Solubility of Mesalazine in Pseudo-Binary Mixtures of Choline Chloride/Ethylene Glycol Deep Eutectic Solvent and Water at 293.15 K to 313.15 K. *BMC Chem* **2023**, *17* (1), 171;

(259) Wang, K.; Jiang, H.; Li, W.; Qiang, M.; Dong, T.; Li, H. Role of Vitamin C in Skin Diseases. *Front Physiol* **2018**, *9*;

(260) Ling, J. K. U.; Chan, Y. S.; Nandong, J.; Chin, S. F.; Ho, B. K. Formulation of Choline Chloride/Ascorbic Acid Natural Deep Eutectic Solvent: Characterization, Solubilization Capacity and Antioxidant Property. *LWT* **2020**, *133*, 110096;

(261) Rogošić, M.; Zagajski Kučan, K. Deep Eutectic Solvent Based on Choline Chloride and Propylene Glycol as a Potential Medium for Extraction Denitrification of Hydrocarbon Fuels. *Chem. Eng. Res. Des.* **2020**, *161*, 45–57;

(262) Andrés, A.; Rosés, M.; Ràfols, C.; Bosch, E.; Espinosa, S.; Segarra, V.; Huerta, J. M. Setup and Validation of Shake-Flask Procedures for the Determination of Partition Coefficients (LogD) from Low Drug Amounts. *Eur. J. Pharm. Sci.* **2015**, *76*, 181–191;

(263) Mustafa, N.; Spelbos, V.; Witkamp, G.-J.; Verpoorte, R.; Choi, Y. Solubility and Stability of Some Pharmaceuticals in Natural Deep Eutectic Solvents-Based Formulations. *Molecules* **2021**, *26* (9), 2645;

(264) Serna-Vázquez, J.; Ahmad, M. Z.; Boczkaj, G.; Castro-Muñoz, R. Latest Insights on Novel Deep Eutectic Solvents (DES) for Sustainable Extraction of Phenolic Compounds from Natural Sources. *Molecules* **2021**, *26* (16), 5037;

(265) Rengstl, D.; Fischer, V.; Kunz, W. Low-Melting Mixtures Based on Choline Ionic Liquids. *Phys. Chem. Chem. Phys.* **2014**, *16* (41), 22815–22822;

(266) Aroso, I. M.; Paiva, A.; Reis, R. L.; Duarte, A. R. C. Natural Deep Eutectic Solvents from Choline Chloride and Betaine – Physicochemical Properties. *J Mol Liq* **2017**, *241*, 654–661.